MASSEY UNIVERSITY
COLLEGE OF SCIENCES

MODELLING FOOD BREAKDOWN AND BOLUS FORMATION DURING MASTICATION

A thesis presented in partial fulfilment of the requirements for the degree of

Doctor of Philosophy in Bioprocess Engineering

at Massey University, New Zealand

Eli Mark Gray-Stuart

2016

ABSTRACT

Mastication is a complex process that transforms food into a bolus which can be swallowed safely. However, it can be simplified within an engineering context, where the mouth is the equipment carrying out a unit operation to convert ingested food (raw material) into a safe-to-swallow bolus as the process output. Two questions emerge from this observation (i), 'What processes transform the food from its initial state into a bolus?' and (ii), 'How do humans assess when the food is ready to initiate swallowing?' This research examines these questions and a mathematical model is developed which can track the bolus properties during mastication.

A range of common foods with contrasting textures were examined in an observational study to investigate the rate processes of mastication. A wide range of breakdown pathways and textures were observed, from the brittle fracture of carrots to the work softening of a fibrous beef steak. However, despite differences in their structure and properties, breakdown is dominated by a small number of rate processes. Size reduction and work softening occur at occlusion and account for majority of the structural breakdown. Absorption, dissolution and melting are generally more subtle. These are facilitated by mixing, which is the circulation, gathering, folding and placement of food on the occlusal plane.

Mechanical sensory testing (MST) occurs simultaneously to breakdown as the food is manipulated around the mouth during occlusion and between chews. During occlusion this provides gross information about the toughness and hardness, whereas between chews the tongue-palate interactions provide more detailed information about yield and flow. These MST's assess the properties of volume, adhesion, bolus deformation, particle deformation and particle size. Adhesion refers to the binding forces between the food particles and the oral surfaces. Bolus deformation is important for boluses that do not contain individual particles. If they do then swallowability is constrained by their size and individual deformability.

In order for safe swallowing, thresholds for each of the MST properties must be met. These were justified using a *hazard and operability* study of swallowing, on the premise that attempting to swallow a bolus which does not meet the threshold property could result in aspiration or choking. As mastication proceeds, the properties assessed by the MST's are evaluated against the required threshold properties and contribute to the decision making process of whether to swallow or continue chewing.

From this analysis, this work proposes a universal conceptual model of mastication that combines the rate processes, the MSTs and a decision making model. The conceptual model was then described mathematically. It is universal, that is, it is not specific to any food type, because solid foods follow similar physical breakdown paths where occlusion is of primary importance followed by the incorporation of saliva and the other rate processes. Model parameters require *in-vivo* experiments about the breakdown dynamics of specific foods. Subject variability was avoided by using single subject studies for three separate foods; brown rice, a sweetened gelatine gel and peanuts embedded in a food matrix. Each case study explored a limited number of rate processes and food properties. Bolus properties predicted by the model were compared to the experimental data. The output of the model, including particle size distribution and moisture content, closely matched the data during mastication and at swallow point using input parameters fitted from the single subject experiments.

This work provides a platform for further research into mastication modelling. It is recommended the mathematical model be expanded to mechanistically describe the mixing and work softening of non-particulate food boluses. Additional experimental work would achieve a better understanding of the heat transfer in the mouth which would improve the models ability to handle heat sensitive foods.

The model developed here has the potential to aid future food design where a particular breakdown pathway is desired and will reduce the number of time intensive *in-vivo* experiments needed.

ACKNOWLEDGEMENTS

I would like to thank my supervisors Professor Jim Jones and Professor John Bronlund for their enduring and unwavering support and encouragement throughout this project. I will be forever grateful. Also a special thank you to Marco Morgenstern for his support, input and kind words over the years.

Thank you to the Riddet centre of Research Excellence for funding this project and to the School of Engineering and Advanced technology at Massey University for accommodating me. Furthermore, the support and encouragement from the academic, technical and administrative staff was fantastic and made this work possible. I would like to particularly thank Warwick Johnson, Anne-Marie Jackson, John Edwards, Linda Lowe and Michelle Wagner.

Thanks to all my friends, colleagues and class mates who have shared this journey and experience with me. Being able to shoot the breeze and share our trials and tribulations made this process so much more enjoyable and manageable. In no particular order, thank you Konrad, Melissa, Yashwant, Gonzalo, Georg, Colin, Sureewan, Mazidah, Sadia and Tiyaporn.

A special thanks to Scott Hutchings for his thoughts and guidance and to Anuchita Moongngarm, Camille Ollier and Jenny Loi for their help in the lab. I must also thank my volunteers who helped throughout this project.

Last but definitely not least, I would like to thank my family. They have graciously shared, or should I say endured, this journey with me. To my Dad and wicked step mother, I am so very grateful for your love, encouragement, and unfaltering support over the years. Thank you Mum for your love, support and kind words. Luke you have been an incredibly understanding brother and housemate and have been generous to a fault. Chris, Fleur and Olivia your encouragement and all the times you have helped me relax and unwind from the daily grind was a godsend. To Oliver, thank you for keeping me on my toes and for your consistent hard line of enquiry.

Lastly, it would be remiss of me not to end this section with some noble insight or pearl of wisdom. Therefore, I leave you with this. There are two types of people in the world, those who can extrapolate from incomplete data sets.

Warning: This thesis may contain traces of nuts!

LIST OF PUBLICATIONS AND PRESENTATIONS

Refereed conference papers:

Gray-Stuart E., Jones, J. R., Bronlund, J. E., & Morgenstern, M. P. (2012) Rate processes during mastication important for modelling mastication. In: *Chemeca 2012*. Wellington, New Zealand 23-26 September 2012.

Gray-Stuart E., Jones, J. R., Bronlund, J. E., & Morgenstern, M. P. (2012) Control loops in mastication: whether to keep chewing or prepare for swallowing. In: *Chemeca 2012*. Wellington, New Zealand 23-26 September 2012.

Gray-Stuart E., Jones, J. R., Bronlund, J. E., Moongngarm, A., & Morgenstern, M. P. (2011) A discrete population balance to simulate the particle size distribution in a bolus of chewed rice. ICEF 2011, Athens, Greece.

Conference presentations and posters:

Gray-Stuart. E., J R Jones., Bronlund, J.E. and Morgenstern. M. Modelling the Food During Mastication. Oral presentation, Food Oral Processing, Wageningen, 29th Jun - 2nd July 2014.

Gray-Stuart E., Jones, J. R., Bronlund, J. E. A mathematical model to simulate the breakdown of a gelatine based gel during chewing (2010). Oral presentation, International Conference on Food Oral Processing, 5-7 July 2010, Leeds, UK

Gray-Stuart E., Mongngarm, A., Jones, J. R., Bronlund, J. E. (2010). A conceptual model of particle size reduction during chewing of brown rice. Poster presentation, International Conference on Food Oral Processing, 5-7 July 2010, Leeds, UK

TABLE OF CONTENTS

LIST OF FIGURES

LIST OF TABLES

CHAPTER 1 PROJECT OVERVIEW

Food is celebrated across the world and is central to many social interactions. The complex texture and flavour profiles are complimented by our olfactory senses to deliver a pleasurable eating experience. However, mastication can be simplified rather crudely within an engineering context, where the mouth is the equipment carrying out a unit operation to convert ingested food (raw material) into a safe-to-swallow bolus as the process output. Two questions emerge from this observation (i), 'What processes transform the food from its initial state into a bolus?' and (ii), 'How do humans assess when the food is ready to initiate swallowing?' This research examines these questions, and proposes an engineering framework to represent/analyse human mastication.

The transformation of food during oral processing of food is complex. Foods have a great variety of structures and properties which breakdown via a number of common rate processes Occlusion between the teeth is a crushing and grinding action which either breaks apart the food into many particles or work softens it. At the same time saliva is continually produced and is blended with the food. When saliva coats particles it facilitates the dissolution of soluble solids and release of flavour compounds. If the food is porous it can absorb excess moisture which generally softens the food. Heat from the mouth surfaces and added saliva warms the food which contributes to melting of solid fats, if present. These rate processes are explored qualitatively in chapter 3, then mechanistically using a process engineering approach in chapter 4. This answers the first research question.

Mastication concludes when the food is formed into a bolus ready for swallowing. Defining when a bolus is ready for swallowing is still an open question. Theories date back to the nineteenth century when Horace Fletcher proposed that food should be masticated until it reaches a liquid-like consistency (in Christen and Christen, 1997). His ideas did not gain traction, however, because this requires a conscious effort to override the usually involuntary initiation of bolus transport and of swallowing. Modern consensus on the criteria for swallowing is credited to Hutchings and Lillford (1988) who described a dual threshold model of *structure* and *lubrication*. Their model is conceptual, however, and quantitative approaches have yet to be developed. This thesis addresses the second research questions by first considering how the mouth measures food and what food properties these measurements align with. Then, using a hazard mitigation engineering tool, it is shown that these food properties must have thresholds that must be met in order for safe swallowing to occur. They

define the endpoint of mastication and are critical because of the dangers involved with incorrect swallowing, a decision making process for swallowing is then proposed.

In this work, across the various sections of chapter 4 the rate processes, food properties and thresholds for swallowing are brought together as a conceptual model of mastication. This is then developed into a mathematical model which is described in chapter 5. In chapter 6, it is tuned to experimental data for three case studies to explore the robustness of the model assumptions.

In summary the primary objectives of this thesis were;

For research question 1: 'What processes transform the food from its initial state into a bolus?'

- Conduct a qualitative analysis of bolus formation for a range of solid foods. This task was used to formalise an understanding of how foods are broken down during oral processing by identifying the key rate processes.
- Describe mechanistically the rate processes identified above.

For research question 2: 'How do humans assess when the food is ready to initiate swallowing?'

- Describe how the mouth measures food properties and identify which properties are important to track as the bolus approaches swallow point
- Apply a hazard and operability study (HAZOP) to swallowing to confirm the set of criteria that define a 'safe-to-swallow' bolus. This then leads to a review of decision making models for mastication.

The outcome of the four objectives above is a conceptual model of food breakdown that links the effect of rate processes to food and bolus properties and their thresholds as the swallow point is approached. There were two further objectives, to;

- Develop the conceptual model of food breakdown described by the effect of rate processes on food properties into a quantitative mathematical model.
- Validate the model using three case study foods, by comparing model predictions to experimental data from human subjects for the best fit model parameters. The foods examined are brown rice, a sweetened gelatine gel and peanuts embedded in a chocolate and gelatine matrix.

CHAPTER 2 LITERATURE REVIEW

2.1 Introduction

The oral processing of food results in the formation and swallowing of a bolus. However, food breakdown and bolus formation are not simple processes to describe because the different parts of the oral apparatus operate in synergy to process the food from its initial state into a safe-to-swallow bolus. It is the objective of this thesis to explore the concepts required to develop a mathematical model of food breakdown and bolus formation. In order to do so, the mastication process needs to be clearly understood. How the food is processed in the mouth, how the different physiological aspects of the mouth and the physical and mechanical properties of the food contribute to food breakdown and bolus formation all need careful consideration.

Conceptual models of food oral processing have been postulated by different researchers (Hiiemae, 2004; Lucas et al., 2002). These models can help visualise the mastication process and provide some insight when developing a mechanistic (i.e. mathematical) model, particularly the formation and swallowing of multiple boluses during a complete mastication sequence. However, they tend to describe the breakdown process in terms of what the mouth is doing rather than the changes that food undergoes during mastication, where industrial comminution models provide more insight. These models successfully simulate the particle size distribution in the food bolus for a limited range of hard and brittle foods which, when fractured, produce several daughter particles (Lucas and Luke, 1983b, van der Bilt et al., 1987 van der Glas et al., 1992).

Developing a predictive model framework is the aim of this thesis. Lucas et al. (2002) purport that if the initial properties of the food and the final properties of the bolus can be characterised together with the principal features of the process, testable models possessing predictive values can be developed. One of the potential difficulties to overcome will be characterising the final properties of the bolus. A bolus needs to be cohesive, lubricated and deformable to be safely swallowed, but measuring such properties is difficult although progress has been made (Peyron et al., 2007, Nagatomi et al., 2008 and Loret et al., 2011). The comminution models mentioned above predict only particle size, not bolus properties. Textural profile analysis (TPA) is one such method which has been used to measure the rheological properties of the food bolus. However, TPA has not been able to be used to define

threshold swallowing properties that are applicable across a range of foods. Further work using TPA may prove useful in correlating parameters in a mathematical model and rheological properties of the bolus.

The purpose of this review is to provide information on the current literature relating to food breakdown and bolus formation during oral processing. Both food properties and oral physiology of an individual influence how food is processed in the mouth. The oral cavity in terms of how the teeth, tongue and saliva contribute to food breakdown is discussed. Food oral processing is discussed as a series of sub processes from the first bite through to the final mouth clearance (Hiiemae, 2004, Lucas et al., 2002). These mechanisms are influenced by the initial physical and mechanical properties of the food and are discussed in this review. The end point of mastication is a safe-to-swallow bolus, which means it is important to explore the criteria of a safe swallow and how to quantify bolus rheology. While researchers have shown that the particle size distribution for brittle foods in the bolus can be simulated using models adapted from industrial comminution processes, it is important to review how these models perform for softer foods and matrices of soft and hard foods.

2.2 Oral Physiology

The oral cavity is where food is processed before it is swallowed and is the void space between the lips and the velum (Chen, 2009) and contains the teeth, tongue and saliva. This section provides some background information on the roles and contribution these physiological aspects have on the consumption of food.

2.2.1 The Oral Cavity

The volume of the oral cavity and the nominal bite size varies significantly between people. Medics and Hiiemae (1998) have shown that a normal mouthful for an adult male is 30.5 ± 10.1 g water and for adult females it is around 25.2 ± 8.1 g water. Assuming the water fills the void space in the mouth, the measurement gives an estimation of the volume of the oral cavity. Intuitively, the initial volume of a mouthful of solid food is much less than that of the water measurements. The same study found for each mouthful, males take on average 18 ± 4.9 g of banana and females take 13.1 ± 1.4 g. The mouthful is smaller still for peanuts, 5.5 ± 2.3 g for males and 3.6 ± 1.4 g for females. The amount of food varies not only between people but is also dependent on the food type. Although these results were reported as a mass, a volume measurement may be more useful as the density difference between foods can be

significant. The volume of a mouthful decreases from a maximum with liquid to soft solids and a minimum for hard solids (Chen, 2009).

Chewing studies tend to either give subjects a pre-determined amount of food or allow them to take their own bite or mouthful. A study conducted by Hutchings et al. (2009) examined the variation in natural bite weight, volume and length of different food bars in order to assess which method of serving is best for mastication studies. Six food bars were chosen for the study each with distinctive physical properties. They found that bite length rather than bite mass or bite volume, was consistent between food bars. An ideal method for serving size in mastication studies has not been identified. Hutchings et al. (2009) were the first to conclude that the serving method needs to be chosen to match the requirements of the study.

The number of chewing strokes required to prepare a food for swallowing is correlated with the portion size. If subjects used a low number of strokes for the smallest portion they used relatively fewer strokes for the largest portion (Fontijn-Tekamp et al., 2004).

2.2.2 Teeth

The teeth physically break the food down into smaller pieces enabling a bolus to be formed. A fully dentate adult has 32 teeth, 16 in each jaw. The teeth serve different purposes. Incisors are used for cutting and only usually participate in the first bite. Canine teeth are used for cutting and tearing. The molars (or post canines) are used for chewing and shearing and perform most of the comminution.

Teeth form the occlusal area where the food particles are fragmented. The extent of fragmentation depends on the total occlusal area and thus on the number of post-canine teeth (Pereira et al., 2006). A linear relationship between the number of occluding teeth and masticatory performance has been found (van der Bilt et al. 2006). The number of chewing strokes before swallowing is influenced by dentition but is independent of age or gender (Fontijn-Tekamp et al., 2004).

People with incomplete dentition have a reduced masticatory function and use more chewing strokes before swallowing compared to fully dentate people. However, subjects with good masticatory function do not necessarily swallow their food in fewer chewing strokes than

people with reduced masticatory function because it was found that people with reduced masticatory function swallow boluses with larger food particles (Fontijn-Tekamp et al., 2004).

2.2.3 Tongue

The tongue which is essential for speech and appreciation of food also plays an important role in mastication, where it helps manipulate food and assists in swallowing. After the first bite, the tongue moves food distally through the oral cavity from the incisors to the post canines. The tongue then helps position food between the post-canines during mastication and finally moves the food to the pharynx for bolus formation and swallowing (Hiiemae, 2004). After a mouthful of food has been chewed and swallowed, the tongue often performs a 'sweep' to collect small particles which remain in the mouth attached to the gums, teeth and other tissues in the mouth. The particle 'sweepings' form the terminal swallow.

2.2.4 Saliva

Saliva is the first physiological secretion associated with the ingestion of food and serves many important functions. It helps to maintain overall oral health by maintaining tooth integrity, provides antibacterial activity, lubricates and protects oral tissues and acts as a barrier against irritants (Chen, 2009 and Pederson et al., 2002). In addition the saliva affects food properties through solubilisation and absorption. It is essential for the perception of taste, aids bolus formation and facilitates deglutition. Saliva initiates the first stage of digestion because it contains amylase, a digestive enzyme that hydrolyses starch (Froehlich et al., 1986). Saliva flow is affected by different stimuli as discussed below.

Ninety percent of saliva is produced by three pairs of salivary glands (Humphrey and Williamson, 2001), the paired parotid gland, the sublingual gland and the submandibular gland (Table 2-1). Sources responsible for the remaining 10% are the gingival crevicular sulci (area between tooth and marginal free gingiva), an estimated number of 450–750 minor accessory salivary glands, situated on the tongue, the buccal mucosae and the palate, and oro-naso-pharyngeal secretion (Aps and Martens, 2005).

Table 2-1: Mean contribution (expressed as % of the total) of the different salivary glands to the total salivary production under different stimulation (from Aps and Martens, 2005)

	Sleep	No Stimulation	Mechanical stimulation	Citric acid stimulation
Parotid glands	0	21	58	45
Submanidubular glands	72	70	33	45
Sublingual gland	14	2	2	2
Minor glands	14	7	7	8

The flow rate and composition of saliva varies with stimuli. The stimulation can be intra oral such as taste or mechanical stimulation, or extra oral from ambient factors such as odours (Engelen et al. 2003). Froehlich et al. (1986) studied the change in flow rate and the secretion rate of protein and alpha amylase of saliva secreted by the parotid gland in response to different stimuli. Aqueous solutions of sodium hydroxide, citric acid, starch and glucose were made up at various concentrations to simulate a range of similar sensory intensities. Citric acid produced the most dramatic increase in flow rate, followed by sodium hydroxide, sucrose and starch. Citric acid at the lowest level elicited a higher flow rate than the highest level of the other three stimuli. The protein secretion rate and amylase secretion rate depended on the stimulus concentration.

Many studies have measured the whole salivary flow rate generated while chewing on natural and artificial foods. In these studies, the saliva flow rate while chewing on natural food was taken as the difference between the initial mass of the food and the mass of the bolus. Watanabe and Dawes (1988) measured the saliva flow rate in response to citric acid and a range of foods (Table 2-2). A similar study by Gaviao et al. (2004) used toast with and without margarine and three different size portions of Dutch breakfast cake (9.2, 14.0 and 20.0 cm^3) (Table 2-3) . Engelen et al. (2003) measured the flow rate of whole saliva after stimulation with custard odour, citric acid and after subjects had chewed on Parafilm, an inert tasteless material (Table 2-4).

Table 2-2: Salivary flow rates in response to citric acid and chewing various foods (from Watanabe and Dawes, 1988)

	Flow rate (ml/min)
Stimulus	Mean and SD
Unstimulated	0.72 ± 0.28
52 mmol/l citric acid	4.35 ± 1.92
156 mmol/l citric acid	5.94 ± 2.08
260 mmol/l citric acid	7.07 ± 2.16
Rice	3.15 ± 1.48
French fries	3.82 ± 1.32
Cheeseburger	3.92 ± 1.85
Cookie	4.17 ± 1.32
Chocolate	4.18 ± 1.44
Apple	4.76 ± 1.53
Rhubarb pie	4.94 ± 1.51

Table 2-3: Salivary flow rates in response to chewing different foods (from Gaviao et al., 2004)

	Flow rate (ml/min)
Stimulus	Mean and SD
Unstimulated	0.53 ± 0.28
Parafilm	1.40 ± 0.67
Toast	8.84 ± 5.06
Toast (with margarine)	7.74 ± 4.97
Cake (small)	7.97 ± 5.02
Cake (medium)	7.32 ± 3.97
Cake (large)	7.42 ± 3.61

Table 2-4: Average salivary flow rates at rest and after stimulation with custard odour, Parafilm chewing and citric acid (from Engelen et al., 2003)

	Flow rate (S.D) ml min^{-1}			
	Unstimulated	Odour	Parafilm	Citric acid
Female	0.35 (0.17)	0.52 (0.20)	1.06 (0.40)	2.03 (0.68)
Male	0.45 (0.18)	0.50 (0.24)	1.22 (0.52)	2.69 (0.68)
Morning	0.37 (0.17)	0.47	1.04	2.49
Evening	0.41	0.53	1.16	2.0
Total	0.38	0.51	1.12	1.87

These tables show that saliva flow rates vary widely among subjects, demonstrated by the high standard deviations. When citric acid was used as a stimulus it elicited the highest flow rate. The amount of citric acid and how it is administered influences saliva flow rate and is the reason for the large differences in the values shown in Table 2-2 and Table 2-4 . Watanabe and Dawes (1998) supplied a constant flow rate of citric acid (5ml/min) to the subjects, they swished this around their mouths and expectorated every 10 seconds for a minute. In contrast Engelen et al. (2003) put only three drops of 4% citric acid on the subjects tongue every 30 seconds, their saliva was also collected every 30 seconds for five minutes. Gustatory

stimulation has more of an effect than mechanical stimulation alone; this is shown by the lower flow rates for Parafilm compared with natural food. The comparatively high flow rates in

Table 2-2 and Table 2-3 can be explained by the types of food used, toast and cake are dry foods that would require more saliva to form a bolus (Gaviao et al. 2004) than the moist foods in Table 2-2. Within a single food type, saliva excretion is independent of food volume. This means the amount of saliva secreted per gram varies significantly among the different types of foods (Watanabe and Dawes, 1988; Gaviao et al. 2004); Melba toast elicited the highest flow rate and had the lowest fat and moisture content which supports the thinking that dryer products need more saliva to form a safe to swallow bolus.

Saliva flow rates for females are not significantly different than their male counterparts (Table 2-4). The salivary flow rate is only weakly correlated with the number of chewing strokes required to prepare food for swallowing. Subjects with high salivary flow rates do not necessarily swallow food after less chewing strokes than a subject with a low saliva flow (Engelen et al. 2003).

The method of measuring the flow rate by measuring the food mass before and after chewing can be prone to errors due to food particles remaining stuck in the mouth after expectorating and the possibility of swallowing food before expectoration. Intermediate swallowing can result in less than 50% of the ingested solids being recovered in the expectorated bolus (Flynn, 2012; Jalabert-Malbos et al., 2007). These errors can be reduced by measuring the solids content of the bolus after expectoration to account for solids lost enabling incorporated saliva to be calculated more accurately; Watanabe and Dawes (1998) used this approach in their analysis. Gaviao et al. (2004) had their subjects chew in a natural manner and also told them that all food material needed to be recovered, this was ostensibly achieved by having the subjects using a tongue sweep to recover particles after expectoration. This method could explain the much higher saliva flow rates obtained in Table 2-3 as even a small amount of solids lost through intermediate swallowing will inflate the value of incorporated saliva.

Saliva Properties and Composition

Saliva is a heterogeneous clear fluid consisting of 98% water and 2% organic and inorganic substances, such as various electrolytes of sodium, potassium, calcium, magnesium, bicarbonate and phosphates. Immunoglobulins, enzymes, proteins, urea and ammonia are also found. These components interact in a series of related functions including; (1), bicarbonates, phosphates and urea help maintain pH give saliva its buffering capacity; (2), macromolecule

proteins and mucins cleanse, aggregate, and/or attach to oral microorganisms and contribute to dental plaque metabolism; (3) calcium, phosphate and proteins work together as an anti-solubility factor and modulate demineralization and remineralisation of dental enamel; and (4) immunoglobulins, proteins and enzymes provide antibacterial action (Humphrey and Williamson, 2001). Saliva occupies a neutral pH range between 5.6 and 7.6 with an average of 6.75.

Functions of Saliva

Saliva has multiple functions in aiding mastication and maintaining good oral health. Humphrey and Williamson (2002) organised the functions of saliva into 5 major categories: (1) lubrication and protection, (2) buffering action and clearance, (3) maintenance of tooth integrity, (4) antibacterial activity, and (5) taste and digestion. These functions relate to the unique fluid characteristics and the components of saliva with many having multifunctional roles (Pederson et al., 2002). With respect to mastication, categories 2, 3 and 4 can be grouped as they all concern maintenance of healthy disease free teeth and oral cavity. The functions of saliva pertinent to this study relate to lubrication and bolus formation, taste and digestion. Each of these is discussed below.

(1) Lubrication and bolus formation. Saliva provides a coating that lubricates and protects oral tissues and acts as a barrier against irritants such as enzymes produced in plaque and by exogenous chemicals. Lubrication of the oral tissues is primarily mediated by mucins, which are large extracellular glycoproteins with molecular weights ranging from 0.5 to 20 Mda. Mucins have low solubility, high viscosity, high elasticity and adhesiveness (Humphrey and Williamson, 2002). It is the lubricating action and cohesive properties of the mucins which help to form a bolus that is safe to swallow.

(2) Taste. The sense of taste is activated during the initial stage of ingestion. It only allows for the appreciation of the food and identification of desirable and essential nutrients but also the detection of potentially toxic or harmful compounds (Pederson et al., 2002). Saliva is essential for taste perception, because flavour compounds need to be in solution to stimulate taste receptor cells in the taste buds. Saliva is hypotonic which enhances the ability to taste salty foods and nutrient sources. Another significant aspect of taste is the ability to detect aroma compounds; volatile compounds enter the saliva and then evaporate into the head space of the oral cavity where they are detected.

(3) Digestion. The enzyme amylase is a major component of parotid saliva and is responsible for the early breakdown of starch. Hoebler et al. (2000) found that during the mastication,

about 50% of bread starch and 25% of pasta starch was hydrolysed and transformed into smaller molecules. The different rate of starch hydrolysis was due to the structural differences of the food. Bread is porous and more accessible to saliva. Prinz et al. (2000) performed *in-vitro* experiments with custard and found that the amylase induced breakdown significantly affected viscosity, causing an almost 10 fold reduction over the time of oral processing. The enzyme α-amylase is most active in the pH range of the mouth and becomes inactivated by the acidic conditions of the stomach. Although starch digestion begins immediately in the mouth, for most foods the majority of starch digestion is carried out by pancreatic amylase (Chen, 2009). It is likely that, with the right conditions, starch digestion via salivary amylase may continue in the stomach. For example, if a well formed cohesive bolus does not disintegrate upon entering the stomach, α-amylase incorporated in the bolus may continue to act as long as the gastric acid does not penetrate the bolus.

2.3 Oral Processing of Food

Oral processing is controlled by the central nervous system. It is a physiological and physical process (Chen, 2009). Physiological factors are those relating to the subject, e.g., by age, gender, dental status, while physical factors explain the variation related to the properties of the food (Chen, 2009 and Woda et al., 2006a). Four stages of oral processing can be described that track the food experience: the first bite, comminution and lubrication, bolus formation and swallowing (Hutchings and Lillford 1998; Prinz and Lucas 1997, Prinz and Lucas 1997, van der Bilt et al. 2006, Engelen et al. 2005).

Our metabolic rate demands mastication of food to acquire energy and essential nutrients, comminution increases the surface area exposure of the food particles to the digestive enzymes in the gut, thus providing energy at a higher rate (Prinz and Lucas 1997; Lucas, et al. 2002).

The oral operations occurring between the first bit and the terminal swallow involve a series of decision steps to ensure masticatory operations are co-ordinated and proceed in the right order (Chen, 2009). Lucas et al. (2002) produced a conceptual model (Figure 2-1) with decision boxes to describe different oral operations including, grip, first bite, fracture, size reduction, transportation and swallowing. The decision boxes do not describe decisions made by the central nervous system but are a simple analytical way of describing a general sequence of events. In between each event is some sort of transport whether gathering and placing the

food in the occlusal plane or transport towards the pharynx. This model does not address the sensory input necessary to make the decisions at the steps.

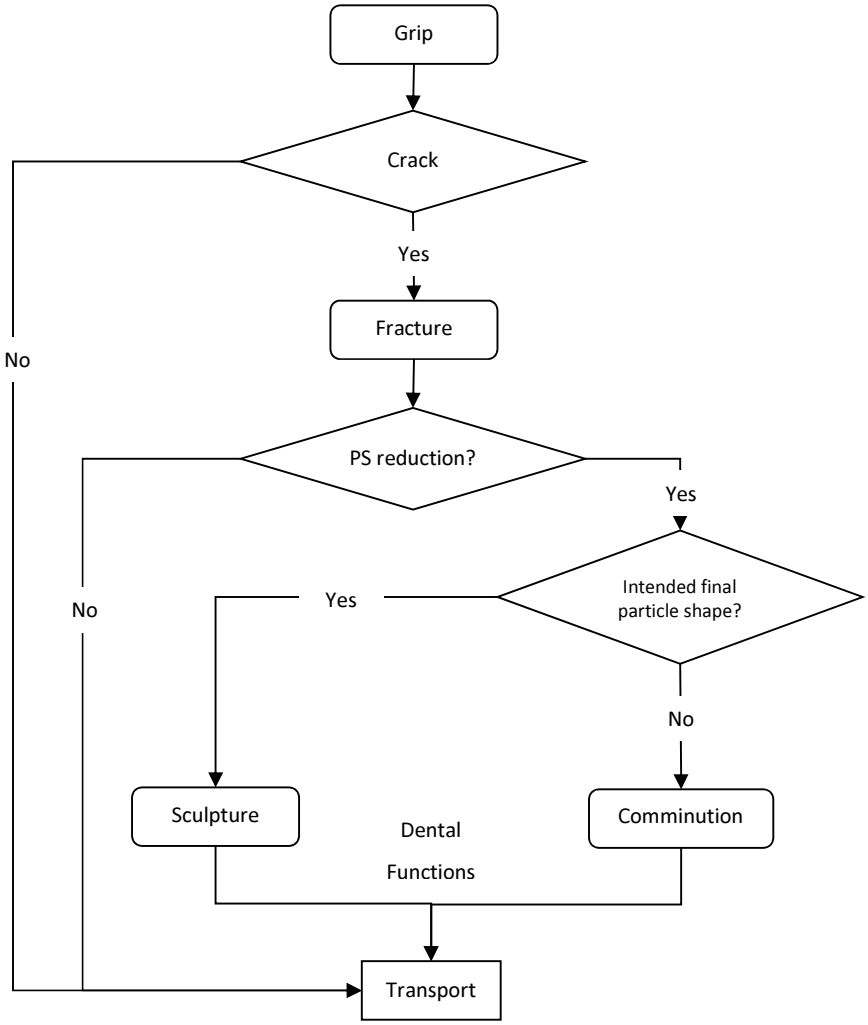

Figure 2-1: A conceptual model depicting food oral processing as a sequence of events. Decision boxes are shown as diamonds while process boxes are rectangular (from Lucas et al., 2002).

Hiiemae (2004) proposed a conceptual model of feeding that involves a series of sequential stages (Figure 2-2). The process model asks three questions and the progress of food from ingestion to swallowing is regulated by sensory input from the orofacial complex. The first question is whether the food is suitable to eat; the second is whether the material is suitable for swallowing. The last gate is a threshold which has time and volume components and asks if there is enough food to swallow. If there is not enough food it implies a below volume threshold, however the bolus will get swallowed after some time regardless.

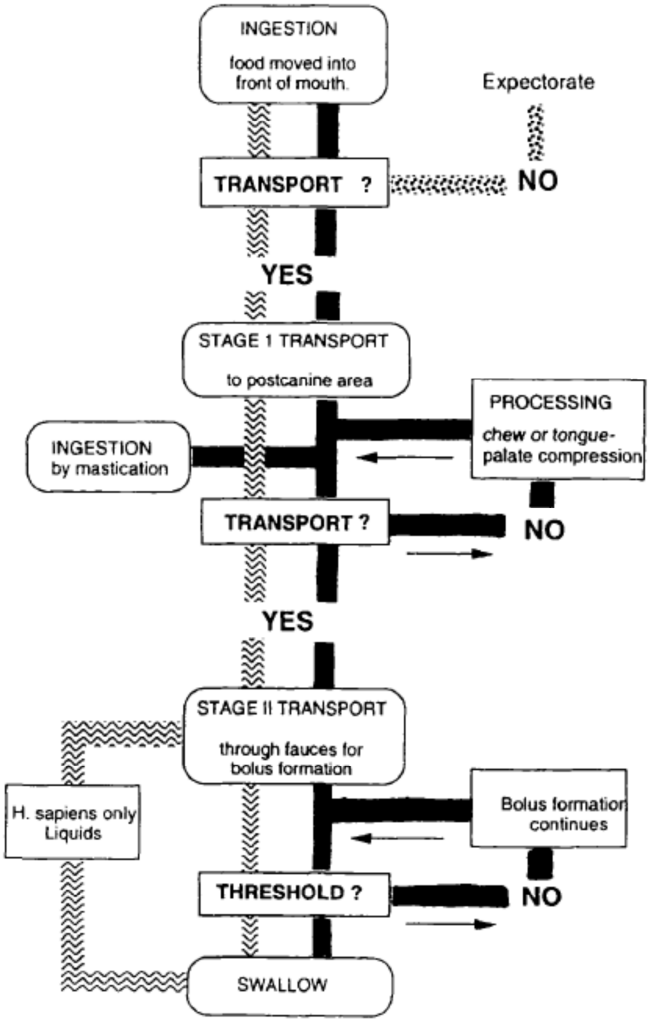

Figure 2-2: The process model of feeding (from Hiiemae 2004).

Stage 1 transport is the act of moving the food from the front teeth after the first bite to the molars for size reduction. During this transport stage, properties of the food such as taste, surface texture are detected. If the food is perceived to be toxic it is spat out at this stage. After the first transport stage processing begins where particle size reduction occurs, and food is mixed with saliva to ready it for bolus formation. Once the food particles are processed sufficiently second stage transportation moves them selectively to the back of the oral cavity to form a bolus. Hiiemae's (2004) model is supported by sirognathographs of 3D jaw movements (Figure 2-3). The different sequences of the mastication cycle can be identified by the changes in jaw movement during swallowing and mouth clearance. Stage 1 transportation is easily distinguishable but the second stage of transport is less evident. It has been postulated that stage 2 transportation occurs simultaneously with the chewing process as more than one bolus is prepared from the one mouthful. Multiple swallows occur for most

feeding sequences. With solid food, some portion of the food may become 'swallowable' before others and be selectively moved to the oropharynx. As mastication continues more food is transported to the oropharynx and ultimately swallowing is completed (Hiiemae, 2004).

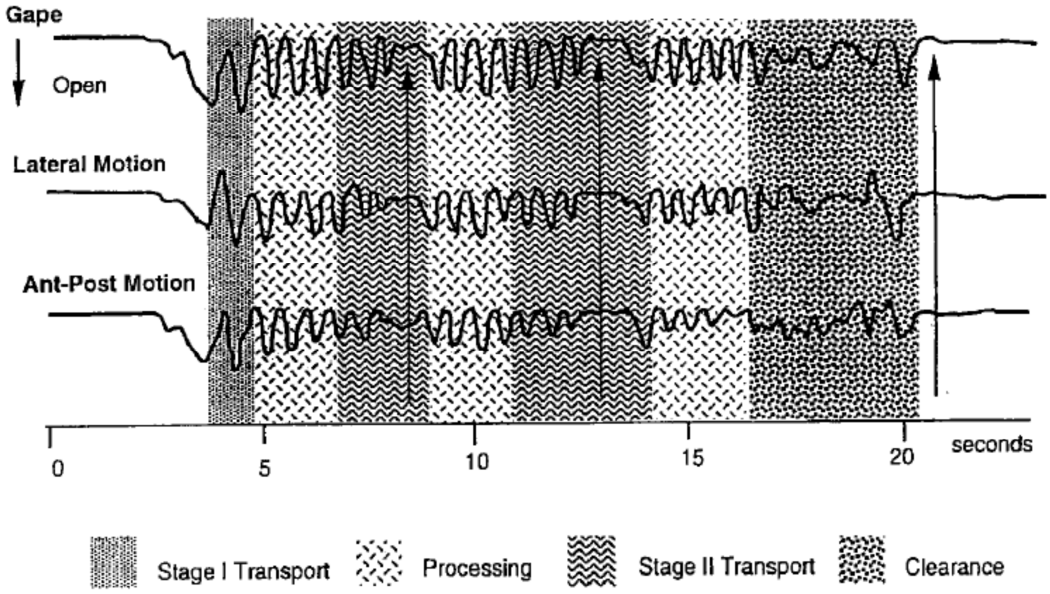

Figure 2-3: Sirognathograph record of a human subject eating an unpeeled apple. The arrows highlight the different jaw movement profile during swallowing (from Hiiemae, 2004).

Accounting for multiple swallows in a mathematical model of bolus formation is an important consideration. The mass or volume of food consumed to produce Figure 2-3 is not mentioned, but the volume of the initial bite would be an important contributing factor to the number and also the mass of the multiple swallows. There is obviously a size threshold for a safe to swallow bolus, which will be governed by an individual's oral physiology and possibly the properties of the food as they contribute to forming a bolus. The composition (solid or liquid) of the intermediate swallows will depend on the food being chewed. In studies on the mastication of meat, the loss of solids during mastication was low, suggesting minimal partial swallows or primarily liquid swallows (Mioche et al., 2002a). Subjects chewing on gelatine sweets used several partial swallows before mastication was completed, the swallows consisted of saliva and dissolved gel and are required to remove excess liquid (Sprunt and Smith., 2002).

The conceptual models presented by Lucas et al. (2002) and Hiiemae (2004) have strong similarities although the later appears more complex and provides a more in-depth explanation of what occurs in each of the stages. The models address the movement of the food and the action of chewing but (apart from comminution) do not address the mechanisms or other physical changes to the food that transform it into a safe to swallow bolus.

It is the aim of this work to extend these conceptual models by critically examining the food experience during mastication and to develop a mechanistic framework necessary to create a quantitative model of food mastication.

2.3.1 The Mouth Process Model

A major step towards a mechanistic framework was made by Hutchings and Lillford (1988) who developed a three dimensional conceptual model to show the dynamic process of food breakdown and texture perception. The model is descriptive rather than quantitative (Figure 2-4). It demonstrates the effect of 'Time' in the mouth and how this affects the 'Degree of Structure' and the 'Degree of Lubrication'. Food follows a breakdown path and in order to be swallowed safely must cross a threshold of structure and lubrication. Although the model was intended for modelling textural change it helps to visualise the rate processes that need to be considered before a mathematical approach to food breakdown can be taken.

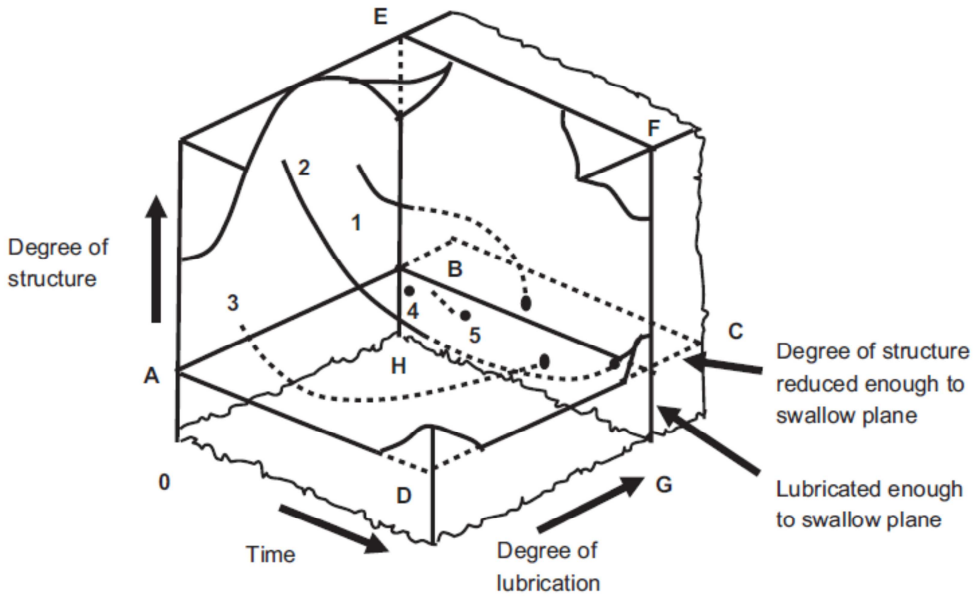

Figure 2-4: The mouth process model. A food may be swallowed when the 'degree of structure' has been reduced below the plane ABCD and its 'degree of lubrication' has crossed the plane EFGH. Key:(1) Tender juicy steak (2) tough dry meat (3) dry sponge cake (4) Oyster (5) liquids and semisolids. From Hutchings and Lillford (1988).

The degree of structure refers to the physical properties of the food which change during mastication. The degree of lubrication is based on the food bolus requiring a specific degree of lubrication to be safe to swallow. The axes in Figure 2-4 have no defined units. Hutchings and Lillford (1988) stated that to assign one physical method to define the 'Degree of Structure' or 'Degree of Lubrication' is unreasonable considering the many factors that contribute to the

process. This approach agrees with current research which finds that the threshold for a safe to swallow bolus consists of particle size and lubrication (Peyron et al., 2004; Jalabert-Malbos et al., 2007). While it remains a challenge to quantify these, it nevertheless provides a useful insight into the oral processes occurring during mastication and helps one consider the rate processes and mechanisms of food breakdown.

2.4 Food Properties that Influence Mastication

Chewing is the dominant process that mechanically breaks down the food so that it can be swallowed safely. This section shows how food properties can influence the mastication process, in particular the number of chewing strokes required to process the food and the rate at which food is broken down.

2.4.1 Hardness and Moisture Content of the Food

The number of chewing strokes required to prepare a bolus for swallowing varies greatly from food to food. This is caused by differences in physical properties, such as moisture, fat content and hardness. This is somewhat intuitive because foods that are softer with more available moisture are going to be broken down and formed into a cohesive bolus faster than a hard or a dry food.

An experiment by Engelen et al. (2005) measured the yield stress and number of chewing strokes for different foods. Chen (2009) plotted this data and found a perfect linear relationship between the chewing strokes and yield stress (Figure 2-5). Foods which are harder require more chewing strokes to form a bolus. Similar conclusions were also made by Jalabert-Malbos et al. (2007) who investigated the particle size distribution and chewing behaviour of 10 subjects eating 8 natural foods and Fontijn-Tekamp et al. (2004) who investigated 87 subjects eating cheese, carrot and peanuts.

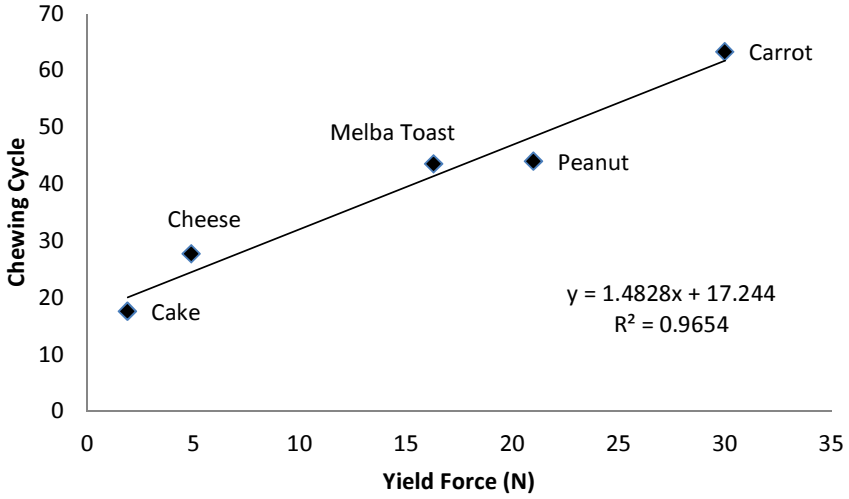

Figure 2-5: Correlation between the hardness of food and the number of chewing cycles. 10 cm^3 samples were fed to 266 healthy adult subjects (from Chen. 2009).

Moisture content is less significant than hardness. This is demonstrated in Figure 2-6 where carrot is approximately 90% water but takes the longest to consume. In carrot, water is bound in rigid cells which, unless they are on the shear plane, do not release their moisture during mastication.

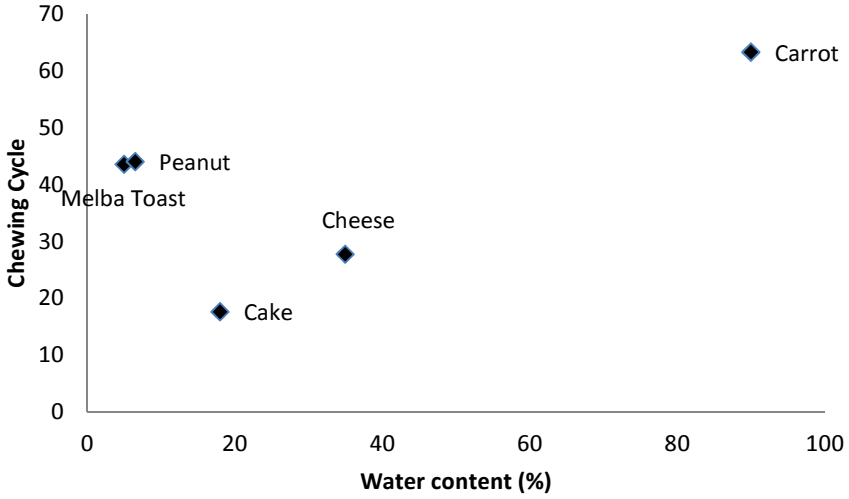

Figure 2-6: Correlation between the moisture content of food and the number of chewing cycles. 10 cm^3 samples were fed to 266 healthy adult subjects (data from Engelen et al., 2005).

The significance of 'liquid' moisture content or extra lubrication on chewing time is demonstrated when water or butter is added to the food. Pereira et al. (2006) studied the texture perception of a number of solid foods (same foods as Figure 2-6) when adding a controlled volume of tap water or applying butter before chewing. The added fluid affects both the physiology (muscle activity and the number of chewing cycles) and the sensory

perception of textural attributes. Muscle activity and number of chewing cycles were reduced for dry products of melba toast, peanuts and cake but were unchanged for the cheese (fatty) and carrot (wet), indicating that for the latter products reaching a safe-to-swallow bolus is dependent on factors other than interstitial moisture content.

Adding liquid or a spread like butter to the food can reduce the number of chewing strokes required in one of two ways; (1), they can help lubricate the surface of the bolus and bind particles together, this may permit the inclusion of larger particles within the bolus; or (2), liquid can reduce the mechanical strength of the food so the structure is broken down faster, thus reaching the swallow threshold in fewer chewing strokes. The average number of chewing strokes required before swallowing toast significantly decreased when 2 g of margarine was spread on it (Gaviao et al., 2004). Also a significant reduction in chewing cycles was also observed when 0.8 g of butter was added to cake, melba toast and toast (Engelen et al., 2005). In these instances the butter aids the lubrication process of the bolus and decreases the time required to form a cohesive bolus. Particle size analysis was not done in these studies but with the significantly reduced number of chewing strokes it is likely that the boluses consisted of larger particles.

2.4.2 Mechanical Properties of the Food

When a food particle is positioned between the occlusal teeth and chewed, daughter particles may be produced by fracture or deformation. The particle distribution resulting from fracture can be described by a breakage function (see §2.7.2), which depends on food material properties. A corollary is the fragmentation index defined by Agrawal et al. (1997) who link the mechanical properties of food to its fragmentation performance. Lucas et al. (2002) later corrected and expanded the approach. Three assumptions were made about the fragmentation during mastication; (1), the food is loaded late in the closing phase of the jaw movement and in the occlusal plane between the molars; (2), the cusps of the molar teeth contact the food particle; and (3), the stored elastic strain energy concentrates at cracks which spread and results in fragmentation as the energy is released.

The response of a solid object to loading stress is a function of the loading geometry and its mechanical properties. The food particle can bend like a beam with at least three points of contact and a crack will form remote from the cusps (Figure 2-7). The crack can then propagate

quickly (Figure 2-8:a) or resist propagation (Figure 2-8:b) which requires the cusp to force the further opening of the crack.

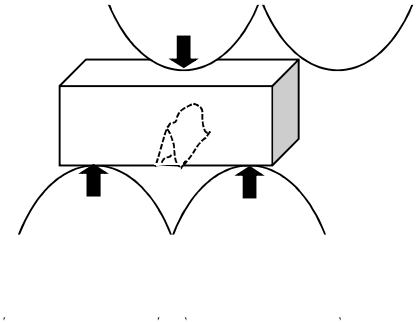

Figure 2-7: Loading of a food particle between the molar cusps. The food particle bends like a beam and the crack starts remote from the cusps (from Agrawal et al., 1996).

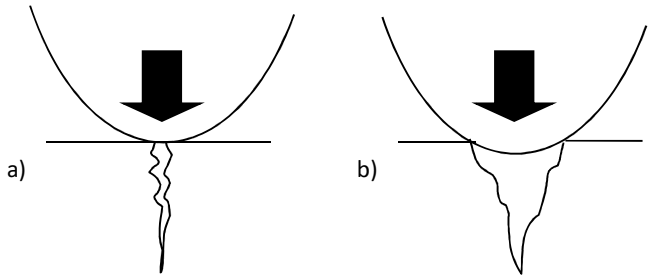

Figure 2-8: Rapid crack propagation and an arrested crack pushed apart by the cusp (from Lucas et al., 2002).

Thus, fracture mechanics theory can be used to analyse mechanical properties of food, where Young's Modulus, *E*, which measures the stiffness of a material and the toughness R measures the resistance to crack growth in a material. Lucas et al. (2002) argued that the modes of crack development depended on whether the fracture was displacement or stress limited. When displacement is limiting, as it will be for most foods trapped in the occlusal plane between the cusps of the teeth, the ratio $\sqrt{R}/\sqrt{E}$,called the displacement index, determines the criterion for breakage. When stress is limiting, the ratio $\sqrt{E}.\sqrt{R}$, called the stress related index, determines the criterion for breakage. For materials that follow this criterion, fractures start at or near the cusp and run rapidly through the material.

The work of Agrawal et al. (1997), which was later extended by Lucas et al. (2002), who investigated the correlation between these two indexes and the breakage function of 28 foods from three food groups: nuts, vegetables and cheese. These foods were chosen because they

are relatively homogeneous and exhibit a linear stress-strain curve, meaning the theories relating fragmentation and mechanical properties should be applicable. The breakage function was measured by having a subject chew once on a particle of food with the post canine teeth. The food was enclosed in a latex bag to prevent interference from saliva. Image analysis was used to measure the apparent surface area of the fragments. The breakage function was expressed as the change in the square root of the specific surface area of the food after one chew. The results are shown in Figure 2-9. It shows that the sugar and many of the nuts have a high breakage function and low $\sqrt{R}/\sqrt{E}$ values. In the middle are the fruits, vegetables and some of the cheeses which have similar values of $\sqrt{R}/\sqrt{E}$ but the fruits and vegetables have a higher breakage function. At the other end are the breads. These foods with values of $\sqrt{R}/\sqrt{E}$ above 25 $mm^{1/2}$ were found to be plastically distorted rather than broken into discrete fragments.

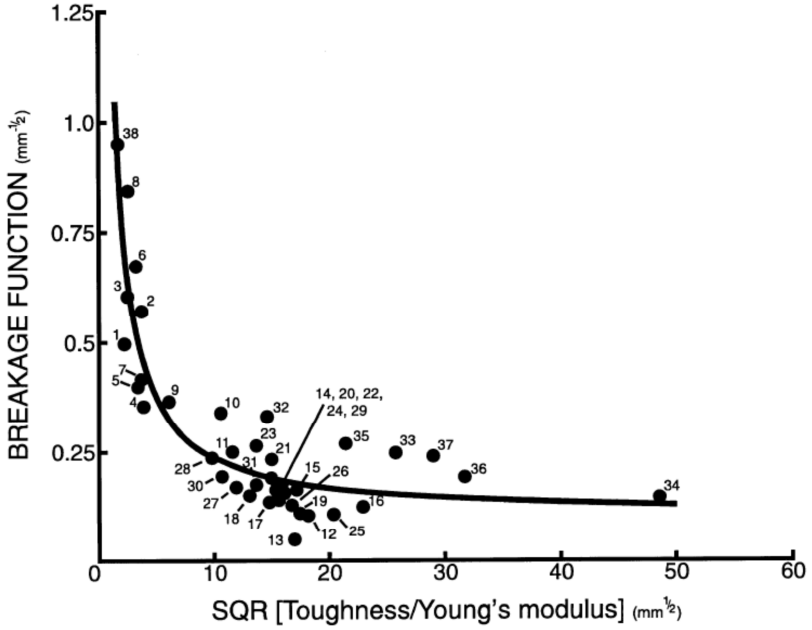

Figure 2-9: The correlation between the breakage function and the mechanical food property group $\sqrt{R}/\sqrt{E}$ .for 38 foods; 1-9 are nuts; 10-27, cheeses; 28-32, fruits and vegetables; 33-36, breads; 37 – a type of soybean curd; and 38, monocrystal sugar.

Figure 2-9 indicates that breakage is inversely related to $(E/R)^{0.5}$ which is shown in Figure 2-10a (Lucas et al., 2002). The other plots, 10b-d show poorer correlations, i.e., the breakage function was significantly correlated with $(E/R)^{1/2}$ and not with $(E.R)^{1/2}$ or E and R alone. Lucas et al (2002) concluded that $(E/R)^{1/2}$ is the best property index at estimating the fragmentation response of food.

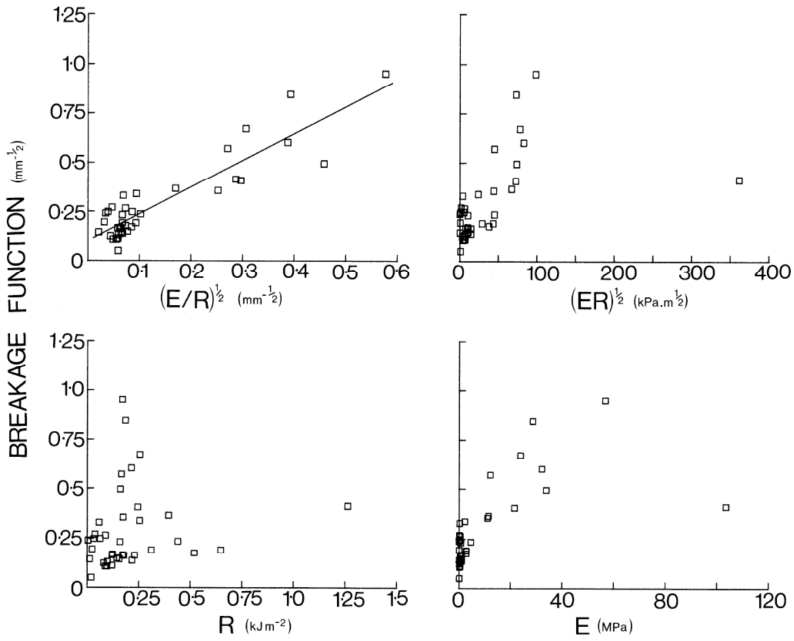

Figure 2-10: The relationship between the breakage function and properties of: (a) $(R/E)^{0.5}$; R^2 = 0.828, (b) $(ER)^{0.5}$; R^2 = 0.230, (c) n.s, (d) R^2 = 0.410. From Lucas et al (2002).

Two issues come out the work by Agrawal et al. (1997) and Lucas et al. (2002.). First, the work investigated only a single chew and excluded saliva, which means that it did not consider the rate processes of moisture absorption or dissolution of dissolved solids. These will affect the rheological properties of the food, meaning the fragmentation behaviour of the food will change during mastication. Second, the work did not consider heating and its effect on softening and then melting, which will occur faster if saliva can transfer heat to the food. Hard cheese is a good example, where the breakage function progresses from fracture to deformation to liquid flow. Third, is inhomogeneity, homogenous foods were chosen simply because theories relating mechanical properties to fragmentation are best applied to homogeneous solids with a linear stress strain curve Agrawal et al. (1997). While this was an excellent starting point, there are many inhomogeneous foods. Meat is one such example, which contains bundles of orientated fibres held together by connective tissue. It is likely that the mechanical properties will depend on the orientation of these fibres to the occlusal surfaces and the stress - strain relationship that they exhibit.

However, fragmentation of food is only one factor in the mastication process. Reaching a safe-to-swallow bolus will most likely depend upon a range of textural properties. As Lucas et al. (2002) point out using evolutionary arguments it is unlikely that, before the advent of modern food processing, humans communicated oral-sensed food texture which might explain why it

is a difficult area to quantify in food science. The next sub-section provides some context to this area.

2.5 Food Texture

Food texture is a collection of characteristics used to describe how a food feels during mastication. There is a plethora of words used across the literature where textural terms are used to describe the sensory experience and characteristics of food. Textural profiling is used to quantify the physical characteristics of food which relate to sensory attributes.

2.5.1 Definition

A definition of texture agreed upon by a number of researchers states "texture is the sensory and functional manifestation of the structural, mechanical and surface properties of foods detected through the senses of vision, hearing, touch and kinesthetics". From this definition the following important concepts are conveyed (Szczesniak, 2002).

1. Texture is a sensory property. Instruments that measure texture only detect and quantify certain physical parameters which are then interpreted in terms of sensory perception.
2. Texture is a multi-parameter attribute, and cannot be described by a single word; it is a collection of characteristics.
3. Texture is derived from the structure of the food, molecular, microscopic or macroscopic.
4. Texture is detected by several senses, where touch and pressure are deemed to be most important.

2.5.2 Texture Profiling

Because texture is a multi-parameter attribute, it is logical to try and introduce some order and to classify the terms into categories. This was first attempted by Szczesniak (1963) for solids and semi-solids (Table 2-5 with definitions in Table 2-6). This led to a profiling method for texture description from sensory and mechanical measurements (Bourne, 1978; Szczesniak et al., 1963). The mechanical method of texture profiling (Figure 2-11) involves compressing and decompressing the food twice between two plates to obtain a force deformation curve. The textural terms in Table 2-5 and Table 2-6 correlate to different aspects of the force deformation curve.

Table 2-5: Classification of textural characteristics (from Szczesniak, 2002))

Mechanical characteristics		
Primary parameters	Secondary parameters	Popular Terms
Hardness		Soft → Firm → Hard
Cohesiveness	Brittleness	Crumbly → Crunchy → Brittle
	Chewiness	Tender → Chewy → Tough
	Gumminess	Short → Mealy → Pasty → Gummy
Viscosity		Thin → Viscous
Springiness		Plastic → Elastic
Adhesiveness		Sticky → Tacky → Gooey
Geometrical Characteristics		
Class		Examples
Particle size and shape		Gritty, Grainy, Course etc
Particle shape and orientation		Fibrous, Cellular, crystalline etc
Other characteristics		
Primary parameters	Secondary parameters	Popular Terms
Moisture content		Dry → Moist → Wet → Watery
Fat content	Oiliness	Oily
	Greasiness	Greasy

Table 2-6: Definitions of mechanical parameters of texture (from Szczesniak, 2002).

	Physical	Sensory
Primary Properties		
Hardness	Force necessary to obtain deformation	Force required to compress a substance between the molar teeth
Cohesiveness	Extent to which a material can be deformed before it ruptures	Degree to which a substance is compressed between the teeth before it breaks
Viscosity	Rate of flow per unit force	Force required to draw a liquid from a spoon over the tongue
Springiness	Rate at which a deformed material goes back to its undeformed condition after the deforming force is removed	Degree to which a product returns to its original shape once it has been compressed between the teeth
Adhesiveness	Work necessary to overcome the attractive forces between the surface of the food and the surface of the other material with which the food comes in contact	Force required to remove the material that adheres to the mouth during the normal eating process
Secondary Properties		
Fracturability	Force with which a material fractures: a product of high degree of hardness and low degree of cohesiveness	Force with which a sample crumbles, cracks or shatters
Chewiness	Energy required to masticate a solid food to a state ready for swallowing: a product of hardness, cohesiveness and springiness	Length of time (in sec) required to masticate the sample, at a constant rate of force application, to reduce it to a consistency suitable for swallowing.
Gumminess	Energy required to disintegrate a semi-solid food to a state ready for swallowing: a product of a low degree of hardness and a high degree of cohesiveness	Denseness that persists throughout mastication; energy required to disintegrate a semi-solid food to a state ready for swallowing.

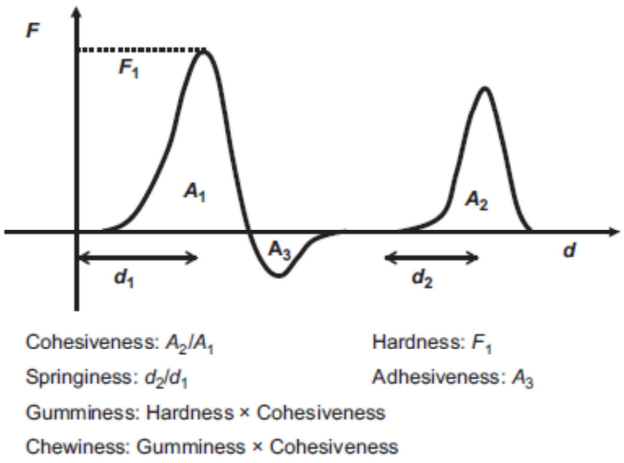

Figure 2-11: Force-displacement curve obtained from a double compression test using the texture profile analysis approach (from Chen, 2009).

The downside with the (two-bite) double compression test for texture profiling is that it only provides information for the initial properties of the food, not the changes that occur during mastication. Furthermore, food is rarely isotropic and so the force deformation curve can vary considerably depending on the orientation of a food sample, particularly for fibrous foods such as meat where the properties differ with fibre orientation.

A relatively new method of quantifying the dynamic texture perception experienced during mastication is called the Temporal Dominance of Sensation (TDS) (Pineau et al., 2003). In TDS the order of dominant textural sensations experienced during mastication are recorded. A subject chews a food sample and identifies the sensation/attribute they perceive to be dominant; a new dominant attribute is picked when a change in dominant sensation is perceived (Lenfant et al., 2009, Pineau et al., 2009). The intensity of the attribute can also be recorded by the subject depending on the experimental protocol being used. When this data for several subjects is combined a TDS curve is produced (Figure 2-12).

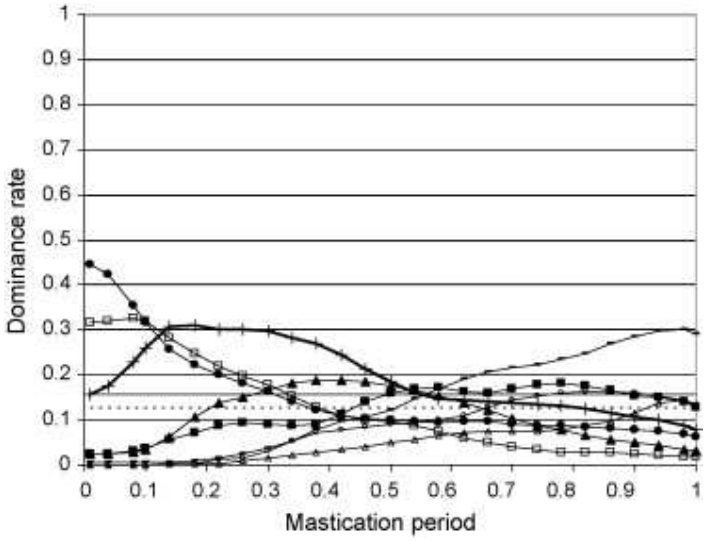

Figure 2-12: Average sequence of texture sensations over the mastication period (▲ brittleness, + crispness, □ crackliness, ▵ dryness, ○ grittiness, ● hardness, ■ lightness, - stickiness). Two horizontal lines account for chance limit (- - -) and significance limit (—), from Lenfant et al. (2009).

The dominance rate is the fraction of times a sensation is cited as dominant over all the experimental runs (Ng et al., 2012). Thus, the sum of the rates for all attributes equals one. The higher the dominance rate is the more there is a consensus between subjects Pineau et al. (2009). Because the mastication period varies significantly between subjects, it is usually normalised as shown in Figure 2-12. An advantage of TDS is that subjects do not require a lot of training before participating in a trial.

2.6 The Bolus

Mastication transforms food into a bolus that is lubricated, deformable, and plastic and most importantly cohesive (Woda et al. 2006a; Woda et al. 2006b & Prinz and Lucas 1997). This is required to prevent aspiration of the food and to ensure a safe passage down the oesophagus and into the stomach (Prinz and Lucas 1997 & Woda et al., 2006a). Swallowing is triggered when some threshold is reached which depends on the aforementioned properties of the bolus.

It is interesting to note that despite the large variation in physiological and anatomical differences among individuals, the particle size distribution (Peyron et al., 2004; Jalabert-Malbos et al. 2007) and moisture content (Flynn, 2012) of food boluses are similar between individuals and are largely dependent on food type. This suggests individuals adjust their chewing behaviour to achieve a food dependant criteria/threshold for swallowing. For many types of food the particle size is an important factor in the bolus reaching the swallow

threshold. Studies on the particle size distribution have been the most common method to analyse the food bolus even though it is accepted that other rheological (and more broadly textural) parameters are also important, but have not been measured.

While there are many technical difficulties to overcome, Peyron et al. (2006) & Nagatomi et al. (2008) have made some attempts to measure the rheological properties of the food bolus. The following sections discuss the particle size and rheological property measurements of these researchers. The discussion then turns to a mathematical model that predicts the point of swallowing.

2.6.1 Particle Size

Many studies have measured the PSD of the bolus at the swallow point (Lucas and Luke 1983a, Olthoff et al. 1984, van der Bilt et al. 1987, Hoebler et al. 2000, Peyron et al. 2004, Jalabert-Malbos et al. 2007) and throughout mastication (Flynn, 2012). Studies carried out by Peyron et al. (2004) and Jalabert-Malbos et al. (2007) on young healthy subjects have shown that the particle size distribution in ready-to-swallow food boluses is significantly different from one food to another, but is similar for a given food across all subjects. These end point similarities are contrasted by high variability in the intermediate measurements of chewing strokes, the amplitude of mandibular movements and the degree of EMG activity during each cycle (Woda et al., 2006[a]). The fact that masticatory parameters vary so much yet individuals produce boluses with similar particle sizes suggests food is chewed to reach a common end-point, a safe-to-swallow bolus. People have physiological and anatomical differences and so employ different chewing strategies to produce a bolus that is safe-to-swallow.

The difference in the particle size threshold in boluses between different foods suggests that the particle properties in conjunction with size influence bolus swallowability. Chen et al. (2013) examined the relationship between the food hardness, measured with a texture analyser, and the mean particle size in the bolus at swallow point for several test foods.

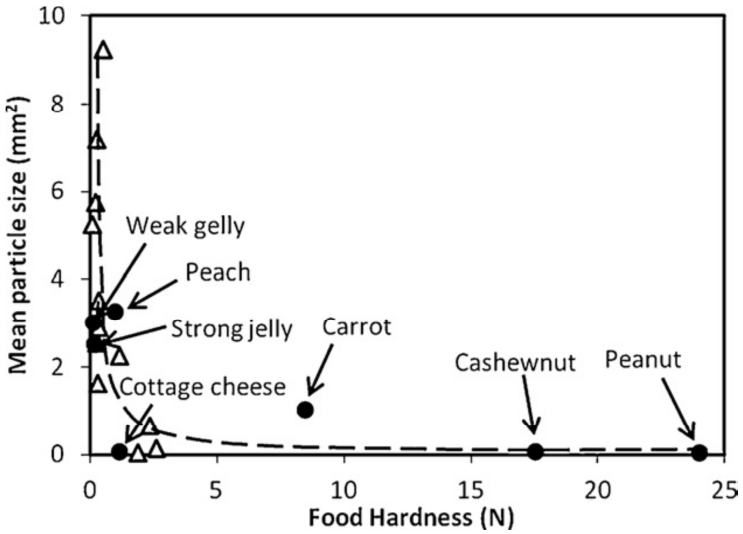

Figure 2-13: Relationship between the mean particle size of food boluses and the measured food hardness for 19 different types of food (from Chen et al., 2013). The correlation between mean particle size and hardness fits a power law relationship.

The results indicate that all particles beyond some threshold hardness, somewhere around 2 N, must be reduced to very small sizes. If particles are soft, e.g jelly and Peach, they can deform under the forces applied during swallowing and so larger particles will be permitted in the bolus. There is a similar relationship between the inverse fragmentation index (see §2.4.2) and bolus d_{50} as shown in Figure 2-14 below.

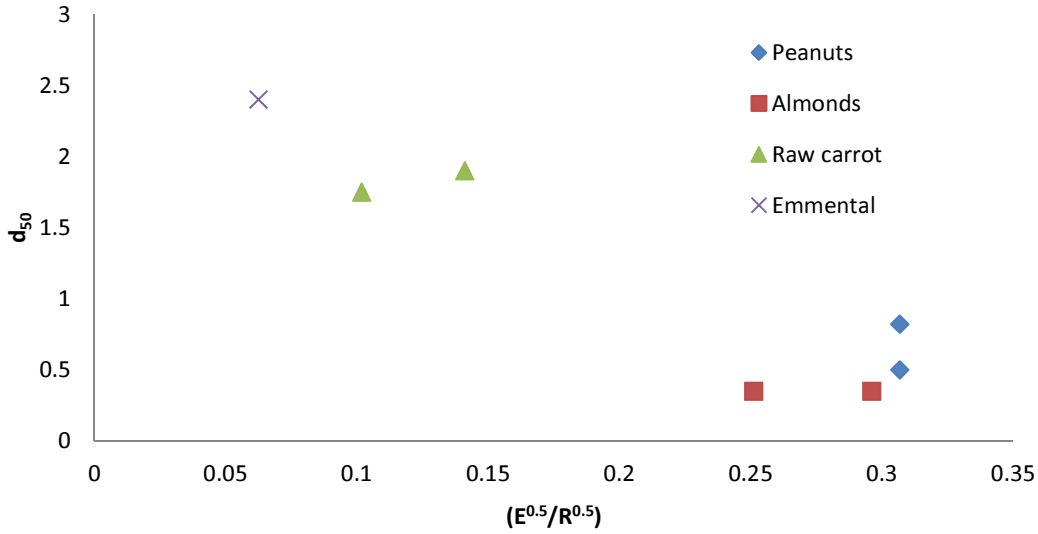

Figure 2-14: Relationship between the d_{50} in expectorated boluses and the inverse of the fragmentation index for peanuts, raw carrot and cheese (data adapted from Lucas et al. (2002), Peyron et al. (2004) and Jalabert-Malbos et al. (2007).

Emmental is a medium hard cheese and of the foods shown has the largest particles in the bolus. Larger particles of carrot are swallowed compared to nuts despite it being unlikely that they can yield during oral manipulation and swallowing. The difference in bolus particle size could be explained by the foods breakage function (see Figure 2-9). Nuts produce smaller particles when they are occluded, thus in reaching the required threshold for lubrication or non-adhesion the PSD in the bolus will be lower compared to foods producing fewer particles during occlusion. Furthermore, the surface properties and shape of the particles could influence the acceptable size in the bolus.

The safe-to-swallow bolus must be cohesive, lubricated and deformable. Particle size alone is not a criterion, but size reduction relative to the particle properties along with saliva addition, mixing and kneading are the processes through which the criteria are achieved. Eating a biscuit illustrates these processes. Biscuits are brittle, hard and dry and both size reduction and lubrication are important. It may be due to brittleness that the biscuit is easily comminuted into small particles but additional chewing strokes are needed to mix in saliva so that the particles adhere together and become lubricated enough so that a bolus can be formed and swallowed without risk of aspiration. In contrast, an oyster is essentially one large particle which is the size of a bolus, is deformable and well lubricated and apart from the desire to taste the oyster, there is no reason to chew it.

2.6.2 Rheological Properties

Limited research has been carried out on the rheological properties of the bolus. Peyron et al. (2011) and Nagatomi et al. (2008) used Textural Profile Analysis (TPA) to characterise the rheological properties of hardness, adhesiveness, springiness and cohesiveness. Peyron et al. (*ibid.*) studied boluses of breakfast cereal where subjects chewed on the food and expectorated the bolus at different stages of the masticatory sequence. They found that, during the course of mastication, the hardness decreased whilst the cohesiveness, adhesiveness and springiness all increased (Figure 2-15). Hardness and adhesiveness were accentuated best when tested at a 65% deformation. TPA compression tests were performed, either at 20% or 65% deformation, whereas springiness and cohesiveness were more profound at 20% deformation.

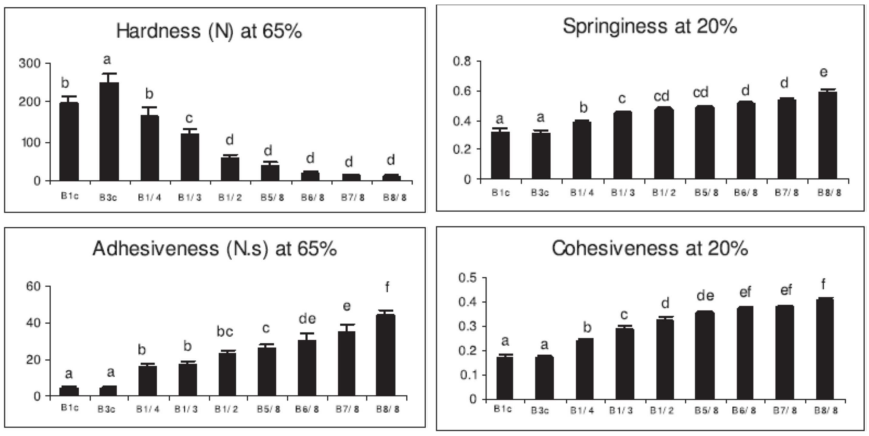

Figure 2-15: Rheological characteristics of the bolus during the course of mastication, measured at either 20% or 65% deformation (from Peyron et al., 2006). The mastication sequence was divided up into nine stages and normalised. Definitions are given in Figure 2-11.

Another area of research interest is to ask subjects to chew beyond the point they felt like swallowing. It would be reasonable to expect that the adhesiveness, springiness and cohesiveness would start to decrease as the bolus moisture content increases. From this it may be possible to identify optimal values of the rheological characteristics that correspond with the bolus at the natural swallow point.

In a similar study, Nagatomi et al. (2008) measured six mechanical properties of the bolus for three foods, rice cracker, cheese and peanuts. They found the minimal cohesiveness (measured by TPA) for swallowing was constant for all three food samples, which suggests that food needs to be chewed to a desirable consistency. The standard deviations for the other five parameters varied considerably which made it difficult to draw reliable conclusions as to how the properties could be related to the swallowable bolus. The mixed results from the study highlight the difficulties in quantifying the rheological and mechanical properties of the bolus.

2.6.3 Bolus Cohesion – A Mathematical Model

Prinz and Lucas (1997) also postulated the point of swallowing occurred when bolus reached its most cohesive point. To illustrate this, they developed a mathematical model to predict the point of swallowing for two foods (carrot and Brazil nut). Their model incorporated comminution and lubrication. The food particles and the bolus were both assumed to be spherical. After breakage, particles are coated in oral fluid and then either adhere to the walls of the oral cavity or cohere together. Given that these forces are in opposite directions within the oral cavity, the net cohesion is the difference between these two forces, $F_C = F_V - F_A$, where

F_V is the viscous force that must be overcome to shear a bolus of cohered particles, and F_A is the adhesion force due to surface tension sticking particles to the wall of the oral cavity (Eq. 2-1). During mastication the food particles are pressed against the hard palate to pack them into a bolus and the oral fluid fills the void spaces which increases the viscous cohesion between the particles. The force that holds the bolus together was modelled using an equation developed by Cottrell (1964) for viscous cohesion between two parallel planes. If a section was cut through the centre of the bolus, two disc-like surfaces would result. The viscous force required to separate the discs is given by Eq. 2-2 (Prinz and Lucas, *ibid*.).

$$F_A = 4\pi r\gamma \qquad \textbf{Eq. 2-1}$$

$$F_V = 3\pi\eta R^4/64d^2t \qquad \textbf{Eq. 2-2}$$

$$F_C = F_V - F_A \qquad \textbf{Eq. 2-3}$$

The symbol η is the viscosity of the oral fluid, *R* the radius of the bolus of food particles, *r* the radius of food particles, *t* the time span over which the separation of the discs takes place, *d* the average distance between particles, and γ the surface tension of oral fluid. Prinz and Lucas (ibid.) propose that particles will agglomerate when $F_V - F_A > 0$, but that particles will cohere best when $F_V - F_A$ is at a maximum, which they call the optimum swallow point. In order to test their ideas, they generated particle size distributions using the comminution model of Lucas and Luke (1983b) was used to, and developed a two dimensional packing model to simulate the bolus and calculate the viscous force.

Figure 2-16 shows the results of the simulation. The initial negative values for cohesion indicate the food particles fall apart rather than form a bolus. The cohesive force increases and peaks around 20-25 chews, this is the point at which swallowing is thought to occur. This range is in some agreement with data from Lucas and Luke (1986) where the mean number of chewing strokes was 31 (35 subjects) for carrot and 25 (15 subjects) for Brazil nuts. Carrot does not tend to form a very cohesive bolus rather it is a loose aggregation of particles which could possibly be described as a slurry. The model predicts much lower cohesion values for raw carrot which is in agreement with the above observations.

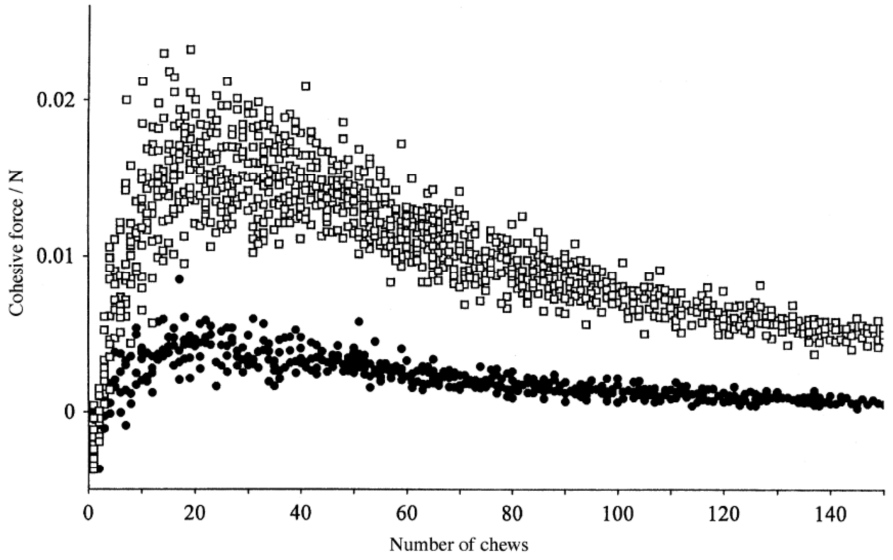

Figure 2-16: The cohesive force plotted against the number of chewing strokes for brazil nuts (top) and raw carrot (from Prinz and Lucas 1997).

The authors sited some shortcomings and simplifications of the cohesion model. The two-dimensional packing algorithm is a simplification of a three dimensional problem. Further the surface properties of the particles are assumed constant as are the properties of the saliva, which may be applicable for carrot and nuts but many foods either become sticky through dissolution and melting in the mouth or by absorption if they are dry foods. The model also does not account for loss of particles or saliva through partial swallowing before the final bolus is formed. In the chewing experiments that this model was compared to, subjects were asked not to swallow but, when mastication occurs in a natural manner, the loss of particles through multiple swallows can occur. A study by Jalabert-Malbos et al. (2007) found that expectorated bolus comprised around 50 per cent of its original mass. Nevertheless, mass must be conserved and so solids loss needs to be apportioned to either the linings of the oral cavity, which are typically recovered as rinsings, or to intermediate swallows, or are an artefact of the methods used to recover the solids; for example, recovery on sieves can lead to undersized solids being washed through the sieves.

While the work of Prinz and Lucas (1997) explores the concept of cohesiveness and suggests that the maximum cohesiveness defines the swallow point, the link to what constitutes a safe-to-swallow bolus has not been made. There are as yet no agreed criteria to define a-safe-to-swallow bolus. Cohesiveness, deformability, plasticity, slipperiness are mentioned by most researchers, but the discussion has remained qualitative.

2.7 Comminution Models

Particle size is an easily measured quantity and it is no surprise that a considerable amount of effort has gone into developing population balance models of mastication. Industrial comminution models have been adapted as analogues to help understand and model the mechanical broken down of food during mastication (Lucas and Luke, 1983a). Epstein (1947), cited by Lucas and Luke (1983a), studied the particle distributions resulting from coal degradation and introduced the idea that the rate of breakdown is determined by two factors; (1), the probability of selection relating to the position of the material within the comminution apparatus; and (2), the degree of fragmentation which describes the particle size distribution of daughter particles after fracture (Lucas and Luke, 1983a). These are termed the selection and breakage function, the development of which is discussed in the next sections first with respect to mastication.

2.7.1 Selection Functions

The selection function defines the chance particles of a given size have of being chewed during a masticatory stroke. It is size dependent because not all particle sizes have an equal chance of being chewed. Experimental determination by Lucas and Luke (1983a) hypothesised a generalised form of selection function then conducted experiments to test their hypothesis. They assumed the percentage of particles in a size fraction declines in a power series with the number of chews. If P_1 is the percent of particles of average size x after C_1 chews and P_2 percent remain after C_2 chews, then P_2 is related to P_1 by

$$P_2 = P_1(1 - S(x))^{C_2 - C_1} \qquad \textbf{Eq. 2-4}$$

and rearranging yields the average selection function,

$$S(x) = 1 - \left(\frac{P_2}{P_1}\right)^{\frac{1}{(c_2 - c_1)}} \qquad \textbf{Eq. 2-5}$$

where x is approximated as the mid-point size of the fraction, three different methods of estimating particle selection were used. By assuming $S(x)$ is constant for a given particle size Eq. 2-5 can be used to calculate selection between any two chew numbers.

The method is amenable to experiment. While the selection value for the largest particle size in a distribution is easily determined, it is more difficult to measure the selection value of a particle within a distribution. The particles of interest need to be labelled in such a way that particles entering into the size range can be distinguished from the original particles. To do this Lucas and Luke (1983a) conducted experiments on carrot using three methods to determine the selection function.

Method (A): The largest size fraction at any time is only subject to selection because no larger size fractions are able to break and produce fragments of this size. So the change in the number of particles within this fraction can be used to calculate a value of S (x).
Method (B): Similar to method A but carried out to measure the selection of sizes more central to the particle distribution. An initial volume of carrot was chewed and then sieved to establish a particle size distribution. A size fraction was then dyed and all the particles were then re-chewed and re-sieved. The stained particles left on the lower boundary sieves were collected and weighed, values of S(x) were determined using Eq. 2-4.
Method (C): Cylinders of carrot with 4-10 mm diameter were produced. The particles were equal in height and diameter. Subjects were given approximately 5 g samples of the different size cylinders. After a number of chews (3-20, depending in particle size) the number of unbroken particles was counted and *S*(x) was calculated using Eq. 2-4.

In all three experiments particle selection depended significantly on particle size. Method B showed the selection values decline for 3.08 and 2.4 mm particles with the number of chewing strokes but as chewing progresses, the proportion of 3.08 and 2.4 mm particles of the total food volume decreases. This trend indicates that particle selection may also depend on particle number. The chance of selecting the remaining particles of this size will decrease because of competition with the increasing population of smaller particles. A multi chew experiment using Eq. 2-4 and Eq. 2-5 works well when calculating the selection chance for the largest particle size in a mixture or if the particles are all initially the same size, because the initial number of particles is known and can only decrease. However, it is not possible to perform a multiple chew experiment and back calculate a selection value for any other particle size because, even if the particles are labelled according to initial size, the equations do not account for the flux of particles entering and leaving the size range of interest.

Van der Glas et al. (1987) also measured the particle size distribution resulting from various numbers of chews. A mixture of particle sizes was composed so that the weight distribution of

the particles matched the average distribution attained in the mouth during an early phase of the chewing (mixture A) and a late phase of chewing (mixture B). The particles were cubes or half cubes and coloured according to their size. This allowed for the origin of particle fragments to be determined and whether particles had been damaged or broken. Subjects chewed either five or ten times. The experiments were performed with mixtures of particles and the selection chance of particles in the different size classes were calculated using Eq. 2-5. From the calculated selection chances of the different sizes a size dependent power law selection function, Eq. 2-6, was fitted

$$S(x) = v.(x)^w \; where \; [0 \leq S(x) \leq 1] \qquad \textbf{Eq. 2-6}$$

where $S(x)$ is the chance that particle has of being selected, *v* represents the selection chance of a particle of unit size (for example 1 cm or 1 mm) and exponent *w* is a subject dependent constant, which varied between 1.6 and 2.6 . For any subject, *w* is constant for the duration of chewing and is independent of the phase of chewing (van der Bilt et al., 1987). Chewing experiments with different mouthfuls of peanuts showed also that exponent *w* is independent of the volume of food offered (Lucas & Luke, 1984). Thus different values of *v* can account for different volumes of food (Voon et al*.,* 1996). In chewing particle mixtures, *v* was found to be larger in the late phase of chewing in two of the four subjects (van der Glas et al., 1987). Although the selection defined above has been used in mastication studies, it makes sense to define a dimensionless selection function:

$$S\left(\frac{x}{x_o}\right) = v.\left(\frac{x}{x_o}\right)^w \; where \; \left[0 \leq S\left(\frac{x}{x_o}\right) \leq 1\right] \qquad \textbf{Eq. 2-7}$$

where x_o is the upper limit of particle size and *x* is the particle size of interest. Writing the equation in this way also limits $v \leq 1$ and means *w* can take any value. Otherwise for a given value of *v*, only a limited range of values for *w* can be used because the selection chance has to be ≤ 1. The experimentally validated selection functions given in Eq. 2-5 and Eq. 2-6 (Lucas and Luke 1983a; Van der Glas et al, 1987) have been used in a number of simulation studies on chewing (Lucas and Luke, 1983b; Voon et al*.,* 1986; van der Bilt et al*,* 1987 and van der Bilt et al*.,* 1992) . These simulations are discussed in §2.7.3.

Selection based on Particle Number and Size

Earlier it was noted that the trend in the results of Lucas and Luke (1983a) may indicate that selection is based on particle size and number. This concept was explored fully by van der Glas et al. (1992). His model considers the positions between the post-canine teeth to be breakage sites and the particles occupying these sites restrict other particles from selection. The number of breakage sites is limited and therefore the selection chance depends on the number of particles present.

Van de Glas et al. (1992) derived a mathematical description of the selection chance as a function of particle number, breakage sites and the particle affinity of the oral system. Three models were proposed; (i), for particles of a single size; (ii) a one-way competition model whereby larger particles inhibit the selection chance of smaller particles; and (iii), a two-way competition where particles of all sizes have the chance to occupy the breakage sites. The following subsections summarise these three models. The advantage these models have over Eq. 2-6 is that they account for the number of particles present. Predicting selection chance from a power law relationship fitted from experimental data means it will only be applicable to bolus conditions similar to the experimental conditions. When particle number as well as size is factored in, the selection function has the potential to give meaningful predictions over a much wider range of initial bolus conditions.

(i) Particles of a Single Size

If n particles of size X are in the mouth, the number of selected particles per chew depends on X and n, this is denoted as $n_s(X, n)$. The number of breakage sites between the teeth is limited and given by $n_b(X)$ [where $n_b(X) \geq 1$]. The number of breakage sites is size dependent where smaller particles can fit more of their number into the occlusal zone. All particles are assumed to have the opportunity to occupy breakage sites. The total occupied fraction of breakage sites after i particles have tried to occupy these sites is denoted as $O(X, i)$, being equal to $n_s(X, i)/n_b(X)$. The unoccupied fraction of breakage sites left is denoted as $U(X, i)$, being equal to $[1 - O(X, i)]^i$. The selection chance of this single particle is $S_i(X, i)$. When n particles are present, the first particle to move between the post canine teeth has an opportunity to occupy a breakage site while all breakage sites are available [$U(X, 0) = 1$]. The average chance of the first particle of being selected is denoted as $S_1(X, 1)$ ($0 < S_1(X, 1) < 1$). The first particle will occupy a fraction of the breakage sites given by:

$$O_1(X, 1) = S_1(X, 1)/n_b(X) \qquad \textbf{Eq. 2-8}$$

$O_1(X, 1)$ is dependent on particle manipulation of the tongue and individual variation in dentition. $O_1(X, 1)$ is called the particle affinity and is the selection chance of a single particle of size X per breakage site. It is assumed that particle manipulation is on average the same for all particles. The number of selected particles, $n_s(X,n)$, out of n particles offered is given by:

$$n_s(X, n) = n_b(X).[1 - (1 - O_1(X, 1))^n] \quad \textbf{Eq. 2-9}$$

Intuitively the average selection chance of a particle in a chew when n particles are present is:

$$S(X, n) = n_s(X, n)/n \quad \textbf{Eq. 2-10}$$

Thus the selection chance of an individual particle when n particles are present is

$$S(X.n) = n_b/n\,.[1 - (1 - O_1(X, 1))^n)] \quad \textbf{Eq. 2-11}$$

Saturation of the sites is mathematically achieved by defining a fraction that remains unoccupied, arbitrarily defined as 1/e (where e is the base of the natural logarithm). The choice of e is tidy mathematically, but otherwise arbitrary. Setting this to equal the unoccupied fraction, $U(X,n)=[1-O(X,1)]^n$ where the power term defines a critical particle number, $n_c(X)$, gives.

$$[1 - O_1(X, 1)]^{n_c(X)} = 1\ /e \quad \textbf{Eq. 2-12}$$

$$n_c(X) = -1/ln[1 - O_1(X, 1)] \quad \textbf{Eq. 2-13}$$

Experiments were carried out to validate Experiments were carried out to validate the theoretical relationship that had been derived. Four subjects participated in a series of one chew experiments using particles of Optosil. Eight different particle sizes (XE) were used and the number of particles in a mouthful ranged from 1-16 for the largest particle size and 64 – 2048 for the smallest particle size. Table 2-7 summarises the experimental details.

Table 2-7: Particle sizes and number of particles used in the one-chew experiments

X_E (mm)	n (range)
1.2	64 – 2048
1.7	32 – 1024
2.4	16 – 512
3.4	8 - 512
4.8	4 – 128
6.8	2 – 48
9.6	1 – 16

Figure 2-17 shows the results for three of the particle sizes, the largest, and smallest and one size in-between. The number of selected particles, normalised with respect to the number of breakage sites is plotted against the number of particles offered. The data fitted the theoretical function, Eq. 2-9, allowing the parameters $O_1(X,1)$, and $n_b(X)$ to be determined.

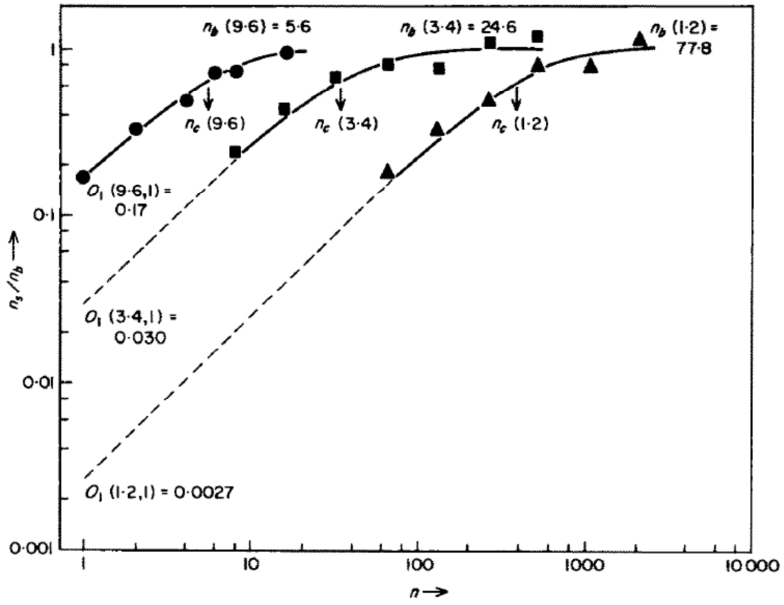

Figure 2-17: Ratio of n_s/n_b as a function of n for a single chew. The data is fitted to Eq. 2-9 (from van der Glas et al., 1992). Where O_1 is the particle affinity, n_s is the number of selected particles, n_b is the number of breakage sites and n is the number of particles offered.

The particle affinity increased with increasing particle size, the number of breakage sites decreased as the particle size increased. This can be explained by larger particles occupying more of the tooth area; therefore fewer particles can fit on the surface of the teeth (van der Bilt et al, 1992). Particle affinity depends on many anatomical and physiological factors; the number of breakage sites is a tooth-dependent variable. The model for single particle size allows the subject dependent parameters $O_1(X,1)$ and $n_b(X)$ to be determined by curve fitting with experimental data.

(ii) One-Way Competition

The basis for the one-way competition is that large particles will hamper the selection of smaller particles but the reverse does not occur. In this construct there are k size classes present, where X_1 is the largest and X_k the smallest, each with particle numbers $n_{X_1}, n_{X_2} \ldots, n_{X_k}$, and the sum total particle number being n_T. During a chewing stroke when the jaw is closing, the largest particles, X_1, are engaged first. The smaller particles are free to move but do not compete with the largest particles for the available breakage sites. As the jaw continues to close smaller particles may become selected onto the remaining available sites according to the same one-way model where the largest remaining particles have preference. The breakage sites of the smaller particles are assumed to be dispersed over the post canine teeth. Particles of size X_i will occupy a fraction O_{Xi} of their possible breakage sites $n_b(X_i)$. This means they exclude smaller particles of size X_j occupying the same fraction of their possible breakage, $n_b(X_j)$, where $X_i > X_j$ for $i > j$ in the one-way model (van der Glas et al., 1992). Cumulatively, the sum of all occupied fractions cannot exceed 1, so therefore, as larger particles have first preference to occupying sites, the fraction of sites available to smaller particles becomes increasingly limited. Nevertheless, as mastication proceeds, the number of larger particles decreases and so more sites become available to smaller particles. The theory is developed by van der Glas (1992), with the result given in Eq. 2-14 below for the number of selected particles of size X_i from a population containing n_{X_i} of that size.

$$n_s\left(X_i, n_{X_i}\right) = \left[n_b(X_i).\prod_{p=0}^{i-1} U\left(X_p, n_{X_p}\right)\right].\left[1-\left(1-O_1(X_i,1)\right)^{n_{X_i}}\right] \qquad \textbf{Eq. 2-14}$$

The similarity to Eq. 2-9 can be seen with the additional term which accounts for the already occupied sites of all particles larger than size X_i, which reduce the number able to be selected. When no particles are present, all the breakage sites are available, hence $\left(X_0, n_{X_o}\right) = 1$. For any defined particle size, the possible non-occupancy is calculated in the same way as for the single size model above, $U\left(X_p, n_{X_p}\right) = \left[1 - O_1(X_p, 1)\right]^{n_{X_p}}$. The saturation limit of breakage sites can be defined in the same manner as Eq. 2-12 above to define a critical number of particles, n_{c,X_i}.

(iii) Two-Way Competition

The two-way competition model assumes smaller particles may be locked between the antagonistic teeth by the tongue and cheeks limiting the freedom of displacement and thus

occupying the breakage sites of larger particles. Similarly, the two-way competition model considers *k* particle size classes with the number of particles in each class $n_{X_1}, n_{X_2} \ldots, n_{X_k}$, and the sum total number of particles is n_T. Like the on-way model when a particle X_i occupies a fraction of its breakage sites $n_b(X_i)$ it also occupies an equal fraction of the breakage sites $n_b(X_j)$ of another particle size X_j. However, unlike the one-way model, all the breakage sites, $n_b(X_i)$, are initially available for any particle size X_i.

The full derivation is shown in Appendix A; the final equation is given below. The number of selected particles, n_s, of size X_i in the mixture containing n_{X_i} particles of this size is given by

$$n_s(X_i, n_{X_i}) = n_b(X_i).\left[n_{X_i}.\ln(1 - O_1(X_i, 1))\Big/\sum_{j=1}^{k}(n_{X_j}.\ln(1 - O_1(X_j, 1)))\right] .\left[1 - \prod_{j=1}^{k}(1 - O_1(X_j, 1))^{n_{X_j}}\right] \quad \textbf{Eq. 2-15}$$

where $n_b(X_i)$ is the number of possible breakage sites if the system only contained particle of this size. The term enclosed in the middle bracket is the fraction of the possible breakage sites able to be occupied by particles of size X_i in the two-way competition construct, where the counter *k* is the number of size classes. It is noted that the natural logarithm terms are the inverse of the critical particle numbers, $1/n_{c,X_i}$ and $1/n_{c,X_j}$. The last term is the total fraction of breakage sites occupied by the particle mixture which, for a normal mouthful of food, will equal 1 as there will be enough food particles to saturate the occlusal zone. Again, the saturation limit of breakage sites can be defined in the same manner as Eq. 2-12 above to define a critical number of particles, n_{c,X_i}.

Validation of Selection based on Particle Number

Van der Glas et al. (1992) used previous data (Lucas and Luke, 1983a; van der Glas et al., 1987) to investigate the validity of the models, starting with the established power law function used to describe selection

$$S(x) = v.(x)^w \; where \; [0 \le S(x) \le 1] \quad \textbf{Eq. 2-6}$$

The exponent *w* was found to be constant for each subject and does not vary with food volume. Van der Glas et al. (1992) concluded that *w* does not depend on the number of particles of different sizes in a mixture, rather just on the size. Therefore the ratio of the selection chances for two arbitrary particle sizes X_p and X_r can be written

$$S(X_p)/S(X_r) = (X_p/X_r)^w \quad \textbf{Eq. 2-16}$$

The different selection models for particle mixtures can then be tested by calculating the ratio between selection chances. However the ratio for the one-way competition model is found to depend on the particle numbers and thus the one-way completion model is incompatible with experimental evidence. The ratio for selection chances between two particle sizes for the two-way competition model does not depend on the particle numbers in the mixture but rather the ratio of breakage sites and the inverted ratio of critical particle number of the two sizes (van der Glas et al. 1992). This is obtained by assuming the last term of Eq. 2-15 is unity, then taking the ratio between the two size classes *p* and *r*, reduces Eq. 2-15 to

$$S(X_p)/S(X_r) = \left[n_b(X_p)/n_b(X_r)\right].\left[n_c(X_r)/n_c(X_p)\right] \quad \textbf{Eq. 2-17}$$

Partitioning Eq. 2-16 allows the two parts of Eq. 2-17 to be described

$$n_b(X_p)/n_b(X_r) = (X_p/X_r)^g \quad \textbf{Eq. 2-18}$$

$$n_c(X_p)/n_c(X_r) = (X_p/X_r)^h \quad \textbf{Eq. 2-19}$$

Thus

$$w = g - h \quad \textbf{Eq. 2-20}$$

The two-way competition model predicts the exponent *w* in equation Eq. 2-6 is equal to the difference in the exponents between the number of breakage sites and the critical particle number. Values of $n_b(X)$ and $n_c(X)$ from the one chew experiments were used with equation Eq. 2-17, a value for *w* of 1.3 was predicted using Eq. 2-19 and data from the one chew experiments. This value compares favourably with the value of 1.6 obtained from experiments using labelled particles (van der Glas et al. 1987). The two-way competition model enables selection of particles to be calculated during a normal chewing sequence using variables related to particle affinity and the number of breakage sites obtained from one chew

experiments with various particle sizes. Testing the two-way model, which considers competition between large and small particles, with data obtained from a one chew experiment using a single particle size seems counter intuitive, because it relies on size distributions. The usefulness and relevance of such an experimental approach is questionable and indeed van der Glas et al. (1992) recommend testing Eq. 2-9 by carrying out one-chew experiments with controlled particle mixtures of initial known number and size. Furthermore, the data was obtained in experiments where subjects were instructed not to swallow and the number of chewing strokes used was sometimes extended beyond what would be considered natural.

Selection based on a Threshold

The chance of selection becomes increasingly tiny for small particles. Even if there are only a few large particles amidst an otherwise small particle size distribution, the selection chance for a small particle is considerably lower than for selection for a large particle. This is somewhat intuitive and demonstrated by previous experiments where Eq. 2-6 was validated (Lucas and Luke, 1983b; van der Bilt et al., 1986; van der Glas *et* al., 1987). In experiments with dyed carrot particles Lucas and Luke (1983a) found that small particles were not always selected and thus not broken when larger particles are present. Voon et al. (1986) suggested a floating threshold whereby only the top specified proportion of particles can be selected. However, this threshold could be very difficult to detect because the threshold is not tied to a particular size.

Discussion of Models

The chance a particle has of being selected depends primarily on particle size but is influenced also by numerous factors including the total volume of the mouthful, the relative sizes of other particles in the mouth and the number of particles present. Variability in selection chances among people chewing the same food will arise due to differences in oral physiology.

Equation 2-6 is not mechanistic; the selection function is fitted to a power law function and parameters are best fit to data from chewing experiments. However, it has proved adequate in describing mastication in chewing simulations. Mechanistic selection equations have been developed based on the number of breakage sites available, the size of the particles and the order in which they present themselves to the occlusal plane (van der Glas et al., 1992). Selection chance decreases as more of the breakage sites are occupied until all sites are saturated.

The selection model for a single particle size was validated with one-chew experiments. The model describes the selection in terms of the occupied fraction of breakage sites of a single particle (called particle affinity) and the number of breakage sites. The particle affinity depends on physiological factors, including the efficiency of the tongue and cheek to position particles on the occlusal surface for selection. Low affinity values for small particle sizes are attributed to the difficulty in collecting and positioning small particles. The number of breakage sites is a tooth dependent variable and as particle size increases, the number of breakage sites decreases. Larger particles will take up a larger area so less can fit on the occlusal surface of the teeth (van der Glas et al., *ibid*.).

Of these mechanistic models, the two-way competition model is the most appropriate. It would be best tested by performing one-chew experiments with particle mixtures of pre-determined particle sizes and numbers. The downside to the two-way selection model is that it requires many subject dependent constants to be determined. The number of breakage sites and the particle affinity factor need to be determined for each size class of particle before the selection model can be used in a chewing simulation. In contrast the selection function based purely on particle size, requires only two subject dependent constants, *v* and *w*,

To date, the experiments performed to measure the selection chance of particles have used only one food in the mouth at a time; carrots, peanuts or Optosil. If selection was based purely on particle size, then Eq. 2-7 could be used in a simulation where different foods were present in the same mouthful. However if the mouthful contains foods of differing physical properties, it may require different selection functions for the respective foods and consideration of interaction effects.

2.7.2 Breakage Functions

A breakage function is a cumulative distribution function which describes the particle size distribution resulting from the fracture of a single particle (Kelly and Spottiswood, 1990). Breakage functions were first used in industrial comminution processes and have proved useful in chewing simulation studies. Lucas and Luke (1983b) used an empirical power function which fitted their experimental data well although it had no mechanistic basis.

$$B(X, X_o) = (X/X_o)^a \qquad \textbf{Eq. 2-21}$$

Here $B(X, X_0)$ defines the weight or volume fraction of particles of size X_0, which break into particles smaller than size X, where $X \leq X_0$ (Lucas and Luke 1983b; van der Glas et al., 1987; van der Bilt *et* al 1992). Larger values of a correspond to a lower degree of fragmentation. Converting from a cumulative distribution to the fraction within a size class yields

$$B(X_i, X_0) = \left(\frac{X_{i+1}}{X_o}\right)^a - \left(\frac{X_i}{X_o}\right)^a \quad \textbf{Eq. 2-22}$$

where X_{i+1}, is the next largest size class after X_i.

Van der Bilt et al. (1987) used a breakage function described by Austin (1971) which was derived to describe the distribution of particles resulting from a single breakage event.

$$B(X, X_0) = 1 - (1 + r.X/X_0).(1 - X/X_0)^r \quad \textbf{Eq. 2-23}$$

where r is related to the degree of fragmentation; higher values of r result in a higher the degree of fragmentation. The constants in these breakage functions can be determined experimentally. A subject chews once on a particle of known initial size and the resulting distribution of particles is sieved. The cumulative distribution of particles undersize is then plotted against the sieve sizes. The breakage function is then fitted to the data by a least squares method to obtain the value of the constant. Lucas and Luke (1983a) performed this with ten subjects chewing on carrot particles, they obtained values of a between 2.29 and 3.27. Van der Bilt et al. (*ibid*) had subjects chew once on Optosil (a silicone dental material) in their study and found values of r between 0.18 and 0.50.

Lucas and Luke (1983b) used the breakage function Eq. 2-21 to simulate the breakdown of carrot particles during chewing. They found good agreement between the experimentally determined particle size distributions and their simulations. Van der Bilt et al (1987) used a different breakage function (Eq. 2-23) to successfully simulate the particle size distribution of Optosil particles in a bolus; the modelling method used for the simulation is described in §2.7.3.

Applicability of Breakage Functions to Food

These breakage functions do not account for all types of breakdown. The breakage functions Eq. 2-22 and Eq. 2-23 have only been used in chewing simulations for hard and brittle foods.

They may not be suitable foods that are cleaved rather than fractured and do not produce many daughter particles, or for foods that resist fracture and are plastically distorted, or for foods where the breakage function changes during chewing due to softening or melting. It is likely that alternative breakage functions will have to be developed to model the breakdown of foods of this nature including the effect of saliva-food interactions.

2.7.3 Analysing and Simulating the Particle Size Distribution

The result of selection and breakage is an evolving particle size distribution. While a mouthful of particles is a discretised system, mathematically it is convenient to model distributions as continuous functions. The most used function in mastication is the Rosin-Rammler which is discussed below.

Rosin-Rammler Distribution

The Rosin-Rammler distribution function is used to describe the cumulative particle size distribution in the bolus of some foods (Olthoff et al., 1984; van der Bilt et al., 1987).

$$Q_w^-(x) = 1 - 2^{-(-x/x_{50})^b} \qquad \textbf{Eq. 2-24}$$

where $Q_w^-(x)$ is the weight fraction of particles with a size smaller than x, and x_{50} is the aperture of a theoretical sieve through which 50 % of the weight can pass and b indicates the broadness of the distribution ($0 < b < \infty$). Olthoff et al. (1984) found the masticatory performance of individuals could be quantified by expressing x_{50} as a power function of the number of chewing strokes, N, according to Eq. 2-25, where c and d are subject dependent constants that relate to chewing efficiency.

$$X_{50} = c.N^{-d} \qquad \textbf{Eq. 2-25}$$

Figure 2-18 shows the cumulative size distributions for one subject after a various number of chewing strokes. Chewing shifts the Rossin-Rammler curves to the left, but the slopes of the curves remained relatively constant. The shift towards smaller particle sizes was greater for fewer chewing strokes for the peanuts indicating the peanuts are more easily commuted than Optosil (Olthoff et al., 1984).

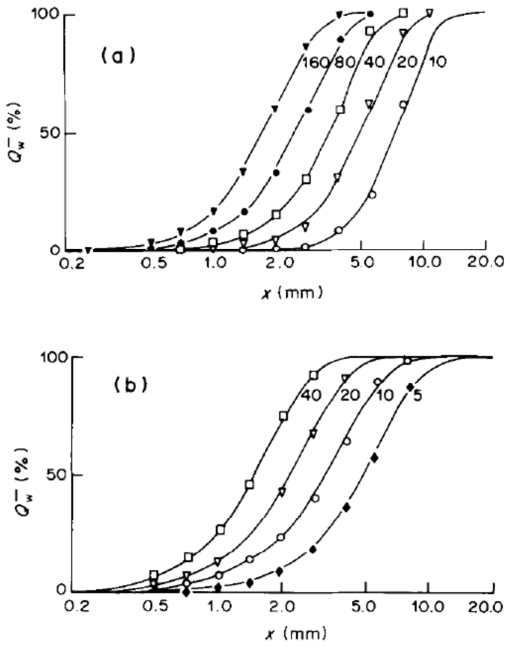

Figure 2-18: Cumulative weight percentage undersize as a function of the logarithm of the sieve aperture for an individual after various numbers of chewing strokes for a) Optosil and b) peanuts. The solid lines are best fits through the data points using Rossin-Ramler distribution (from Olthoff et al., 1984).

A linear relationship is obtained when x_{50} is *plotted* against the number of chewing strokes on a double log plot (Figure 2-19). The values obtained for *c* and *d* are displayed in Table 2-8.

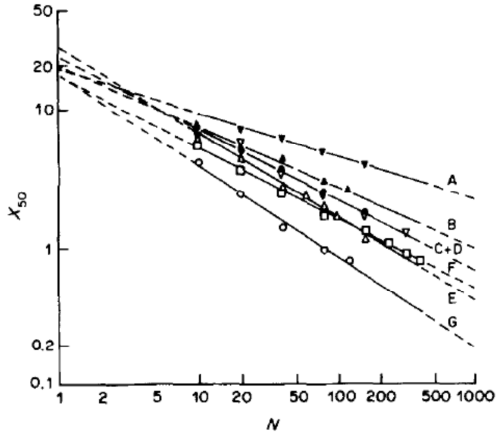

Figure 2-19: X_{50} versus the number of chewing strokes *N* on a log log plot for the seven subjects chewing Optosil, lines are best fit according to Eq. 2-25, (from Olthoff et al., 1984).

Table 2-8: Values and standard deviations of points from Figure 2-19.

	c	*d*	*c*	*d*
	(mm)		(mm)	
Subject	Optosil		Peanuts	
A	19.2(0.7)	0.32(0.03)		
B	21.4(1.3)	0.46(0.05)		
C	24.6(0.4)	0.52(0.01)	16(5)	0.6(0.1)
D	23.6(1.3)	0.52(0.04)		
E	26.1(0.9)	0.61(0.03)	15(5)	0.6(0.1)
F	16.8(0.6)	0.51(0.02)	14(5)	0.6(0.1)
G	17.2(1.2)	0.66(0.06)		

Limitations of the Rossin-Rammler Distribution

The Rossin-Rammler function cannot be used to accurately describe the particle size distributions in the beginning of the chewing process where large particles remain unbroken and the size distribution of particles is not settled. Good fits were obtained with the Optosil and peanuts once the x_{50} value had dropped to around 70 percent of its original value, this equates to about 10 chewing strokes for Optosil and 5 for peanuts (Olthoff et al., 1984). The reproducibility of the Optosil results is good but for the peanuts it is poor, demonstrated by the larger values of the standard deviation for the variables *c* and *d* (Table 2-8).

Although the Rossin-Rammler function is capable of describing the particle size distribution of peanuts and Optosil, it may not be applicable for all foods. Bimodal distributions have been reported by Hoebler et al. (2000) and in the work presented in §6.1 on rice boluses. Hoebler et al. (2000) examined the particle size distribution of food boluses for three starchy foods; bread, spaghetti and tortiglioni. Bread was found to have a bimodal distribution with two peaks at mean diameters of 30 ± 3 and 620 ± 192 μm. The detection of small particles is due, in part to the use of laser light scattering which can measure particle sizes in the micron range. Conventional sieving is restricted to +45 μm and typically in mastication research the smallest size is 125 μm. Thus, bimodal may well be the norm.

This raises the importance of using the method of particle size analysis that suits the food type and also the goals of the experiment. To evaluate masticatory performance focussing on the larger particles is necessary especially considering the particles less than 100 μm only make up around 10 per cent of the bolus volume. If changes to the food microstructure or digestion of starch by amylases on the saliva are to be investigated then particles < 100 μm will be relevant.

The Matrix Model

Because the selection functions may be size dependent, they can be used with matrices to predict the product size distribution. Matrix methods were first developed by Broadbent and Callcot (1956) and Berenbaum (1961) and have been adapted to mastication by van der Bilt et al. (1986). The comminution matrix, *A*, describes the effect of one chewing stroke on a feed distribution of particles, *f*, the product of *A* and *f* yields the product distribution, *p*.

$$p = Af \qquad \textbf{Eq. 2-26}$$

The comminution matrix *A* contains the information on how each size class of particles are distributed after each cycle, thus *A* is expressed in terms of the selection and breakage matrices in the following manner,

$$A = [BS + (I - S)] \qquad \textbf{Eq. 2-27}$$

where *I* is a unit matrix, *B* is the breakage matrix which describes the particle distribution resulting when particles are comminuted. *S* is the selection matrix which describes the selection chance for each size class of particle. The product of *BS* describes how the selected particles are fragmented. I – S is simply the proportion of feed particles not selected for breakage.

The breakage matrix is a lower triangular matrix; each element represents the fraction of fragments originating from the top sieve.

$$B = \begin{bmatrix} b_{1,1} & b_{1,2} = 0 & b_{1,3} = 0 \\ b_{2,1} & b_{2,2} & b_{2,3} = 0 \\ b_{3,1} & b_{3,2} & b_{3,3} = 1 \end{bmatrix}$$

$b_{1,1}$, $b_{1,2}$ and $b_{1,3}$ are the fractions of fragments originating from the particles on the top sieve, $b_{2,1}$ and $b_{2,2}$ are fraction of fragments resulting from the breakage event of particles on the second sieve.

The selection matrix *S* is constructed with the diagonal elements being the chance a particle in each of the size ranges has of being selected in each chewing stroke. In the chewing simulation Eq. 2-6 was used, the variables *v* and *w* were not determined experimentally but determined

using a least squares method by fitting the data for the experimentally determined particle size distribution with the comminution model. The comminution matrix *A* is related to one chewing cycle. However, because of the assumptions made with breakage and selection functions, matrix *A* needs only to be calculated once and then for a given feed distribution the resulting product particle size distribution (product vector) can be determined for a given number of chews, *n*,

$$p = A^n f \qquad \textbf{Eq. 2-28}$$

Van der Bilt et al. (1987) used the matrix model to predict the particle size distribution in a bolus of Optosil particles from a known feed distribution. The elements of the breakage matrix *B* were calculated using Eq. 2-23 with experimentally determined values for *r*, these ranged from 0.18 to 0.50. The selection matrix, *S,* was expressed using the unknown variables *v* and *w*. Using a known feed distribution a theoretical product distribution, *p*, was calculated by assigning values to *v* and *w*. The optimum values of *v* and *w* were found by changing *v* and *w* to minimise the difference between the theoretical and experimentally determined product distribution. The Theoretical product distributions were compared with the experimental data of van der Glas et al. (1985). In this way, good agreement was obtained between the experimental and model product distributions.

These comminution models do not account for loss of particles during chewing. For some foods the bolus comprises only 50% of the original mouthful Jalabert-Malbos et al. (2007). The losses are attributed to either, small intermediate swallows to rid the mouth of excess fluid and fine particles, or particles getting stuck in the teeth and to the inside of the mouth after swallowing. From an engineering perspective, predictive models need to include a mass balance and so must account for particle and moisture losses and multiple swallows.

2.8 Relevance of the Literature to the Objective of this Thesis

The goal of this thesis is to develop a model framework for mastication between the first bite and swallowing, as outlined in chapter 1. The literature presented in this review considers only some of these factors. The purpose of this discussion is to highlight the extent of current research and point out the new knowledge needed to convert a model framework into a working predictive model applicable to a wide range of foods.

Conceptual models of mastication are presented in §2.3 which describe generally the decision steps of whether or not to continue chewing or to prepare the food for swallowing. These models do not define the criteria for these decisions. In §2.3.1 the criteria are suggested to relate to food structure and lubrication where, once the food meets an undefined threshold, it is ready to swallow. However, structure and lubrication are complex terms that are difficult to quantify, especially when we do not yet know what needs to be measured. To provide more context around them, §2.5.2 shows that the discipline is moving towards sensory assessment to define the dominant sensory response as mastication proceeds.

Particle size is the most obvious and easily measured food property during mastication and so it is not surprising that it has received attention. Models of comminution and experimental validations are discussed in §2.7. These have been discussed in some detail because they are quantitative, which is necessary in any model. They divide size reduction into selection and breakage. Selection defines the portion of the particle selected for occlusion. Breakage defines the resulting distribution of daughter particles. It is related to particle properties and is discussed in section §2.4.2, where the ratio of the moduli of toughness to elasticity is the best indicator of the ease of breakage for a range of common foods.

Also clear from the experimental work covered in this literature review, is that variability in bolus properties is greatest between different foods and less so between human subjects. Even so, for a particular food type, the human subject variability is greater for the number of chews than the final PSD at the swallow point. This remarkable fact, which is not highlighted in the literature, suggests that there must be a common set of criteria which define a swallowable bolus. Unveiling this ‘swallowable bolus’ set of criteria is one of the goals of this thesis. This will be done using a chemical engineering tool called a hazard and operability analysis (HAZOP) which has never before been applied to mastication. The basic premise of this approach is that humans, over millions of years, have evolved a mastication-swallowing

mechanism that avoids choking and aspiration, both of which are extremely rare in healthy people. It is also important to only set criteria that are assessable by the sensory system; for this reason, particular attention is paid to the tongue and palate to and how they measure and respond to the changing bolus properties.

Food properties change during mastication. The comminution models examined in §2.7 focus on particle size because this is easily measured. They are not multi-dimensional which they need to be because there are a range of other rate processes occurring. These include moisture absorption, moisture expression, dissolution, melting, softening, and comminution mechanisms other than fracturing which require significantly different breakage functions, e.g., cutting and shear pulverisation. The food circulation or mixing system is also important. These rate processes then change the food properties which, for expediency, need only be those properties that relate directly to the criteria that must be satisfied for swallowing. And, as mentioned, the criteria must relate directly to the sensory cues that measure them.

In this way, this research hopes to shed new light on the criteria for swallowing and on describing how a range of rate processes affect the food properties during mastication. This will be framed in as a model concept rather than a fully working model, simply because foods are extremely complex. Three simplified case studies are explored in the Chapter 6.

CHAPTER 3 QUALITATIVE ANALYSIS OF FOOD BREAKDOWN DURING MASTICATION

3.1 Introduction

Rigorous observation is the foundation on which mechanistic understanding is developed. Numerous researchers have taken this approach. For example, Hutchings and Lillford (1988), Foster et al. (2011), Salles et al. (2007) and Lillford (2011) all found that food breakdown and bolus formation is largely dictated by food structure and mechanical properties. In contrast, differences in human oral physiology have only a limited influence on these processes (Engelen et al., 2005; Chen 2007). Similarly, this section of the thesis provides an observational study of a range of foods but with particular emphasis on the rate processes at play and their extent. These rate processes allow us to take a chemical engineering science view of the food experience during mastication. Naturally, mastication changes the food properties where the dynamic texture profile is affected by shear forces, temperature, interaction with saliva or a combination of these (Bourne, 2004). These eventually produce enough structural breakdown and lubrication so that the food meets the qualitative threshold criteria of Hutchings and Lillford (1988) where a bolus is assembled and swallowed safely.

The natural foods that humans have evolved to eat can be broadly placed in four separate categories according to their structures (Aguilera and Lillford, 2007)); (1) fibrous hierarchical structures (meat) (2) fleshy materials from plants comprised of cells (fruits, vegetables, tubers) (3) embryos from plants that contain a dispersion of starch, protein and lipids (cereal grains, nuts and pulses) (4) milk, a complex oil in water emulsion. Foods of the first three types are examined; solid food is the focus here so liquids are not investigated. Manufactured foods are increasingly common in the modern diet, where a manufactured food is defined as one whose raw materials have extensively altered chemical and physical properties resulting in a significantly different microstructure (common examples include cheeses and baked products). Foods have many different structures and mechanical properties which mean that different rate processes will dominate the breakdown. The purpose of this work is to observe the range of behaviours across a variety of foods and so to understand the rate processes that are important when developing a generalised food breakdown model.

3.2 Methodology

The eight foods in Table 3-1 cover many of the common structures of natural and processed food. They are also expected to cover a wide range of breakdown pathways encountered during mastication. Furthermore, some of the foods were chosen as they have been used in some capacity in mastication studies by other researchers. The focus of this experiment was to observe the rate processes of mastication and bolus formation for a range of foods. Therefore, a single subject study was sufficient because the food properties influence breakdown much more than the inter subject variability owing to physiological differences (Engelen et al., 2005). The subject who participated in this experiment was a 25 year old male with good dentition and oral health.

3.2.1 Sample Preparation

The foods used in this study were sourced from a local supermarket; their composition and nutritional information is given in Appendix B. The beef was prepared by cooking a 250 g rump steak in a non-stick fry pan on a gas element. The pan was lightly sprayed with canola oil and pre-heated on a medium heat for five minutes before adding the steak. It was fried for three minutes on each side and then removed from the pan and rested for five minutes before being cut into cubes of equal size. The chewing experiments with the cooked beef were conducted separately from the other foods so that the meat would be chewed at its usual serving temperature. The other foods were all served at room temperature.

Table 3-1: Size and description of the food samples. (The dimensions are given as width x height x length for the cuboid samples, diameter x height for the cylinders and the peanut is half an ellipsoid).

Food Sample	Volume (cm^3)	Dimensions (cm)	Sample description
Cooked Beef Steak	3.0	1.5 x 2 x 1	Cuboid cut from a cooked steak
Raw carrot	3.7	2.5 x 0.75	A circular slice cut from a carrot
Banana	3.7	2.5 x 0.75	A circular slice cut from a banana
Roasted peanuts	0.85	0.8 x 0.6 x 0.5	Five half peanut pieces
Wine biscuit	4.0	4.5 x 0.5	Half a wine biscuit
White bread	6.3	2.5 x 2.5 x 1	Square piece cut from centre of bread slice
Edam Cheese	3.4	1.5 x 1.5 x 1.5	Cube cut from cheese block
Milk Chocolate	4.0	2 x 2 x 1	Single piece from a king size block

3.2.2 Procedure

To determine the 'natural' swallow point for each food, a sample was chewed in a natural manner until it was completely swallowed. This was repeated four times to get the average number of chews required for each food sample. To show the how the food changes during mastication the bolus was expectorated and photographed at various chew numbers up to and

past the swallow point (Table 3-2). The chewing intervals used for expectoration and photographing the bolus were chosen to be approximately equally spaced with respect to the complete mastication sequence. This enabled the boluses to be observed and compared at the same early, midpoint and later stages of oral processing rather than after an arbitrary number of chews. The order in which the samples were chewed and expectorated was randomised. Between each sample water was sipped and swished around the mouth to remove particles that remained attached to the oral surfaces. A toothpick was used to remove stubborn particles from the teeth when necessary.

Table 3-2: Number of times the food was chewed before being expectorated and photographed, the last two columns are the average normal swallow point and twice this number.

Food	Number of chews					sp	2*sp
Cooked Beef steak	1	3	6	12	15	21	42
Raw carrot	1	3	6	9	15	21	42
Banana	1	3	5	7	9	10	20
Roasted Peanuts	1	3	6	9	15	21	42
Wine Biscuit	1	3	6	9	15	21	42
White Bread	1	3	5	7		9	18
Edam Cheese	1	3	5	7		9	18
Milk Chocolate	1	3	6	9	15	20	40

3.3 Observations

The following sub-sections discuss the solid food structures typical of the natural categories defined by Aguilera and Lillford (2007): fibrous hierarchical structures, fleshy materials from plants, and embryos from plants, as well as the modern category of manufactured foods. Then the observations for the breakdown pathway selected foods in each category are described.

3.3.1 Fibrous Hierarchical Structures

Skeletal muscle tissue has a hierarchical structure (Figure 3-1); muscle fibres are arranged and held in place by a series of connective tissue components that act as wrappings and dividers. The entire muscle is then surrounded by a final layer of heavy connective tissue sheaths called the epimysium, which forms the tendon that connects the muscle to the bone. Each muscle fibre is surrounded by a layer of connective tissue called endomysium. The muscle is divided into a bundle of muscle fibres grouped together by another layer of connective tissue called the perimysium, into primary and secondary bundles. The perimysia surround adjacent fibre bundles and form a continuous network which is easily seen by the naked eye in a piece of meat cut across the grain. Fibre bundles are 1-5 mm across and individual fibres range from 10 – 100 μm in diameter and 1- 40 mm in length sometimes spanning the entire length of the

muscle (Swartz et al, 2009). The muscle fibres are multinucleated, elongated, cylindrical cells and contain approximately 1000 myofibrils. The myofibrils have parallel striations owing to regular repeating sarcomere units, which can be easily recognized under light microscopy. The major structural features affecting the meat are connective tissue, myofibrillar proteins and the cytoskeletal system.

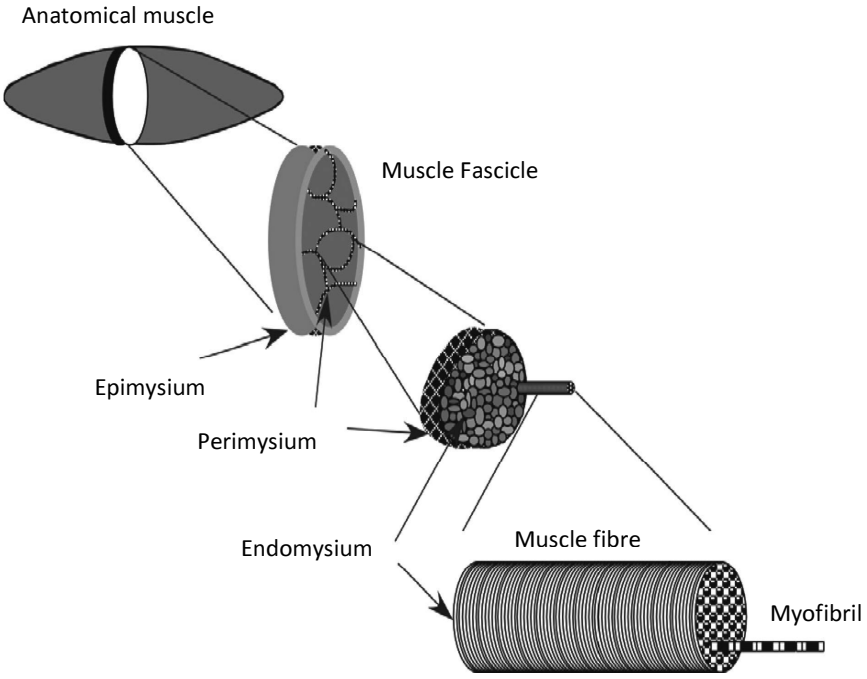

Figure 3-1: Schematic diagram of a skeletal muscle (from Swartz et al., 2009)

Humans nearly always cook meat before consuming it. Cooking meat, apart from reducing the risk of pathogenic microorganisms, is done to improve texture, taste and the energy required to chew and digest it. Raw meat is tougher than cooked meat which requires mechanical strains greater than what many people (elderly and the young) can generate (Vincent and Lillford, 1991). During cooking the muscle fibres shorten, protein denatures, and moisture is lost. Collagen begins to denature at 39°C, and collapses at 65°C, causing the meat to shrink. Other proteins also denature and lose their water-binding capacity which results in moisture loss. These can contribute to a sensation of toughness.

Cooked Rump Steak

For the first chew shown in Figure 3-2, the piece of meat was placed in the occlusal zone and the chewing direction was aligned with the fibres. The first chew disrupts the meat structure

by separating some fibres and connective tissue but the meat is not fragmented into separate pieces or particles. Further disruption occurs at successive chews in a combination of compression and shear, eventually also cutting the meat fibres. Whether disruption or cutting occurs is probably related to the proximity of the upper cusps to the lower cusps. Early in the mastication sequence, these will not approach closely as the meat is a single large particle, but they will later as the meat softens and breaks down. In this case fibres and bundles within close proximity to both cusps, if orientated correctly, are likely to be cut. This is shown by the change in appearance of the bolus where longer fibres are no longer visible and the bolus starts to resemble 'minced meat' (from 15 chews onward). After several chews some of the meat may remain un-chewed as only a portion of the piece is caught between the teeth in each chewing stroke. Behaviour follows that observed by Mioche et al. (2003) where the meat changes from having an initially ordered anisotropic structure to a bolus with separated and shortened fibres, and where connective tissue and saliva all mixed together, resembling minced meat. Even in this state, connective tissue still appears to hold some of the fibre bundles together. Moisture is expelled from the fibrous meat matrix during occlusion and this gives the meat a 'juicy' texture. Longer cooking times result in lower moisture content, e.g., for a 'well done' steak, which results in a more leathery texture. Before the meat is ready to be swallowed excess of moisture may need to be removed. If so, the bolus is held on the tongue, pushed against the palate and the expressed liquid is swallowed. This may occur multiple times before the final bolus is swallowed.

What's happening to the food during mastication?

- Fibres bundles are disrupted, i.e., separated from each other, by compression and shearing.
- Individual fibres and bundles may be cut when they are proximate to both shearing cusps of the teeth.
- The meat begins to resemble minced meat, where individual fibre bundles are difficult to identify. The connective tissue, although damaged, still holds some of the damaged fibres together.
- Moisture is a combination of added saliva and that expelled from meet matrix at occlusion.
- Excess liquid means more than one swallow may be required.

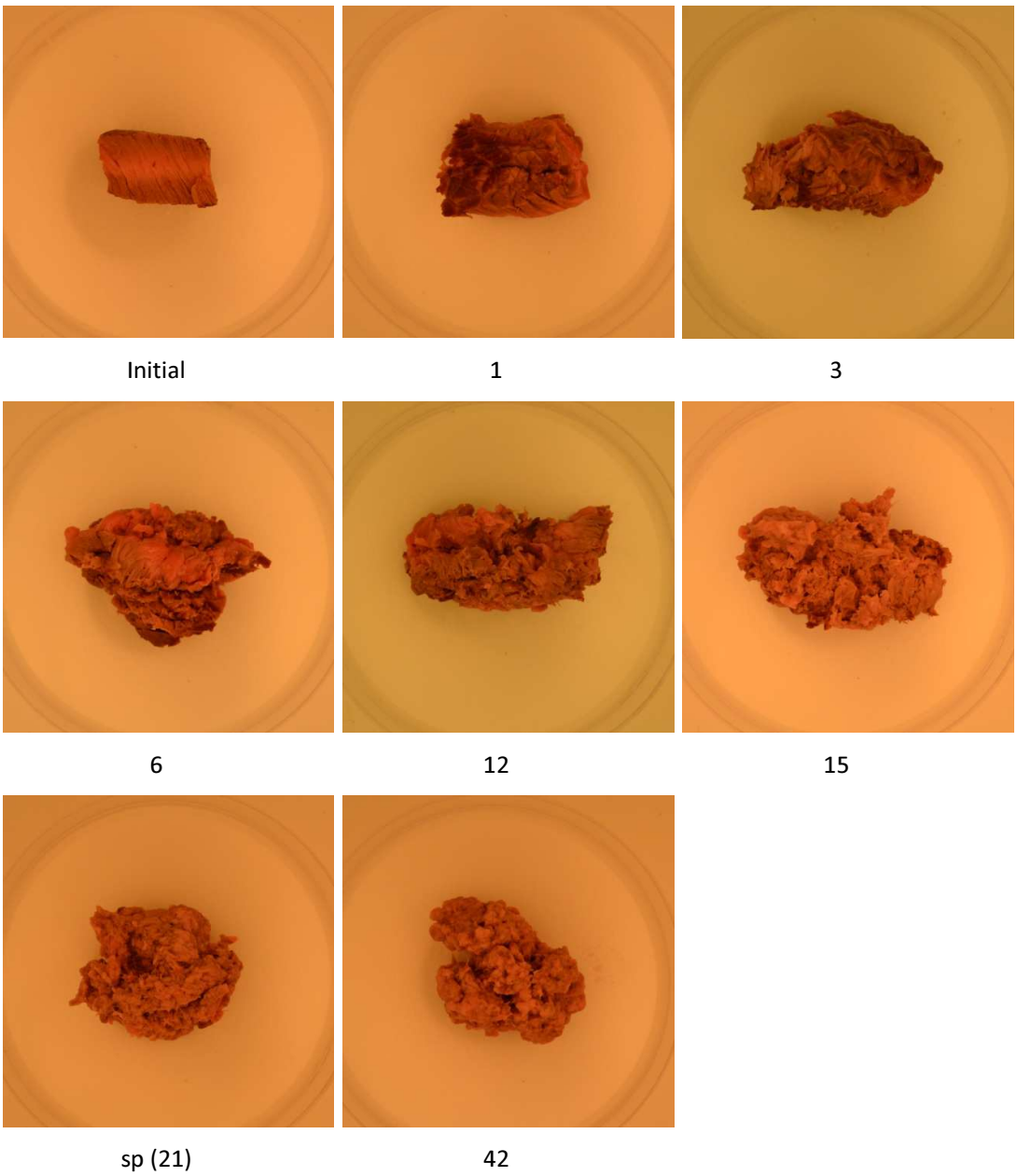

Figure 3-2: Cooked beef steak expectorated after different numbers of chewing strokes up to and past the swallow point (sp).

3.3.2 Fleshy Materials from Plants

Fleshy materials from plants are characterised by fruits and vegetables which are primarily composed of parenchyma cells. Mature cells typically range from 50 – 500 µm across and are polyhedral in shape. Intercellular air space is common, approximately 20-25% in apple, 15% in peach and 1% in the potato. Depending on the rigidity of the cell wall some of this air space

will be removed during occlusion. Most of the cell volume is taken up by a vacuole which contains water and various solutes. The vacuole is enclosed by a semi permeable membrane which maintains the cells turgor by allowing water molecules to pass and restricting the movement of larger molecules. It is the turgor pressure which gives the tissue its textural properties of rigidity and crispness. Fracture occurs through the cells of most raw fruits and vegetables and the watery cell contents are released (Lillford, 2011). The cell wall is composed primarily of cellulose, hemicellulose, pectin, and some other proteins. When cooked, the parenchyma tissue is significantly altered because heat destroys the semi permeable membrane, which greatly reduces the internal pressure of the cells. When cooked vegetables are eaten fracture occurs between softened cell walls and the watery contents are not released. Thus the food goes from being crisp with a sensation of moistness to a soft and tender mouth feel.

The two foods studied here in this category are raw carrot and banana. Carrot is described texturally as crisp and moist but banana is noticeably soft and yields rather than fracturing like crisp fruits and vegetables.

Raw Carrot

From the first bite it is instinctive that significant particle size reduction is required before swallowing can occur. Particles are fragmented by the post canine teeth, producing at least two daughter particles when they are occluded, as seen after the first chew (Figure 3-3). The shape of the teeth and the jaw trajectory during occlusion mean there may be multiple cracks generated in a single particle during occlusion, which will produce several daughter particles. Furthermore, fragments generated in a breakage event may be broken again in the same chewing stroke (Lucas and Luke 1983). Liquid from the vacuole of the carrot cells is released when particles are fragmented which gives the carrot a moist feel. Size reduction is by comminution only; there is no obvious softening of the particles as a result of shear or from the addition of saliva and heat. As a result the mechanical properties of the carrot at the individual particle level appear to be unchanged throughout mastication; i.e. the carrot does not feel any less rigid than the first bite. During mastication most of the carrot seems to be on the dorsal surface of the tongue; particles are not readily left in the buccal pouch or stuck to the oral surfaces during chewing. In the early stages of mastication while the carrot particles are large they do not adhere together. As mastication progresses the median particle size decreases considerably (to 1-2 mm at swallow point Lucas & Luke 1983b), the interstitial space between particles decreases as they pack closer together and is filled by saliva. Thus the

particles adhere together weakly at the swallow point. However, the carrot bolus does not appear as cohesive as other brittle foods like nuts and biscuits, an observation which is supported by the model of the bolus peak cohesive force by Prinz and Lucas (1997). Before the carrot bolus was swallowed an intermediate swallow was required before the final mouth clearance after approximately 15 chews. The solid particles were not ready to be swallowed but a predominantly liquid swallow was required to remove excess liquid. The carrot bolus becomes saturated from the addition of saliva and expelled juice from the carrot cells. The excess liquid was swallowed while the remainder of the bolus was retained on the surface of the tongue and compressed against the palate. In the work of Peyron et al. (2004) partial swallows were significant with as little as 50% of the ingested carrot expectorated when the subjects felt the urge to swallow. In this instance the solid mass swallowed is small when compared to what is retained. At the swallow point very fine particles are not present in high numbers and it is easy on visual inspection of the bolus to distinguish between the solid and liquid phases.

What's happening to the food during mastication?

- Size reduction with every chew stroke and individual particles are easily identified.
- Expression/expulsion of cellular contents during breakage.
- Intermediate swallow of mainly liquid.
- A weakly cohesive bolus is formed.

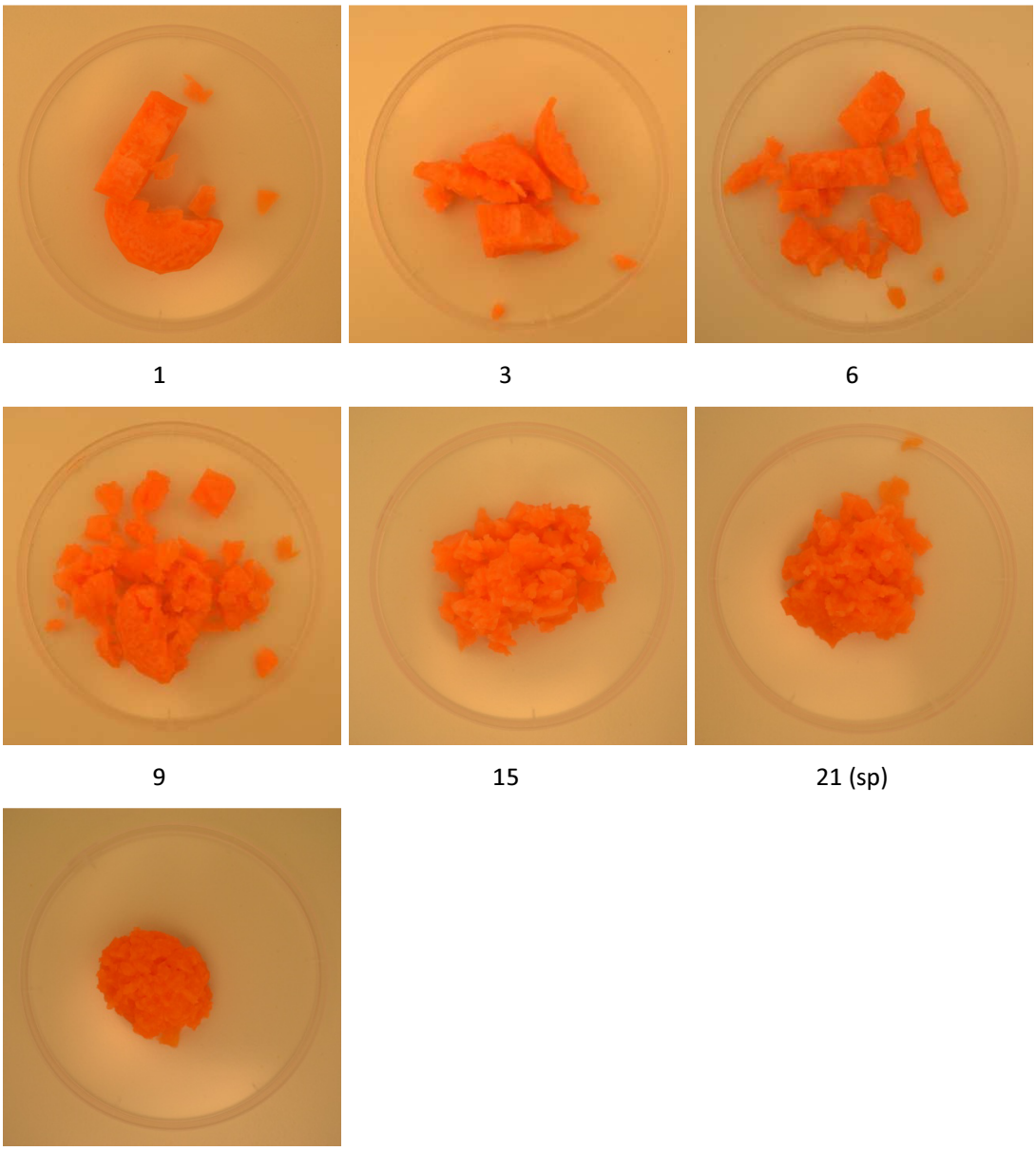

Figure 3-3: A carrot bolus expectorated after various numbers of chewing strokes up to and past the swallow point (sp).

Banana

In the first chew the banana subdivides into two particles (Figure 3-4). During occlusion cracks do not propagate through the food; rather the teeth are forced through the banana during the jaw closing phase and the banana separates. As mastication progresses the banana is deformed irreversibly to a pulp and does not form easily discernible daughter particles. In contrast to the carrot, the banana bolus after three chewing strokes could not in theory be reassembled to give the original piece of food. From three chews and onwards, the pulping is obvious and the bolus becomes a weakly cohesive mass of deformed and extruded banana well mixed with saliva. The purpose of chewing appears to be to re-shape and soften the food into a swallowable form and provide some additional lubrication. It is worth noting that if a banana is sufficiently ripe chewing is not required, the necessary forces to reshape the banana can be achieved simply by forcing it against the palate with the tongue or simply extruding it through the teeth. Chewing the banana past the desired swallow point the bolus reaches a texture of a thick semi solid food with some lumps present.

The banana is swallowed as a single bolus, i.e., there are no partial swallows. Also, the relatively low number of chewing strokes required to swallow the banana, as seen here and in other studies (Hiiemae 2004, Palmer et al. 2007) suggest that banana in its natural ripe state has properties close to the threshold properties required for swallowing.

What's happening to the food during mastication?

- Size reduction in first few chews.
- Deformation of food matrix to a pulp. Individual particles are not easily identifiable.
- Added saliva helps form a well lubricated and weakly cohesive bolus.
- A single swallow for the banana bolus.

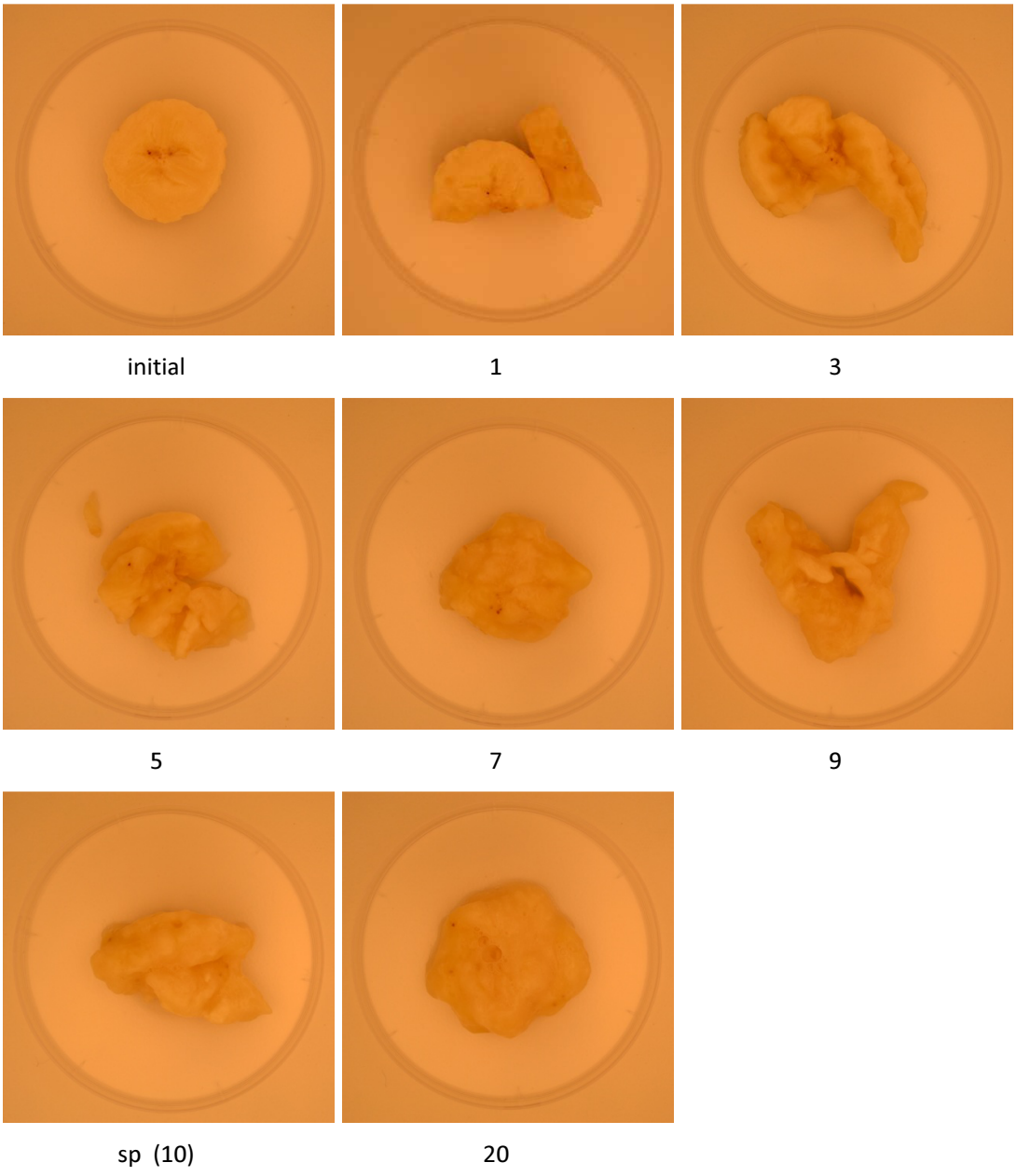

Figure 3-4: Chewed banana expectorated after different numbers of chewing strokes up to and past the swallow point (sp).

3.3.3 Embryos from Plants

Cereal seeds, nuts and legumes are composed of storage tissue containing tightly packed lipids and or protein bodies. In contrast to the fleshy fruits and vegetables these cells have no vacuole and little free water (Aguilera & Stanley, 1999). The range of properties that these foods can have is large. Nuts are most often roasted which changes the flavour and makes the

texture more brittle. Cereals and legumes are generally too hard to eat raw and so are cooked, often after further processing to remove husks, shells and/or kernels. The cooking renders them soft and palatable. The one example of this category chosen for observation is roasted peanuts (which are a member of the legume family), although cooked brown rice is used in a later case study presented in Chapter 6.

Roasted Peanut

The initial serving of peanuts is different from the other foods in this exercise as it contained five particles as opposed to a single piece of food. In the mouth the half peanuts are moved to the occlusal zone by the tongue and jaw during the jaw opening phase. Breakage occurs by brittle fracture and many daughter particles are produced (see Figure 3-5). Only some of the particles are fragmented with each chew stroke and the selection and breakage mechanisms described in §2.7.1 and §2.7.2 are clearly applicable here. After three chew strokes there are still two half peanuts that have not been occluded, after six chews all the original half peanut particles have been occluded at least once. The mastication progresses in the manner described by Peyron et al. (2004) where greater particle size reduction occurs in the early stages of the mastication sequence and the bolus d_{50} plateaus as the swallow point approaches. This makes sense as initially there are several large particles which have a high chance of being occluded and will produce many small daughter particles. As mastication progresses the chance of further size reduction is reduced as the bolus contains many small particles which have a much lower chance of being occluded. It is likely that some chew strokes prior to swallowing serve the purpose of adding extra saliva for lubrication rather than reducing the particle size. Initially the bolus has a lot of interstitial void space as the particles are large and do not adhere to each other (1, 3 and 6 chews). Not a lot of saliva has been added at this point. However, the bolus becomes more paste like as mastication progresses; the interstitial moisture content continually increases whilst the mean particle size decreases. This can be seen from the midpoint of mastication where particles become more closely packed and adhere together as liquid bridges form between them in the manner described by Prinz and Lucas (1988). At the swallow point the bolus resembles a paste of fine particles with liquid filling the space between the particles, the bolus is cohesive and does not readily separate. After several chew strokes moistened peanut particles get stuck between the cusps of the molars and in the buccal pouch. As the swallow point approaches the bolus feels grainy and abrasive and no large outlier particles are detected. When chewing past the natural swallow point, an excess of saliva is present and the bolus feels slurry like, size reduction is hard to detect due to the small size of the particles. After expectoration particles can be felt in

the molars and in the buccal pouch, and very fine particles immersed in saliva are still present on the tongue and palate.

What's happening to the food during mastication?

- Individual particles are easily identified.
- Selection and breakage mechanisms are apparent.
- A cohesive bolus is formed.

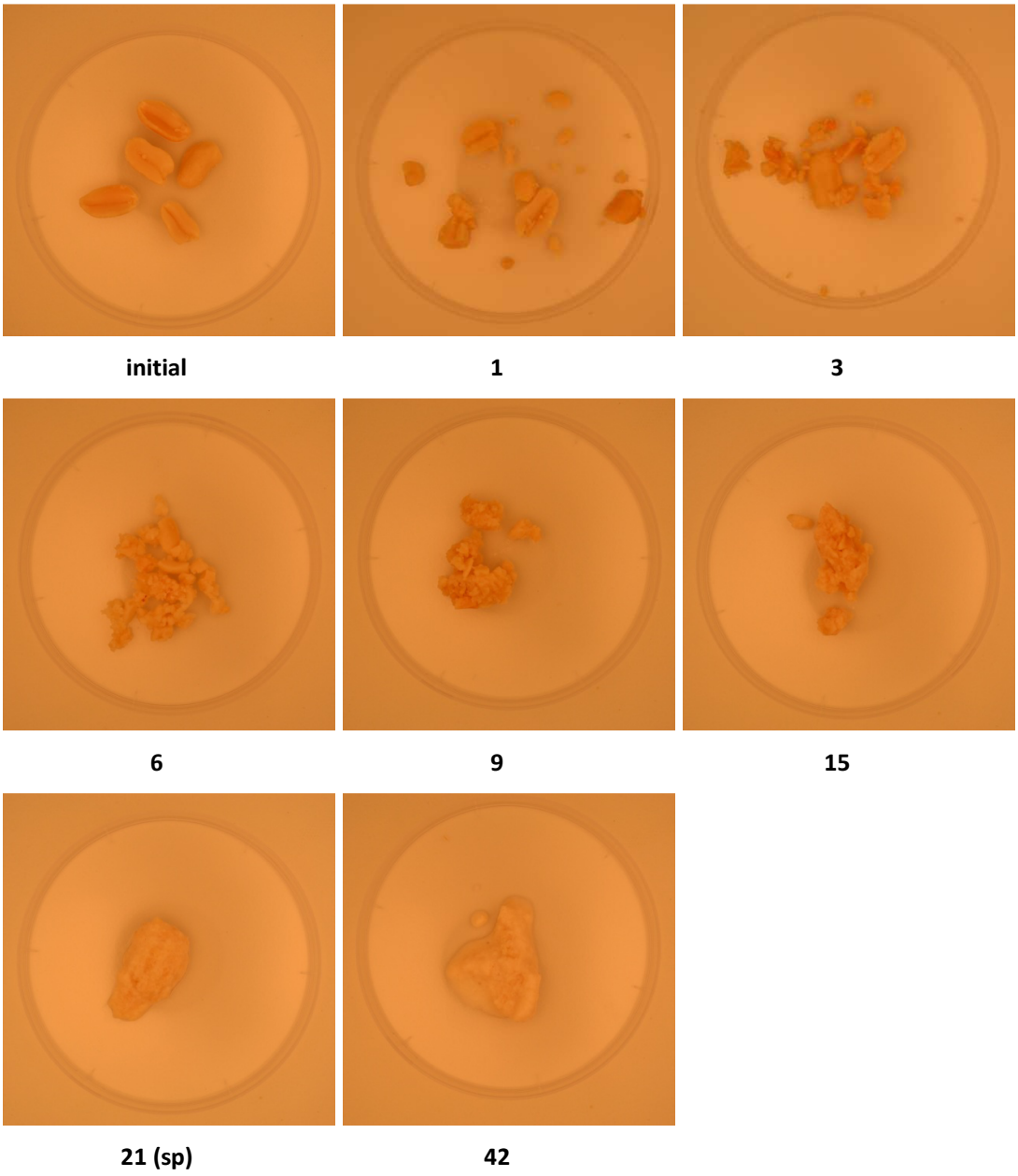

Figure 3-5: Peanuts after different numbers of chewing strokes up to and past the swallow point.

3.3.4 Manufactured foods

Humans did not evolve to eat manufactured foods, yet they constitute a significant proportion of many modern diets. This observational study selects three of these, the baked products of wine biscuit and white bread, the animal products of Edam cheese, and milk chocolate.

Baked products usually have one of two typical textures that we know from eating experience. Either they are the moist and soft texture of cakes, breads and sponges or the dry and brittle texture of biscuits and crackers. These contrasting textures and the way in which the food responds during occlusion depend on the properties of the cell walls. Water acts as a plasticiser which directly influences the mechanical properties of the cell walls, which are a composite of protein; for bread it is (usually) gluten and for cakes typically egg white and starch (Lillford 2011). Moisture absorbed by the food matrix affects the mechanical properties of the cell wall and hence the texture and breakage function/mechanism will change. In mastication, it is moisture uptake rather than loss that is of interest. It has been shown that adding water to different baked goods significantly reduced the number of chewing strokes before swallowing (Engelen et al, 2004). A wine biscuit and white bread were sampled to provide an overview of two common and contrasting oral experiences of baked products.

Cheese has featured in the human diet since as early as the 8th century B.C and there are over 2000 varieties manufactured all over the world (Walstra et al, 2005). Cheese is the fresh or matured, solid or semisolid product obtained by coagulating milk using rennet or another suitable coagulating agent, where the whey is drained from the resulting coagulation (Gunasekaran and Ak, 2002). The cheese may be consumed fresh or undergo a ripening and maturation stage. The removal of the whey is critical to the process as products concentrated by only the removal of water are called milk products. The majority of the fat and protein is retained in the cheese curd while most of the lactose is removed with the whey. A typical cheese curd from whole cow's milk contains ≈27% fat, ≈26% protein, ≈1.5% lactose, ≈1.5% ash and 44% moisture (Walstra et al, 2005). The composition in the final cheese can vary considerably from these values depending on the variety and processing techniques used to make it. The cheese selected for observation here is an Edam cheese which is mass produced in New Zealand and has a firm isotropic texture.

Chocolate as we know it today is a relatively recent addition to the diet first being made in the mid nineteenth century (Tanabe and Hofberger, 2006). It is a suspension of sugar, cocoa solids and milk solids in a continuous fat phase (30-40%) of cocoa butter (Afoakwa, 2011). Cocoa

butter is a polymorphic fat and thus chocolate melts over a temperature range of ≈25-35°C. This melting range of chocolate can be manipulated during manufacturing via the composition and tempering process to deliver a desirable mouth feel.

Biscuit

Biscuits are frangible; that is, they undergo brittle fracture in the early masticatory cycles producing many daughter particles. The biscuit has a very dry mouthfeel and in the initial stages of mastication most of the saliva produced is absorbed or wicked into the porous biscuit matrix, which can be seen by the subtle change of colour of the expectorated particles (Figure 3-6. Mastication has two particular functions for such textures where supplying sufficient moisture to lubricate the particles appears as important as size reduction. After half of the chewing cycles, most of the particles are below 2 mm, size reduction is now much less noticeable, the audible and distinctive crunch from fragmentation no longer occurs, the area between the molar cusps becomes jammed with moist fine particles, and there is still no sign of interstitial saliva because it continues to be absorbed by the dry particles. This last observation also means there is no noticeable dissolution of soluble solids from the biscuit, although this must occur within the absorbed liquid. As the liquid content increases and is expressed to the surfaces of the porous crumbs, it becomes the mechanism for flavour release as the forming bolus is circulated across the taste buds. As swallow point approaches the bolus resembles a cohesive grainy paste that appears saturated with the added saliva. There were no intermediate swallows before the bolus was ready at the final swallow point. After expectoration, some of the food remains in the buccal pouch and stuck in the teeth. This was also observed by Flynn et al. (2011) who proposed a compartmentalisation model where food can circulate between the buccal pouch and main bolus during mastication and is usually retrieved after the swallowing. When chewing past the natural swallow point further size reduction is difficult to detect. The sticky bolus becomes an over-saturated paste tending towards a slurry, where there is a definite urge to swallow.

What's happening to the food during mastication?

- Size reduction and individual particles are easily identifiable for the first half of the masticatory cycles.
- The audible crunch of chewing ceases by the halfway point.
- From halfway, particle breakage is less noticeable in the later stages of mastication as they are much smaller and a cohesive bolus is formed from the small particles and added saliva.

- From halfway, biscuit material is jammed between the cusps of teeth in the occlusal plane.
- The bolus remains crumb-like in appearance until only a few strokes before the swallow point because saliva continues to be absorbed into the porous biscuit matrix
- When the bolus is visibly saturated it is ready for swallowing
- A single swallow

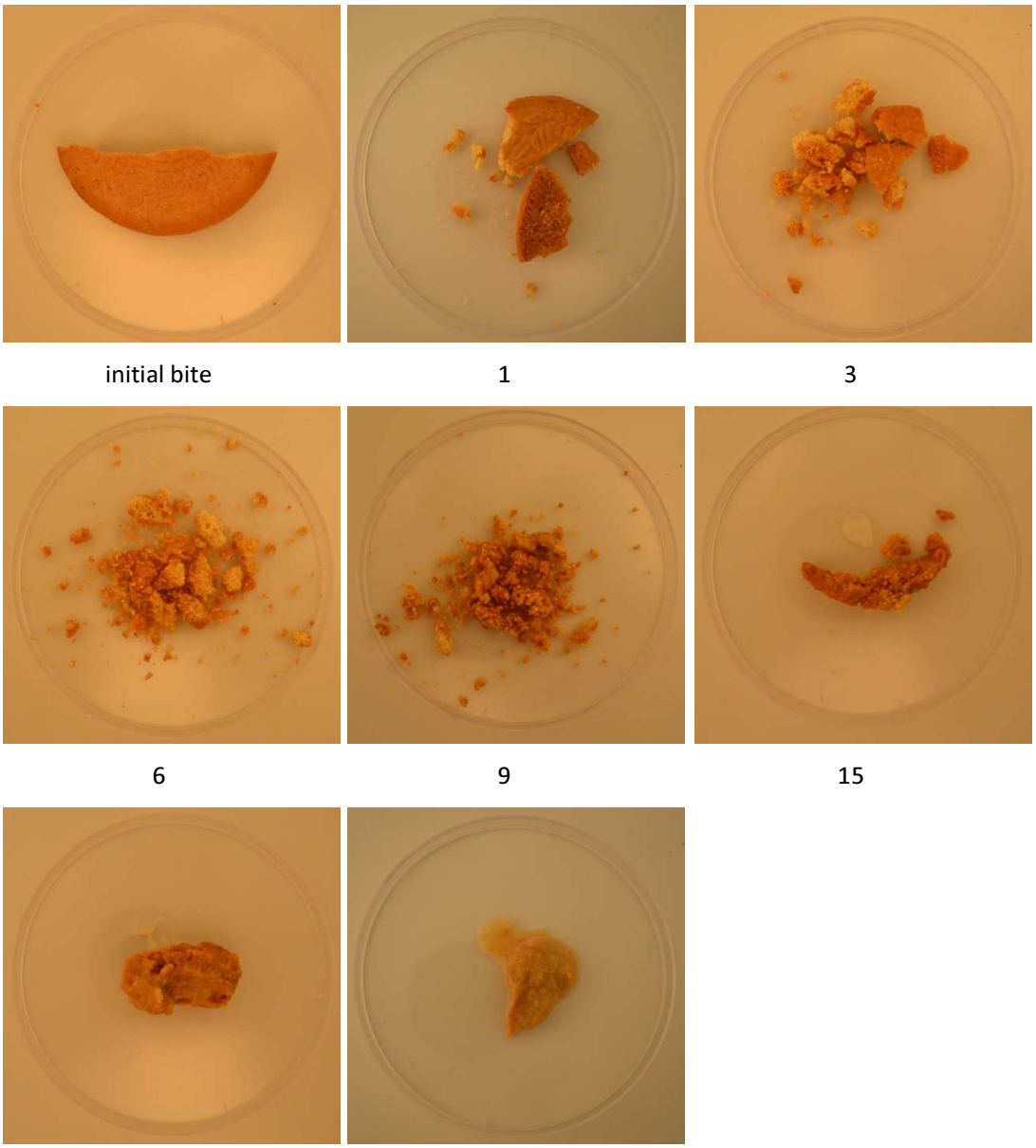

Figure 3-6: Wine biscuit expectorated after different numbers of chewing strokes up to and past the swallow point.

Bread (Soft cell walls)

Bread contains a lot of air in a porous matrix. When occluded, the matrix bends, buckles and sometimes ruptures reducing the air fraction (Ashby and Medalist 1983). At the first chew the indentations from the teeth are visible as compression imprints (Figure 3-7). In subsequent chews, the matrix is further compressed and deformed, and it is difficult to make out individual particles of bread in the bolus. Interestingly, it mostly stays as a single cohesive mass, appearing to be manipulated in a similar way to chewing gum with a rhythmic mixing and folding motion (van der Bilt et al. 2010, Schimel et al. 2007). The mixing and folding assists with saliva incorporation and surface coating which gives the bread a sticky doughy texture and helps it reach the requisite properties of a safe-to-swallow bolus, where it must be suitably deformable and well lubricated. Only nine chews were required to get to the swallow point and there was no urge for any partial swallows.

What's happening to the food during mastication?

- Deformation of the bread matrix by compression, resulting in loss of voids.
- Individual particles are difficult to identify, but the bread remains as a single mass appearing to be manipulated by stretching and folding each chew cycle.
- The stretching and folding incorporates saliva into the bread and coats the bolus with saliva. Both assist to create a deformable and well lubricated bolus for safe swallowing.

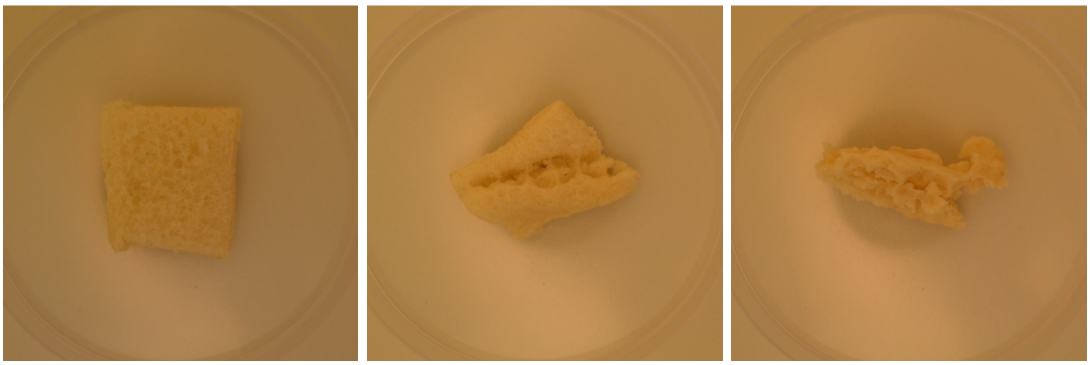

before 1 3

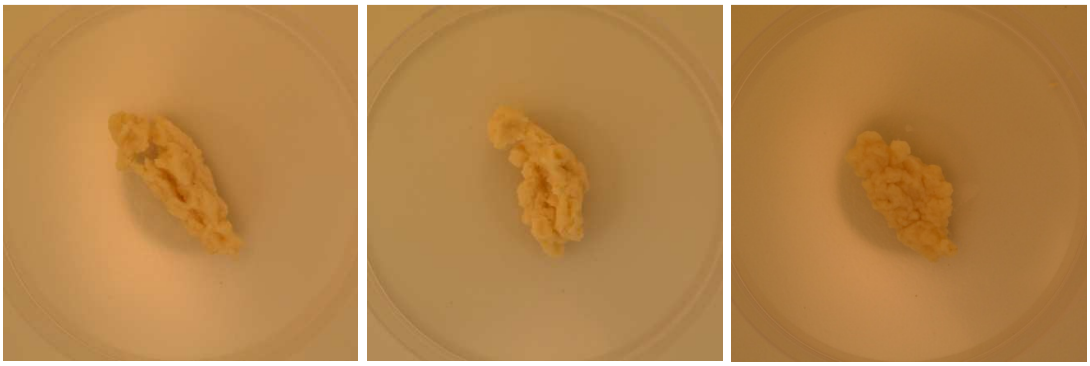

5 7 9 (sp)

18

Figure 3-7: White bread expectorated after different numbers of chewing strokes up to and past the swallow point.

Cheese

Cheese is soft to the bite and deforms elastically during the chewing stroke. It 'crushes' and fragmentation occurs when the teeth cut through the particle and contact during jaw closure (see Figure 3-8). This is similar to the banana and in contrast to carrots, peanuts and biscuit. The cheese has a naturally high cohesiveness and deformation rather than fragmentation dominates after the first few chewing strokes. It is difficult to distinguish between particles in the bolus after five chews as they stick together. The cheese sticks to the oral surfaces as it is chewed and swallowing requires a conscious gathering action of the tongue to collect the bolus just before swallowing is initiated. After swallowing a residual coating is left on the tongue and oral mucosa which takes some time to clear. The bolus is very cohesive and it appears that melting, which occurs as the cheese heats during mastication, helps the particles stick together.

What's happening to the food during mastication?

- The cheese is initially fragmented as the teeth cut through it.
- Individual particles not easily discernible after midway point.
- Strongly cohesive bolus with a single swallow.
- Noticeable mouth coating after swallowing and expectoration

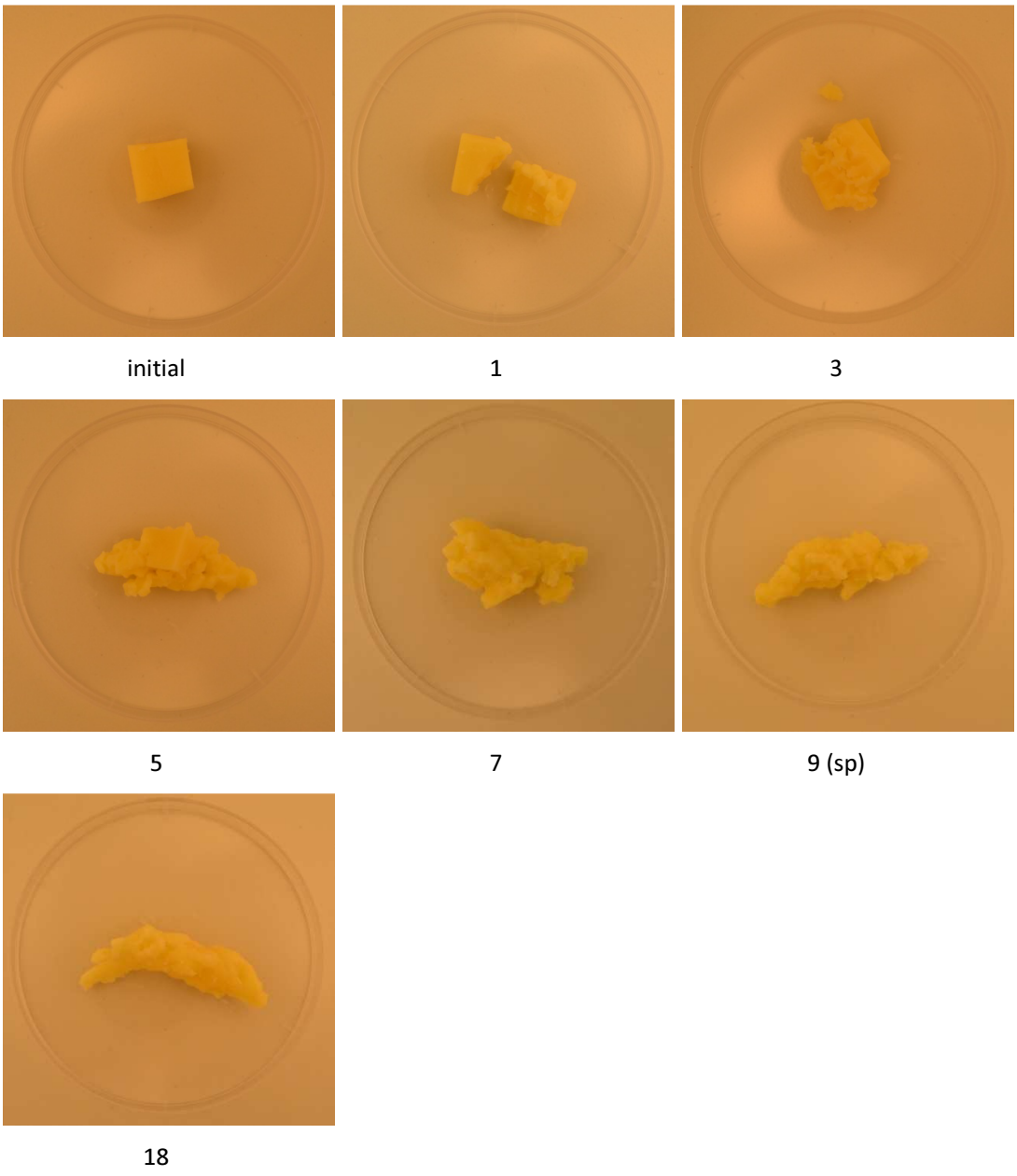

Figure 3-8: A cube of Edam cheese expectorated after different numbers of chewing strokes up to and past the swallow point (sp).

Milk Chocolate

Chocolate at room temperature is initially brittle so that in the first few chews, it breaks and produces a distribution of mostly large daughter particles. Two additional processes start to occur and are noticeable after the third chew; the melting of the fat and dissolution of the sugar. In subsequent chew strokes some particles are crushed but distinguishing smaller individual particles is difficult (see Figure 3-9 after six and nine chews). By the middle of the

mastication sequence the numbers of daughter particles do not appear to increase and the particles appear less angular and stickier. Individual particles are harder to differentiate from one another as the melting at the particle surfaces helps them adhere together. As the swallow point approaches there is an onset of rapid melting and any remaining larger particles are less noticeable. At the swallow point the bolus is a saturated cohesive agglomeration of un-melted chocolate particles, melted chocolate and saliva. The un-melted chocolate particles that are swallowed will fall in relatively narrow size range because small particles produced as a result of occlusion will melt in between chew strokes. After swallowing there is a residual chocolate mouth coating and the chocolate also sticks between the teeth and to the gums. Chewing past the natural swallow point resulted in the chocolate being completely melted giving a liquid mixture of saliva and molten chocolate.

What's happening to the food during mastication?

- Brittle fracture distribution of predominately large particles
- Melting and dissolution become noticeable after three chews
- Rapid melting of chocolate occurs as the swallow point approaches.
- Bolus is a mixture of un-melted chocolate particles in a liquid phase of saliva and molten chocolate
- Significant mouth coating after swallowing

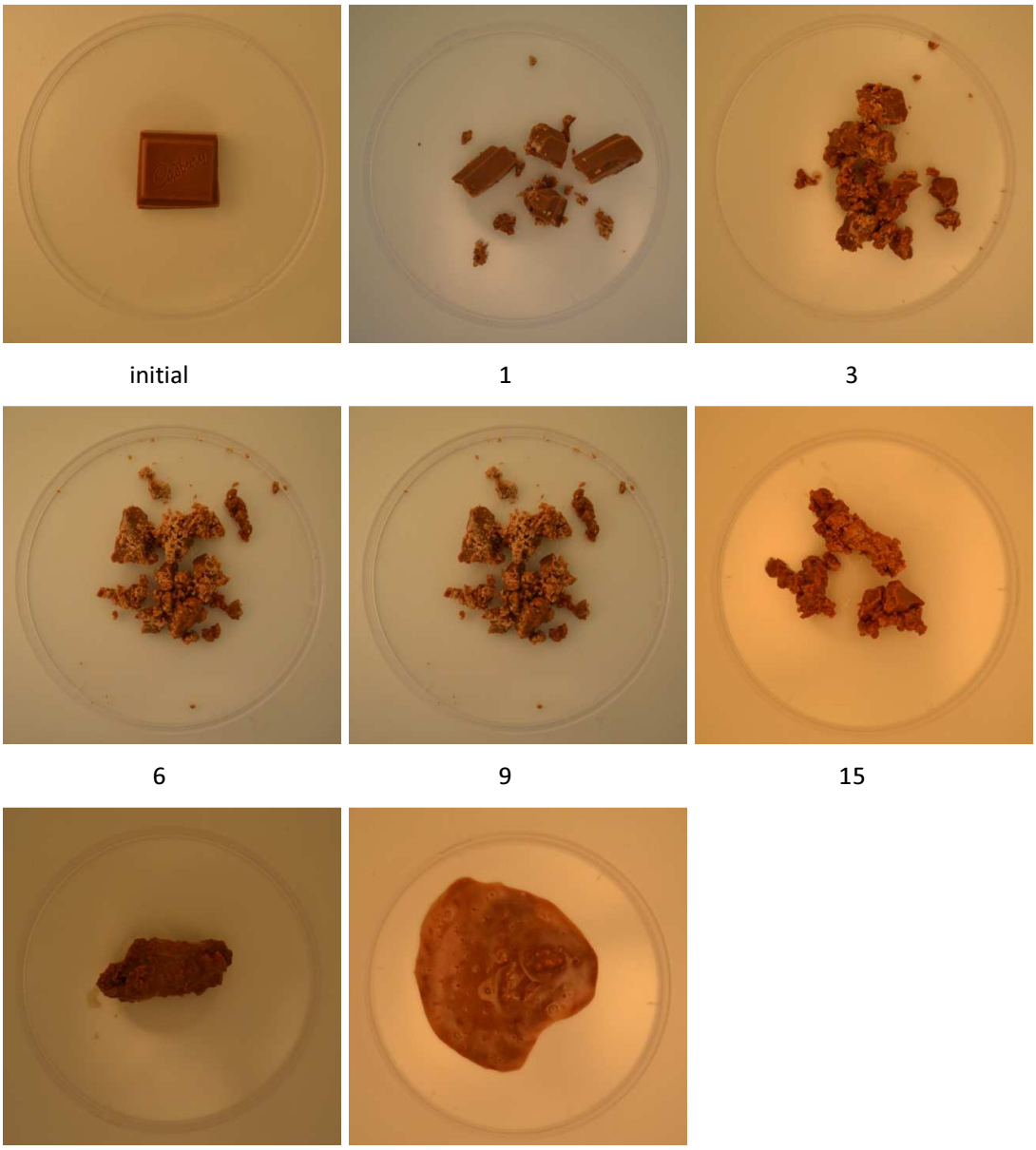

Figure 3-9: A piece of chocolate expectorated after different numbers of chewing strokes up to and past the swallow point (sp).

3.4 Discussion and Conclusions

The eight foods examined here displayed a range of break down pathways which transformed the food into a swallowable bolus. However, despite the differences, size reduction from occlusion and the bolus liquid content were important for all foods and the addition of heat had an important role in the development of the cheese and chocolate boluses.

Size reduction is complex because it interacts with the food properties. Some foods like carrots and peanuts fracture producing easily identifiable daughter particles through mastication. Others mostly yield like banana, cheese and bread. Some foods change their behaviour, chocolate initially fragments like carrot but as the particles heat up and become smaller they are fragmented less and yield in a similar manner to cheese. Meat, representing the fibrous hierarchical foods, needs to be work-softened by a combination of compression and shear in order for the jaws to come close enough together that the cusps provide enough proximate shear to cut the fibres and separate fibre bundles.

The liquid component of the bolus is important and serves two important functions; it is needed to saturate the bolus interstitial space and to lubricate its surface. Saturation of the bolus is required to ensure that the bolus is malleable and can deform easily as it moves through the pharynx and into the oesophagus. The surface lubrication is required to ensure it does not adhere to surfaces during transit. Heat is important where fats are present, because these add to the bolus liquid content when they melt. In most instances saliva makes up the majority of the liquid phase, but some foods release liquid and so saturation or an excess of liquid can be quickly achieved. Although this doesn't automatically mean the swallow point is reached in fewer chews. Carrot releases a small amount of liquid as it fractures through the cells. Banana rapidly became slurry like, indicating far more rapid cellular breakdown was achieved. The meat expressed liquid as it was compressed and together with saliva addition partial swallows were needed to remove excess liquid while mastication continued to soften and breakdown the meat to meet the requisite swallowable bolus properties. The baked goods did not contain obvious free moisture, but they absorb it which was particularly noticeable with the biscuit. As a result the swallow point for the baked goods was dictated more by the time required to saturate and lubricate the bolus than by the necessary size reduction which occurred somewhat more quickly. The cheese and chocolate were different again, where in both cases the added heat, aided by size reduction and mixing within the

mouth, appeared to provide an onset of fat melting which quickly gave the requisite bolus properties for safe swallowing.

All observations showed that the different boluses at the swallow point had a degree of sameness about them. They appeared homogeneous at the macro level, a well-mixed agglomeration of solids with saturated interstitial space or a soft solid such that it was surface wet. There were no larger outlier particles or un-chewed portions for any of the food. This was distinctly different from the slurries that resulted when chewing occurred far past the swallow point. These observations support the idea that the ideal swallow point is when the bolus reaches some threshold properties.

In the next chapter the methods of breakdown observed here are examined from an engineering perspective with a view to developing a mathematical description of the breakdown mechanisms. Swallowing is examined using a hazard and operability (HAZOP) study to identify the criteria of a safe-to-swallow bolus.

CHAPTER 4 PROCESS ENGINEERING OF MASTICATION

Mastication is a dynamic process which transforms food into a bolus that can be safely swallowed. Two questions emerge from this; (i), 'What processes transform the food from its initial state into a bolus?' and (ii), 'How do humans assess when the food is ready to initiate swallowing?' The answers to these questions lie in understanding the food-centric *breakdown* and the mouth-centric *mechanical sensory testing* regime. At some point in the breakdown cycle the food properties, as measured by the mechanical sensory tests, meet as yet undefined thresholds, which then permit phase II transport to the oropharynx in preparation for swallowing. There is a plethora of research on food breakdown as discussed elsewhere in this thesis (see §2.3 in particular). The threshold properties required for swallowing has received little attention since Hutchings and Lillford's (1988) insight that food properties must reach thresholds for structure and lubrication, upon which swallowing can occur. Others have also attempted to measure the bolus properties as swallow point approaches (Mioche et al. 2002a, Seo et al. 2007, and Peyron et al. 2007). With respect to the sensory testing that occurs simultaneously to the breakdown, Hiiemae (2004) has proposed a decision-making pathway for swallowing. While this is profound in terms of the decision-making, it does not go as far as defining the mechanisms of the testing regime or the way they fit within a safety-focussed decision-making hierarchy. It is the aim of this chapter to provide further insight in this area.

No-one is expecting that a generalised mechanistic model of mastication is just around the corner. Nevertheless, it is possible to propose the structure of such a model. An engineering approach considers the mouth as a unit operation with two sub-volumes, the oral cavity and the buccal pouches, and which contains a number of physical structures that perform both breakdown and mechanical sensory testing. These are; (a), the post-canine teeth; (b), the tongue; and (c) the palate. The post canine teeth are selected because mastication is the post-bite processing of foods (and so is a boundary of this analysis) responsible for most of the breakdown. The tongue is both a sensory organ and a mixing device which together with the jaw trajectory moves the food around the oral cavity. As a sensory organ, the tongue is complemented by the palate against which it pushes food. It is the mechanical sensory testing performed by the tongue-palate system that is of interest here. While the mouth contains many more structures, this short list is sufficient as a first attempt at understanding how oral processing affects and assesses the progress of bolus formation. It is reasonable to assume the testing occurs every chew cycle and are linked by *mixing* as the food is gathered, folded and repositioned into the occlusal plane. Thus, three mechanical processes are at play,

breakdown, *mixing* and *testing*. Figure 4-1 shows this construct and the remainder of this chapter describes each of these processes.

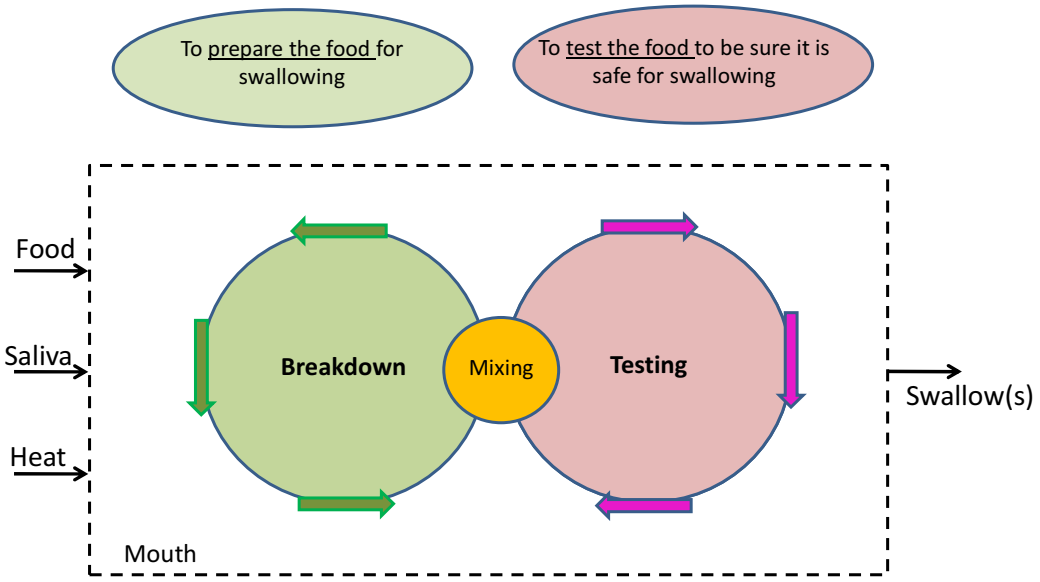

Figure 4-1: Mechanical processes of mastication. The mouth is considered as a process unit operation containing oral structures (teeth, tongue and palate) housed in a volume (oral cavity, buccal pouches). During mastication *mixing* facilitates both food *breakdown* and the continuous *mechanical sensory testing* to facilitate decision making.

4.1 Breakdown

Mechanical breakdown of the food occurs by a range of rate processes. Quantitative studies of food breakdown have been centred on the particle size distribution (Lucas & Luke, 1983a van der Bilt et al, 1987), dissolution of gels (Harrison & Hills, 1996, Wright & Hills, 2003) and more recently the salt release from a model dairy food (de Loubens et al., 2011). However, there are other rate processes occurring during mastication, as highlighted in the qualitative study in Chapter 3. Collating these, the rate processes that apply to food can be grouped into the following categories; (i), *size reduction*; (ii), *work-softening*; (iii), *dissolution*; (iv), *absorption*; and (v), *melting*. The sections below discuss these rate processes.

Note that size reduction and work-softening are separated. This is because occlusion differentially affects the food properties where work-softening becomes relatively more important for fibrous and rubbery foods. Most foods are heterogeneous and have multiple failure mechanisms at different levels of structure, each associated with a particular stress profile, which is further complicated by the changing jaw trajectories, applied forces and the

shape of the teeth (van der Bilt et al., 2006). The relationship between structure, stress profiles and the resulting shear or breakage is complex and rarely mimics simple tests like uniaxial tension or compression from instruments (Jeronimidis, 1991). Furthermore, as size reduces, the occlusal gap becomes important. Below a minimum size, particles maybe smaller or similar in size to the occlusal gap so do not deform enough to fracture. While size reduction and work-softening are intimately related, the following discussion is limited to size reduction

4.1.1 Size Reduction

Size reduction results from occlusion of brittle foods between the teeth during chewing and has received a lot of attention. It has been modelled by Lucas and Luke (1983a), van der Bilt et al. (1987) and van der Glas et al. (1992), who all divide size reduction into breakage and selection functions. Breakage describes the size distribution of daughter particles and depends upon tooth morphology, the jaw-muscle activity, mechanical properties of the food and particle size and shape (Lucas et al., 2002). It can be regarded as size independent and described by a power law (Lucas and Luke, 1983b), a cumulative distribution (van der Bilt et al., 1987, van der Glas et al., 1987 and Olthoff et al., 1984) or size dependent where a small size limit may be specified below which particles are no longer reduced (Voon et al., 1986). An alternate mechanism, not reported in the literature is where breakage can follow a pasting mechanism where the occluded portion of the particle is immediately pasted to below the limit size and several large residual daughter particles are produced; this mechanism is explored later in this work (see §6.1.3). Other breakage functions are discussed in detail in §2.7.2.

The selection function describes the probability of a food particle being contacted by the teeth during a chew stroke. It is described often by a size dependent power law (Lucas and Luke 1983b, van der Bilt et al., 1987 and van der Bilt et al., 1992). Selection can also be affected by the number of particles and how they 'compete' for space on the teeth during occlusion (van der Glas et al. 1992). Selection is an interesting mathematical construct because it is the outcome of mixing which circulates food around the mouth. However, selection and, by implication, mixing are influenced by physiological factors such as the total occlusal area of the post canine teeth, tooth morphology, the relationship between antagonistic teeth, movement of the jaw, the action of the tongue and cheeks, and food factors such as portion size, particle size and number (van der Glas et al. 1992). Selection functions are discussed in detail in §2.7.1.

For brittle foods, occlusion changes the surface area and number distribution of particles which are important for the other rate processes discussed later. For non-brittle foods, the effect of occlusion results in structural breakdown described by work softening.

4.1.2 Work Softening

Work softening occurs when a decrease in apparent viscosity, viscoelasticity, or degree of structure of a system persists when the shear is discontinued. This behaviour is also called shear breakdown (IUPAC, 2012).

For non-brittle foods, occlusion progressively breaks down the food matrix, reducing the toughness, hardness and yield properties. For example, Mioche et al. (2002a) measured the mechanical shear stress of un-chewed cooked meat and the resulting bolus after chewing for different numbers of chew strokes. The shear stress was highest for the un-chewed samples and decreased proportionally with more chews. Peyron et al. (2007) used texture profile analysis (TPA) to analyse expectorated boluses of wheat flake cereals at different stages of the masticatory sequence. They found that bolus hardness decreased whilst the cohesiveness, adhesiveness and springiness all increased.

To develop a modelling platform, relationships must be established between occlusion and the degradation of mechanical properties of the food and bolus. The rate of degradation will depend on; (i), the food structure and texture; (ii), the occlusion forces and their direction; and (iii), the frequency of occlusion. Points (i) and (ii) require an understanding of the yield behaviour of a particular food subjected to the normal and shear forces within the occlusion zone. Point (iii) requires an understanding of the mixing mechanisms which are discussed later in §4.3.

4.1.3 Absorption

Absorption processes are the wicking of liquid into the pores by capillary action and hydration of the solid matrix. Both processes occur at different food specific rates and result in changes to the mechanical properties of food (Lillford, 2011). Hydration is the swelling absorption by diffusion of moisture into foods (e.g., starch). The volume of liquid involved is generally small and is a relatively insignificant rate process.

Wicking is of particular interest. It is controlled by the surface tension of the liquid, the pores sizes and the distribution of pore volume throughout the matrix, and the availability of liquid from the oral mucosal surfaces. Hapgood et al. (2002) describe the wicking time for a droplet

placed on porous powders. They found that the limiting factor to wicking is the size of the macro voids within the matrix and that wicking time increases with fewer pores (low porosity), closer packing of the powder, more viscous liquids, high surface tension and low contact angle. Hapgood et al. (2002), predicted for fine, medium and coarse lactose powders ($d_{3,2}$ = 32.0, 48.3 and 69.7 μm) wicking times between 0.16 seconds to 17.4 seconds. If similar wicking times occur in food, at the fast end, it is significantly shorter than the circulation time (i.e., the time between occlusal events for a packet of food). Using a similar approach, a wicking velocity can be established for porous foods prior to mastication by measuring the absorption rate into a food with known void volume and surface area. Such a method avoids needing to know the pore size distribution or the interfacial properties.

As stated above, wicking is dependent on the availability of liquid, which comes mostly from saliva but also from expression from the food matrix (apple), melting (fats and gels) and dissolution (sugars). The liquid continues to be absorbed until the voids are full or the matrix is sufficiently softened. The detection of dryness or adhesion to the oral mucosa means that mastication must continue, during which time more saliva is added. Eventually the bolus becomes saturated and a layer of saliva appears on the outside of the bolus. Compaction may aid this process, as it does in granulation (Iveson & Page, 2005). The bolus is sufficiently lubricated when it will not stick to the mucosa and swallowing can be initiated. Thus the end-point of the absorption process is saturation. Indeed, some foods will become saturated before the food is ready to swallow because other thresholds are not satisfied like particle size. In these cases, if safe to do so, liquid is partitioned and an intermediate liquid swallow is initiated. The conceptual model for absorption is further developed in §5.4.6.

4.1.4 Melting

Heat transfer to the food occurs via conduction from the oral surfaces and by convection. The latter is influenced by the rate of saliva addition and its mixing into the food, and by the surface renewal rate of the food against the oral surfaces of the mouth (high surface renewal of particles to the contact surface results in faster heat transfer). This added heat can melt fats at the exposed surfaces which will then enter the liquid phase. At a single particle level, heat transfer occurs by conduction if the food is non porous or by conduction and convection if it is porous when absorption is occurring. Each mechanism is a dynamic process describable by the melting properties of the food, a heat transfer resistance, a driving force and a surface area across which the exchange of heat occurs. For nonporous foods at the beginning of chewing, when particles are large and the total surface area is small, conduction will be the limiting

resistance to melting. Later, when particles are small and the total surface area of the system is high, convection will be the limiting resistance. Thus, when chewing chocolate, anecdotally there is a point when the chewed particles rapidly melt to liquid, as was observed in §3.3.4. Similarly for cheese, melting is important for the dynamic sensory experience during eating.

As described, melting involves complex interactions which require simplification in a conceptual model, based on the dominate mechanisms at play. It is reasonable to assume constant temperature for the added saliva and the walls of the oral cavity. Conduction from the wall can be approximated from the surface renewal rate of the food to the wall as it circulates within the mouth, which can be derived from the mixing model discussed later in §4.2. It is simplest to assume that heat enters the mobile liquid phase, after which it transfers to the particles, melting them as shrinking cores from their surfaces based on their size distribution. Thus, melting is dominated by the size reduction process, the amount of latent heat required to affect phase change and the available mobile liquid phase. The concept model for melting is further developed in §5.4.5.

4.1.5 Dissolution

When saliva coats the surface of particles, soluble solids on the surface such as salt, sugar or flavour compounds will be transferred to the liquid phase. Dissolution occurs at the solid-liquid interface. Concentration gradients within the food particle can be assumed not to develop because the mastication time (10-40 seconds) is short compared to the characteristic time of solute release (in the manner described by de Loubens et al. 2011). Knowledge of the particle surface area and mobile liquid phase volume is thus sufficient to simulate this mass transfer phenomenon. The mass transfer coefficient is dependent on the food and can be determined experimentally with *in vitro* experiments; for example with sugars, will be dependent on whether the sugar present is amorphous or crystalline.

Dissolution is arguably more important for its influence on sensory properties than physical properties of the bolus, unless there is associated melting such as for gels, which are a special case requiring further discussion. Gelatine gels are common in confectionary. In these, the sugar and flavour release is dominated by gel melting, where the onset temperature is influenced by the local amorphous sugar concentration. If the melting point of the gels is at first above 37°C, dissolution begins by surface diffusion of sugar out of the gel, which then lowers the melting temperature of the surface layer. When the gel melting temperature decreases below the mouth temperature, gel then melts which releases significantly more sugar and flavour (Harrison & Hills, 1996, Wright & Phillips, 2003). Thus, the melting of the

surface layer dominates the rate of release. Experimentally, the rate of flavour/sugar release into the saliva can be calculated by determining the rate of the change in the solid volume between chews (Wright & Hills, 2003) from which a velocity of the melting surface layer can be calculated. For model development, dissolution of gelatine gels is analogous to that of melting.

4.2 Mixing

Mixing is the management of the food within the mouth cavity. Researchers divide mixing into 'manipulation' which is the processing stage of eating after the first bite, and 'movement' which occurs when swallowing is initiated and moves the food back into the oropharynx. Oral processing is complex as it relates the central nervous system to the muscle actions of the jaw and cheeks, the movement of the food about the oral cavity and the changes in properties of the food (Hiiemae, 1983). If the food experience is considered in isolation then a simpler diagram can be drawn (see Figure 4-1), where mixing is the connector between the food breakdown and mechanical sensory testing.

The movement of the food around the mouth is controlled by the tongue in synchrony with the jaw trajectory and cheek movements. The management of food from the first bite to the terminal swallow is well described by the process model of feeding proposed by Hiiemae (2004), which describes the feeding sequence in several steps and processes. A mixing model needs to simulate, with respect to the food, the cycles of mastication between the first bite and before the terminal swallow. During this rhythmic chewing phase, the tongue cycles in the mouth and maintains food on the occlusal surface through a series of rotating, pushing and tilting motions. This mixing profile is dependent on food structure and texture.

Mioche et al. (2002b) observed using videoflurography three types of processing cycles; (i), chewing on one side, 'unilateral cycles', (ii), chewing with food on both sides of the mouth 'bilateral cycles,' and (iii) shift cycles,' in which the bolus or part of it was moved from one side to the other, or to the midline of the mouth for initiation of swallowing. The types of processing cycles varied significantly with food type. Unilateral cycles occurred 83% of the time for tender meat, 70% tough meat, 58% for banana and 22.5% for biscuit. In contrast, bilateral mastication constituted 11% of the cycles for tender meat, 19% for tough meat, 40 % for biscuit and 46% for banana. Differences may be due to the natural cohesiveness of the foods; for example, meat stays more or less in one piece, biscuits break up and banana is extruded between the teeth. The bolus was manipulated onto the occlusal surfaces by 'tongue pushing'

(41% of unilateral cycles) 'cheek pushing' (28%) and the remaining 31% with no clear mechanism. The 'cheek pushing' results from food ending up in the vestibule (cheek pouch) which after several chew cycles is pushed by the cheek back onto the occlusal surface. In summary, Mioche et al. (ibid) observed that mixing is highly variable.

From a biological viewpoint, it makes energetic sense to use as few chew strokes as possible to prepare a 'safe-to-swallow' bolus. Our dentition and digestive system is suited to particular foods which deliver our energy requirements. Thus, it is not unreasonable to assume that mastication and swallowing strikes a balance of delivering a safe swallow of a bolus with ideal properties for gastric digestion with the minimum energy input. Indeed, Prinz & Lucas (1997) state that our high metabolic rate demands mastication because small particle sizes provide rapid access to digestive enzymes in the gut. However, there is an energy cost to reducing particle size that also wears out the teeth, which implies some optimum exists between the energy cost of chewing and the energy extractable during digestion. This manifests itself in the relationship between particle size and food properties (Lucas et al. 2002, refer to §4.4). Mastication also increases the bioavailability of important nutrients, affects the glycemic response and, through sensory perception, can safeguard us from consuming unsafe foods. Furthermore, sensory signals generated during mastication can initiate a central nervous system response to increase the digestion of some nutrients (Peyron, 2011). Here, the focus is on mechanical properties rather than other sensory responses. Therefore, a generalised mixing model must consider the least amount of work required to break down the food structure.

Some conjecture is worthwhile. The most parsimonious energy efficient mixing process in mastication would optimise two outcomes; (i), minimal wear on the teeth; and (ii), mechanical sensory testing. When viewed this way, the mixing circulation of food around the mouth is logically somewhat plug-flow involving stretching, folding and rotation, and preferential selection of particles requiring further breakdown which together minimise the number of chew cycles and thus wear on the teeth. The second optimal outcome, mechanical sensory testing, is intimately dependent on the mixing because it relies on the food being presented continually to the oral surfaces when the tongue and palate mechanoreceptors assess the food supplying the central nervous system with information. Interestingly, surface renewal is also important for the overall heat transfer rate in meltable foods (§4.1.4), although the evolution of this is more likely to be related to the need for continuous mechanical sensory testing. While Mioche et al. (2002b) have provided videoflurography of the bulk motion, the exact path

that an element of food takes in the mouth is unknown. While clearly complex, any mathematical description of mixing should yield, with respect to size reduction, the same mathematical result as the selection functions arising from existing studies with brittle foods (Lucas and Luke, 1983a; van der Bilt et al., 1987; van der Glas et al., 1992). It is also safe to assume that the surface renewal is sufficient to avoid any swallowing problems as discussed in detail in §4.3.3. Therefore, with these assumptions, a conceptual model of mixing reduces to the already defined selection function and need not attempt to fully describe the oral mixing system. Nevertheless, it is a recommendation of future work, that this assumption be tested.

Mixing also facilitates absorption, dissolution and melting depending on the rate of saliva addition, heat flow and surface area change as packets of food are occluded. It may take several chew cycles before a packet of food is chewed again (Hiiemae & Palmer, 1999); this period is called the circulation time and will vary depending on the portion size, particle size and number, and type of food being chewed. One chew cycle lasts between ~0.5-1.0 seconds and varies between people and foods (Jalabert-Malbos et al. 2007; Hutchings et al. 2011). The travel path of a particle or packet of food, while not known, will most likely not exceed four chew cycles. This defines an upper limit of about 2-4 seconds for the rate processes of absorption, dissolution and melting to occur between chews.

4.3 Mechanical Sensory Testing

The question 'How do humans assess when the food is ready to initiate swallowing?' is qualitatively well understood. A swallowable bolus must be lubricated, deformable, plastic and cohesive (Woda et al., 2006[a]; Woda et al., 2006[b]; Prinz & Lucas, 1997; Peyron et al., 2011) so that the movement of food from the mouth to the stomach occurs without the possible deadly consequences of aspiration into the lungs or choking. Swallowing is triggered when a bolus with acceptable levels of these properties has been prepared, although for a mouthful of solid food there is usually more than one bolus swallowed (Hiiemae & Palmer 1999, Okada et al. 2007).

Hiiemae (1983) suggest that the mouth detects and measures bolus properties through some testing regime. The previous section argues that these tests occur mostly during the mixing phase of the chew cycle and that they are mechanical in nature, because information on strength, yield, flow, volume and texture are required. In this way, mastication acquires both feed-back and feed-forward control advantages. Feed-back determines whether more

chewing cycles are needed (or perhaps a partial swallow of excess liquid is required). Feed-forward control determines the future jaw trajectory and forces to apply.

Swallowing occurs when the bolus reaches the requisite properties defined by a list of criteria, which will be discussed shortly. Figure 4-2 shows an extended version of the mastication system from Figure 4-1, but now with the rate processes of breakdown and the elements of the mechanical testing regime. The discussion now proceeds to the mechanical sensory tests by; (i), examining the oral structures and their sensory detection architecture (§4.3.1); (ii), discussing how this information translates into assessment of bolus properties (§4.3.2); and (iii), defining the thresholds necessary for safe swallowing (§4.3.3). This chapter then links the rate processes to the outcome bolus properties and explains how a conceptual model needs to use the rate processes to predict the bolus properties (§4.4). Lastly, the decision making process of whether to swallow or continue chewing is discussed in §4.5.

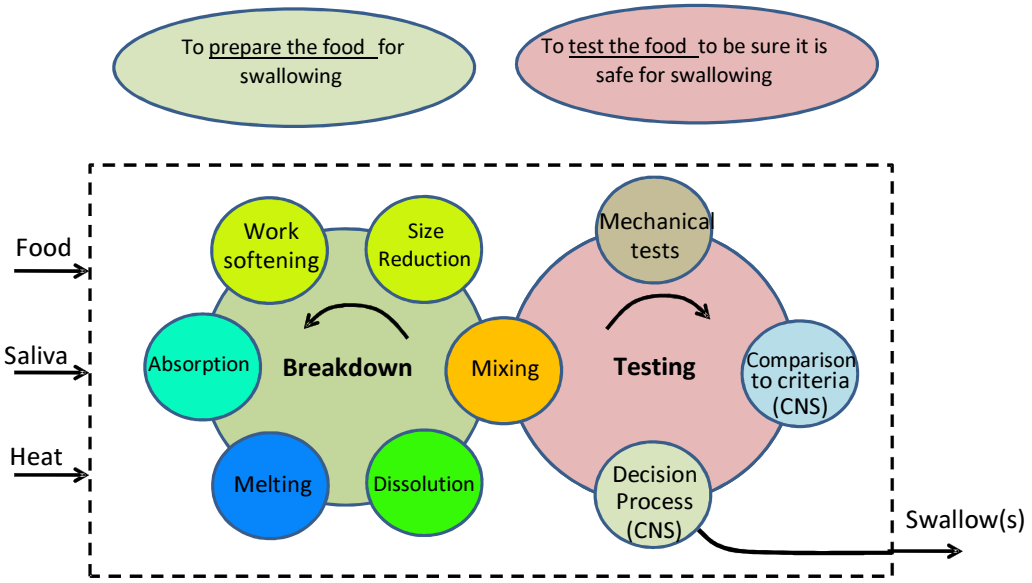

Figure 4-2: The mechanical processes of mastication showing how mixing both circulates the food which simultaneously undergoes breakdown by a number of rate processes and is subjected to mechanical sensory tests which are then compared to some criteria stored in the central nervous system. The outcome is a decision whether to continue chewing or prepare for partial or terminal swallowing.

4.3.1 Oral Structures that Perform Mechanical Sensory Tests

It is implicit that the same oral structures that mix the food also conduct the mechanical sensory tests: the teeth, tongue, palate and buccal pouches. Of interest here is the capacity of these structures to make measurements. The teeth break down the food matrix through size

reduction and work softening. Incisors are used for cutting and only usually participate in the first bite. Canine teeth are used for cutting and tearing.

The molars are used for chewing and shearing and are of particular interest here as they make up the occlusal area where most of the comminution and work softening occurs. In terms of their capacity to make measurements, occlusion of the teeth can measure gross forces involved (Trulsson, 2007) using the periodontal mechanoreceptors as shown schematically in Figure 4-3. These receptors are important in controlling the level of force required by the teeth during manipulation and positioning of food (Trulsson & Johanson, 2002), and also in measuring the mechanical properties of the food and the spatial contact patterns with the dentition (Trulsson, 2007). The distance and components of force are measured by the periodontal mechanoreceptors, which can measure in all directions although they have preferred reception to distal (towards the back) and lingual (towards the front) forces as well as the normal compressive force (Foegeding et al., 2011). Anterior periodontal mechanoreceptors have especially low range sensitivity. It is these measurements combined with the spatial movements of the jaw which gives information on the food/bolus properties. To protect the teeth an upper limit toughness threshold exists. Thus, the periodontal mechanoreceptors give vital information needed for feed forward control to determine the future jaw trajectory and forces to apply.

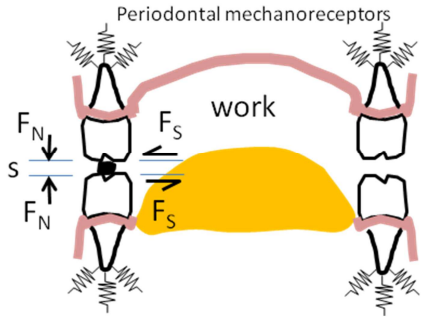

Figure 4-3: Forces applied during occlusion are measured by the periodontal mechanoreceptors. Shown is a particle caught between the upper and lower teeth a distance *s* apart and to which a normal force F_N and a shear force F_S are applied.

The tongue helps manipulate food and assists in swallowing. It moves food distally through the oral cavity from the incisors to the post canines after the first bite, then helps position and re-position food between the post-canines for occlusion and finally moves the food to the pharynx for bolus formation and swallowing (Hiiemae, 2004). After a mouthful of food has been chewed and swallowed, the tongue often performs a 'sweep' to collect small particles which remain in the mouth attached to the gums, teeth and other tissues in the mouth.

Of most interest to this discussion are the opposing positions of the tongue and hard palate because they offer the opportunity to test the mechanical properties of the food. The tongue, palate and oral mucosa all contain mechanically sensitive tactile receptors, called mechanoreceptors, which provide sensory information to the brain to control oral processing (Peyron et al. 2011) by ensuring efficient and safe completion of the masticatory sequence, from the acquisition of food until swallowing (Kapur et al. 1990, Ertekin et al. 2000, Foegeding et al. 2011). Three types of receptors are present in the tongue and oral mucosa: Meissner corpuscles, Merkel cells, Ruffini endings and free nerve endings (Jacobs et al., 2002). Two subgroups are further distinguished based on the receptive field area; type I receptors with small and distinct receptive field areas and type II with large and diffuse receptive field areas. Furthermore, rapidly adapting (RA) receptors respond during the dynamic phase of stimulus application; for example, to a stroke across the tongue surface. Slow adapting (SA) receptors respond to dynamic and static application of force; for example, a constant indentation on the mucosal surface.

In opposing each other, the tongue contains elastic papillae whilst the palate has smaller more rigid papillae (van Aken, 2010). The palate provides a rough and hard friction surface and the tongue a sensitive, conforming friction surface capable of measuring compression and shear forces. The papillae on the tongue surface are innervated by tactile sensors; thus, forces measured by the mechanoreceptors relate to the deformation of these papillae (van Aken, 2010). In the language of engineering, it is reasonable to expect that the papillae-mechanoreceptor combinations must be able to measure normal and shear forces with enough sensitivity to differentiate properties across a response surface, e.g., a soft solid pulp or an expressing free liquid.

In addition, the tongue is able to measure distance between itself and the palate (Trulsson & Essick, 1997). Indeed, the resolution of size detection is quite remarkable. Strassburg et al. (2007) established that plastic discs of 3 mm diameter could be discerned apart when the difference in thickness was as little as 25 μm. In further research, Strassburg et al. (2009) proposed two methods for the thickness differentiation by the tongue-palate interaction, where the method of detection depends on the material properties. For a compliant disc that aligns with the palate, the thickness differentiation is achieved by evaluating the normal stress distribution across the disc, which depends on the disc stiffness and diameter. The deformation of the tongue approximately equals the disc thickness. Instead, if the disk is non-compliant when compressed by the tongue, peaks in stress are detected at the contact edges

with the palate and tongue, which are registered by the deep mechanoreceptors. The force exerted by the tongue/papillae was evaluated by van Aken (2010) who examined experimental data from Trulsson & Essick (1997). For the mechanoreceptors in the tongue, assuming that if forces across a receptive field area are additive, they determined that the detection threshold is 30 μN/2.4 mm^2 giving a minimum detection stress threshold of 12 Pa.

The aim here is to translate these temporal measurements of the tongue-palate interaction into a food property assessment. The concept for this is given in Figure 4-4. The papillae on the tongue and palate effectively provide 'pixel-like' resolution about the compressive and shear forces, the area over which they apply and the separation distance between the tongue and palate. This means they deliver a time varying response surface map of force vectors and separation distance that characterises food behaviour, and which can be used by the central nervous system (CNS) to decide whether to continue chewing or to prepare the bolus (or a portion of it) for swallowing. For simplicity, the cheeks are ignored in this discussion, although they have an important role in positioning of food for occlusion (Mioche et al, 2002b).

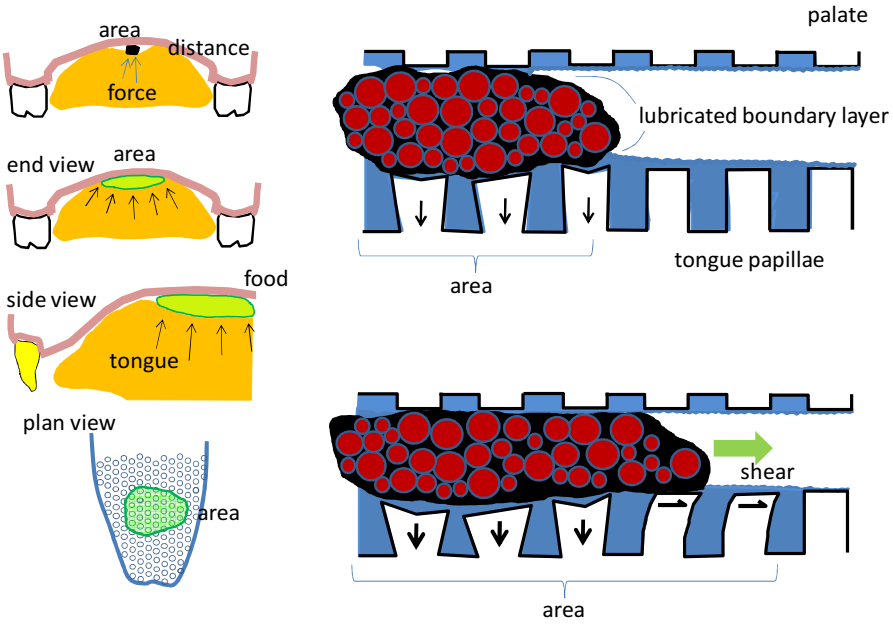

Figure 4-4: Schematic of particle and bolus measurement between the tongue and palate showing the papillae measuring both compressive and shear forces during mild and stronger compression.

4.3.2 Translation from Response Surface to Food Properties

The previous discussion describes the oral structures that conduct the mechanical sensory tests. In summary, the mechanoreceptors of the tongue and palate and the periodontal mechanoreceptors of the teeth assess the particle size, the particle deformation and the bolus deformation. This is achieved through a *response surface* of normal and shear stress as detected by the mechanoreceptors, as well as distance both as local deformation of the tongue surface and the proximate distance between the tongue and palate. The response surface responds to the applied force delivered by the tongue, and its applied motion termed the strain rate and strain distance. Furthermore, it is dynamic, meaning that it continually changes as the food is circulated in the mouth.

The resultant dynamic response surface provides information that can be translated into a list of food properties. These will be the food properties used in the next section by the HAZOP procedure to reverse engineer their threshold values for safe swallowing. They also become the properties that need to be tracked in a conceptual model of mastication. The following list contains the proposed properties. They are illustrated in Figure 4-5 and are justified in the following paragraphs.

- Temperature
- Volume
- Adhesiveness
- Particle size
- Particle deformation
- Bolus deformation

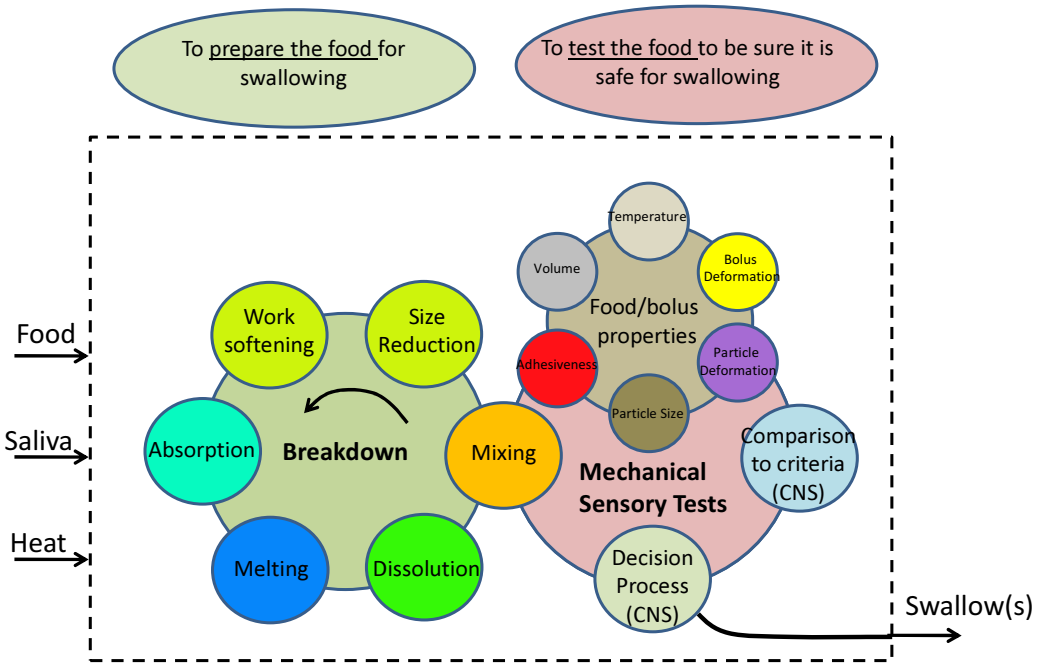

Figure 4-5: Mechanical processes of mastication. The rate processes of breakdown affect the bolus properties detected through the mechanical sensory testing by the oral structures within the mouth. The criteria define a safe-to-swallow phase space of properties.

Temperature

The property of **temperature** is self-explanatory. Food that is too hot must be expectorated. Food that is too cold must either be expectorated or warmed to avoid discomfort. Temperature perceptions in the mouth are divided into two categories, warm and cold, which are perceived by specific receptors throughout the mucosa. The receptors which induce a feeling of pain relating to temperature extremes are called thermal nociceptors (Jacobs et al. 2002). Stimulation of these is expected to induce bolus expectoration. As temperature is not a mechanical or rheological bolus property it is of little interest here in terms of defining a safe-to-swallow bolus. However, it is of interest in the dynamics of melting of fats and gels, as discussed in §4.1.4.

Volume

For volume, it is intuitive that there is an upper limit, although defining this limit is difficult and will vary between individuals. The following examples show that it is likely that the tongue and palate are principally involved with volume determination. Ertekin et al. (2000) conducted experiments where subjects had their oropharyngeal mucosa topically anaesthetised. They experienced swallowing difficulties and aspiration with liquid swallows, which were partially attributable to inadequate sensory inputs necessary for the perception of the bolus volume and viscosity being relayed for initiation and control of swallowing. Kutter et al. (2011) tested

proprioception (knowledge of tongue position and movement in the mouth) and tactile response (of the mechanoreceptors). They found that the tactile mechanoreceptors were responsible for the perception of thickness in semi-solid foods and that proprioception of the tongue had no influence. Furthermore, no correlation between a mouthful size and bolus size has been determined, although Hiiemae et al. (2004) and Okada et al. (2007) observed subjects taking multiple swallows for a single mouthful, for which there were variations between people and the food type.

Adhesion

It is reasonable to expect that adhesion is mostly a result of liquid wicking from the mucosal surfaces, which removes the saliva boundary layer that lubricates food motion across the surface (see Figure 4-4). This increases the coefficient of friction preventing surface slip. There may also be a tactile response where the mucosal surface may detect the removal of the liquid boundary layer. Adhesion can be avoided if wicking behaviour no longer occurs and the saliva boundary layer is restored. Therefore from a model perspective, it is not necessary to predict adhesion (initially), but rather to track the liquid requirements of the food in terms of pore absorption by capillary action, the interstitial saturation and swelling absorption of the food matrix. The mechanisms of these behaviours are described in §4.1.3. Once the food is saturated with liquid, which can be upwards of 50% of its mass, it may or may not be necessary to determine its flow behaviour, such as slurry-like, paste-like, a semi-solid or a highly viscous liquid.

Kokini et al. (1977) state that the tongue and palate can be approximated as two flat parallel plates squeezed together generating a normal force, while moving relative to each other generating a shear force. In their work they defined various mechanical sensory properties such as 'thickness', 'smoothness' or 'slipperiness', which are important to defining the low limit boundary of adhesion for safe swallowing. These are discussed further in the paragraph below with respect to deformation.

Prinz & Lucas (1997) postulated that the criterion for swallowing is when the bolus reaches its peak cohesive force, i.e., when the difference between the cohesive force and adhesive force is greatest. The cohesive force is a measure of the cohesive strength between food particles in the bolus and the adhesive force is that required to separate food particles from the oral lining. Adhesion is also important during stage II transport where a squeeze-back action of the tongue and palate is used to transport the bolus to the oropharynx. An analogy for this process is squeezing a tube of toothpaste (Hiiemae, 2004). Here, the hard palate is non-

deformable whilst the tongue deforms to accommodate the food, and so applies sequentially a pressure which creates a peristaltic wave to propel the food into the pharynx. This indicates that slippage is required at the adhesive boundary between food and the oral surface. Considering each of the approaches above, it is argued here that wicking is the first phenomena that must be avoided, which brings the adhesion to within some proximity of the low limit for safe swallowing.

Particle Size

Particle size is widely regarded as an important criterion for a safe-to-swallow-bolus. Peyron et al. (2004) and Jalabert-Malbos et al. (2007) found that particle size distribution in the bolus is consistent between subjects for similar foods (raw vegetables or nuts) but different between foods. This result indicates that an acceptable particle size threshold may relate to the individual particle properties; for example, the particle size of pasta, at the swallow point, is larger than peanuts (Flynn et al. 2011). Hutchings et al. (2011) embedded peanuts in different food matrices (chocolate and gelatine) and found the size distribution of peanuts in the boluses to be similar despite the gelatine matrix being chewed for nearly twice as many chew strokes as the chocolate. These findings indicate that particle deformation (discussed below) and particle size are linked with respect to the threshold for swallowing. Also, the variation in particle size distribution may be a result of more or less size reduction simply because the bolus has or has not met other swallow threshold criteria. In the study on wheat flake boluses, Peyron et al. (2011) found the d_{50} and bolus hardness values did not change much after the half-way point of mastication, giving further evidence that the initiation of swallowing requires several thresholds to be satisfied. Particle size distribution will also affect the bolus yield properties, by interfering with deformation applied to the bolus at various stages of the swallowing process. In the context of the response surface map obtained from the mechanical sensory testing, detection of particle size is most likely for the identification of outlier large particles that can be preferentially selected for occlusion. A secondary assessment will be angularity.

Particle Deformation

Measurements of particle deformation occur during occlusion by the periodontal mechanoreceptors shown schematically in Figure 4-3. These force-distance maps translate into the important food properties of modulus of elasticity (Young's modulus) and toughness (Williams et al., 2005). The Young's modulus (E) is a measure of stiffness or rigidity and is the linear slope of the stress vs strain graph during elastic deformation. The toughness (R) is the energy required to propagate a crack per unit crack area. For food particles that are basically

two dimensional, toughness mostly dictates the fragmentation (Lucas et al., 2002). The quantity $(R/E)^{0.5}$ is called the displacement index and is of interest if the number of food fragments is limited by the displacement available when the food particle is loaded. Some foods can withstand high strains or displacements before crack propagation begins. For the typical early human or hominid diet, the shape of the cusps have evolved so that foods (eaten at that time) fail by fracture rather than compression or shear, both of which would take more energy [Lucas, ibid.]. The quantity $(ER)^{0.5}$ is important if stress is limiting, where fractures start at or near the cusp and run straight through the material. Thus, these two quantities $(R/E)^{0.5}$ and $(ER)^{0.5}$ describe the progress of particle breakdown. While the periodontal mechanoreceptors give gross information (greater force/low resolution) *cf* the tongue-palate interaction (low force/high resolution), this information is important in defining the work-softening of tough and fibrous foods. Also, they detect the presence of hard bodies amidst what may otherwise be a soft food.

Bolus Deformation

During the mixing circulation of the food within the mouth, the tongue squeezes the bolus against the hard palate and pushes it towards the molars for occlusion (Hiiemae & Palmer, 1999), which allows the deformation properties of the bolus to be measured. Prinz & Lucas (1997) suggested that after compression against the palate the particles either stick together or fall apart. They suggest that falling particles are sensed by the mechanoreceptors in the tongue. A similar line of argument is proposed here, that bolus deformation properties are derived from the rate of change of the normal and shear forces detected by the mechanoreceptors as the bolus is circulated around the mouth. In addition, it is proposed that the variability and distribution of the forces is important particularly in the early stages of mastication when large particles are present. This is not too dissimilar to the case where particles do not stick together, but fall apart as suggested by Prinz & Lucas (ibid.). These mechanoreceptors will also account for the sensation of slipperiness and the presence of free liquid which, if in excess, can be segregated for partial swallow.

As the swallow point approaches, the bolus becomes softer, more homogeneous and paste-like. The forces measured across the tongue will be more evenly distributed and the internal bolus cohesion becomes greater than the adhesion to the oral surfaces. It is reasonable to expect that the deformability must be below some threshold value, indicated by both the magnitude and slope of the plastic deformation part of the stress strain curve. For a fibrous food like meat this describes the threshold for work softening. For crisp foods that release a lot of liquid during occlusion like apples, compression of the bolus by the tongue against the

palate will trap the solid or pulp phase and a response surface of forces will be detected. Partially chewed apple with many firm particles will yield a different response surface to a pulp. This supports the argument that the regularity of the force distribution is as important as the value of the force profile. A regular distribution indicates a homogeneous paste or pulp-like bolus; where the value of the forces averaged across an area indicate the yield properties of that bolus. In this way, a model can be constructed that links the parameters of food type, liquid content and particle size to the deformation properties of the bolus. Through this logic train, a similar model concept to that used by Prinz & Lucas (ibid.) is developed.

4.3.3 Thresholds of Safe Swallowing

The above discussion promotes the bolus properties of temperature, volume, adhesion, particle size, particle deformation and bolus deformation as being determinable from response surface maps of the tongue-palate and periodontal mechanoreceptors. These record the normal and shear stresses as well as distance. For the tongue-palate interaction, distance is both the local deformation of the tongue and the proximate distance between the tongue and palate. These bolus properties change with chewing time until a decision is made to swallow. It has already been postulated that humans have a safe-to-swallow system that balances the energy cost of mastication against the dietary gain for the types of food we evolved to eat. Therefore, having identified the bolus properties that are measured within the mouth, it is now necessary to define the threshold values that allow a safe-to-swallow decision to be made.

The methodology applied here is a chemical engineering methodology called a *hazard and operability study*, or HAZOP, which is applied to the transit passageway from the mouth to the stomach. HAZOP is a risk mitigation tool in plant design. Streams into and out of process unit operations are examined to determine if dangerous unexpected consequences are possible. If so, the design is modified to mitigate or eliminate their effect. When applied to swallowing, evolution is assumed to have already mitigated the consequences in normally functioning humans so that mastication does not result in the unexpected consequences of choking and aspiration. Thus, design changes are not required. Instead, HAZOP is used to reverse engineer the food property thresholds that satisfy this evolutionary outcome.

Hazard Operability Study

The HAZOP procedure examines the streams that leave a unit operation and asks a series of questions about the stream using GUIDE WORDS, such as MORE, LESS and NONE, which are applied to *properties* of the stream such as *temperature*, *composition* and *flow*. In studying the

passage of food from the oral cavity to the stomach, the **properties** selected above are examined. HAZOP explores the possible **causes** of the GUIDE WORD/*property* combination, and then proposes some likely **consequences**. If these consequences are likely to be problematic, **actions** are proposed, which are typically then integrated into the process plant design (e.g., control systems). **Actions**, in the context of swallowing are not to change the design of the passageway or mouth as it would be in a process plant (for the unit operation and piping), but to require that chewing continue until the food is safe to swallow. In this way, the end-point of mastication becomes defined by the food reaching a safe-to-swallow property phase space.

Table 4-1 contains the HAZOP. Each **property** and **guide word** combination then explores the **causes** and **consequences** of involuntary swallowing. **Actions** state the masticatory response needed to avoid the consequence. It is important to note that only the involuntary (natural) swallow is being considered here: of course, it can be overridden consciously even when the natural urge is to chew; e.g., swallowing a large pill.

Table 4-1: Hazard operability study of the passage of food during swallowing. The table explores the cause and consequence of involuntary swallowing food with the property/guide word combination. Actions are inherent within the natural masticatory decision making processes.

Property	**Temperature**	
Guide word	MORE THAN	LESS THAN
Cause	Attempt to eat something that is too hot.	Attempt to eat something that is too cold.
Consequence	Burns the tissues of the mouth and pharynx. Potentially irreversible damage if too hot.	Discomfort.
Action	DO NOT attempt to swallow. Reject and expectorate.	Hold in mouth until an acceptable temperature is reached, or expectorate.
Property	**Volume** Volume refers to the volume of the bolus at swallow	
Guide word	MORE THAN	LESS THAN
Cause	Attempt to swallow a bolus that is greater than a threshold, which relates to the volume able to be transported by peristalsis.	N/a
Consequence	An attempt to swallow a bolus that is too large carries more than one risk: 1. The bolus is too large for safe pharyngeal transit and may leave residue along the transit passageway. 2. A bolus that is too large may hide within it other risk factors, e.g. see **particle size**. Inability to clear the blockage may result in death.	
Action	DO NOT attempt to swallow. Partition food into swallowable volumes that are smaller than the threshold.	
Property	**Adhesion** Adhesion refers to the binding forces between particles of food and the oral mucosal surfaces	
Guide word	MORE THAN	LESS THAN

Cause	1. Unsaturated, dry porous food absorbs moisture by capillary action which removes surface liquid on the mucosa and binds the particles to the mucosa by surface tension. 2. Food that does not have a lubricating layer (early on in mastication sequence) removes the saliva coating which then allows food to adhere to the mucosa.	1. Excess liquid separates from the solid phase of the bolus.
Consequence	1. Food adheres to the mucosal or 'swallow' transit surfaces and remains there after the swallow reflex has finished. If so, this can cause discomfort and may aspirate into the lungs or cause choking. 2. Same as 1.	The liquid could be aspirated if continue to masticate.
Action	DO NOT attempt to swallow. Continue to masticate until adhesion is below a 'safe' threshold. This implies that the threshold requires that several conditions are met; (i) moisture is no longer absorbed from the surrounding mucosal surfaces; (ii). the mucosal surface returns to a saturated state with free liquid at its surface; and (iii) the bolus is saturated so that it has free surface liquid. Note: in its limit, this is satisfied when the bolus is reduced to a pulpy slurry and can be swallowed like a liquid.	Stop chewing. Perform a liquid swallow, whilst retaining the solid phase of the food in the oral cavity. Then continue chewing.
Property	**Particle size** Particle size refers to discrete particles within the bolus. A threshold particle size exists which is a function of particle deformation.	
Guide word	MORE THAN	LESS THAN
Cause	The particle size distribution has not been sufficiently reduced during occlusion such that large outlier particles are present.	N/a. There is no lower limit threshold for mastication.
Consequence	If swallowed, large outlier particles may separate from the bolus and get stuck in the transit passageway and remain there after the swallow reflex has finished. Large particles may penetrate or remove the passageway lubricating linings increasing the likelihood of other particles getting stuck. If so, this can cause discomfort and may later aspirate into the lungs, or cause choking.	
Action	DO NOT attempt to swallow. Continue mastication until particle size and particle size distribution criteria are met.	
Property	**Particle Deformation** Particle deformation refers to the individual particles rather than the bolus	
Guide word	MORE THAN	LESS THAN
Cause	Individual food particles may yield elastically or plastically when an external force is applied. The following are causes for food NOT yielding: 1. Food particles above a small limit size do not yield or break during occlusion (i.e., between the teeth). 2. Food particles above a small limit size are texturally gritty, detected by high friction with the oral surfaces despite having sufficient free liquid (i.e., despite satisfying the adhesion property threshold). These particles also do not yield or break during intra-oral manipulation (i.e., between the tongue and palate), which indicates the particles are angular and tough.	N/a. There is no minimum particle deformation.

Consequence	1. Particles are inedible. Further chewing may damage the teeth. 2. If swallowed, particles may injure the mucosa or may get stuck in pharyngeal transit and during peristalsis. If so, this can cause discomfort and may aspirate into the lungs, or cause choking.	
Action	1. Expectorate inedible particles (which cannot be chewed or digested) 2. DO NOT attempt to swallow. Continue chewing to reduce the particles to below the intra-oral threshold size.	
Property	**Bolus Deformation** Bolus deformation refers to the bolus, not the individual particles held within the bolus	
Guide word	MORE THAN	LESS THAN
Cause	1. The cohesion of the bolus (i.e., the forces binding the bolus together) is less than the adhesion of the particles within the bolus to the mucosal surfaces.	The bolus does not deform sufficiently under the applied stress of the tongue-palate compressions, i.e., the bolus yield stress is too high.
Consequence	1. Consequence is the same as for **adhesion** (see above).	The bolus will not deform sufficiently during the pharyngeal and oesophageal stages of swallowing and could result in choking
Action	1. DO NOT attempt to swallow. Continue mastication to mix in more saliva to reduce surface adhesion (see adhesion above). The criterion may also be satisfied if the cohesive forces between particles become greater than the adhesive forces between the particles and the oral surface (per Prinz and Lucas, 1997); again this is a subset of the adhesion criterion above and is equivalent to wet massing in granulation where the bolus is bound with liquid binder and the mucosal layer is saturated and able to lubricate the bolus surface.	DO NOT attempt to swallow. Continue mastication to work-soften the food matrix.

Phase Space of Safe Swallowing

The outcome of the HAZOP study is a series of criteria that must be satisfied for each property, either as a range or as a threshold. While these are also obtainable from deductive reasoning, the HAZOP procedure provides a formal framework focussed on the safe swallow. Furthermore, in doing this analysis, it is postulated that the swallow point is defined not by individual property thresholds, but by *phase space* of criteria. When the properties fall in this allowable phase space the bolus (or a portion of it) is deemed safe to swallow. Figure 4-6 captures the essence of the argument, that each property has a range and, when masticated, a phase space diagram emerges in which properties change with chew number until they all lie

within a safe-to-swallow zone. The thresholds of the properties are not quantified, because they vary between individuals, change with an individual's dentition (Fontijn-Tekamp et al. 2004, van der Bilt et al. 2006) and are somewhat defined by a person's eating history, although it is expected that thresholds will be generally consistent across food types. On this latter point, while boluses prepared from eating different foods will not have the same properties, it is expected that they will have met the threshold criteria for each food bolus property.

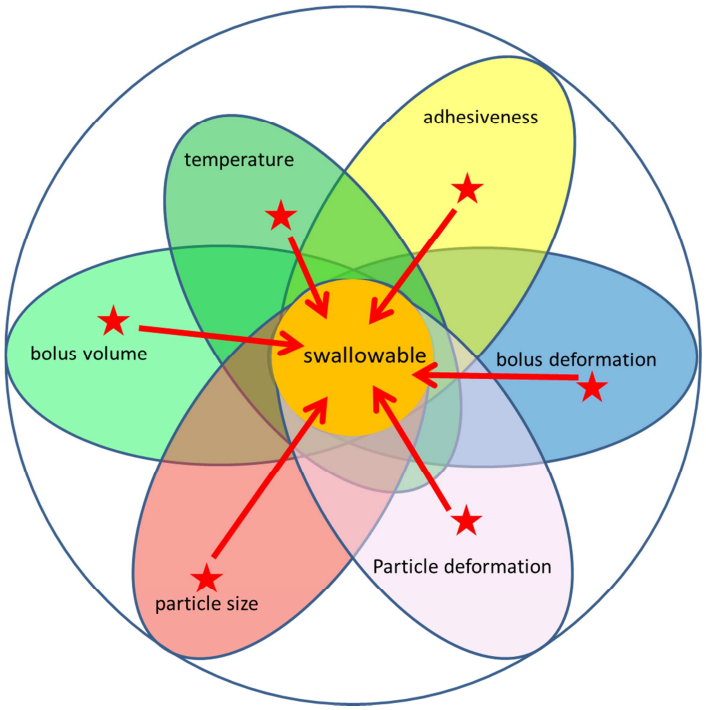

Figure 4-6: Phase space diagram that defines a swallowable region. Stars and arrows indicate the direction of change in properties from the initial chew to the swallow point for a hypothetical food.

4.4 Linking the Rate Processes to the Bolus Properties

The rate processes of breakdown affect the detectable food or bolus properties. Therefore within a modelling framework it is important to develop constitutive relationships to relate these to each other. It is also important in a mathematical framework not to expend unnecessary computational effort. Figure 4-7 demonstrates the connections between the food/bolus properties and the rate processes of breakdown that have arisen in the discussions within this chapter. Importantly, not all rate processes affect each bolus property. Thus, when

the objective is defining the bolus properties at swallow point and the effort required to get there, mastication is reduced from a highly complex process to one that is feasible to model. This is especially the case if the system has no melting or dissolution.

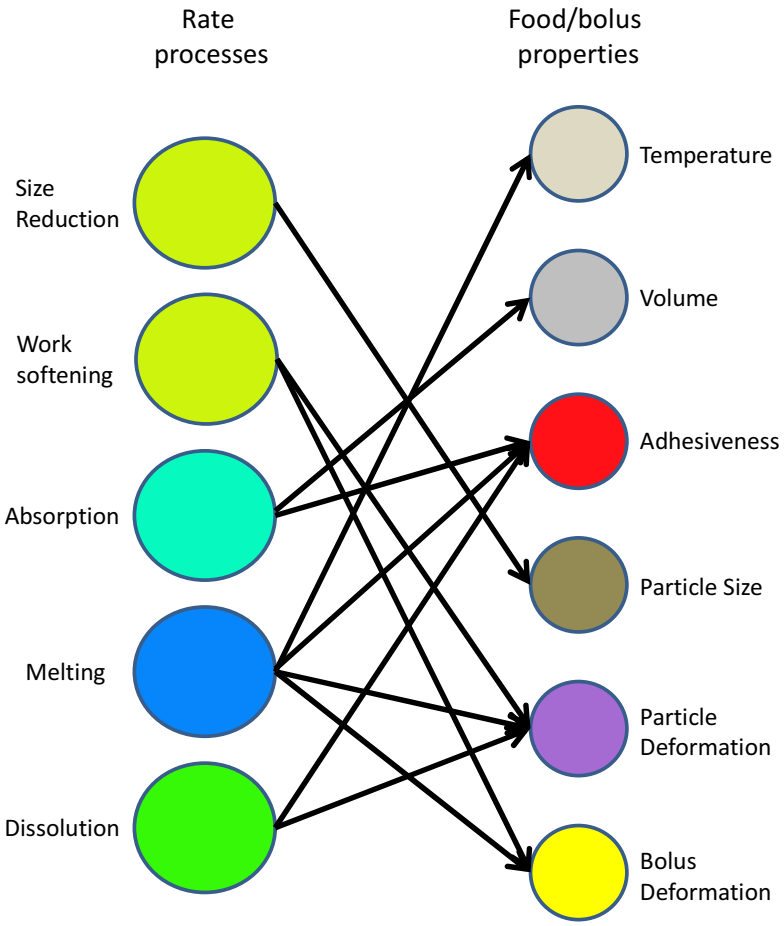

Figure 4-7: Connections between rate processes and the food/bolus properties assessed by the oral structures within the mouth and for which a phase space of threshold values defines a swallowable bolus.

The constitutive relationships that link the rate processes to the food/bolus properties are further discussed in Chapter 5, where the conceptual model is developed into a set of mathematical equations. However, one relationship that needs exploring is the identified link between particle size and particle deformation, this was previously discussed in §2.6.1 and §4.3.2. Here a state diagram (Figure 4-8) is proposed which links the particle properties, namely deformability, with particle size and a swallowable threshold.

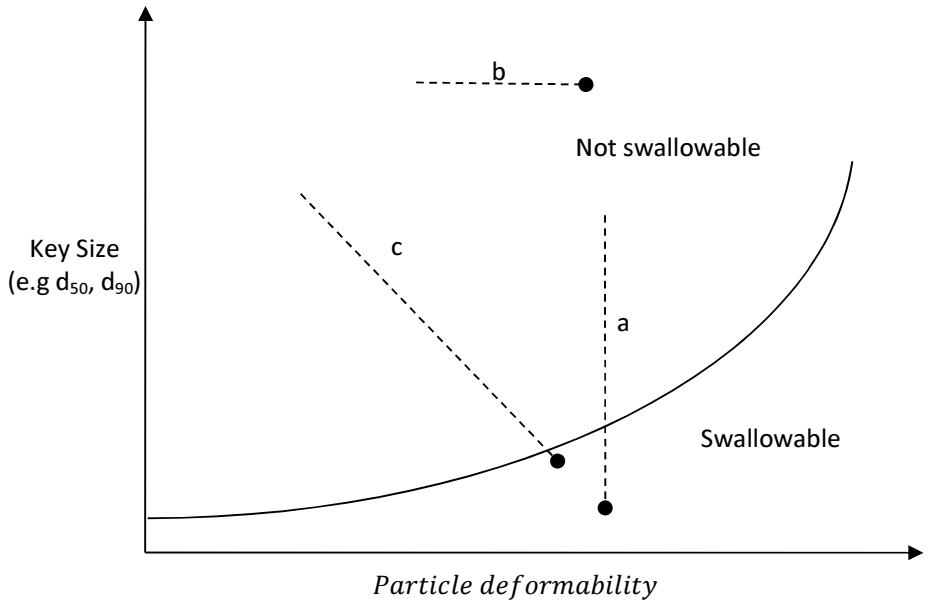

Figure 4-8: Proposed state diagram relating size and particle properties to the swallowable threshold, a) represents a brittle food with constant mechanical properties, , b) represents chewing gum and c) represents a food that work softens and decreases in size.

Above the curve, foods are not swallowable and must be chewed further. Below the curve, foods are swallowable (conditional on meeting the other threshold criteria). Thus, the plot of size versus the inverse fragmentation index is effectively a state diagram, where the properties of the food change with mastication. The diagram shows three contrasting foods, *a* ,*b* and *c*. Food *a* is a brittle food whose properties do not change with chewing. On the state diagram, this represents a vertical movement from the initial particle size to the swallowable threshold. The end point of mastication for these foods is therefore predictable using only a comminution model. Food *b* represents an extreme case such as chewing gum, where size does not change and work-softening does not occur beyond the first few chew strokes and therefore remains in the non-swallowable zone. Food *c* represents a food that work softens and size reduces, possibly via a range of mechanisms; for example, fibre linkages may break, or softening may occur by absorbing heat from the mouth or by mixing in saliva. Such foods will track downward and to the left on the state diagram. This requires a model for how mastication work softens food.

Work softening is detected during occlusion and by compression between the oral surfaces during circulation about the mouth. This was discussed in §4.1.2. The rate of work softening will depend on; (i), the food structure and texture; (ii), the occlusion forces; and (iii), the

frequency of occlusion. Points (i) and (ii) require some measure of how the yield behaviour changes when subjected to the normal and shear forces within the occlusion zone. Here, it is postulated that instead of trying to quantify these forces, a food specific work-index can be used to characterise the rate of change of the fragmentation index as a function of the chew cycles. By specifying a food specific work-index in this way, the forces involved in work softening are assumed to be significantly below the maximum human bite force, thus allowing them to be neglected.

It is necessary to round out this discussion on oral processing by examining the decision-making process of whether to swallow or continue chewing within the context of the conceptual model.

4.5 Decision Making

The conceptual model of Figure 4-5 can be recast as a subset of oral processing which is shown schematically in Figure 4-9 bounded by the dotted line, which also defines the scope of this work, i.e., after the first bite until the terminal swallow. Here, the breakdown of food is based on simulating rate processes which affect the physical properties of the food and saliva mixture which constitutes the bolus. The food is sensed in the mouth which we consciously perceive as the dynamic textural experience of the food. These sensory measurements provide information for the oral food management of the food including jaw trajectory, bite force, circulation, compartmentalisation, selection and liquid-solid separation. Of particular interest here is the decision-making process about whether to continue chewing or to prepare the food for a full or partial swallow. It must be noted that the ensuing discussion focuses on the food and not on the physiology. Also, it is confined to solid food.

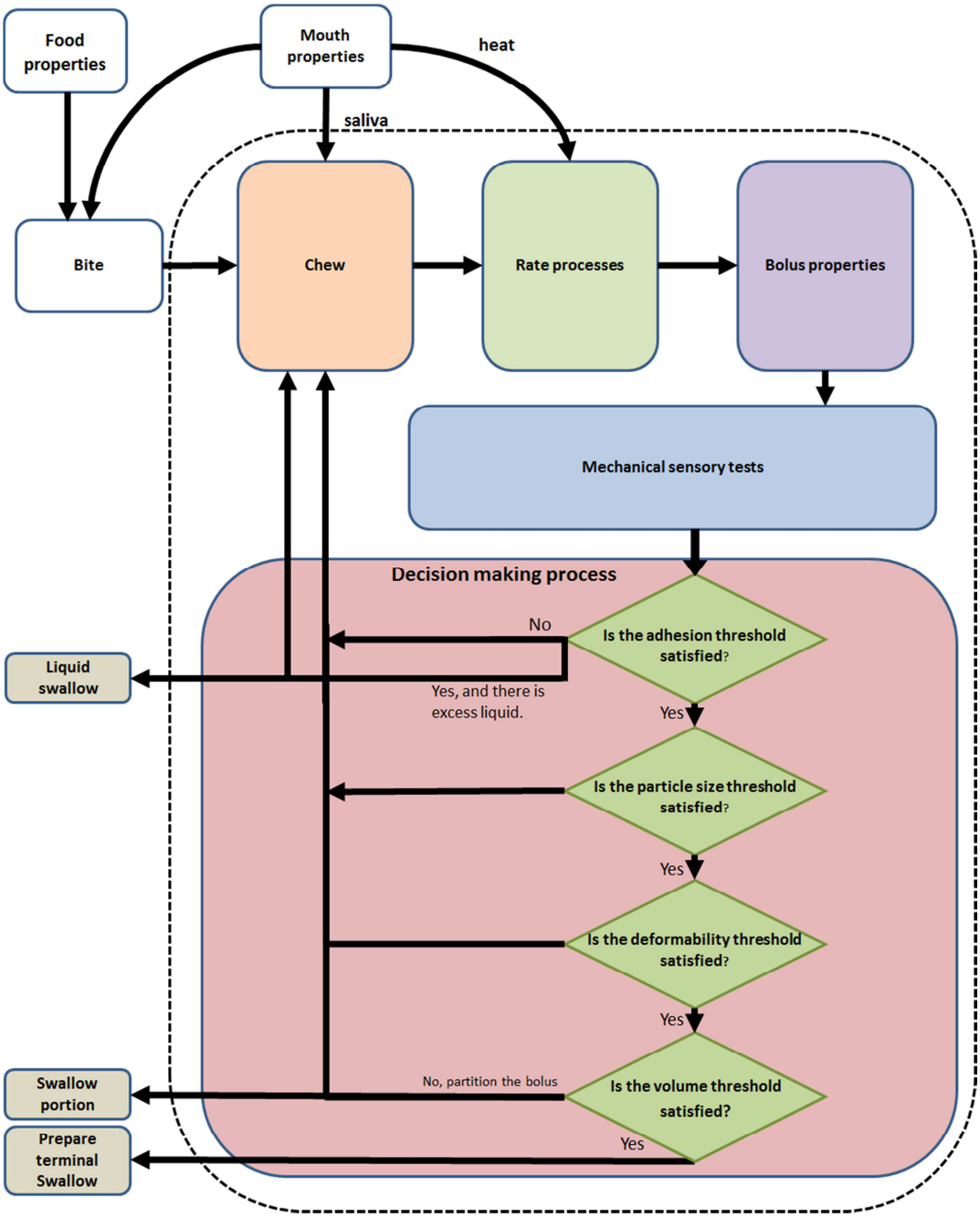

Figure 4-9: Overview of oral processing. The dotted line shows the conceptual mastication model.

By treating the decision-making as a continuous process as the food is mixed (i.e., circulated), the steps involved can be interrogated in more detail. It combines elements from the mouth process model of feeding (Hiiemae, 2004) and from Lucas et al. (2002) with the focus on the decision of swallowing relating to the required bolus properties as discussed in §4.3.3. It is a simplistic overview which is not intended to show every nuance of this complex process in detail. The aim is to demonstrate the linkages between the rate processes and the development of bolus properties which are important to the mechanical sensory tests from

which threshold criteria determine whether the bolus is safe to swallow. It illustrates how modelling of mastication and bolus formation is approached where the typical outcome is a full or partial swallow.

4.6 Conclusions

This work describes a conceptual model which incorporates food breakdown, mixing and testing of the food properties. A chemical engineering approach is taken where the mouth is regarded as a unit operation into which the food, saliva and heat are added and out of which is the swallowed food. It addresses how food is transformed into a bolus and how it is assessed to determine whether it is safe to swallow.

Breakdown is dominated by occlusion. Occlusion of the food both size reduces the particles and work softens them. Other rate processes are also at play, namely absorption, melting and dissolution. Each is described as they affect the food.

Mixing involves stretching, folding and rotation of the food to deliver the most parsimonious energy efficient process to deliver a swallowable bolus. Existing mastication models are strong on particle selection and breakage because these are amenable to mathematical description. While mixing has not been integrated into models, the selection function is the mathematical outcome.

Together, breakdown and mixing can be used to predict how bolus structure changes during mastication. Eventually, the food reaches a safe-to-swallow state. To assist in determining the range of properties the food must have, a methodology called a hazard and operability study (HAZOP) was used, which is common practise in designing chemical process plants. There, it determines what changes are needed to the process design in order to avoid catastrophic consequences. Here, it is performed in reverse, to determine the food properties required to avoid the consequences of choking and aspiration which are very rare in normally functioning humans. The methodology reveals that temperature, volume, adhesion, bolus deformation, particle deformation and particle size are the determinant food properties. Together, these describe a phase-space of threshold properties which each food must achieve in order to be swallowed.

While developing the HAZOP methodology, it was also important to address how the mouth measures food properties. The chapter presents a discussion of the literature on the

mechanoreceptors present in the mouth where the tongue – palate interaction is the most significant. It is revealed that stress can be detected both locally and summatively over an area for both normal and shear components, and that local surface deformation and distance between the tongue and palate can be also detected. This information is then used to propose a conceptual model of the mechanical sensory testing system.

Thus, with the rate processes of mastication described, the role of mixing defined, the mechanical sensory tests framed in engineering terms of response surfaces, and by identifying the threshold properties of a swallowable bolus, this study is now well placed to, somewhat ambitiously, begin to develop the mathematical framework around the conceptual model.

CHAPTER 5 MODEL DEVELOPMENT

Chapter 4 has presented the rationale for a conceptual model of mastication where the rate processes of size reduction, work softening, absorption, dissolution and melting relate to the food properties that are able to be measured in the mouth which are temperature, volume, adhesiveness, particle size and deformability, and bolus deformability. The relationship between these rate processes and properties is paramount in tracking the progress of mastication where the objective to define the amount of mastication effort required to produce a swallowable bolus and the properties of that bolus. This chapter develops the conceptual model into a set of mathematical equations.

The model presented here is generalised; that is, it is not specific to any food type. The basic premise is that solid foods follow the same physical breakdown path where occlusion, i.e., size reduction and work softening, is of primary importance followed by the incorporation of saliva and the other rate processes.

5.1 General Assumptions

The model contains the following assumptions. Most have arisen in the discussion in Chapter 4.

1. The bolus is regarded as having two phases, a mobile interstitial free liquid-phase and a food particle-phase. The liquid-phase may contain, in addition to liquids (e.g., water, alcohols, vinegar, oil), the components of saliva, dissolved solids, molten fats and suspended solids. The particle-phase will contain solid, liquid, and air pores. The solid component may contain dissolvable solids, meltable fats and meltable gels.
2. The bolus occupies a single compartment and is well mixed meaning the interstitial liquid is evenly distributed into the interstitial spaces between the food particles.
3. The properties of the interstitial liquid are calculated using the simple mixture rule based on composition.
4. Saliva flow rate is continuous.
5. The properties of specific heat capacity, and component solubility do not change with temperature.
6. The heat of dissolution is negligible.
7. Constant values of fat and soluble solid densities are used.

8. Melting of fat is temperature dependent and is reliant on the known temperature range and latent heat for melting of fats.
9. Heat transfer into the food is assumed to occur in two steps. First, heat enters the mouth from incoming saliva and the walls of the oral cavity, where heat transfer from the oral cavity is described by an overall heat transfer coefficient. This heat is blended into the well-mixed liquid phase of the bolus by convection (assumptions 1 and 5). Subsequently, heat transfers from the blended liquid phase to the particles.
10. Particles increase in temperature uniformly. The Biot number gives the ratio of the heat transfer resistances inside and at the surface of a body. When this is ≤ 0.1 the internal resistance is low and the body can be assumed to have a uniform temperature. For a spherical food particle in the mouth this occurs when it had a diameter ≤ 0.25 mm. Therefore, this assumption is a gross simplification for large food particles. However, given the short lifespan of solid particles before they are occluded, modelling a temperature profile would add significant complexity without significantly improving the model.
11. A discrete population balance model is used where particles are individually tracked. If particles are below a small size limit they are no longer individually tracked but are attributed to the liquid-phase as suspended solids.
12. Each particle has a chance of being selected for occlusion defined by a selection function.
13. Occlusion causes size reduction and/or work softening. When size reduction occurs, the breakage function is food type dependent. When work softening occurs, the degree of softening is dependent on the initial toughness and Young's modulus of the food and a food specific Work Index.
14. Dissolution occurs from the particle surfaces into the liquid phase. However, generally comminution dominates size reduction and so the effect of dissolution on particle size is negligible and here is manifested only in the change in concentration of dissolvable solids within particles. It is assumed that the rate of dissolution can be approximated by a mass transfer coefficient. The rate of dissolution is constrained by the available free liquid and the concentration gradient. The mass transfer coefficient is food type dependent.
15. Melting occurs when the particle temperature reaches the melting temperature of the fat contained within the particle. This may occur over a range of temperatures for various fat fractions. The rate of melting is constrained by the heat flux. All

molten fat is assumed to transfer from the particle phase to the interstitial free liquid.

16. Occlusion of food can also compress the void volume within porous foods. This is food specific and is defined by a fractional compression per occlusion event.
17. Occlusion of food can express a mobile liquid phase. When size reduction occurs the amount of mobile liquid phase released is proportional to the new surface area created which is both related to subject dentition and the food type. For the latter, some foods (like fresh carrot) fracture through cells, resulting in the liquid from the cells being released, whereas others (like cooked carrot) fracture along cellular boundaries and do not release liquid (Lillford, 2011). For foods that work-soften rather than reduce in size, occlusion can also express a mobile liquid phase where the amount expressed is food type and force dependent. It is assumed to be proportional to the food specific Work Index.
18. Wicking is simplified from the Washburn equation and assumed proportional to the surface area available and the potential for wicking defined by the difference between the liquid saturation and 100% saturation.
19. Swelling by hydration is not considered.
20. The food property thresholds are food dependent.

5.2 System Composition

The bolus system containing the two phases, an interstitial free liquid-phase and a particle-phase, each have components that need to be tracked during mastication. The following subsections describe composition by mass and volume and how they are related by density.

5.2.1 Mass

The bolus contains food particles and interstitial fluid. Every chew cycle, the mass balance is

$$M_{bolus} = M_{liq} + M_{\mathrm{p}} \qquad \textbf{Eq. 5-1}$$

The components are

$$M_{\mathrm{liq}} = M_{\mathrm{liq,\ saliva}} + M_{liq,\ expressed} + M_{liq,\ diss.\ sol.\ solids} + M_{liq,\ molten\ fat,\ oil} \qquad \textbf{Eq. 5-2}$$

$$M_p = M_{p,\ solids} + M_{p,liq} \qquad \textbf{Eq. 5-3}$$

The term, $M_{p,solids}$ is the solid-phase contained in the food particles. It is regarded as including the insoluble solids, the undissolved soluble solids and the solid fat, given by

$$M_{p,\,solids} = M_{\mathrm{p},insol.\,solids} + M_{p,undiss.\,sol.\,solids} + M_{p,solid\,fat} \qquad \textbf{Eq. 5-4}$$

The term, $M_{p,liq}$ is the liquid-phase contained in the food particles, which may be either bound or mobile and residing in pores and may be either water, dissolved, or solids oil given by

$$M_{p,liq} = \; M_{p,liq,water} \; + \; M_{\mathrm{p,\,liq,\,diss.\,solids}} \; + \; M_{p,liq,oil} \qquad \textbf{Eq. 5-5}$$

The definitions are:

- M_{Bolus} is the mass of the bolus [kg];
- M_{liq} is mass of the free liquid phase [kg];
- M_p is mass of the food (particles) [kg];
- $M_{liq,\,saliva}$ is the mass of saliva in the free liquid phase [kg];
- $M_{liq,\,expressed}$ is the mass of expressed liquid in the free liquid phase [kg];
- $M_{liq,\,diss.\,sol.\,solids}$ is the mass of dissolved soluble solids in the free liquid phase [kg];
- $M_{liq.\,molten\,fat,\,oil}$ is the mass of molten fat and oil in the free liquid phase [kg].
- $M_{p,\,solids}$ is the mass of solids in the food particles [kg];
- $M_{p,liq}$ is the mass of the liquid-phase contained in the food particles which may be either bound or mobile and residing in pores [kg];
- $M_{p,\,insol.\,solids}$ is the component of M_p solids that is insoluble solids [kg];
- $M_{p,\,undiss.\,sol.\,solids}$ is the component of M_p solids that is the mass of undissolved soluble solids [kg];
- $M_{p,\,solid\,fat}$ is the component of M_p solids that is the mass of solid fat [kg];
- $M_{p,\,liq,\,water}$ is the component of $M_{p,liq}$ that is water [kg];
- $M_{p,\,liq,\,diss.\,solids}$ is the component of $M_{p,liq}$ that is dissolved solids [kg]; and
- $M_{p,\,liq,\,oil}$ is the component of $M_{p,liq}$ that is oil [kg];

The volume of the bolus consists of particles and an interstitial space between the particles. The particles may contain solid, liquid and air in pores, and the interstitial space may contain liquid and air.

$$V_{bolus} = V_{\mathrm{interstitial}} + V_{\mathrm{p}} \qquad \textbf{Eq. 5-6}$$

The components are

$$V_{interstitial} = V_{interstitial,liq} + V_{interstitial,air} \qquad \textbf{Eq. 5-7}$$

$$V_{\mathrm{p}} = V_{p,solid} + V_{p,liq} + V_{p,air} \qquad \textbf{Eq. 5-8}$$

The term $V_{interstitial,liq}$ is the volume of the fluid occupying the interstitial space within the bolus, which has the components

$$V_{interstitial,liq} = V_{interstitial,saliva} + V_{interstitial,expressed} + V_{interstitial,\ diss.\ solids} + V_{interstitial,\ molten\ fat,\ oil} \qquad \textbf{Eq. 5-9}$$

The term $V_{p,solid}$ is the solid component of the particle-phase and has the sub-components

$$V_{p,solid} = V_{p,insol.\ solids} + V_{\mathrm{p},undiss.\ sol.\ solids} + V_{\mathrm{p},solid\ fat} \qquad \textbf{Eq. 5-10}$$

The term $V_{p,liq}$ is the liquid component of the particle-phase and has the sub-components

$$V_{p,liq} = V_{p,liq,water} + V_{p,liq,diss.\ solids} + V_{p,liq,oil} \qquad \textbf{Eq. 5-11}$$

The definitions for the volume composition equations are:

- V_{bolus} is the volume of the bolus [cm^3];
- $V_{interstitial}$ is the volume of the interstitial space between the particles but within the volume of the bolus [cm^3];
- V_p is the volume of the food particles [cm^3];
- $V_{interstitial,liq}$ is the volume of the liquid-phase occupying the interstitial spaces [cm^3];
- $V_{interstitial,\ air}$ is the volume of air occupying the interstitial spaces [cm^3];
- $V_{interstitial,\ saliva}$ the component of $V_{interstitial,\ liq}$ that is saliva [cm^3];
- $V_{interstitial,\ expressed}$ the component of $V_{interstitial,\ liq}$ that is expressed from the food [cm^3];
- $V_{interstitial,\ diss.\ solids}$ the component of $V_{interstitial,\ liq}$ that is dissolved solids [cm^3];
- $V_{interstitial,\ molten\ fat,oil}$ the component of $V_{interstitial,\ liq}$ that is the molten fat and oil [cm^3];
- $V_{p,solid}$ is the volume of the solid-phase within the food particles [cm^3];
- $V_{p,liq}$ is the volume of the liquid within the food particles [cm^3];
- $V_{p,air}$ is the volume of the air within the food particles [cm^3];
- $V_{p,\ insol.\ solids}$ is the component of $V_{p,solid}$ that is insoluble solids [cm^3];
- $V_{p,\ undiss.\ sol.\ solids}$ is the component of $V_{p,solid}$ that is undissolved soluble solids [cm^3];
- $V_{p,\ solid\ fat}$ is the component of $V_{p,solid}$ that is solid fat [cm^3];
- $V_{p,\ liq,\ water}$ is the component of $V_{p,liq}$ that is water [cm^3];
- $V_{p,\ liq,\ diss.\ solids}$ is the component of $V_{p,liq}$ that is dissolved solids [cm^3]; and
- $V_{p,\ liq,\ oil}$ is the component of $V_{p,liq}$ that is oil [cm^3].

The degree of saturation is a well-known parameter which defines the progress of powder granulation using a liquid binder (Hapgood, 2000). It is defined by the ratio $V_{interstitial,\ liq}/(V_{interstitial,\ liq} + V_{interstitial,\ air})$ using the terms in Eq. 5-7. As the degree of saturation increases from a dry basis, it reaches a value where the cohesion of the powder (or here the bolus) is greatest. Further increases result in it becoming a paste (called wet massing in granulation) then a slurry. However, in mastication, the interstitial pore volume is impossible to measure because the food is continually being circulated. An alternate approach is needed. Because the objective is to define a threshold for the adhesiveness criterion (§4.3.3), it is proposed here that such an objective is reached when a critical excess liquid content is reached. The ratio of interest then becomes $V_{interstitial,liq}/V_p$. This then means that the unknown $V_{interstitial,air}$ is not required in Eq. 5-7.

5.2.2 Density

Density links mass and volume. The aim here is to practically link them, two simple tests are possible. The first is the drying test which evaporates the water and can be done at a temperature (including freeze drying) which avoid melting fats. The second is the immersion test which can determine the open pore volume. Given that the drying test removes water and assuming no other volatiles are removed, the water-free food density is

$$\rho_{food} = \frac{\left(M_{particle} - M_{dried}\right)}{V_p - V_{p,water} - V_{p,air}} \qquad \textbf{Eq. 5-12}$$

where the undefined terms are:

- $M_{particle}$ is the mass of the particle prior to the drying test [kg]; and
- M_{dried} is the mass after the drying test [kg].

The denominator contains $V_{p,water}$ whereas Eq. 5-8 above contains $V_{p,liq}$. Because the simple evaporation test only separates the water component, which means that equation Eq. 5-12 is an approximation of the solid-phase density of the food, i.e., $\rho_{food} \approx \rho_{p,solids}$. This is reasonable because $V_{p,liq}$ will generally only be slightly larger than $V_{p,water}$ where the difference is associated with liquid-phase dissolved solids and oils.

The food solid-phase density also equates to the sum of the ratios of mass fraction and component densities, which is important when accounting for mass flow between phases. Constant values of fat and soluble solid densities are used.

$$\rho_{p,solids} = \frac{1}{\left(\frac{X_{p,insol.solids}}{\rho_{p,insol.solids}} + \frac{X_{p,sol.solids}}{\rho_{p,sol.solids}} + \frac{X_{p,solid\ fat}}{\rho_{p,solid\ fat}}\right)} = \frac{M_{p,solids}}{V_{p,solids}} \qquad \textbf{Eq. 5-13}$$

where

- $X_{p,insol.solids} = M_{p,insol.solids}/M_{p,solid}$ and $\rho_{p,insol.solids}$ are the mass fraction and density of the insoluble solids [-, kg m^{-3}];
- $X_{p,sol.solids} = M_{p,sol.solids}/M_{p,solid}$ and $\rho_{p,sol.solids}$ are the mass fraction and density of the soluble solids [-, kg m^{-3}]; and
- $X_{p,solid\ fat} = M_{p,solid\ fat}/M_{p,solid}$ and $\rho_{p,solid\ fat}$ are the mass fraction and density of the solid fats [-, kg m^{-3}].

5.3 Governing Equations

Four balances are important in mastication: mass, volume, heat and population. Each balance is tracked for both the mobile liquid-phase and particle-phase within the mouth. Volume is important to track the porosity of the particles and to track progress towards the adhesiveness threshold for swallowing. The heat balance is important because fats and gels melt to release liquid. The population balance is important because it defines the available surface area necessary for the rate processes of absorption, dissolution and melting. It also defines particle size and when particles are occluded which is important for progressive work-softening. Each balance is presented below.

Size reduction, compression of pore volume, and expression of liquid occur at occlusion. The other rate processes are time dependent and occur between chews. The length of time between chews is determined by the chewing frequency.

5.3.1 Rate of Change of Mass

For food already in the mouth, the dynamic mass balance is given schematically in Figure 5-1.

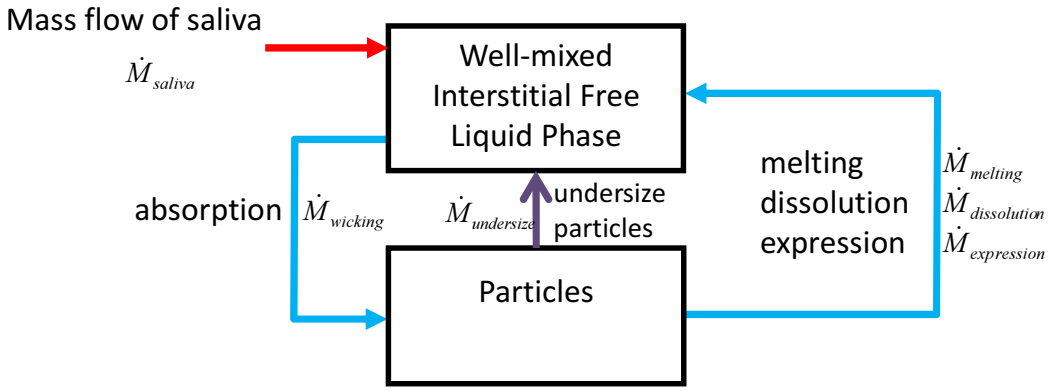

Figure 5-1: Mass flow balance within the oral cavity during mastication. Saliva is the only addition of mass during mastication. Flows of mass occur between the food particles and the interstitial free liquid phase due to processes of wicking absorption, the release of molten fats, dissolution of soluble solids and expression of liquid from food during occlusion. Small particles below a threshold size are also assumed to enter the liquid phase.

The overall rate of increase in system mass is $\dot{M}_{saliva}$ if no intermediate swallow has occurred, which relates to the net rates of change of material between the free liquid and particle phases,

$$\frac{dM_{\text{bolus}}}{dt} = \dot{M}_{\text{saliva}} = \frac{dM_{\text{p}}}{dt} + \frac{dM_{\text{liq}}}{\text{dt}} \qquad \textbf{Eq. 5-14}$$

The rates of change of mass of each phase are given respectively by

$$\frac{dM_{\text{p}}}{dt} = \dot{M}_{\text{wicking}} - \dot{M}_{\text{p,undersize}} - \dot{M}_{\text{melting}} - \dot{M}_{\text{dissolution}} - \dot{M}_{\text{expression}} \qquad \textbf{Eq. 5-15}$$

$$\frac{dM_{\text{liq}}}{dt} = \dot{M}_{\text{saliva}} + \dot{M}_{\text{p,undersize}} + \dot{M}_{\text{melting}} + \dot{M}_{\text{dissolution}} + \dot{M}_{\text{expression}} - \dot{M}_{\text{wicking}} \qquad \textbf{Eq. 5-16}$$

The constitutive equations for the rate terms are discussed after the rate balances

5.3.2 Rate of Change of Volume

For food already in the mouth, the dynamic volume balance is given schematically in Figure 5-2.

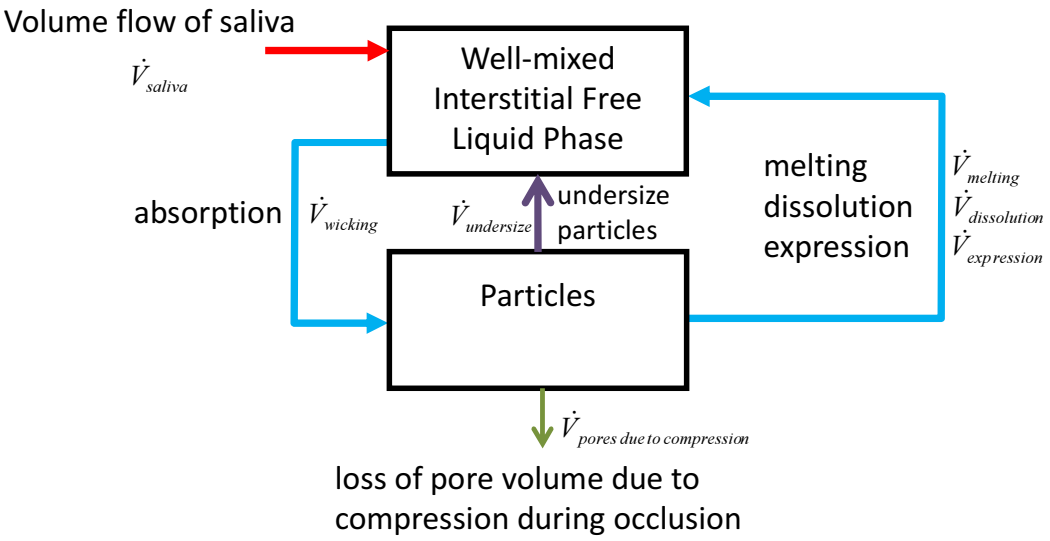

Figure 5-2: Volume flow balance within the oral cavity during mastication. Only saliva enters the oral cavity, which enters into the well-mixed interstitial free liquid phase. Subsequently there is a volume flux between the free liquid-phase and particle-phase due to the rate processes of wicking absorption, melting, dissolution of soluble solids, expression of liquid from foods at occlusion and some transport of undersize particle which are below a threshold are assumed to exist in suspension in the liquid. Occlusion can also cause some loss of pore volume in porous foods.

The overall rate of increase in system volume is $\dot{V}_{saliva}$ -$\dot{V}_{pores\ due\ to\ compression}$ if no intermediate swallow has occurred, which relates to the net rates of change of material between the free liquid-phase and particle-phases,

$$\frac{dV_{bolus}}{dt} = \dot{V}_{saliva} - \dot{V}_{pores\ due\ to\ compression} = \frac{dV_p}{dt} + \frac{dV_{liq}}{dt} \qquad \textbf{Eq. 5-17}$$

The rates of change of volume of each phase are given respectively by

$$\frac{dV_p}{dt} = \dot{V}_{wicking} - \dot{V}_{p,undersize} - \dot{V}_{melting} - \dot{V}_{dissolution} - \dot{V}_{expression} - \dot{V}_{pores\ due\ to\ compression} \qquad \textbf{Eq. 5-18}$$

$$\frac{dV_{\mathrm{liq}}}{dt} = \dot{V}_{\mathrm{saliva}} + \dot{V}_{\mathrm{p,undersize}} + \dot{V}_{\mathrm{melting}} + \dot{V}_{\mathrm{dissolution}} + \dot{V}_{\mathrm{expression}} - \dot{V}_{\mathrm{wicking}} \qquad \textbf{Eq. 5-19}$$

The constitutive equations for the rate terms are discussed after the rate balances.

5.3.3 Rate of Change of Heat

This work does not consider foods that are hotter than the oral cavity, which are generally expectorated. Neither does the work consider frozen foods. A schematic of the heat balance is shown in Figure 5-3. The heat that enters particles goes to sensible heating and phase change of fat to oil.

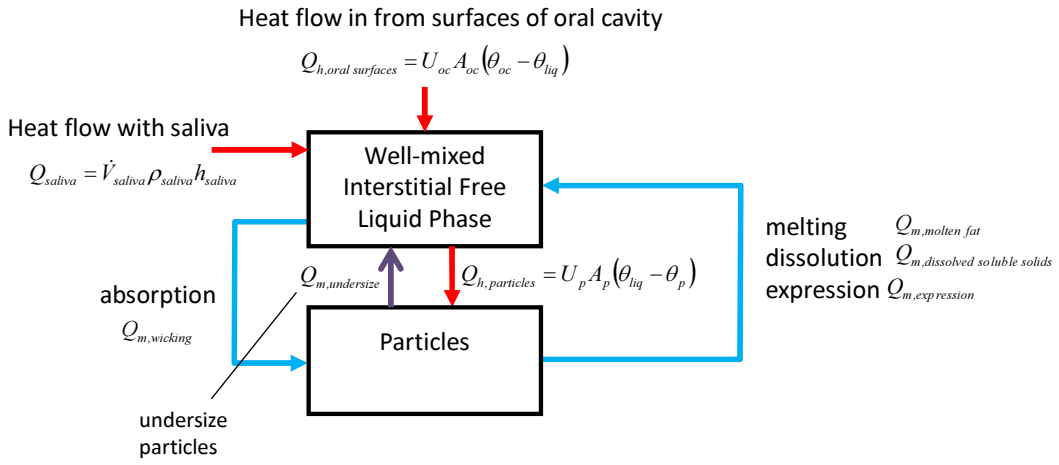

Figure 5-3: Heat balance within the oral cavity during mastication. Heat is added from saliva and the walls of the oral cavity to the well-mixed interstitial free liquid-phase. From here, it transfers between the particles and the liquid-phase by heat convection and mass convection. The mass convection processes are wicking absorption, melting, dissolution of soluble solids, expression of free liquid during occlusion and some transport of undersize particle which are below a threshold are assumed to exist in suspension in the liquid. There are no heat losses from the oral cavity. *U* is the overall heat transfer coefficient [W m^{-2} K^{-1}], C_p is the specific heat capacity [J kg^{-1} K^{-1}], $\dot{V}_{saliva}$ is the saliva flow rate [m^3 s^{-1}], *A* is area [m^2], *M* is mass [kg]. Subscripts *saliva*, *oc*, *liq* and *p* are saliva, oral cavity, interstitial liquid and particle respectively.

The heat flow into the bolus from the saliva and heat transfer through the walls of the oral cavity then flows into the well-mixed interstitial free liquid-phase and the particle-phase, given by

$$Q_{bolus} = Q_{m,saliva} + Q_{h,oral\ surfaces} = Q_{liq} + Q_p \qquad \textbf{Eq. 5-20}$$

The component heat flows to the liquid and particle-phases are described by

$$Q_{liq} = Q_{m,saliva} + Q_{h,oral\ surfaces} + Q_{m,moltenfat} + Q_{m,diss.sol.solids} + Q_{m,expressedliq} + Q_{m,undersize} - Q_{h,liq-to-particles} - Q_{m,wicking} \quad \textbf{Eq. 5-21}$$

$$Q_p = Q_{h,liq-to-particles} + Q_{m,wicking} - Q_{m,moltenfat} - Q_{m,diss.sol.solids} - Q_{m,expressedliq-Q_{m,undersize}} \quad \textbf{Eq. 5-22}$$

The mass of the dissolved soluble solids is very small and therefore the influence on the heat balance is negligible. It is assumed that expression of liquid from particles and the transfer of the undersize particles to the liquid phase occur instantaneously at occlusion. Therefore, the accumulation of heat in the two phases between chew strokes is,

$$\frac{d\theta_{liq}}{dt} = \frac{\dot{V}_{saliva}\rho_{saliva}C_{p,saliva}\theta_{saliva}}{M_{liq}C_{p,liq}} + \frac{U_{oc}A_{oc}(\theta_{oc} - \theta_{liq})}{M_{liq}C_{p,liq}} - \sum_{i=1}^{i=n_t} \frac{U_pA_{p,i}(\theta_{liq} - \theta_{p,i})}{M_{liq}C_{p,i,liq}} - \frac{\dot{M}_{wicking}C_{p,liq}\theta_{liq}}{M_{liq}C_{p,liq}} \quad \textbf{Eq. 5-23}$$

and the temperature of a given particle between chew strokes is,

$$\frac{d\theta_{p,i}}{dt} = \frac{U_pA_{p,i}(\theta_{liq} - \theta_p)}{M_{p,i}C_{p,p,i}} + \frac{\dot{M}_{wicking}C_{p,liq}\theta_{liq}}{M_pC_{p,p,i}} \quad \textbf{Eq. 5-24}$$

The temperature of the liquid phase after occlusion is the equilibrium temperature resulting from the assumed instantaneous mixing of the existing liquid phase with the newly formed undersize particles and any expressed liquid.

$$\theta_{liq,n+1} = \frac{M_{liq}C_{p,liq}\theta_{liq,n} + M_{undersize}C_{p,p}\theta_p + M_{expressed}C_{p,p}\theta_p}{M_{liq,n}C_{p,liq,n} + M_{undersize}C_{p,p} + M_{expressed}C_{p,p}} \quad \textbf{Eq. 5-25}$$

If a particle is at the melting temperature of its solid fat component, the heat gained by the particle melts the fat and the particle temperature remains constant and the left hand side of **Eq. 2-25** is zero, the rate of melting is explained in §5.4.5.

The terms are defined as follows:

- θ_{liq}, θ_p, θ_{saliva} and θ_{OC} are the temperatures of the interstitial free liquid-phase, the particle, the incoming saliva and the walls of the oral cavity respectively [K];
- $\dot{V}_s$ is the saliva flowrate [$m^3\ s^{-1}$];
- A_{OC} is the active area of the oral cavity between which the food is mixed, i.e., the top surface of the tongue and the palate [m^2];
- $C_{p,liq}$ and $C_{p,p}$ are the specific heat capacities of the saliva, liquid phase and particles respectively which are determined by the mixture of the component specific heat capacities [kJ $kg^{-1}\ K^{-1}$];
- $h_{fat\text{-}to\text{-}oil}$ is the latent heat of fat melting [kJ kg^{-1}];
- U_{oc} is the overall heat transfer coefficient (*HTC*) for the oral cavity to the interstitial liquid [W $m^{-2}\ K^{-1}$];
- U_p is the HTC for the interstitial liquid to the particles [W $m^{-2}\ K^{-1}$]; and

Of particular interest are the two heat transfer coefficients (*htc*), the oral cavity *htc* U_{oc} which is assumed universal to all foods but person (subject) dependant and the free liquid to particle *htc* U_p which is expected to be food dependent. Further research is recommended to establish the true relationships.

5.3.4 The Rate of Change of Particle Population

The population balance is, by definition, discrete because occlusion dominates the death and birth of particles. A discrete approach is taken here which is also supported by the fact that size analysis is discrete, done by sieving or image analysis, and that mastication often starts with one or a few particle(s) and continues only for about 40 chew cycles. This discrete approach is further justified because each particle has seven properties that need to be tracked; these are size, insoluble solid content, solid fat content, solid-phase soluble-solid content, liquid volume, air void volume, inverse fragmentation index and temperature. To do this effectively, particles in the bolus are individually tracked through all chew cycles. Particles 'die' if they are occluded whereby they give birth to new 'daughter' particles, and in being reborn, they carry their other properties within them. When particles are comminuted below a lower limit threshold size they are not tracked, but their volumes are summed together and thereafter are regarded as suspended solids in the liquid-phase. This approach is practical because numerous particles in the low micron range can become computationally expensive. Figure 5-4 shows a schematic of the population balance.

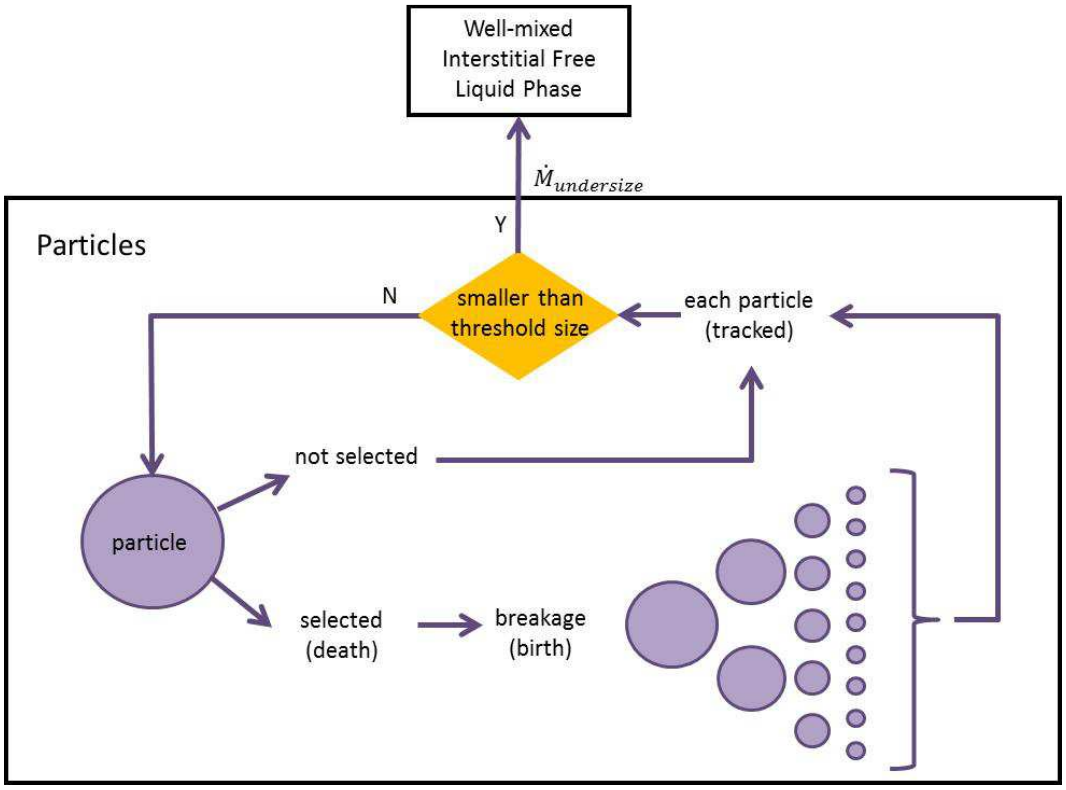

Figure 5-4: Discretised population balance within the oral cavity during mastication. Particles are tracked individually. A particle selected for occlusion is recorded as a death and the resulting daughter particles are births. Any particles that fall below a threshold size are no longer tracked; their death means their mass and volume are apportioned to the interstitial free liquid-phase.

Mathematically, the population can be represented by an array, V_p, where the elements are individual particles with some volume, V_i. If particles less than the threshold size are created from occlusion, their volume is summed and apportioned to the liquid-phase as described previously in the mass and volume balances.

where $V_p = \begin{bmatrix} V_1 \\ V_2 \\ \vdots \\ V_{i-1} \\ V_i \\ V_{i+1} \\ \vdots \\ V_{max} \end{bmatrix}$

The particles in V_p are sorted into size classes, i, where i ranges from the minimum threshold size to the maximum size class used to describe the PSD. The PSD is given by the array $N_{t,k}$ whose elements are the number of particles in each size class, k, denotes the chew number.

$$\underline{\underline{N}}_k = \begin{bmatrix} n_{1,k} \\ n_{2,k} \\ \vdots \\ n_{i-1,k} \\ n_{i,k} \\ n_{i+1,k} \\ \vdots \\ n_{max,k} \end{bmatrix}$$

At occlusion all particles in the same size class are assumed to have the same chance of being selected. This selection chance is calculated from either the size dependent power law (Eq. 2-6) or the two-way competition selection model (Eq. 2-15). For the array of particles V_p, another array is generated with the corresponding chance of selection for each particle V_i. To determine if a particle is selected a random number is generated from a uniform distribution for each particle. If the random number is less than the theoretical selection chance the particle is selected.

These selected particles 'die' and undergo breakage producing daughter particles. Breakage is approximated by a continuous breakage function $B(X,X_i)$ of 'cumulative fraction less than' where the particle undergoing breakage has characteristic dimension X_i and the function gives the cumulative fraction less than size X. **Eq. 2-22** and **Eq. 2-23** give common breakage functions used in mastication. To discretise this, it is necessary to calculate the volume fraction falling within the bin of a single size class; this is achieved by calculating the difference $B(X_j,X_i)$-$B(X_{j-1},X_i)$ where the subscript j refers to the size classes from j=1 to j=i, after occlusion of a particle of size X_i. For a particle in size class X_i the volume of births in size class X_j is given by

$$Volume_{births,j,i} = V_i \left(B\left(X_j, X_i\right) - B\left(X_{j-1}, X_i\right) \right) \qquad \textbf{Eq. 5-26}$$

For each j from j=1 to j=max, the array of birth volume for all size classes for particle X_i is given by,

$$Total\ Volume_{,births} = V_{births} = \begin{bmatrix} \sum_{i=1}^{i=\max} \left(B\left(X_1, X_i\right) - B\left(0, X_i\right)\right) V_i \\ \sum_{i=1}^{i=\max} \left(B\left(X_2, X_i\right) - B\left(X_1, X_i\right)\right) V_i \\ \vdots \\ \sum_{i=1}^{i=\max} \left(B\left(X_{j-1}, X_i\right) - B\left(X_{j-2}, X_i\right)\right) V_i \\ \sum_{i=1}^{i=\max} \left(B\left(X_j, X_i\right) - B\left(X_{j-1}, X_i\right)\right) V_i \\ \sum_{i=1}^{i=\max} \left(B\left(X_{j+1}, X_i\right) - B\left(X_j, X_i\right)\right) V_i \\ \vdots \\ \sum_{i=1}^{i=\max} \left(B\left(X_{\max}, X_i\right) - B\left(X_{\max-1}, X_i\right)\right) V_i \end{bmatrix} \quad \textbf{Eq. 5-27}$$

This matrix allows the number of birth particles in each size class to be calculated. The breakage process described by Eq. 5-27 is applied to all the selected particles. The newly created particles are combined with the unselected particles and a new array V_p is obtained. The MATLAB® model which generates the population balance is explained in Appendix F.

5.3.5 Work Softening

Work softening is the change in mechanical properties of the food due to occlusion with or without size reduction. Earlier discussion (see §4.1.2) proposed that a food specific work-index, W_I, be used to characterise the rate of change of the inverse fragmentation index, $(E/R)^{0.5}$, as a function of the number of occlusion events experienced by the food, where R is the toughness [Pa] and E is the Young's modulus [Pa] of the initial food. By specifying a work-index in this way, the forces involved in work softening are assumed to be significantly below the maximum human bite force, thus allowing them to be neglected. It is proposed that the work index influences the inverse fragmentation index by the following relationship, which is determined for each particle upon occlusion

$$\left(\frac{E}{R}\right)_{k+1}^{0.5} = W_I \left(\frac{E}{R}\right)_k^{0.5}, \qquad \text{where } \left(\frac{E}{R}\right)^{0.5} > \left(\frac{E}{R}\right)_{min}^{0.5} \quad \textbf{Eq. 5-28}$$

where k is the chew number and noting that when the food particle is not selected for occlusion, there is no change in $(E/R)^{0.5}$. The work index, W_I = 1 for brittle foods that do not change their properties. Therefore, all other foods have $W_I < 1$.

The property $(E/R)^{0.5}$ is carried by each particle. However, the work-soften threshold criteria relies also on the particle size distribution as discussed in §4.4, where a food independent (generic) state diagram defines a threshold boundary for the two properties considered together. After each occlusion event the model updates the inverse fragmentation index and particle size distribution then locates the position of the food on the state diagram which is a plot of the d_{90} (by mass) *vs* the inverse fragmentation index, $(E/R)^{0.5}$. The d_{90} is chosen due to the hazard associated with large particles (see HAZOP §4.3.3). Each particle is compared to their threshold value (see Figure 4-8). If its location on the state diagram falls below the threshold curve, then the deformation criteria is satisfied.

Further research is recommended to validate this approach.

5.4 Constitutive Relationships

These relate the terms of the dynamic mass balances to the measured variables.

5.4.1 Flowrate of Undersize Particles

The difference in mass between successive chews represents the mass of undersize which is apportioned to the liquid-phase as suspended solids. Including the time interval between chews converts this to a rate suitable for the mass (and volume) balances given previously,

$$\dot{M}_{undersize} = \frac{\underline{\underline{M}}_{k+1} - \underline{\underline{M}}_{k}}{\Delta t_{chew}} \qquad \textbf{Eq. 5-29}$$

5.4.2 Compression

Compression of porous particles may reduce their void volume. The degree to which this occurs is a food specific (and complex) parameter and further work is recommended to explore both how this could be measured and an appropriate form of mathematical representation, which will need to cover the range of behaviours from brittle porous to soft porous foods. Here, a simple approach is proposed, that the air volume, V_{air}, of the occluded particles is reduced by some fraction, $f_{compression}$, for each chew event. The particle volume after occlusion for a single particle (where the '$|_p$' indicates for a single particle,

$$V_{p,air,k+1}\big|_p = f_{compression} V_{p,air,k}\big|_p \qquad \textbf{Eq. 5-30}$$

noting that when particles are not occluded, $V_{air,k+1}|_p = V_{air,k}|_p$. When aggregated across all particles in the system, and divided by the chew period, Δt_{chew}, gives the dynamic rate of change of volume, $\dot{V}_{pores\ due\ to\ compression}$.

5.4.3 Expression

Expression of liquid from particles occurs when particles are cleaved across cellular boundaries (see §3.3.2). The liquid release by this mechanism will be proportional to the new surface area created, but also to the quantity of liquid residing within the occluded particles and will be food specific. Expression will also result from compression of the food due to stress-strain work-softening which may force liquid out of the food via internal cell rupture or simply compression of the food structure: this mechanism will be important for tough, fibrous foods. Again, future research is recommended to determine how expression can be measured and an appropriate mathematical construct for a food specific rate function to cover the range of food behaviours. Combining these influences we propose a two term relationship. The first term relates the liquid expression to the creation of new surface area and the amount of liquid residing in the occluded food. The second term relates the expression to the Work Index: brittle foods with W_I=1 will not express liquid. Both parameters $f_{expression}$ and f_{work} are food specific. For a single particle after occlusion the updated volume of liquid contained in that particle is

$$V_{k+1,p,liq}\Big|_p = f_{\exp ression} A_{p,i}\Big|_p V_{k,p,liq}\Big|_p + f_{work}\left(1 - W_I\right) V_{k,p,liq}\Big|_p \qquad \textbf{Eq. 5-31}$$

where $A_{p,i}|_p$ refers to the surface area of the particle being occluded.

5.4.4 Rate of Dissolution

Dissolution is the transfer of soluble solids from the surface of food particles into the liquid phase. Soluble solids are typically salts and sugars. The model assumes dissolution is proportional to the surface area of the particles and is defined by a velocity and a potential for mass transfer. For the k^{th} chew cycle and for a single particle (denoted by the '$|_p$' nomenclature), the rate of dissolution is

$$\dot{M}_{k,dissolution}\big|_p = k_d \rho_{k,p,sol.solids} A_{p,i}\big|_p \left(X_{p,sol.solids}\big|_p - X_{liq,diss.sol.solids}\big|_p \right) \quad \textbf{Eq. 5-32}$$

where k_d [m s^{-1}] is the mass transfer coefficient, $A_{p,i}|_p$ is the area of a particle [m^2], $X_{p,sol.solids}$ is the soluble solid mass fraction [kg kg^{-1}] in the particle-phase, $X_{liq,diss.sol.solids}$ is the concentration of soluble solids in the interstitial liquid phase [kg kg^{-1}].

Aggregating over all particles gives the mass and volume rates of dissolution, $\dot{M}_{dissolution}$ and $\dot{V}_{dissolution}$, where they are related by the mean density of dissolvable solids, $\rho_{p,sol.solids} = \frac{M_{p,sol.solids}}{V_{p,sol.solids}}$. When performing these calculations, it is also assumed that the change in particle size is negligible during dissolution, because size reduction is a more dominant mechanism than dissolution. The aggregate mass lost from the particles is accounted for by reducing the particle-phase dissolvable solids concentration, for the next chew cycle, $\rho_{k+1,p,sol.solids}$.

5.4.5 Rate of Melting

The net heat flow into the particles is given by Eq. 5-22. At first heating is sensible until the melting temperature of the fats is reached, here it is assumed that the solid fat melts at a fixed temperature. At this point, further inflow of heat is not associated with a temperature rise until the fat has melted, which means the left hand side of Eq. 5-22 equals zero. Thus, for the *i*th particle in the bolus, the rate of change of its mass due to melting is,

$$\frac{dM_{p,i}}{dt} = \frac{U_p A_{p,i} \left(\theta_{liq} - \theta_{p,i} \right)}{h_{fat-oil}} \quad \textbf{Eq. 5-33}$$

and when divided by the density of the molten fat, corresponds to a volumetric rate, $\dot{V}_{melting} = \dot{M}_{melting} / \rho_{liq,oil}$, noting that there may be a (negligibly small within modelling error) volume change between the volume of fat lost and the volume of oil created.

A gel is a unique case where there are no insoluble solids and where dissolution and melting are both concentration and temperature dependent. For gels with a melting temperature

above 37°C, the melting is limited by the diffusion of sucrose from the gel surface, described by Eq. 5-32. As sucrose diffuses from the surface of the gel the concentration of sucrose in the surface layer is lowered which consequently lowers its melting temperature below 37 °C. If the gel melting temperature is below the mouth temperature, melting is relatively fast and limited by the thermal diffusion into the gel. Wright and Hills (2003) showed that the melting of gelatine gels could be descried by

$$dV_{p,i} = -A_{p,i} v_m dt \qquad \textbf{Eq. 5-34}$$

where V_p is the volume of the gel, A_p is the surface area and v_m is the melting velocity (m s^{-1}).

5.4.6 Rate of Absorption

Wetting of dry foods occurs by addition of saliva which is wicked into particles and into the interstitial spaces. The dynamics of the wicking phenomenon are discussed in §4.1.3 and occurs into the open pores and interstitial spaces. It is distinct from swelling of the solid food matrix through hydration, which is not considered here. Wicking need only be calculated for dry foods.

The overall rate of moisture uptake into a particle will be food specific and will depend on a wicking velocity, as simplified from the Washburn equation. An averaged wicking velocity can be experimentally determined for a food by measuring the absorption rate into a known pore volume across a known surface area. (See §4.4.1 for further justification of this approach.) Foods that do not absorb liquid simply have a wicking velocity of zero. Absorption of liquid into the particles will slow down as it nears saturation. The mass and volumetric wicking rates are

$$\dot{V}_{wicking}\Big|_p = k_{wicking}\, A_i\Big|_p \left(X^*_{k,p,liq} - X_{k,p,liq}\right) \qquad \textbf{Eq. 5-35}$$

$$\dot{M}_{wicking}\Big|_p = \rho_{k,liq} \dot{V}_{wicking}\Big|_p \qquad \textbf{Eq. 5-36}$$

where $K_{wicking}$ is the mass transfer rate constant (ms^{-1}) $X^*_{k,p,liq} = \left(\rho_{k,liq} V_{k,p,air} + M_{k,p,liq}\right) / M_{k,p}$ is the saturation liquid content of the particle at the k_{th} chew cycle if all the pores volume were filled with liquid and $X_{k,p,liq} = M_{k,p,liq} / M_{k,p}$ is the actual liquid content. Aggregated over all

particles gives the rates of mass and volume transfer due to wicking and associated heat flow, $\dot{M}_{wicking}$, $\dot{V}_{wicking}$ and $Q_{wicking}$.

5.5 Thresholds to a Swallowable Bolus

The proposed thresholds define a set of criteria that the bolus must meet in order to be swallowed. They are derived from the *HAZOP* analysis in §4.3.3. The following summarises how these are met in the model. The discussion is generic realising that the individual thresholds will be food specific, thus numerical values are not defined here.

Temperature: The temperature of the liquid phases and the solid particles is tracked in the model; however, foods where their temperature presents a safety issue which would prevent a safe swallow from occurring are beyond the scope of this work.

Volume: The volume of the bolus (particle-phase plus liquid-phase) is tracked with mastication. If it exceeds an upper limit threshold then the food has to be partially swallowed. The model, as developed to date, does not include partial swallowing.

Adhesiveness: This threshold requires that no wicking occur and that an excess of interstitial free liquid-phase be present to ensure that the bolus is appropriately lubricated. When too much excess liquid is detected a partial swallow is required. The adhesiveness of the bolus is defined by the ratio of the interstitial free liquid to the solid phase.

Particle size and deformability: The threshold is defined by the state diagram relating particle size to the inverse fragmentation index. Occlusion both reduces particle size and work-softens the particles which approach the threshold with successive occlusion events.

Bolus deformability: The work softening of food is primarily responsible for the bolus reaching its deformability threshold. For particulate boluses this can be satisfied by sufficiently reducing the particle size and a safe-to-swallow threshold can be predicted from the relationship between particle size and inverse fragmentation index (as defined above). For boluses which do not contain easily identifiable particles, cooked steak for example, the bolus deformability is the important threshold. For foods undergoing work softening, this is an avenue for future research where the deformability of the bolus needs to be quantified and related to a change in bolus properties by a work index (see §5.3.5)

Thus, the model as presented here has the potential to determine the end point of mastication when sufficient particle size reduction and work-softening has occurred, when wicking no longer occurs, and when sufficient excess liquid-phase is present to ensure the bolus is

sufficiently lubricated. The case studies in chapter 6 explore the bolus properties to determine the validity of these relationships in defining a safe swallow point.

5.6 Model Implementation

The model framework is shown schematically in Figure 5-5. This diagram demonstrates how the model of food breakdown is implemented. The MATLAB ® for the model described in Figure 5-5 is given in Appendix E.

Firstly the initial conditions of the system need to be defined. This includes specifying the size and constituent properties of the food before the first bite. Subject and food dependent parameters such as chewing frequency, saliva flow rate, and selection/breakage function variables. The rate constants and important parameters for dissolution, absorption and melting are specified. The number of chew strokes and number of simulations are also user inputs.

The outputs of the model are the particle size distribution, total bolus volume, the volume, temperature and composition of the interstitial liquid and the individual particles. The model can either run for a specified number of chew strokes or until some predefined bolus criteria are satisfied.

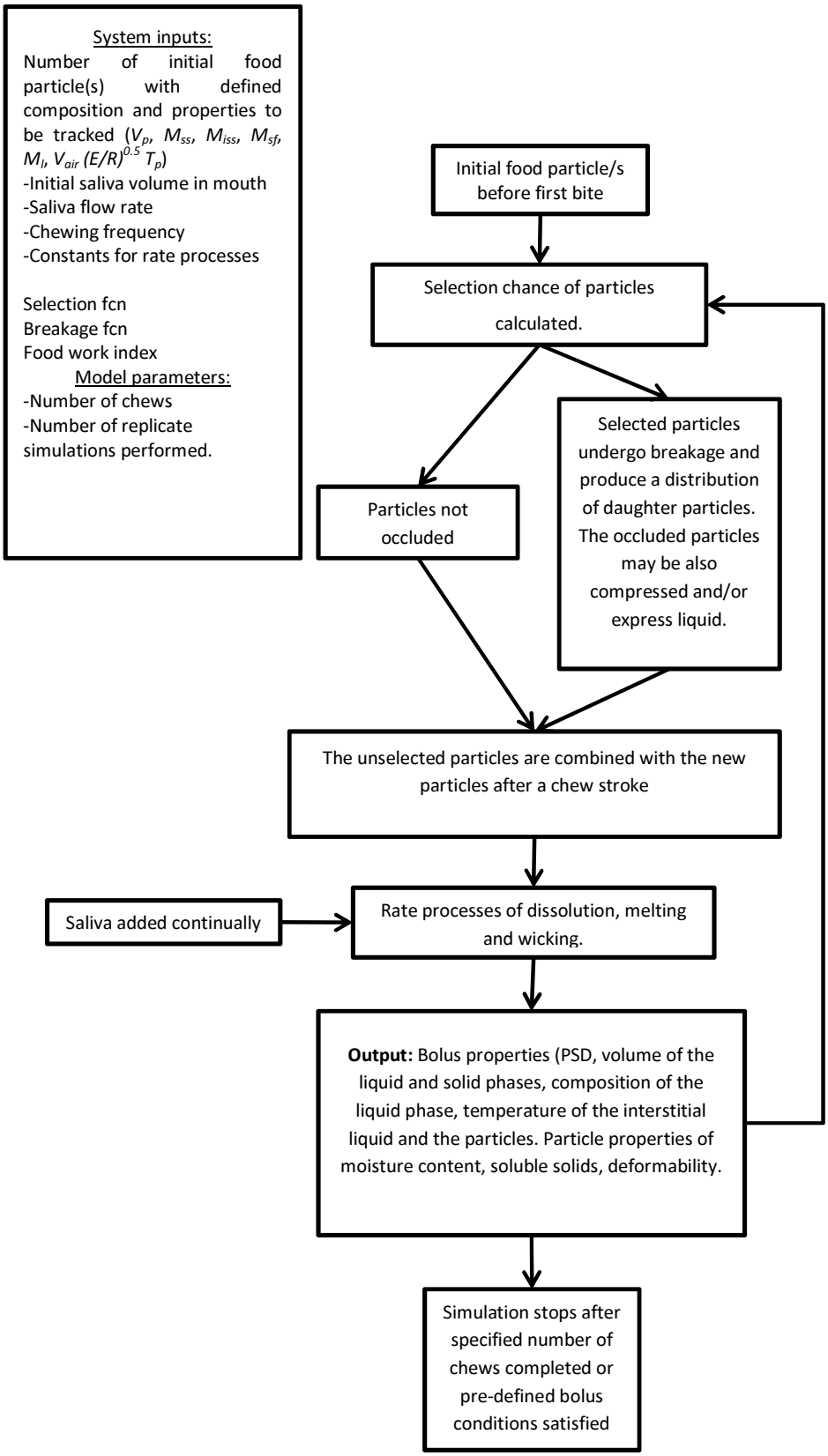

Figure 5-5: Process flow diagram showing schematically how the model is implemented.

5.7 Summary

The model presented here can be used to simulate the solid food bolus during oral processing. The discrete population balance simulates food breakdown using selection and breakage functions. This defines the PSD of the bolus as a function of chew number. Particle size is fundamentally important as in conjunction with the particle properties it can give an indication of the swallowability of the bolus. The surface area of the particles is also important for the rate processes; here the absorption of the liquid, dissolution of soluble solids and melting for the individual particles are all defined. The particle size reduction and the rate processes allow the breakdown pathway of a wide range of solid foods to be examined.

The applicability and versatility of the model is tested in the following chapter where it is applied to three case study food systems with contrasting properties; (i) brown rice, (ii) sweetened gelatine gel and (iii) peanuts embedded in two food matrices (chocolate and gelatine).

CHAPTER 6 CASE STUDIES

In the previous chapter the mathematical model framework was developed which allows the bolus to be simulated as a function of chew number. In this chapter the model is applied to three case studies which demonstrate the model. The mastication of brown rice is examined first where the PSD of the rice is modelled using selection and breakage functions. A sweetened gelatine gel is the focus of the second case study, there are two key processes at play; size reduction at occlusion and melting at the surface of the gel between chew strokes. In the third case study the PSD of peanuts embedded in chocolate, and gelatine matrices is examined. This is done in two parts; firstly only the peanuts are considered and comminution model is used to examine how the matrix influences the selection of the peanut particles. Secondly the matrix component of the food is incorporated and melting is included for the chocolate and dissolution for the gelatine.

6.1 Case Study One – Brown Rice

Brown rice was chosen for this study primarily for two reasons. First, it is a food that has not featured prominently in the literature on oral processing. Second, because rice forms a particulate bolus it is a suitable choice to apply the mechanistic competition model of selection developed by van der Glas et al. (1992) which has not been previously applied to simulations of real food boluses.

Brown rice is interesting in that in contrast to most foods, a mouthful consists of many particles which are already small; however, a large number of chews are required before swallowing. While size reduction is achieved through occlusion, the swallowable bolus end-point appears to be constrained by saliva addition which is needed both to form a suitably deformable bolus and to lubricate in order to prevent adhesion of the rice to the oral surfaces during swallowing. In a six subject study involving five types of rice the number of chews to reach swallow point was 30.23 ± 12.6 (mean ± stdv) (Moongngarm et al., 2012).

In this case study the main objective is to simulate the particle size distribution and the interstitial liquid content of the rice bolus during mastication. The model characterises mixing by the two-way competition selection function and size reduction by the breakage function, which describes the distribution of daughter particles resulting from occlusion. The parameters for selection and breakage were obtained from a series of single chew studies with a single

subject. The following section covers the methodology and experiments followed by a discussion of the pertinent results.

6.1.1 Methodology

Subject Screening and Selection

Two subjects were used in this study. The first subject was taking part in a study undertaken by another researcher within the institute (Moongngarm et al., 2012). The study was approved by the Massey University ethics committee (Southern A Application 09/22). Additional bolus data was obtained from one subject for analysis and modelling in this case study. The second subject was selected using the screening method outlined in §6.3.1. They were chosen because their bite weight and number of chews for both food bars were consistent and within one standard deviation of the population mean (Table 6-1). The study was approved by the Massey University ethics committee (Southern A Application 11/33). The advertisement and questionnaire used to select the subject for this study is contained in Appendix B.

Table 6-1: Bite weight and number of chews Crunchie and Fruit and Nut bars of previous population and the selected subject (mean ± SD).

	Bite weight	Number of chews	n
Population (Crunchie)	6.43±2.46	21.4±5.23	10
Subject (Crunchie)	5.91±0.51	19.2±2.4	1
Population (Fruit and Nut)	8.84±3.22	39.7±18.0	10
Subject (Fruit and Nut)	8.14±0.45	35.2±2.1	1

Rice Preparation

Cooked brown rice (*Oryza sativa*) was used in this study and was prepared immediately before a session with each subject. Whole rice grains were cooked using an electronic rice cooker following manufacturer's instructions using a water-to-rice ratio of 3:1 (v/v). After cooking, rice samples (50-80g) were placed in a plastic container and kept warm at 60±2°C. The rice was served to the subject after cooling down to approximately 40°C, which is the temperature at which rice is commonly consumed.

Experimental Procedure for Bolus Collection

The first subject's natural serving size and number of chews to swallow point were determined in a previous study by Moongnarm et al. (2012). To determine natural serving size and swallow point the subject was instructed to take rice using a tablespoon from a container as they would do at home. The rice in the container was weighed before and after the subject took a

spoonful of rice to record the portion size. The natural swallow point of the subject was determined by having them chew the spoonful of rice in a natural manner and swallow when they felt the need to do so. This was repeated three times with the subject having some water between each spoonful of rice. The number of chews taken to reach the swallow point was counted and when the subject swallowed the bolus they raised their hand to signal they had finished. The serving size for the experiments where the boluses were collected was fixed and set at the average natural serving of the subject. The subject had a natural swallow point of 32 chews and a serving size of ≈10 g. Two further trials were performed to obtain measurements on bolus particle size and moisture content after various numbers of chews.

Bolus collection from the first trial

The subject was given a spoonful of rice and was instructed to take it and chew naturally and expectorate the bolus when instructed to do so into a pre-weighed plastic container. The container was stored on ice before analysis with the Mastersizer. The subject was asked to rinse their mouths before and after chewing the rice. Boluses were collected after 8, 16, 24, 32 or 40 chews; the subject did not know when they would be expectorating the bolus. Three replicates of each chew number were completed and the order was randomised, a total of 15 boluses were collected. No boluses were collected before 8 chews as the particles were too large for the Mastersizer, the boluses collected after swallow point were collected to see if there was significant particle size reduction if the bolus was chewed past the normal swallow point. The bolus properties including bolus mass, moisture content, and solid loss were analysed within the day of collection.

Bolus collection from the second trial

The second subject's natural mouthful and chew number to swallow point was determined in the same way as the first subject. Boluses were collected at two extra chew intervals in the early stages of mastication in order to get a better understanding of how the PSD of the bolus changes after a limited number of chews. The wet sieving method had the advantage over the Mastersizer that it allowed for analysis of the larger particles. Boluses were collected after 2, 4, 8, 16, 24 chews and at the subjects natural swallow point. The subject was instructed to chew naturally and expectorate if instructed to do so or to continue chewing until they felt the urge to swallow at which point they would expectorate into a pre-weighed container. After expectorating the subject took a sip of water and swished it around in their mouth to collect particles that were retained in the oral cavity after expectoration of the bolus. The rinsings were collected in a separate container. A total of six replicates of each chew number were

performed and they were conducted in a random order, four replicates were used for PSD analysis using the wet sieve method and were stored prior to analysis by freezing at -20°C. The other two replicates were used to measure the total solids recovered and incorporated saliva and were dried without sieving. The collected mouth rinsings from all of the samples were dried without sieving. This was done because it was assumed that the mass balance closes; that is, the ingested solids are expectorated in the bolus and the rinsings, and so when rinsings are dried, the solid component of the bolus is calculated by difference.

Measuring the Particle Size Distribution

Two methods of particle size analysis were employed in this work. The boluses from the first subject were analysed with a Mastersizer S (Malvern Instruments ltd, Malvern UK), and wet sieving was used on the boluses from the second subject.

The Mastersizer S (Malvern Instruments Ltd, Malvern, UK) uses laser light diffraction. It is equipped with a 1000-mm lens which allowed for analysis of particles between 5 and 3500 μm. The whole food bolus of rice was dispersed in distilled water at ambient temperature (20 ± 2 °C) until an obscuration of 20-25% was obtained. The sample was placed in chamber dispersion for 2-3 min to ensure particles were independently dispersed and thereafter maintained by stirring during the measurement. This method expresses size distributions as a percentage of the total volume occupied in the laser chamber by the particles.

In the second trial, the PSD was measured by a wet sieving. A series of six sieves with apertures 0.355, 0.5, 0.71, 1.0, 1.4, 2.0 and 2.8 mm were used. Smaller sieves were not used as they were below the range of focus for this study. The expectorated bolus was poured onto the 2.8 mm sieve and washed for 30 seconds using tap water at a flow rate of 2 L/min and each subsequent sieve was also washed for 30 seconds. Particles from each sieve were recovered and put in pre-weighed confoil containers which were stored in a desiccator at 20°C. These were transferred to a drying oven where they were dried at 105°C for 24 hours.

The mass and volume of the cooked rice kernels was determined as this information was needed for the model. The density of the cooked rice was determined by the water displacement method. Cooked rice was added to a graduated cylinder and weighed; water was added so that the rice was fully submerged and the volume of the rice and water were recorded. To determine the average individual particle volume, a spoonful of cooked rice kernels were weighed and then spread out on a petri dish and a scanned image was taken. The particles were counted using image J ® software.

Single Chew Experiments

The second subject also participated in a series of single chew experiments. These were conducted to obtain information on the selection and breakage dynamics of the rice to assist in model development, in particular to determine the parameters of the selection and breakage functions. Selection is dependent on the number occluded or damaged particles in a single chew stroke whilst breakage is dependent on the distribution of daughter particles.

The method for the single chew experiments was adopted from van der Glas et al. (1992) where the dental rubber optosil was used as a test food. Either half or whole cooked rice grains were counted out and weighed on a spoon, Table 6-2 shows the different number of particles offered. Half rice kernels were obtained by cutting whole cooked kernels in half with a scalpel blade. The subject was instructed to take the rice in their mouth and to perform a number of pseudo chewing motions without occluding the particles. This enabled the particles to become naturally dispersed and to produce a normal amount of saliva. The subject was then instructed to conduct a real chew. The rice was then expectorated into a plastic sample container and stored on ice. The subject took a sip of water and swished it around in their mouth to collect any remaining particles before expectorating into a separate container which was also stored on ice. Storage on ice was important to minimise the hydrolysis of starch by the salivary α-amylase before the samples were analysed. The samples were later transferred to a petri dish so that the number of un-chewed particles could be counted. Sips of water were taken by the subject between samples to ensure no particles remained stuck in the oral cavity. The replicates for each sample were analysed together; the particle size distribution was determined using the wet sieving method outlined above, except only three sieves were used 2.8, 1.0 and 0.35 mm, i.e., a $2^{1.5}$ series. A total of 54 single chew experiments were conducted over two sessions. In each session three replicates of each different combination were served and the order of serving was randomised.

Table 6-2: Number of either whole or half kernels served in the single chew experiments and the number of replicates

	Number of particles served	Number of replicates
Whole kernels	10, 20, 40, 80, 120	6
Half kernels	20, 40, 80, 160	6

Moisture Content of Rice and Bolus Saliva Content

Before each session, the dry solids content of the rice was determined by drying four replicates of ≈ 10 g of the prepared cooked rice in a pre-weighed confoil container at 105°C for 24 hours.

The saliva added to the bolus was calculated from the difference between the mass of rice in the bolus and the total bolus mass, given by Eq. 6-1.

$$M_{saliva} = M_{bolus} - \frac{M_{(d)bolus}}{S_{rice}} \quad \textbf{Eq. 6-1}$$

Where M_{bolus} is the mass of the expectorated bolus, $M_{(d)bolus}$ is the mass of dried solids in the bolus and S_{rice} is the solids content of the cooked rice. Saliva added to the bolus was calculated for the two replicate boluses that were dried without sieving. This was necessary because the dry solids mass of the bolus was not able to be calculated accurately after sieving due to the significant fraction that passed through the 355 µm sieve. The other two replicates were sieved.

6.1.2 Results and Discussion

PSD of the Bolus measured with the Mastersizer

The particle size distribution of the rice bolus for a range of chews is shown in Figure 6-1 and Figure 6-2, where Figure 6-2 uses a log scale which aligns with the way the Mastersizer data is presented (as a power series) and which provides the normalisation necessary to directly compare distributions.

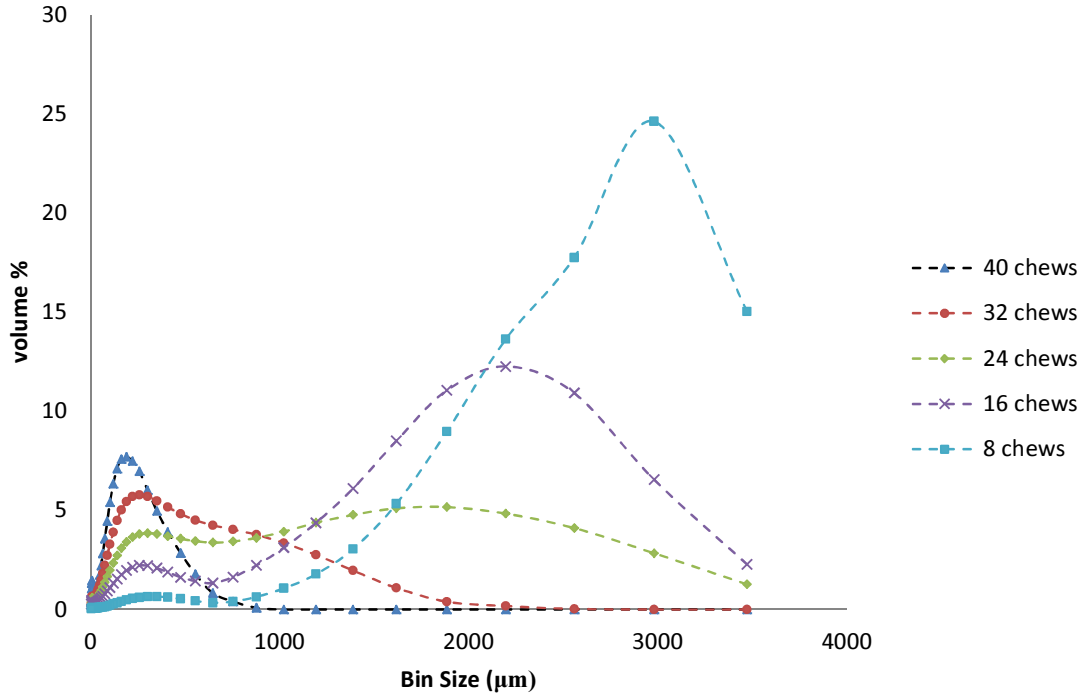

Figure 6-1: PSD of the fractional volume versus the characteristic dimension of rice particles sampled at selected chew numbers. The characteristic dimensions are presented by the Mastersizer in a power series but are plotted here on a linear scale.

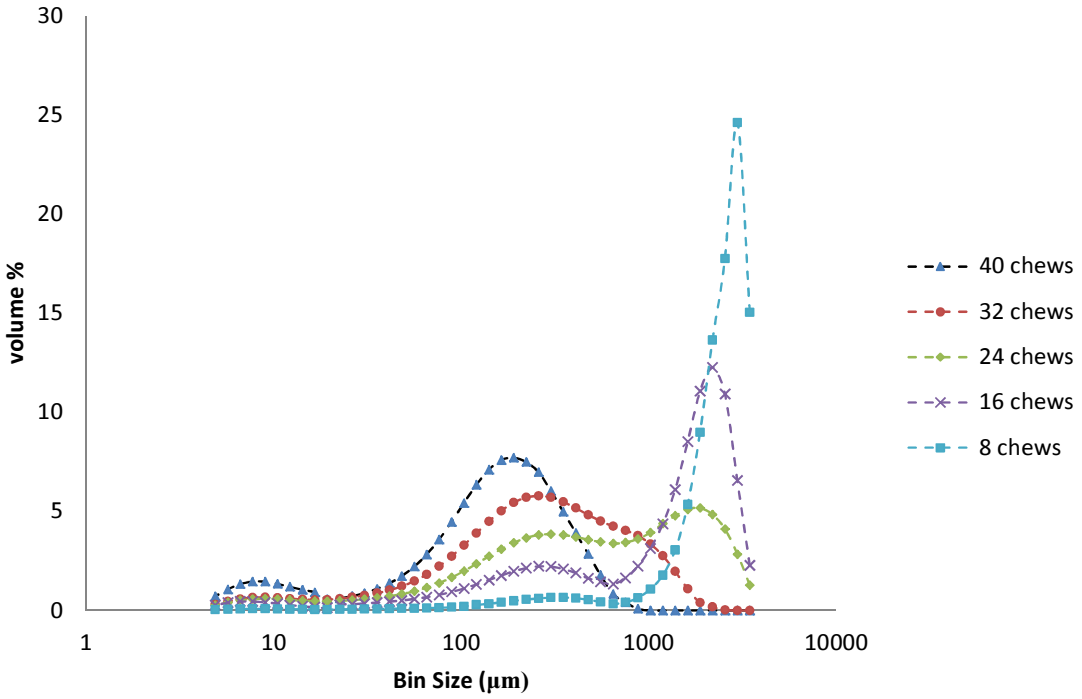

Figure 6-2: PSD of the fractional volume versus the characteristic dimension of rice particles sampled at selected chew numbers. The characteristic dimensions are presented by the Mastersizer in a power series as shown here by the logarithmic scale. .

As mastication proceeds, the rice bolus forms a bi-modal distribution which begins to emerge after 8 chews and is particularly evident at 16 and 24 chews with two distinct peaks in the distribution. After 8 chews 94% of the bolus still consists of particles greater than 1.6 mm in diameter, but this fraction quickly reduces to 49.2%, 23.6% then 1.7% for 16, 24 and 32 chews. Correspondingly, the proportion of smaller sizes increases with a noticeable minimum point between the two peaks of the distribution around 650-750 µm, which increases as a proportion of the PSD from 24 chews. This indicates the mechanism of size reduction where selected large particles are cleaved into one or a few large particles and the remaining pasted into small particles. This mechanism can be called *cleave and paste* where pasting is indicative of significant size reduction. From 24 chews the remaining cleaved particles enter the 650-750 µm size band, but by now the bolus is also becoming relatively cohesive and the *cleave and paste* mechanism reduces to simple *pasting without cleaving*, as shown by the significant shift in the PSD between 32 and 40 chews.

The *cleave and paste* mechanism results in a bi-modal size distribution that can be described quantitatively by a mixed Weibull function,

$$Q = \pi\left(1 - exp\left(-1\left(\frac{X}{d_{50,1}}\right)^{b_1}\right)\right) + (1-\pi)\left(1 - exp\left(-1\left(\frac{X}{d_{50,2}}\right)^{b_2}\right)\right) \quad \textbf{Eq. 6-2}$$

where Q is the volume fraction of particles with a size smaller than X, π is the mixing weight which is the proportion of particles in the smaller distribution, and d_{50} and b are the scale and shape parameters. The scale parameters are the median particle size (i.e. d_{50}) for the respective distributions and shape parameter relates to the width of the distribution, where larger values of b indicate a narrower distribution.

Table 6-3: Fitting parameters for mixed Weibull distribution to the rice bolus for various chew numbers.

Chew number	8	16	24	32	40
π	0.086	0.478	0.544	0.666	0.997
b_1	1.14	0.79	1.03	1.34	1.28
$d_{50,1}$	314	250	272	217	180
b_2	4.37	4.29	1.97	1.93	3.19
$d_{50,2}$	2620	2129	1662	801	700
r^2	0.999	0.999	0.999	0.998	0.997

The mixed Weibull distribution fits the PSD of the bolus very well as demonstrated by the high r^2 values. The values of the fitting parameters confirm the qualitative observations about the distribution. The volume fraction (1-π) of the larger distribution decreases with chew number and the mean size of particles in this distribution also become smaller. The smaller distribution (π) had a more consistent median size, decreasing by a 30% from 8 to 32 chews, compared with 70% for the larger distribution. In the next section, the boluses from the second subject were analysed by wet sieving instead of laser diffraction. The two methods are then compared.

PSD Measured Using Wet Sieve Analysis

The PSD of the rice boluses produced from the second subject after varying degrees of mastication are discussed here. In order to close the mass balance, the methods described in §6.2.1 were employed, which needed to account for the solids in both the bolus and the rinsings. Figure 6-3 shows the dried solids recovered from the boluses and rinsings when the collected samples were either sieved, or not sieved. The obvious difference shows that wet sieving results in less recovered solids.

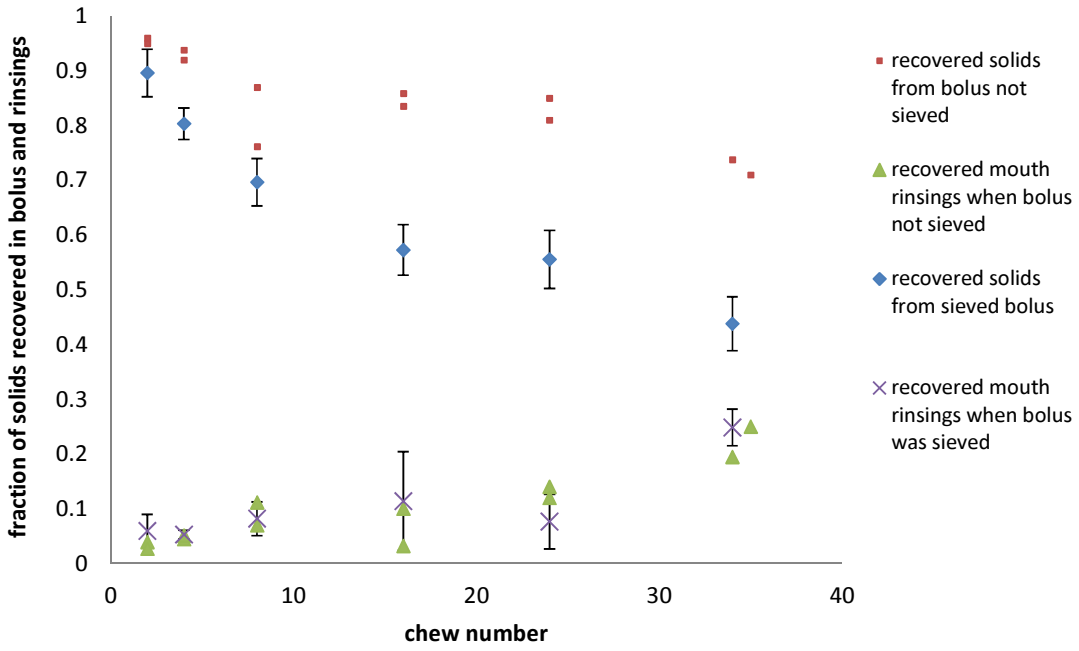

Figure 6-3: Fraction of dried solids recovered from the bolus and rinsings from the second subject. For the boluses that were sieved the data points are the mean of four replicates and the error bars show the standard deviation. The two boluses (and rinsings) that were collected at each chew interval and were dried without sieving are shown as individual points.

These unrecovered solids can be attributed to small particles and soluble solids passing the 355 µm sieve, which went to drain and were not collected. This loss of solids could result from several phenomena occurring both during mastication and after expectoration before analysis is completed; (i) as evidenced from the laser diffraction PSDs on subject 1, small particles < 355 µm are produced during mastication (the PSDs for this subject are discussed below) which wash through the smallest sieve, (ii) washing the bolus could result in further size reduction through shear and attrition during the washing action (Conversely, the shaking action during sieving can agglomerate particles resulting in additional retention.), (iii) starch is hydrolyzed by the amylase from the saliva after expectoration of the bolus, which continues its enzymatic

action during the waiting time before wet sieving and so results in further breakdown of particles and dissolution.

Noteworthy is that when no sieving occurs, the mass balance closes, i.e., the amount of solids not recovered in the bolus is approximately recovered in the rinsings. The trend where the fraction recovered with the rinsings increases with chew number agrees with the findings of Flynn et al. (2012). Other researchers did not obtain mass balance closure; for example, Peyron et al. (2004) and Jalbert-Malbos et al. (2007) obtained ≈50% recovered solids in boluses expectorated at the swallow point for a range of foods. However, their results could be related to the method of analysis as described above where continuing hydrolysis results in dissolution of starch. Hoebler et al. (1998) provide direct evidence where about 50 and 25% of starch in bread and pasta was hydrolysed during oral processing of around 30 seconds resulting in smaller particles being formed. However, the influence this hydrolysis had in size reduction was not quantified. Furthermore, Bornhorst et al. (2014) showed that for in-vivo rice boluses their rheological properties changed significantly over a 180 min incubation period at 37°C. The rheological properties were measured with a compression test, where the change in the measured compression force was due to activity of the α-amylase in the saliva as the controls without amylase did not show an effect.

While starch dissolution by hydrolysis is obviously important, a further test was conducted to determine its effect on the mass balance relative to size reduction below 355 μm. The results reported in Figure 6-3 above involved freezing of the samples to -20°C to halt the enzymatic activity. Thawing the bolus involved standing for three to four hours before sieving. In order to determine the actual mass that passes the 355 μm sieve of a bolus at the swallow point three boluses and rinsings were collected after 35 chews. The boluses were analysed immediately after expectoration so that any post expectoration effects resulting from hydrolysis would be negligible. The results from these experiments are given in Table 6-4.

Table 6-4: Solids recovered in the bolus and rinsings after a serving of rice was chewed to the natural swallow point. The expectorated boluses were either dried without sieving or sieved immediately after collection. (Values are the mean and standard deviation of four replicates).

When was the bolus sieved?	rice serving	solids recovered in bolus	solids recovered in rinsings	unrecovered solids
	(g)	(%)	(%)	(%)
not sieved	9.98 ± 0.24	86.3 ± 2.0	13.2 ± 1.9	0.57 ± 0.35
immediately	9.69 ± 0.41	75.4 ± 2.0	9.4 ± 2.1	15.2 ± 1.1

The boluses that were dried without sieving showed nearly 100% recovery of ingested solids. The boluses that were sieved straight after expectoration had a mean solids loss of 15%, which is indicative of the fraction of solids that are size reduced below 355 μm. Figure 6-3, at 35 chews, produced 27-30% solids loss indicating that the post expectoration hydrolysis induced losses are an additional 12-15%.

More detailed analysis of the PSDs (bolus plus rinsings) from wet sieving for the trials shown in Figure 6-3 are contained in Figure 6-4 to Figure 6-7. These show the PSD of the particles from the boluses recovered on the sieves. Figure 6-4 plots the sieves apertures on a linear scale, Figure 6-5 on a log scale that aligns with the power series of sieves and Figure 6-6 additionally plots the mass fraction axis on a log scale to highlight the tiny amounts collected on the smaller sieves. The first point to note is that the PSD in Figure 6-4 is significantly different to that obtained from the Mastersizer measurements in Figure 6-2. While the subjects were different, the Mastersizer produces many more fines and less large particles which suggest that, as the bolus was dispersed in the mixing chamber and was exposed to shear forces, further size reduction may have occurred. It is unlikely that agglomeration occurred on the sieves as the solids were continually washed which would have prevented cohesive binding of particles. Therefore, it is concluded that sieving produces a more representative PSD at expectoration.

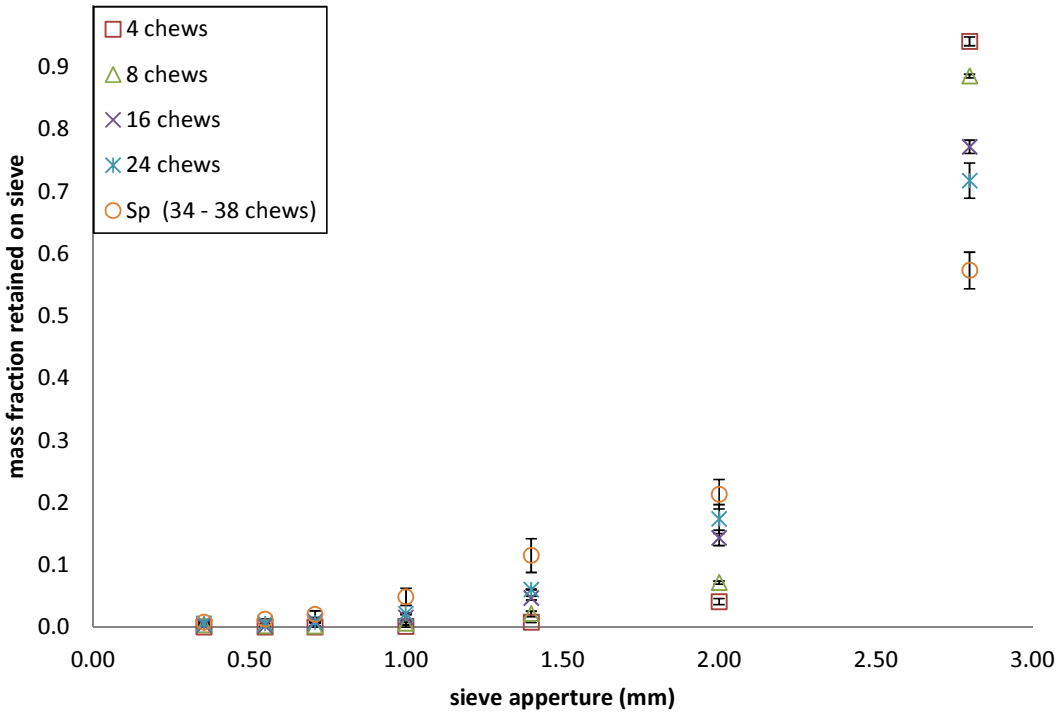

Figure 6-4: Mass fraction of rice retained on each sieve as a fraction of total solids recovered, mean and standard deviation of four replicates. The sieve apertures are plotted on a linear scale.

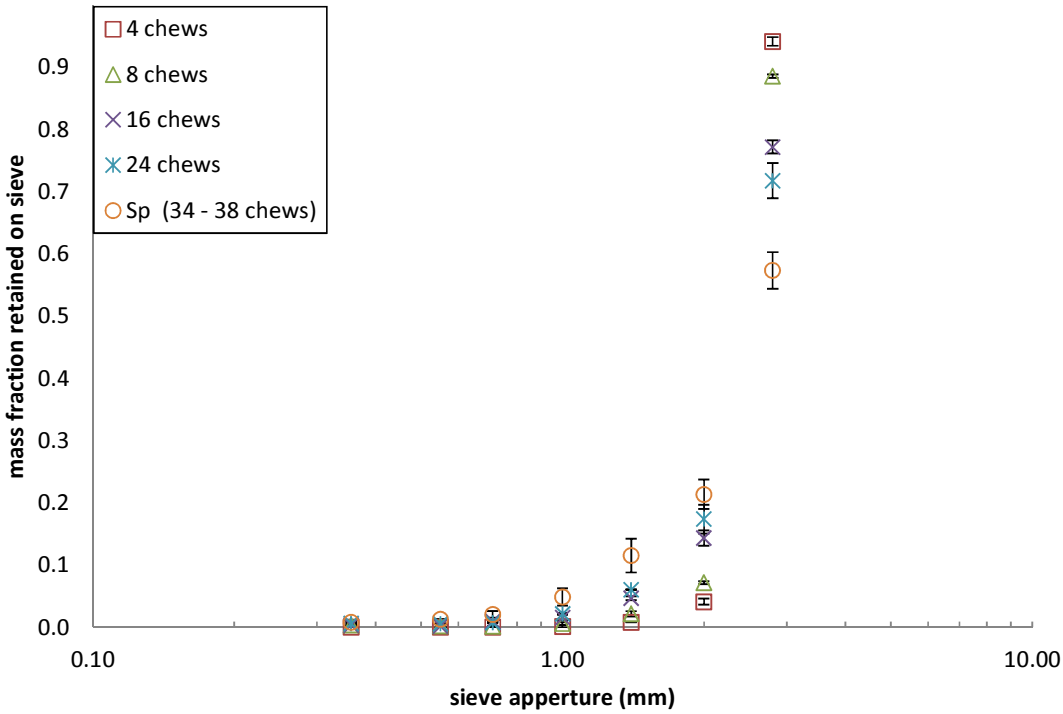

Figure 6-5: Mass fraction of rice retained on each sieve as a fraction of total solids recovered, mean and standard deviation of four replicates. The sieve apertures are plotted on a logarithmic scale.

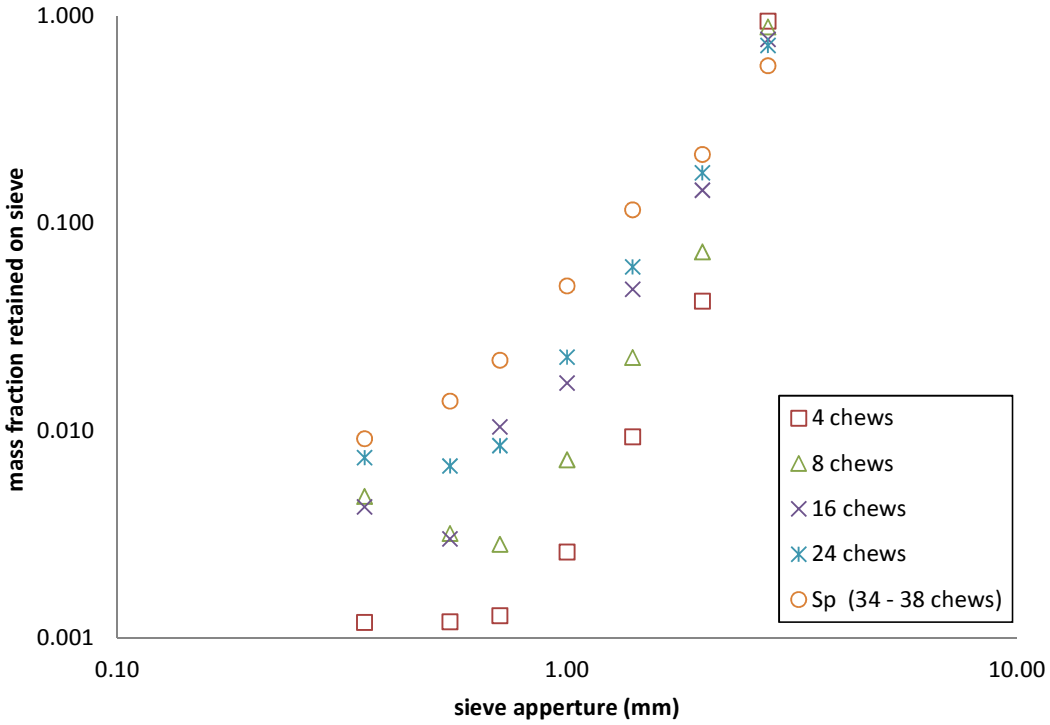

Figure 6-6: Mass fraction of rice retained on each sieve as a fraction of total solids recovered, mean of four replicates. The mass fractions and sieve apertures are both plotted on a logarithmic scale, the purpose being to highlight the small quantities of particles on the smaller sieves.

Of the recovered solids across all chew numbers, the majority fraction was retained on the 2.8 mm sieve, decreasing from 90% after four chews to less than 60% at the swallow point. The fraction of small particles below 1.0 mm was very low and even at the swallow point was less than 10% of the recovered solids, which is contrasted by the large amount of unrecovered solids; 12-14 wt% by chew four rising to 27-29% by the swallow point (Figure 6-2). Discounting the proportion of mass loss due to hydrolysis, this still indicates a bimodal distribution of mass, which reinforces further the *cleave and paste* mechanism already proposed from examination of the Mastersizer PSDs for subject 1. Cleaving tends to produce only a few larger daughter particles and pasting produces many very small particles below the minimum sieve size. The *cleave and paste* mechanism will be explored more in the single subject study.

If starch hydrolysis is removed as a mechanism, the PSD at expectoration can be back calculated as shown in Figure 6-7, where the pan amount is the unrecovered solids, or pasted fraction. The shape of the distribution doesn't change from Figure 6-4, except now the fraction retained on the sieves is lower because the mass fraction below 355 µm is included.

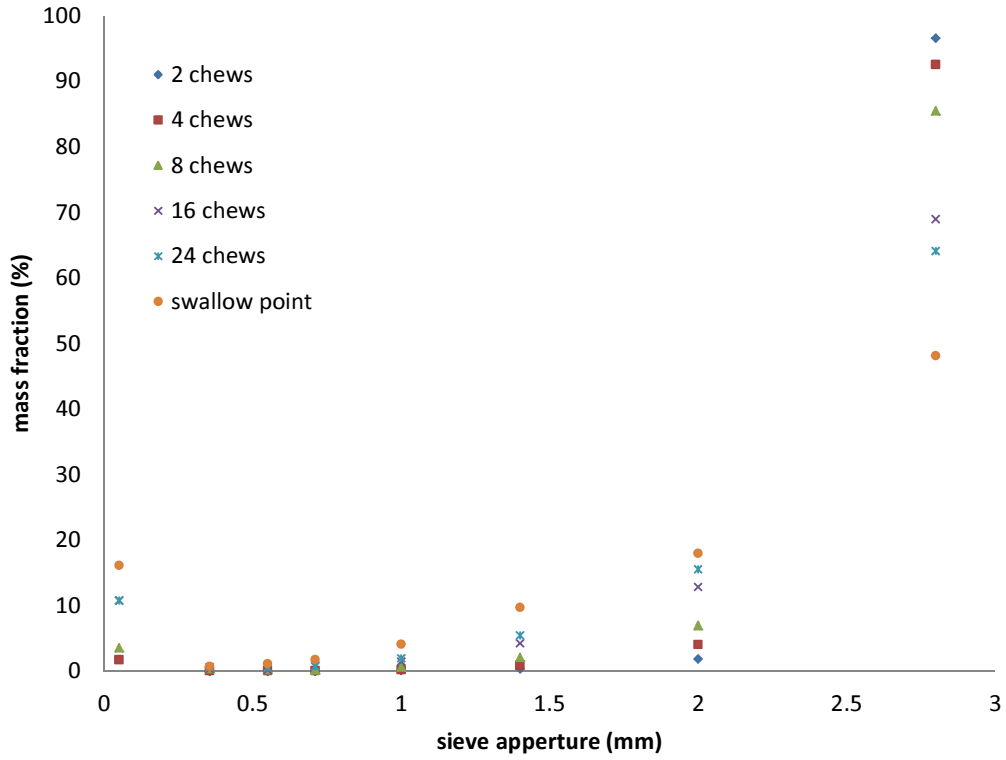

Figure 6-7: Solid fraction recovered in each size class as a fraction of the total solids ingested after removal of the hydrolysis effect in order to determine the influence of mastication alone on the PSD

While it has already been noted that the PSDs from the Mastersizer for subject 1 and the sieve analysis for subject 2 were significantly different but similar enough to indicate bimodality and therefore support a *cleave and paste* mechanism, one further point is important; that is, rice grains above 2 mm were absent in the Mastersizer measurements from 32 chews. This is unlikely when the process of mastication is considered, which involves *selection* of particles into the occlusion zone followed by *breakage*. As will be discussed in more detail later, the selection chance needed to accurately model the Mastersizer PSD is an order of magnitude higher than for the sieve analysis PSD. This result is unfeasible and suggests that the shear in the circulation cell of the Mastersizer also affects the top size particles, which will have been weakened by hydrolysis, post expectoration.

Bolus Saliva Content

The amount of saliva in the bolus steadily increased throughout mastication as shown by Figure 6-8. The saliva flow rate for each subject is calculated form the boluses at the swallow point and is given in Table 6-5.

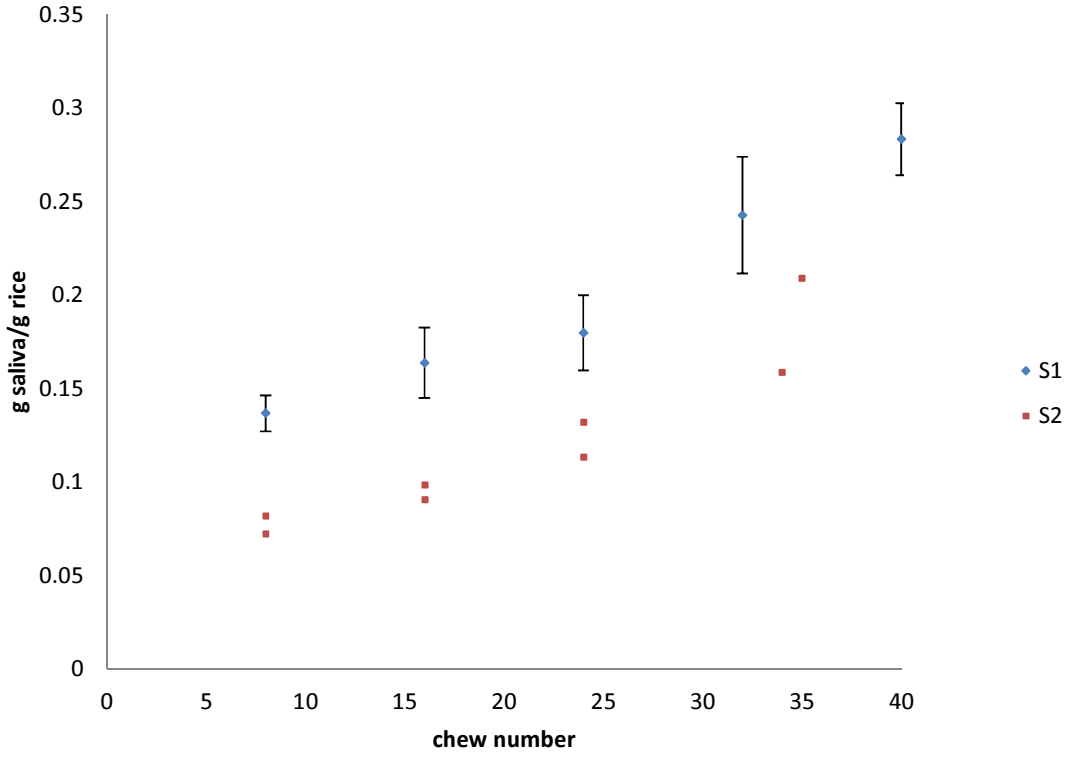

Figure 6-8: Saliva incorporation expressed as grams of saliva per gram of rice in the expectorated bolus for the two subjects throughout mastication, Subject 1 data is the mean and standard deviation of four samples and for subject 2, each replicate is shown.

Table 6-5: Saliva flow rate for both subjects, calculated from the slope of Figure 6-8 between 8 chews and the swallow point. (Note that the chew number is converted to minutes using the subjects chewing frequency).

	Flow rate (ml min^{-1})
S1	2.95 (r^2= 0.95)
S2	2.12 (r^2= 0.87)

The distinguishing feature of the plot is that the slopes are similar, i.e., both subjects add a similar amount of saliva per chew per gram of solids, except subject one has more residual saliva prior to the start of the test. The saliva flow rate on a time basis is different because subject 2 had a smaller bolus with more of the rice ending up in the rinsings component after expectorating the major bolus. The amount of saliva added relative to the amount of solids in the bolus is of particular interest, because the saliva acts as a binder, a carrier and a lubricant and contributes to the bolus reaching the safe-to-swallow thresholds. Adhesiveness is avoided if there is no wicking and the interstitial bolus space is saturated, this is discussed further in §6.1.4.

The single chew experiments described in §6.1.1 enable the parameters for the selection and breakage functions to be determined, which are used in the model to predict the PSD of the rice bolus throughout mastication. The subject was given varying quantities of rice where the number of grains offered, *n*, was known. After a single chew, the number of whole grains remaining was measured in order to determine the number that were selected and occluded, n_s. Another important quantity is the number of breakage sites in the occlusal plane, n_b, which is the maximum number of particles that can be occluded in a single chew. Experimentally, it is determined by giving the subject a large number of particles to saturate the occlusal plane. The number of breakage sites, n_b, is reached when n_s no longer increases with increasing portion size. Table 6-6 gives the number of breakage sites determined for whole and half grains and Figure 6-9 plots the ratio of n_b/n_s as a function of *n*. These show that saturation of breakage sites was achieved when 40 whole grains were served. Noticeably, the results are different for whole and half rice grains, but this is expected as they will occupy the occlusal zone differently. This difference can be further explored using the competition model of selection derived by van der Glas et al. (1992), given earlier in Eq. 2-9. The number of selected particles, $n_s(X,n)$, out of *n* particles offered is given by:

$$n_s(X,n) = n_b(X).[1-(1-O_1(X,1))^n] \qquad \textbf{Eq. 2-9}$$

where $n_b(X)$ is the number of breakage sites and $O_1(X,1)$ is the particle affinity for particles of size *X*. The particle affinity is determined by minimising the sum of the squared residuals between the number of particles occluded $n_s(X,n)$ relative to the number offered, *n*, and is given in Table 6-6.

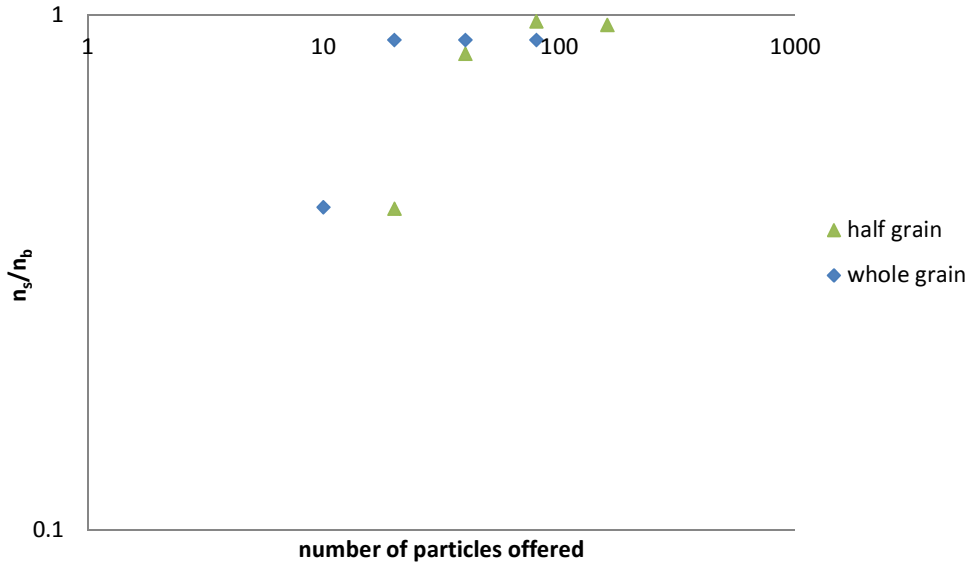

Figure 6-9: Ratio of number of particles selected to the number of breakage sites as a function of the particles offered.

Table 6-6: Number of breakage sites and particle affinity for the subject in the single chew study.

	n_b	O_1
Whole grains	10.7	0.058
Half grains	17.3	0.035

For smaller particles, the affinity is less. For very large particles, the limiting affinity tends to $1/n_b$ as they are easily positioned in the occlusal zone during chewing. The affinity of small particles cannot be approximated in this way and is most easily understood by thinking about the number of particles selected relative to the number of particles offered. The number of breakage sites gives the maximum number of particles of a given size that can be occluded; however, if only a small number of particles are offered they will not all necessarily be selected because the 'affinity' of the particles for selection is low and is dependent on the ability of tongue and cheeks to position particles on the teeth. Thus, smaller particles have a relatively lower chance of being selected as they are less easily manipulated in the mouth.

Breakage

The single chew samples were washed across a $2^{3/2}$ power series of three sieves of 2.8, 1.0 and 0.355 µm. Figure 6-10 shows the mass fraction of the occluded particles retained on the sieves

and passing the 355µm sieve. The error bars represent the variability which is unrelated to the number of particles served.

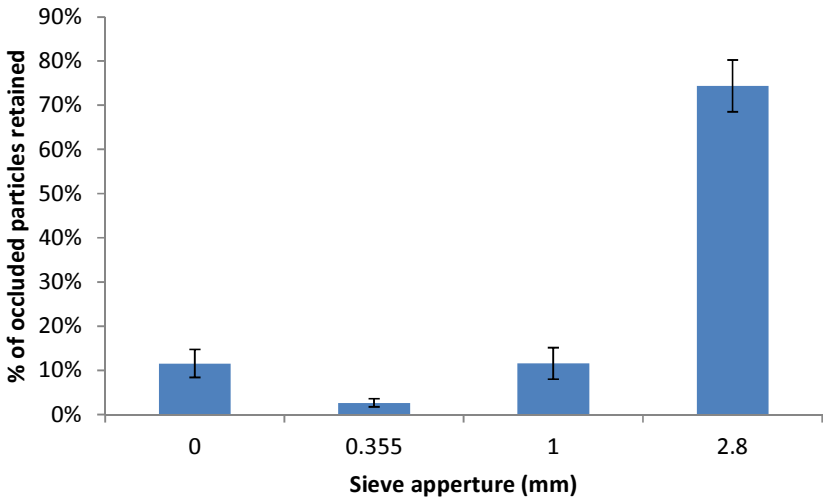

Figure 6-10: Mass fraction (mean ± stdv) of rice from the occluded particles that are retained on the sieves after a single chew stroke, the subject was served 40 grains and six replicates were performed.

When a kernel is occluded one or a few large particles are produced which contain most of the original particle mass alongside several smaller particles as well as a portion that have been pasted into very fine particles. This has previously been named the cleave and paste mechanism and is different from the distribution obtained for more brittle foods such as peanuts (which will be discussed in the peanuts matrix case study, §6.4.3). The cleave and paste mass distribution can be fitted to a breakage function and used in the model to predict the PSD of the bolus.

6.1.3 Model Development

This section describes the mastication model specific to the rice bolus case study. Not all of the rate processes occur (described §4.1 and §5.4). Mixing and size reduction occur but melting, absorption and work softening do not. Dissolution of starch by amylase is ubiquitous but requires time so is mostly significant after mastication, during storage before size analysis; it is a sample preparation issue rather than one affecting the properties of the bolus at swallowing; therefore, it is not included here. For the rate processes that do occur, mixing and size reduction are represented by a selection function and breakage function respectively. These two functions determine the progression of the PSD with chew number, the model for which is described in §5.3.4 and MATLAB® files are in Appendix E.

Particle Selection

The single chew study provided the parameters for the two-way competition model of particle selection derived by van der Glas et al. (1992), which is explained in chapter two (see Eq. 2-15) with complete derivation given in appendix A. The selection chance for a particle, *x*, in a size class X_i is thus given by

$$S(x) = \frac{n_s(X_i, n_{Xi})}{n_{Xi}} \qquad \textbf{Eq. 2-10}$$

where n_{xi} is the number of particles present in the size class. The selection chance of the particles is still probabilistic because a random number generator is used to determine if a particle is selected. The selection chance for particles in each size class is calculated from Eq. 2-10. A random number is generated for each particle, if this number is less than or equal to the selection chance then the particle is selected for occlusion. The nature of this method means the number of particles selected will vary between simulations. Therefore, performing a large number of simulations will produce a result where the average number of particles selected is close to the number predicted by Eq. 2-10.

The selection parameters are dependent on the size of the particles because they have different affinities, and all size ranges competitively occupy occlusal sites, as discussed above. Thus the model continually updates the size distribution by reassigning new particles to the appropriate size class. The sieves were a good starting point for discretisation; however, both the whole and half rice kernels were retained on the 2.8 mm sieve. Therefore additional size classes above 2.8 mm were added. The following size classes were used: >4.06, 3.22, 2.8, 2.0, 1.4, 1.0, 0.71, 0.5, 0.355, <0.355. Figure 6-11 shows the number of breakage sites for the particles in the different size classes fitted to a power function from the measured values for the whole and half kernels. van der Glas et al (1992) measured the selection chance for a various sizes of Optosil half cubes ranging from 9.6 mm to 1.2 mm, their results are shown for comparison.

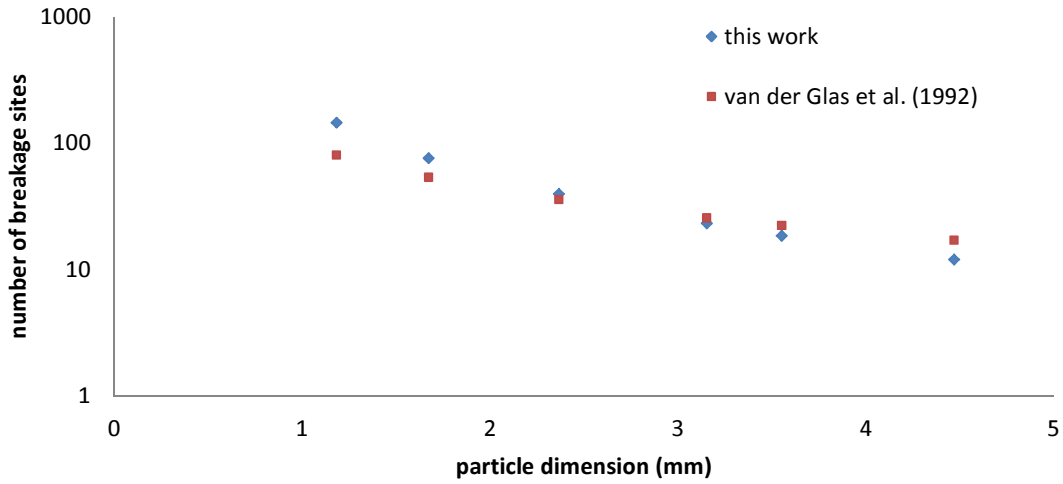

Figure 6-11: Number of breakage sites for the particles in different size classes, these were measured for whole and half rice kernels and extrapolated for the smaller particle sizes from Eq. 6-4.

The results from the single chew study with the rice are comparable that with the Optosil half cubes, although a lot more breakage sites are predicted for the two smallest size classes. This discrepancy likely comes about because these values were obtained by extrapolation. However, the larger number of breakage sites will not adversely affect the simulations because the volume of particles in that range is low and the number selected will not be unreasonably high. The three largest sizes of particles are most relevant as particles in this range dominate the rice bolus throughout mastication.

Particle Breakage

Rice appears to have a *cleave and paste* breakage mechanism as described above in §6.1.2 which, from the single chew experiments, produces several large daughter particles and ≈10% are "pasted" small particles which pass the 355 µm sieve. Assuming that the pasted fraction is constant, the size distribution of the larger particles can be described by a cumulative undersize distribution given by **Eq. 2-23** but adapted to include the pasted fraction, P

$$B(X, X_0) = (1 - P).[1 - (1 + r.X/X_0).(1 - X/X_0)^r] \qquad \textbf{Eq. 6-3}$$

noting that $B(X,X_o)$ is the weight or volume fraction of particles of size X_0, which break into particles smaller than size X, where $X \leq X_0$ and r is the fragmentation variable, which for the results shown in Figure 6-12 is 0.42 (R^2 = 0.98) when fitted to the data. The pasted fraction is under the threshold size and the particles are assumed to occupy the liquid phase (see §5.3.1).

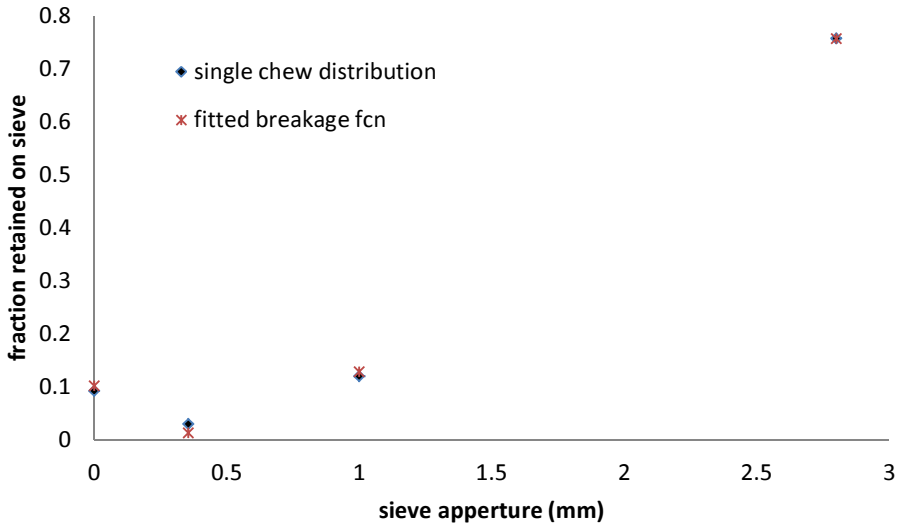

Figure 6-12: Breakage function fitted to the distribution of single rice kernels after occlusion.

In the next section the input parameters and initial conditions to the model are given and a schematic flow diagram shows the structure of the model.

Model Inputs and Initial conditions

An initial number of rice particles needs to be generated as an input for the model. In the experiments the serving size was fixed at 10.0 g and the mean mass of the whole grains was 0.047 g ± 0.002 (stdv). The *randn* function in MATLAB was used to generate a distribution of 200 rice kernels with this mean and standard deviation. The number of chews for each simulation was set at 40 which covered the number of chews used by the subject who used between 32 and 38 chews to prepare a swallowable bolus.

The number of breakage sites and particle affinity for each size class were fitted to a power equation based the values determined experimentally;

$$n_b(x_i) = 200{x_i}^{-1.88} \qquad \textbf{Eq. 6-4}$$

$$O_1(x_i) = 0.005{x_i}^{3.2} \qquad \textbf{Eq. 6-5}$$

The particles are put into size classes and with the information from the above equations the selection chance of all the particles in the bolus is calculated from equations 2-15 and 2-16.

Key assumptions in the model are outlined below:

- The rice particles are spherical. This reduces the complexity of the particle size distribution and is a reasonable approximation of shape for half kernels and subsequent particles resulting from occlusion.
- The breakage function of the rice particles is constant across all size classes. This is also reasonable because the distribution of daughter particles from occlusion of whole and half kernels was measured in the single chew study and were found to be approximately equal.
- Particles within each size class have the same chance of selection. This is an assumption of the two-way competition model which requires particles to be grouped into size classes for their selection chance to be calculated.
- Particles with a diameter ≤ 0.355 mm are not subject to breakage and are considered part of the liquid phase of the bolus.
- There is no loss of solids from the bolus. This is reasonable as the mean total recovered solids from the bolus and rinsings when the bolus was dried without sieving was 94.6%.

A schematic flow diagram of the discrete comminution model is shown in Figure 6-13 below. The model was written in MathWorks® MATLAB 2013a the model files are given in Appendix E.

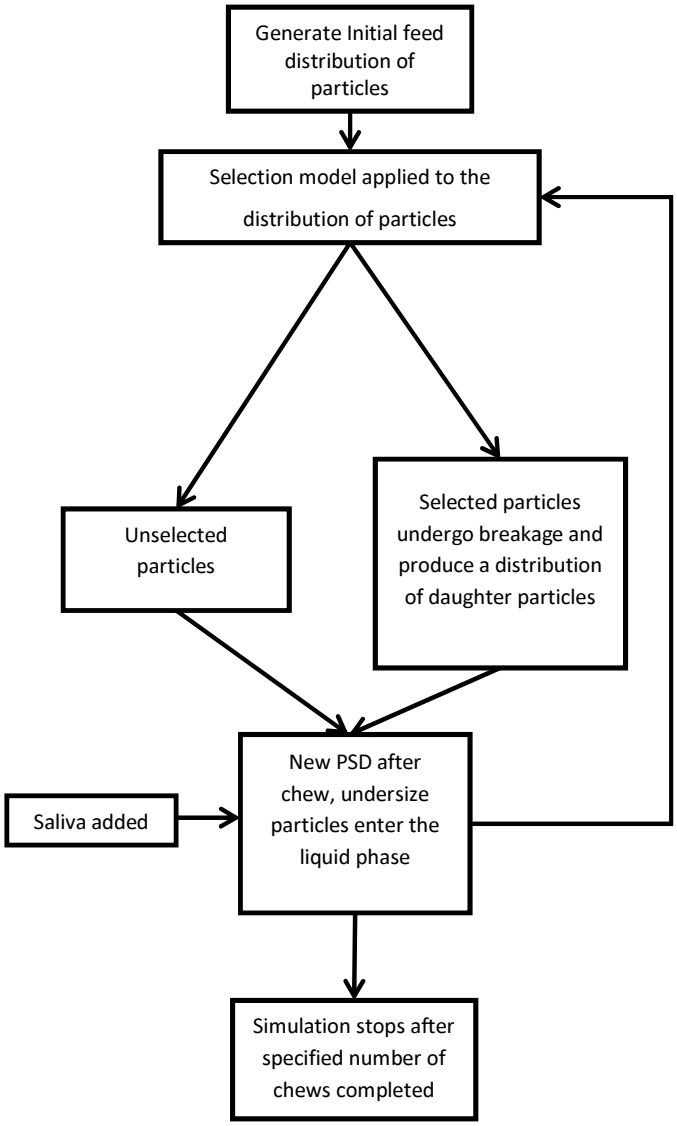

Figure 6-13: Schematic model flow diagram of the comminution model of the rice. This is a specific case of the generalised diagram in Figure 5-5.

6.1.4 Model Results and discussion

The oral processing of the rice bolus was simulated using the competition selection model and breakage function with parameters fitted from the single chew experimental data. This means the parameters are constant across all chew numbers. The model PSDs were collated for comparison with the experimental rice boluses measured by wet sieving, as shown in Figure 6-14 and Figure 6-15 below, where Figure 6-15 uses log scale to better distinguish the smaller size classes.

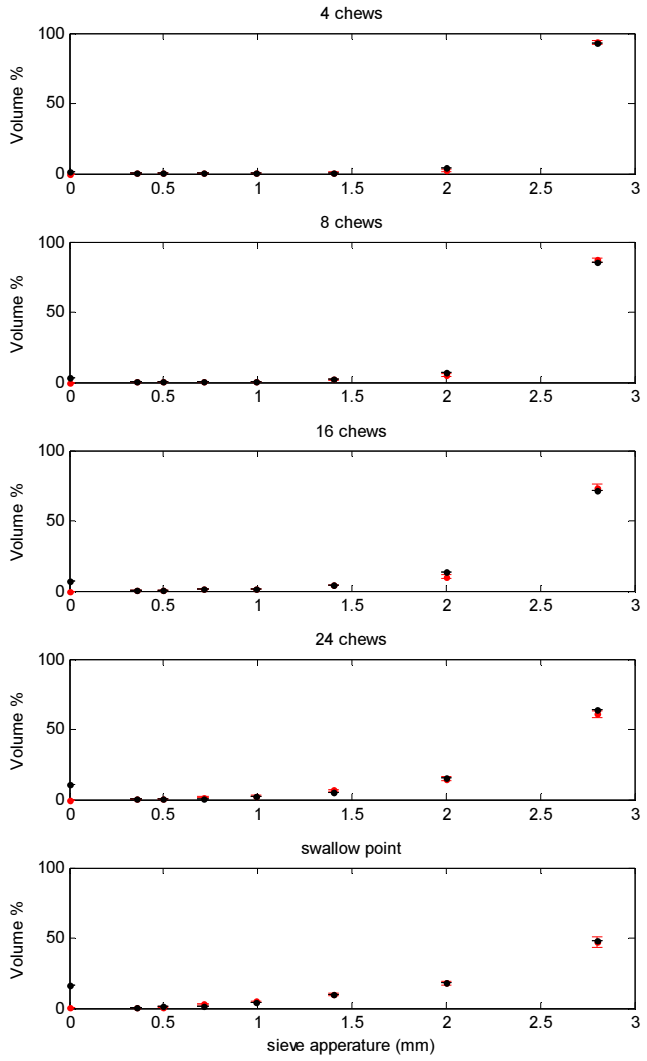

Figure 6-14: PSD predicted by the model compared with the experimental PSD of the rice bolus analysed with wet sieving with the volume fraction on a linear scale. The red dot is the model prediction and the black dot is the experimental data. Simulations were run 20 times and the error bars represent the standard deviation of these. The error bars for the experimental results represent the standard deviation of 4 trials.

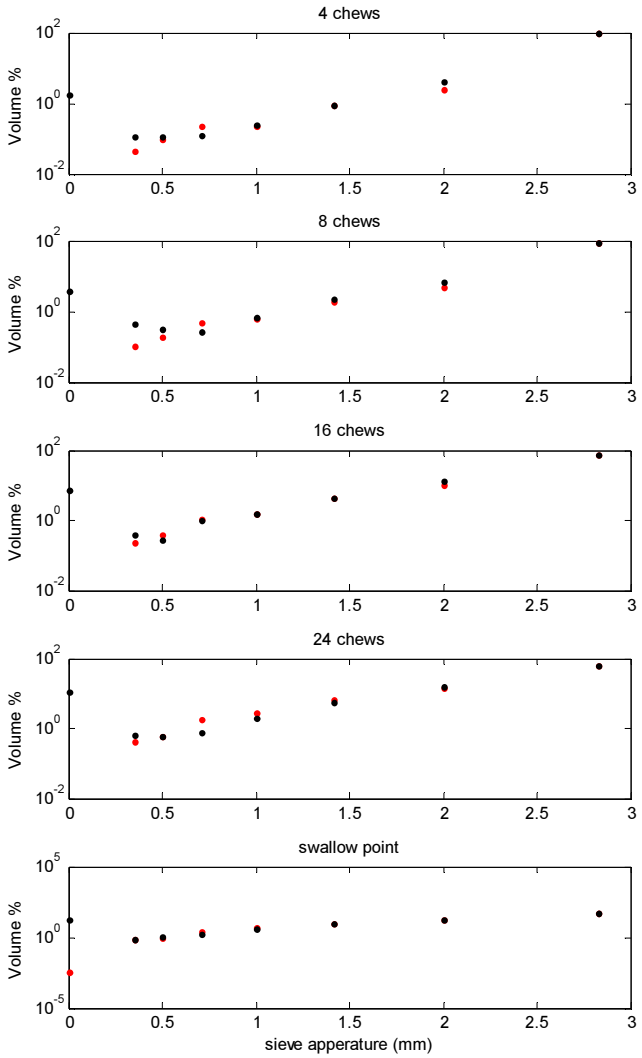

Figure 6-15: PSD predicted by the model compared with the PSD of the rice bolus from the subject which were analysed with wet sieving with the volume faction on a log scale. The red dot is the mean model prediction from 20 simulations; the black dot is the mean value of the experimental data from 4 replicate boluses.

The model predictions fit the experimental data of the expectorated boluses well which demonstrates the accuracy of the single chew experiments in determining the selection and breakage functions. The rate of size reduction between chews is limited by how much of the bolus is occluded every chew. Figure 6-16 shows the volume fraction of the bolus that is selected per chew, which is the sum of the volume of particles that are selected divided by the volume of particles in the bolus.

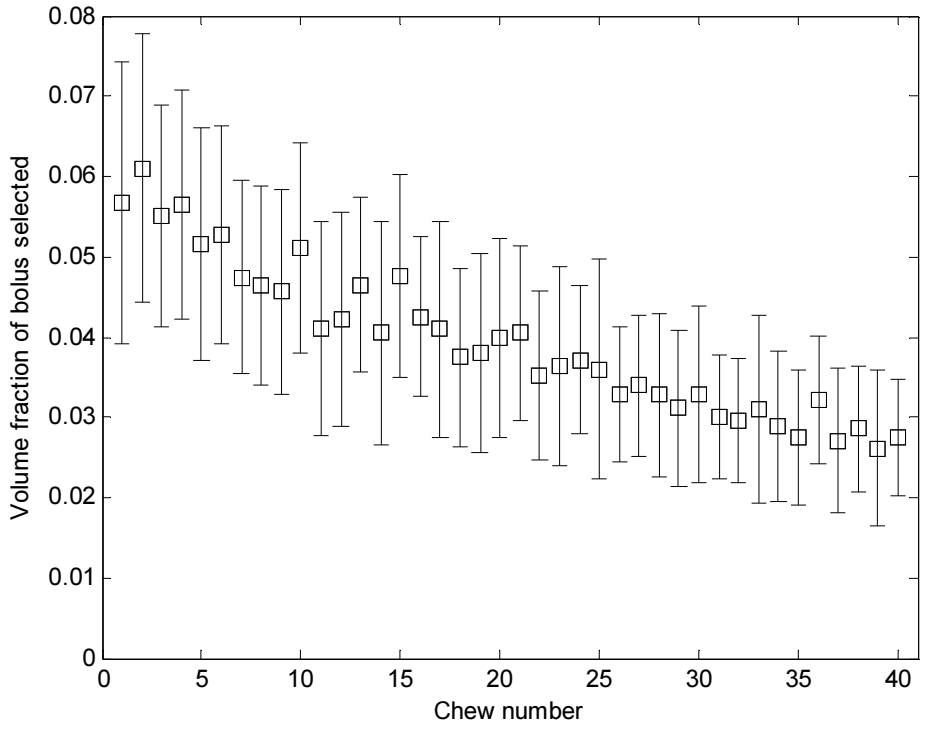

Figure 6-16: Volume fraction of rice selected per chew (mean and standard deviation of 20 simulations).

Around 6% of the bolus is occluded on the first chew and thereafter declines linearly as mastication progresses. The reduction in the volume of particles selected is expected. Smaller particles have a relatively lower chance of being on the teeth at occlusion and particles below the selection threshold are not occluded at all. Thus, as mastication progresses and the particles in the bolus get smaller, the volume occluded reduces. This also means that 'piling' of rice particles does not occur; that is, only a single layer of particles is occluded each chew. All other particles must either be squeezed out of the way or were never in the occlusal zone. When a bolus consists of only a few large particles the volume occluded is much larger, which is illustrated later by the simulations for the peanuts embedded in the matrices (see Figure 6-53). The variation in the fraction selected is due to the method used in the model to select particles (discussed in §5.3.4).

Model Sensitivity

It is useful to study model sensitivity to the parameters for the selection and breakage functions because if the model predications are unresponsive to the changes, then the model may not be as representative of real life oral processing. Figure 6-17 shows the sensitivity to ± 25% changes in the fragmentation variable, *r*, which defines the distribution of daughter

particles after breakage. Sensitivity is recorded as a percentage change in the proportion of particle predicted on each sieve compared to the base case where r = 0.43.

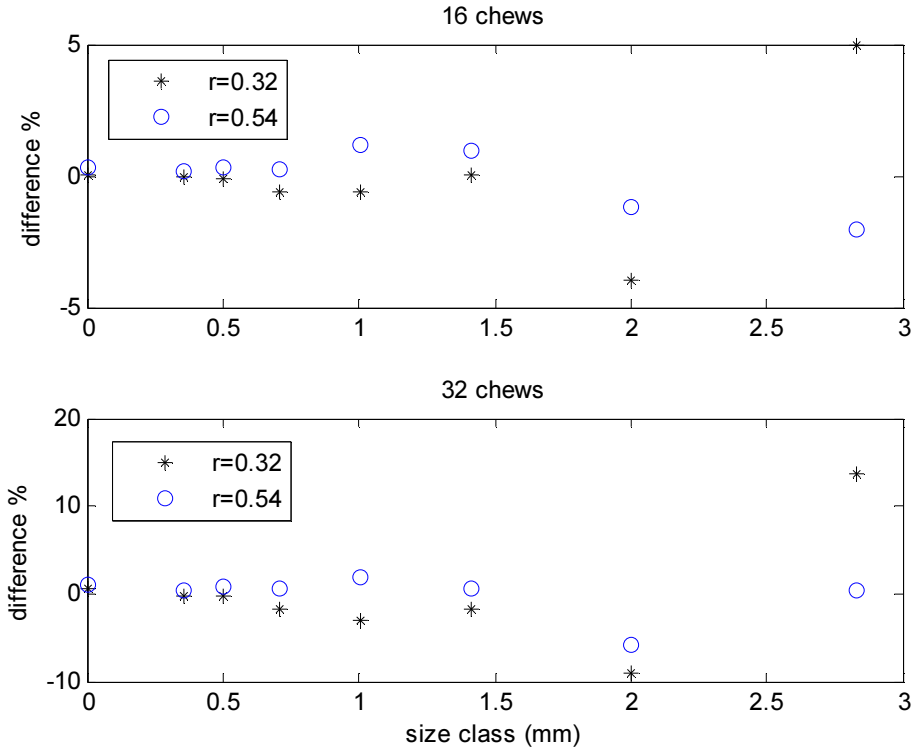

Figure 6-17: Change in mass fraction in the different size classes resulting from changing the fragmentation variable of breakage by ± 25%. The model base case uses r = 0.43.

Decreasing the value of *r* results in less fragmentation and larger daughter particles being produced, meaning that size reduction is slower. The opposite is true if *r* is increased. The number of larger daughter particles produced may not appreciably change with a change in *r*. The mass fraction retained on a sieve might increase or decrease but it may result in a single particle that is either larger or smaller than before. A reduction in the fragmentation variable of 25% results in 10% more volume fraction in the largest size range.

Figure 6-18 shows the sensitivity of the PSD to changes in the pasted fraction by comparing the difference in distributions obtained with the original 10% value (from the single chew experiments) and change of ± 25% meaning a pasted fraction of 7.5 and 12.5% respectively.

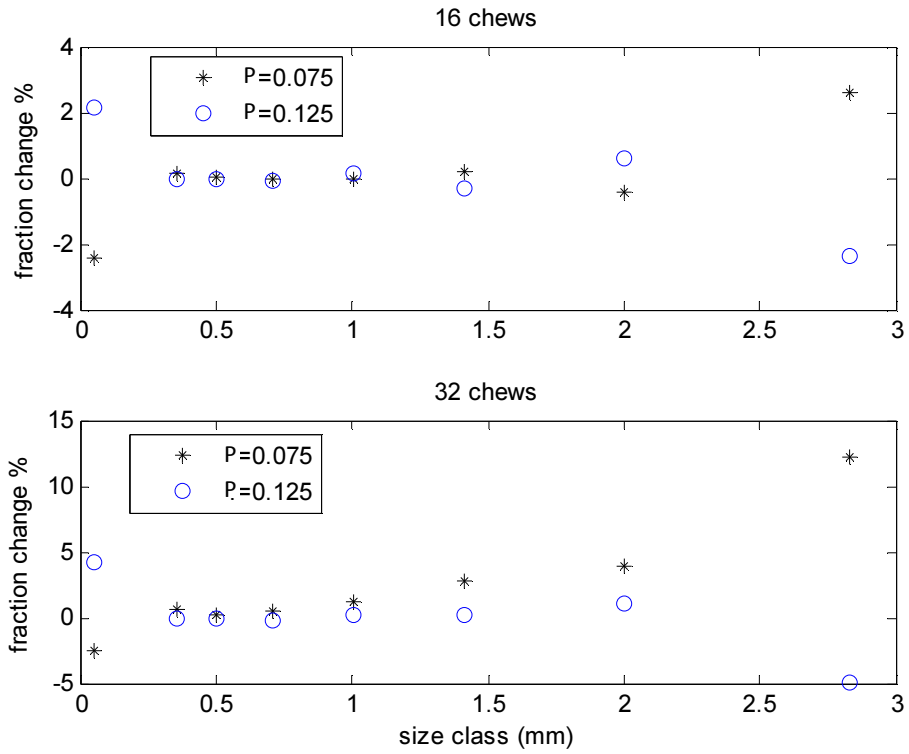

Figure 6-18: Change in mass fraction in the different size classes resulting from changing the fraction of an occluded particle that is pasted to below 355µm by ± 25%.

Increasing the pasted fraction results in more particle mass below 355µm that each occluded particle produces, thus the mass in this size range increases. After 16 chews which is approximately the mid-way point to natural swallowing a two percent increase is seen, this is offset by an equivalent reduction in the fraction of particles larger than 2.8 mm. If the pasted fraction of occluded particles decreases the opposite occurs. The overall mass fraction of the larger sizes increases as less is pasted fraction decreases.

Swallowing Threshold for the Rice Bolus

The bolus properties at the swallow point and how these play a role in in initiating the swallow are of interest. A relevant question is. Can the PSD provide information on why the bolus is swallowed after a certain number of chews and not earlier?

To address this question, three particle size parameters are investigated, the d_{90}, d_{50} and d_{10}. These are obtained from the model simulations by finding the sieve aperture that would retain 90, 50 or 10% of the particles. From the data these are obtained by plotting the geometric mean sieve size against the retained mass fraction and interpolating to get the size parameters

for each chew point. Figure 6-19 compares the d_{90}, d_{50} and d_{10} of the expectorated boluses with the simulations.

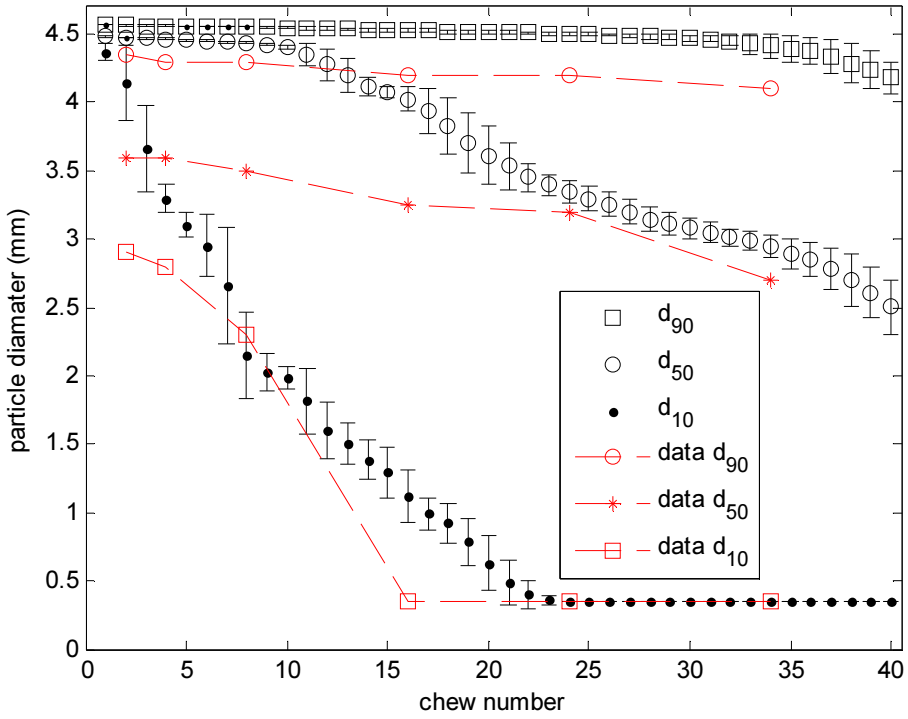

Figure 6-19: Key size parameters of the rice bolus changing with chew number. Model predictions in black compared with values interpolated from the wet sieve data.

The size parameters from the simulated boluses follow the same trend as the values obtained from the sieve data. The primary reason for the discrepancy, particularly with the d_{50} is because the data values are interpolated from the cumulative size distribution from the sieving analysis. The largest sieve aperture used was 2.8 mm and a large fraction of the bolus was retained on this. Interpolating from the cumulative distribution plot is prone to errors because the distribution of particles in this size range cannot be determined from the data. The model predictions provide a better representation of how the size distribution is changing with chew number. The bolus d_{10} decreases steadily with chew number; the plateau shows that at least 10% of the volume is below 355µm in size. The d_{90} remains unchanged up to the swallow point, whilst the d_{50} steadily declines after 10 chews. The unchanged d_{90} shows that 10% of the original particles are not occluded before the bolus is swallowed. The fact that a large portion of the original particles are not occluded indicates that the size of the rice grains is not preventing the bolus from reaching the swallow threshold. Rather, it is the adhesion threshold and interstitial liquid content which is important here. If the adhesion threshold is satisfied when the interstitial space is fully saturated, this would mean an interstitial liquid content of

between 25-40% of the solid volume (based on packing efficiencies of spheres). The interstitial liquid content of the bolus consists of the added saliva and the small undersize particles resulting from occlusion where part of the rice grains are pasted. This is plotted against chew number in Figure 6-20, the subject had a natural swallow point between 32 and 40 chews which corresponds to a mean bolus liquid content over 0.34 -0.44 g/g.

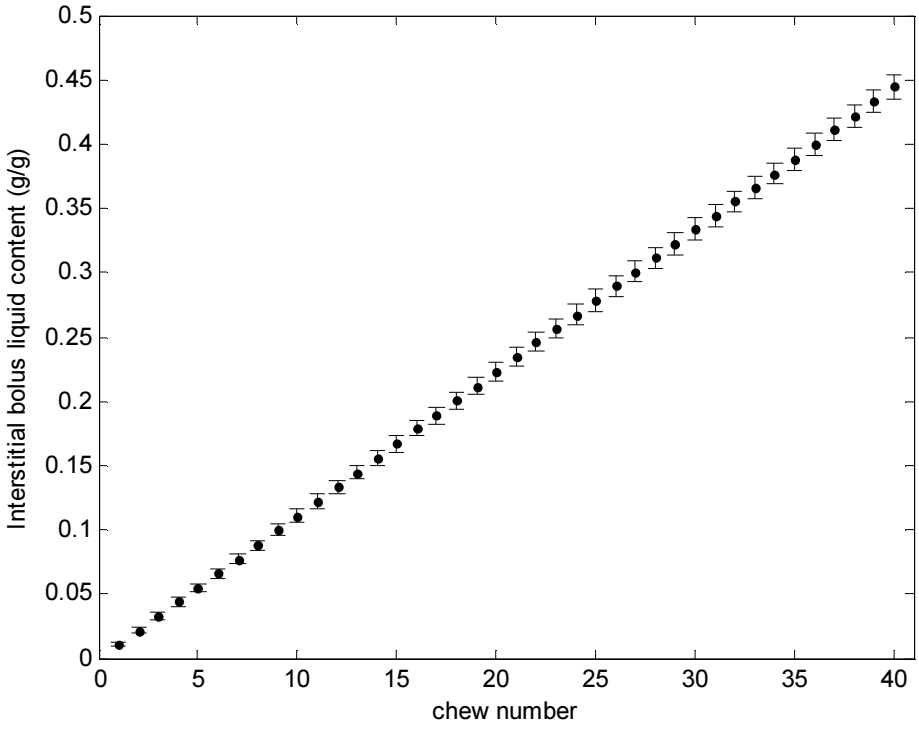

Figure 6-20: Interstitial liquid content expressed as ratio of liquid to solid phase, the liquid phase includes the added saliva and the rice particles pasted to below the threshold size, mean and standard deviation of 20 simulations.

This result showing that the liquid content of the rice bolus is more important than size reduction fits with the anecdotal observation of rice consumption. When consuming rice with liquid, in a curry for example, it can be swallowed with very few chews or even a single chew. In those instances the chewing might be more to facilitate bolus transport rather than being required to modify the bolus properties. Future research is recommended to further investigate the swallowing threshold of rice. This could be done by serving cooked rice on its own and with liquid, coconut milk for example, and varying the rice to liquid ratios. Measuring the PSD, interstitial liquid content and bolus volume would allow the safe-to-swallow threshold for rice to be interrogated. This would verify the observations made here and provide some quantitative values for the safe-to swallow phase space discussed in §4.3.3 and shown in Figure 4-6.

The model used here does not account for 'losses' of solids which occur through partial swallows or through being dispersed throughout the oral cavity. The rice bolus at the swallow point contains ≈80% of the ingested mass, for other foods it can be as low as 40% Peyron et al (2004), Jalebert-Malbos et al. (2007), Flynn (2012). Because the acceptability of the constituent bolus properties are likely to be related to the total bolus volume, being able to more accurately simulate this would be advantageous. The model could be improved by accounting for this food movement, where the volume of the food in the mouth is made up of a primary bolus and food particles which are in the mouth but not part of the bolus which will be swallowed, this model has been proposed conceptually by Flynn (2012) and needs to be developed into a mathematical description of the process.

6.1.5 Summary and Conclusions

The results from the trials with the two subjects show that the wet sieving method provided a more reliable PSD measurement of the rice boluses than the Malvern Mastersizer which shears the particles causing further breakdown. In wet sieving, both whole and half rice grains were retained on the 2.8 mm sieve and passed the next largest aperture sieve in the series and so it was not possible to differentiate between them. In this respect the model is useful as it shows these larger sizes more clearly (Figure 6-19).

The single chew studies conducted with whole and half rice grains provided information on the fragmentation dynamics of the rice in order to determine the selection and breakage function parameters. Inputting these into the model, enabled close matching between the model and experimental trials where the subject chewed until swallow point. The two-way competition model (van der Glas et al., 1992) was used to determine the selection chance of the particles and it was found that a bimodal breakage function best described the size reduction. This is the first known instance of this competition selection model being used in a simulation of mastication; it has previously only been applied to single chew studies.

At the swallow point the rice bolus contains ≈15% un-chewed grains, despite being chewed over 30 times. The model shows that the volume of the rice selected varies from ≈6% at the start of chewing, decreasing to ≈3% by the swallow point. The reason for the decrease is that the affinity of particles for the occlusal zone decreases with size because the particles get smaller and saliva is added, the bolus becomes paste like. As the jaw closes in a chew stroke, particles are squeezed out of the occlusal zone.

As selection and breakage occurred, saliva was being added. It appears that excess interstitial liquid is responsible for the rice reaching the swallow threshold. The subject required 32-40 chews the reach the swallow point and the interstitial liquid content of the rice bolus ranged from 0.34-0.44 g/g. This is enough liquid to saturate the bolus assuming a void volume of the bolus between 25-40%. It is recommended that the swallow thresholds and relationship between interstitial moisture and particle size of the rice be interrogated with future experimental work. Cooked rice should be served to a subject in varying volumes, both on its own and with different volumes of liquid added. The PSD and number of chews to the swallow point should be measured. It is expected that rice with liquid added can be swallowed with fewer chews as the interstitial space will reach saturation with fewer chews.

6.2 Case Study – Gelatine Gels

A confectionary gel is typically made by combining one or more gelling agents such as starch, pectin or gelatine with water and sugar, usually sucrose and glucose syrup. Flavour, colour and food acid are minor additional ingredients (Burey et al. 2009). Gels are usually solid at room temperature. They are isotropic and behave elastically although some will not fully recover their shape after an applied stress and some can undergo brittle deformation. The mechanical properties of a gelatine gel and its melting point depend on the gelatine and sucrose concentrations. Gels are a desirable test food because their composition can be altered to achieve different properties. . Gels are a good model system because of their dissolution and melting behaviour, this makes them ideally suited for the model framework outlined in chapters 4 and 5.

Models for flavour release and melting of gelatine gels have been developed previously (Harrison and Hills, 1996; Wright and Hills, 2003). However, none have incorporated the rate processes of size reduction and melting. Harrison and Hills (1996) developed a mathematical model for the flavour release from gelatine gels by considering the interfacial heat and mass transfer of a spherical particle. Because heat transfer is much faster than mass transfer in the food system, the rate of flavour release was governed by the melting temperature of the gels. If the melting point is below the mouth temperature, then the flavour release is more rapid and melting is limited by the rate of heat transfer into the gel. If the melting temperature is above that of the mouth then flavour release is much slower as the rate limiting step is the diffusion of sucrose from the surface of the gel which lowers the gel melting temperature at the surface so melting can occur. Harrison and Hills (1996) validated their model using data obtained from in-vitro melting of gelatine gels with sucrose concentrations between 20 -50%. Wright and Hills (2003) modelled the flavour release from a gelatine bolus during mastication by assuming that melting at the gel surface controlled flavour release; hence the bolus shrinks at a constant velocity, v, between chews. The mass of flavour released is then calculated from the volume change between chews. To calculate the flavour release they used a simulated mastication pattern which defined the food surface area, chewing and swallow intervals for a complete mastication sequence. These were generated using data obtained by Wright et al. (2003). The bolus surface area was expressed in terms of sphericity; defined as the surface area of a sphere of the same volume divided by the surface area of the bolus. The sphericity was found to be independent of chew number, this implies that the bolus was undergoing a stretch and fold mechanism and being reshaped rather than undergoing size reduction at

occlusion. The latter would result in a continual increase in surface area thus a continually decreasing sphericity. Bolus sphericity plotted against chew time followed a Pearson type IV probability distribution function. The chewing frequency and swallow time interval (the number of seconds between liquid swallows), could be described by the same probability distribution. The distribution functions were fitted to subject's data and a random number generator was used to generate a simulated mastication pattern. The bolus sphericity, chewing frequency and swallow intervals were then used to simulate the concentration of flavour in the saliva during mastication. Wright and Hills (2003) validated their model for flavour release from the chewed bolus by comparing it to flavour time intensity measurements from different subjects. The actual amount of melted gel in the bolus was not measured. The method employed by Wright and Hills (2003) for the surface area is not applicable for a gel that is regularly fragmented as the surface area increases with each chew.

This case study had two main objectives. Firstly, to determine how the gel composition influences the properties of the bolus. Of particular interest is the particle size distributions of the bolus at swallow point, and how the properties of the gel might influence this, i.e. will larger particles of softer more easily deformable gels be swallowed? Secondly, use the model framework to show that the particle size distribution of the bolus and melting of the gels can be tracked during oral processing. Four different gels were formulated using gelatine concentrations of 10 and 15% and sucrose concentrations of 30 and 50% respectively. The physical properties of the gels were assessed with a texture analyzer using a 'two-bite' compression test (displacement rate = 5 mm/s, compression ratio = 75%). A single subject was used for this study as the focus was on the effect the food composition had on breakdown and bolus properties.

6.2.1 Methodology

Subject Screening and Selection

The subject screening and chewing trials were completed in accordance with Massey University Ethics approval (Southern A Application - 10/29). The advertisement and questionnaire used to select subjects for this study is contained in Appendix C.

To avoid significant inter-subject variability and focus on the food effects, a single subject was chosen for this study. Because only one subject was used, a screening procedure was employed to pick a subject with chewing behavior that was representative of the screened population and not extreme in any sense. The screening test was developed by Hutchings et al.

(2009) and was designed to pick a single subject from a population whose chewing behavior was closest to the mean of that group. Here a similar screening test was implemented with ten subjects (6 male, 4 female) participating in the initial screening with the aim of recruiting one subject for the gelatine gel study. To partake, all subjects needed to have good oral and general health, complete natural dentition and no history of orthodontic treatment or jaw injuries. This criteria is in line with previous studies (Lassauzay et al., 2000, Jalabert-Malbos et al., 2007, Hutchings et al., *ibid*).

Two bars were used in the screening process; Cadbury Crunchie and Tasti Fruit and Nut Bar. Participants were presented with either bar and asked to take a bite and chew naturally. Each person did two replicates of each bar. The subjects were observed as they chewed so that the number of chews and total mastication time could be measured. The bite weight and bite dimensions were also measured. The cumulative bite weight fraction for all the subjects and both bars is plotted as a function of the bite weight in Figure 6-21. The cumulative number of chews per bar is shown in Figure 6-22, where the data points show the percentage of the population that had more chews than them or a larger bite weight. To qualify for the study with the gels a subject would need to be between the 25th and the 75th percentile for all the criteria. There were two subjects meeting these criteria, S5 and S6. Participant S6, a 26 year old male, was chosen for the single subject study as he was closer to the population mean for three of the four chewing parameters.

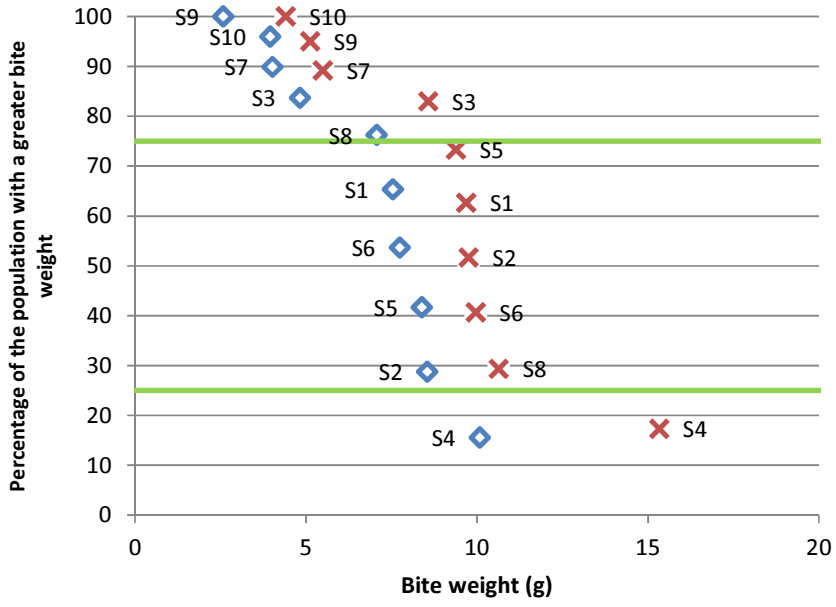

Figure 6-21: Cumulative distribution of bite weight for the ten subjects; Cadbury Crunchie (◇) and Tasti Product Fruit and Nut Bar (x), green line is the 75th and 25th percentile.

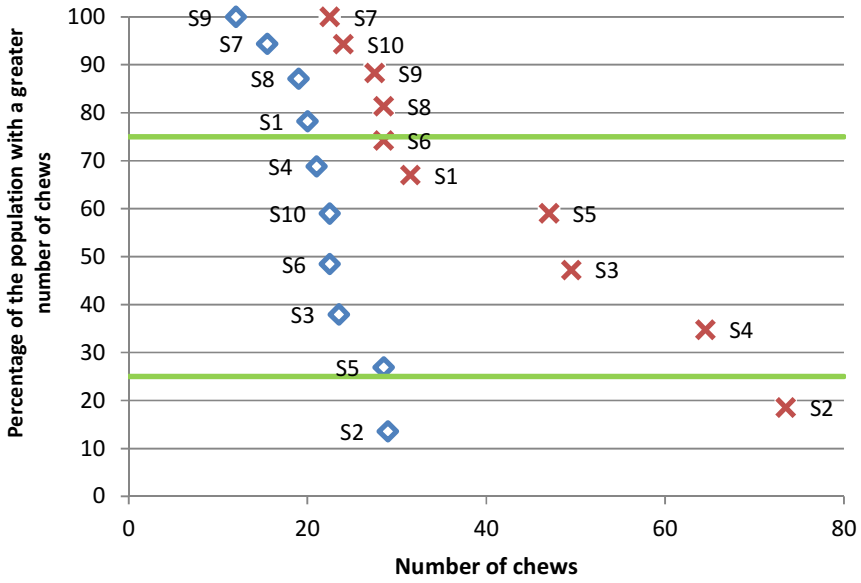

Figure 6-22: Cumulative distribution for number of chews required for each bar; Cadbury Crunchie (◇) and Tasti Product Fruit and Nut Bar (x), green line is the 75th and 25th percentile.

Gelatine Preparation

The four recipes shown in Table 6-7 are derived from formulations used in previous studies (Holm et al. 2009, Lassauzay et al. 2000, DeMars et al. 2001). The citric acid gives the gel a pleasant taste whilst the colour was added to make the gel more visually appealing to the subject and to facilitate the image analysis of the bolus.

Table 6-7: Composition of the gelatine gels used for the study.

Ingredient	(% w/w)			
Sucrose	50	50	30	30
Gelatine (250 bloom)	10	15	10	15
Water	38	33	58	53
Citric acid	2	2	2	2
Colour (g)	0.15	0.15	0.15	0.15

To prepare the gels half the water was added to the sucrose and heated on a stove top until it dissolved and the solution reached 100°C. The gelatine was dissolved in the remaining water in a stainless steel bowl (250 ml volume) which was submerged in a water bath at 75°C. The sucrose solution was removed from the heat and added to the gelatine. The mixture was stirred to ensure it was well mixed, the citric acid and the colour (Ponceau 4r, Bronson and Jacobs) were then added and were stirred through. The mixture was placed back in the water bath at 75°C for 60 minutes to de-gas. After heating, the molten gel was poured into aluminum molds (10 x 10 x 200mm), Figure 6-23, and left to cool at room temperature. The gels were

stored in hermetic plastic bags at room temperature for up to 24 hours. For use in the chewing experiments and analysis the gel was cut into 1cm cubes using a sharp kitchen knife.

Figure 6-23: A gel in the aluminium mould.

Gelatine Properties and Reproducibility

The aim was to make gels with different physical properties to determine if the differences would influence break down and bolus properties. The physical properties of the gels were assessed with a texture analyzer (TA.XT. plus Texture Analyser, Stable Micro Systems). A 'two-bite' compression test (displacement rate = 5 mm/s, compression ratio = 75%) was performed and the hardness of a rectangular piece of gel (1cm x 2 cm x 1 cm) was measured. The hardness is defined as the peak force F1 value on the first compression cycle Figure 6-24.

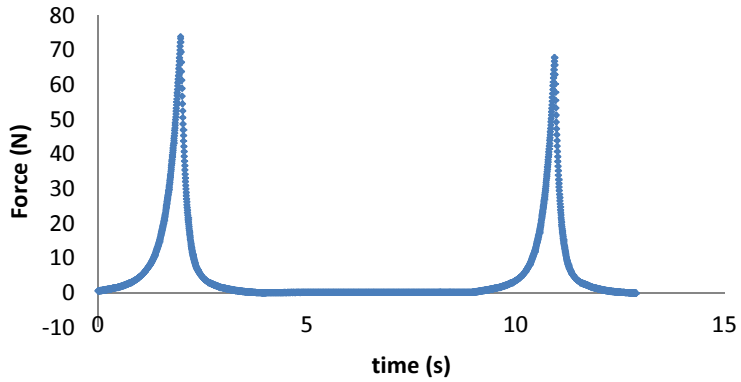

Figure 6-24: Typical force vs time plot for the two-bite compression test on a rectangular sample of 30% sucrose 10% gelatine gel (1cm x 2 cm x 1 cm), displacement rate = 5 mm/s, compression ratio = 75%.

The gels needed to be reproducible so that gels made with the same recipe but prepared on different days were comparable. To test the reproducibility of the gels, the hardness from the

two-bite test was compared for samples of the same recipe gel made on different days. Ten replicate samples were measured from four separate batches. This work was carried out before the relationship between the inverse of the fragmentation index and the particle size in the bolus at swallow point was identified. Therefore, the toughness was not measured as part of this work. However, the Young's modulus can be obtained from the stress/strain data obtained with the TPA measurement from the first compression. However, caution is needed with comparisons to the literature values that have used a different procedure and sample size in their measurements.

Chewing Trials for PSD

The subject was required to participate in four sessions where they would chew and expectorate pieces of gel so that the PSD of the bolus could be analysed. Prior to each session, the gelatine was cut into 1cm cubes and weighed. The natural number of chews required to reach the swallow point was first determined in each session. The subject was presented with six 1 cm cubes of gel and asked to chew and swallow each one in a natural manner. The number of chews was counted and the subject was asked to signal when they had completed the swallow. Between each sample the subject was instructed to sip some water and check that there was no debris or particles remaining in their mouth by doing a tongue sweep. The natural swallow point was taken as the mean of the six replicates. For the remaining samples the subject was asked to chew and expectorate the bolus after 30%, 50%, 70% or 100% of the normal chew number. The subject did not know when they would expectorate; they were told when to stop chewing by the researcher. The subject expectorated the bolus onto a pre-weighed plastic petri dish (100 mm diameter, Biolab Auckland New Zealand) so that the incorporated saliva could be determined; this was taken as the difference between the bolus mass and the mass of the gelatine cube. The order of the number of chews was randomised and three replicates of each were completed; thus, each session contained 18 samples.

Recovered Solids and Saliva Content of the Bolus

The dry solids content of each of gels was measured by drying pre-weighed samples in confoil container in an oven at 105°C for 24 hours. Four replicates of each gel recipe were performed. The saliva content of the bolus was determined from the recovered solids in the bolus.

Particle Size Measurement

Image analysis was found to be the most suitable method to analyse the particle size distribution of the gelatine boluses. Wet sieving was not appropriate as prolonged washing of

particles could lead to loss of solids and the sticky nature of the particles meant accurate separation and sizing of particles would be problematic. The particles were too big for measurement by light diffraction using a Mastersizer.

The expectorated boluses were analysed on the same day as they were collected, straight after a session with the subject was finished. The boluses were expectorated onto a plastic Petri dish (100 mm diameter, Biolab Auckland New Zealand) and 20 ml of water was added to help separate the particles. A plastic toothpick was also used to further separate particles if it was needed. The boluses were scanned at 1200 dpi in grayscale using a flatbed desktop scanner (Epsom Perfection V30). The images were analyzed using Image J ® (1.44, National Institute of Health, USA). The images were converted to binary by applying the black and white threshold and then using the nucleus counter to count the particles and measure their area. The particle size measurements from Image J were saved as Microsoft Excel files for further analysis.

The reliability of the image analysis method was determined by repeating the analysis three times on the same bolus and comparing the measurements. Following the method described above, a bolus expectorated at the swallow point was dispersed in water on a petri dish and scanned. The particles were re-dispersed on the petri dish and another scan was performed. This was repeated three times in total. Assuming the projected particle area, A, was a square the particles were put into size classes based on the side length ($A^{0.5}$). The cumulative area fraction was plotted against the size class in Figure 6-25, which shows that the measured particle size distribution was consistent between scans.

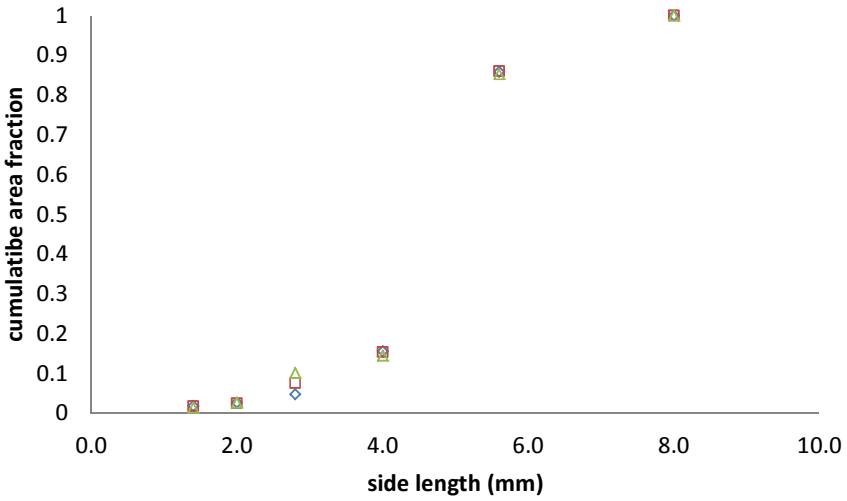

Figure 6-25: Cumulative particle size distribution of the same bolus. The bolus was scanned and re-disbursed and scanned again, repeated three times. Scam 1 Δ, scan 2 □, scan 3 ○.

In-vitro Gelatine Melting Rate

The in-vitro measurement of the gel melting was performed to determine the melting rates that are expected to occur in the mouth during oral processing. The procedure used here is similar to that employed by Harrison & Hills (1996). A beaker with 50 ml of water was placed in a water bath 37.0°C ±0.1°C. A cube (1 cm^3) of gelatine at 20°C was first weighed and then placed on a piece of wire mesh which was held suspended in the beaker above a stirring rod. The mesh allowed the gel to be exposed to water on all sides and not in contact with the stirring rod. The beaker was stirred at a rate of 300 rpm to ensure the water was well mixed. A sample from the beaker was taken every 20 seconds until the gel had fully melted. For the 30% sucrose/10% gel, samples were taken every 10 seconds because the gel melted at a much faster rate. The samples were analyzed with a refractometer (RFM 330 Refractometer, Bellingham + Stanley Ltd.) to measure the sucrose concentration. Three replicate measurements of each gel recipe were performed.

Melted Gelatine in the Bolus

Attempts were made to measure the sucrose concentration in the liquid phase of the bolus with the refractometer. However, this was problematic as the concentration of sucrose in the saliva was too low to obtain meaningful measurements using the refractometer. A method was devised to measure the amount of gel that melted during mastication with a spectrophotometer. Because the gel was coloured, the amount of melted gel in the bolus could be determined from the measured absorbance of the liquid phase in the bolus.

Standard Curve

An absorbance curve was first prepared which enabled the amount of melted gel in the boluses to be measured. Two 1 cm^3 cubes of the gel were weighed and added to 50ml of water in a plastic sample container. The container was partially submerged in a water bath at 40°C until the gel had completely melted. A series of dilutions were prepared from the water and melted gel mixture. The absorbance was measured in the spectrophotometer at a wavelength 510 nm. Four replicates from each dilution were measured. A standard absorbance curve for each of the four gels was produced in this way (shown in Appendix G).

In-vivo Measurements

The liquid phase of the bolus was collected and its absorbance measured, from the standard curve the amount of melted gel in the liquid phase of the bolus could then be determined.

Before the subject chewed a piece of gel a background mouth measurement was obtained. They were instructed to take 5 ml of water from a sample container and swirl it around in their mouth and perform several pseudo chewing motions before expectorating it back into the container. This was done as it would provide a residual or background absorbance value which was subtracted from the value measured from the bolus. Doing this prior to each gel sample ensured the measured absorbance values from the bolus liquid phase would not be over estimating the amount of melted gel.

To measure the amount of gel that melted during mastication the subject was instructed to take a pre-weighed gel cube (1 cm^3). They chewed it in a natural manner until being instructed to stop and expectorate it into a plastic sample container which had 5ml of 0°C water. The lid was put on the container and it was gently shaken to ensure the water mixed well with the saliva. Cold water was used as it would prevent further melting of the gel after expectoration by lowering the surface temperature. Diffusion from the surface of the gel is slow, so the amount of gel in the liquid phase would not increase significantly in the short time before the liquid is separated from the bolus. After weighing the sample container, the bolus and liquid were poured across a small stainless steel kitchen sieve into a separate container to separate the liquid from the particles. A pipette was used to transfer 3.25 ml of the water-saliva mixture into a disposable plastic cuvette. The cuvettes were stored until the session with the subject had finished and then their absorbance was measured at 510 nm. Between samples the subject was instructed to take some sips of water and ensure no small gel particles remained in the mouth from the previous sample. Swishing water around in the mouth also helped to

prevent the colour from the gel being retained on the oral linings. For each of the four gel recipes, the subject was asked to chew and expectorate the bolus either at the half way point or at the natural swallow point for that particular gel. Three replicates of each were performed and conducted in a random order.

6.2.2 Model Development

The oral processing of gelatine gels involves mechanical size reduction through occlusion and melting of the gel into the saliva. The rate of size reduction and the amount of melting that occurs is dependent on the amount of sucrose and gelatine in the gel. The aim of the model is to simulate the particle size distribution of the gel particles in the bolus and the amount of gel in the liquid phase of the bolus. Therefore, the model requires the rate process of size reduction, melting and dissolution.

Size Reduction

Gelatine gels are broken down differently to the peanuts and rice presented in the other case studies in this chapter. When occluded; they are either cleaved into two daughter particles, partially fractured but remain as a single damaged particle or resist fracture and remain intact. How the gel responds during occlusion depends on its physical properties and how it is positioned on the teeth. It is because the gels behave elastically that occlusion does not always result in fragmentation. To account for this, the selection chance given by the size dependent selection function is adjusted so that it reflects the probability of fragmentation occurring. Furthermore, the breakage function cannot be represented by those used for the other two case studies or a generic parameterised form used in mastication (**Eq. 2-21**, **Eq. 2-23**). Another mechanism which better represents the fragmentation of the gel is required. A simple subdivision model is proposed which can describe the size reduction of gels resulting from occlusion. For simplicity it is assumed that the particles are cuboids and when one is cleaved it produces two daughter particles (cuboids). A selected particle is cleaved across its longest dimension. The logic behind this is that a particle is more likely to be orientated this way in the occlusal zone, with the largest surface area of the particle being on the teeth. Figure 6-26 shows schematically how a cube of gelatine is broken down in the model.

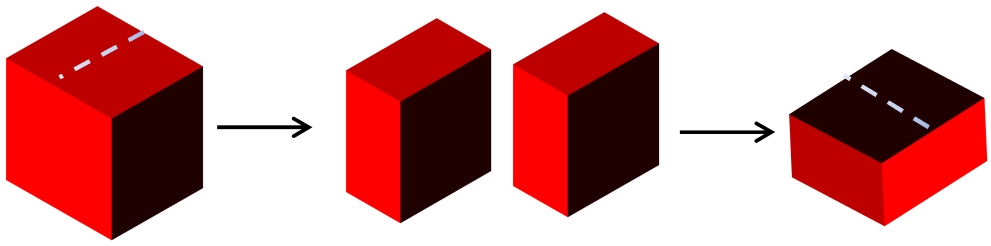

Figure 6-26: Schematic representation showing how a gel particle can be cleaved and is positioned on the teeth during occlusion, the dotted line shows the cleavage point.

There is a larger variation of particle sizes in the bolus so the location of the cleavage point is randomly determined, which should provide a distribution of particles of varying sizes.

The selection chance of the gel particles can be described using the power law selection function, Eq. 2-7, which is also used in the case study of the peanuts embedded in the matrices. The selection chance of a gel particle is given by

$$S(x_m) = v.\left(\frac{x_m}{x_l}\right)^w \qquad \textbf{Eq. 2.7}$$

where x_m is the side length if the particle was a cube (i.e. $V^{(1/3)}$), x_l is the side length of the initial gel cube, v then defines the chance the initial cube has of being fragmented and w is a subject dependent constant that determines how much selection depends on size. Because the gels behave elastically, the threshold for fragmentation is likely to be greater than for harder and rigid foods like nuts. For the peanuts a size selection threshold of 1 mm was defined, here a threshold of 2 mm is used. This equates to an 8 mm^3 particle. There were not many particles with a projected area below 4mm^2 so this is a conservative estimate.

Dissolution and Melting

The melting temperature of gelatine gels is dependent on the sucrose and gelatine concentrations. Harrison and Hill (1996) showed that the rate limiting step for melting of a gel depends on whether its melting temperature is above or below the mouth temperature. For gels with a melting temperature above 37°C, the melting is limited by the diffusion of sucrose from the gel surface and dissolution is described by

$$\dot{M}_{k,dissolution}\big|_p = k_d \rho_{k,p,sol.solids} A_{p,i}\big|_p \left(X_{p,sol.solids}\big|_p - X_{liq,diss.sol.solids}\big|_p\right) \qquad \textbf{Eq. 5-32}$$

where k_d [m s^{-1}] is the mass transfer coefficient, $A_{p,i|p}$ is the area of a particle [m^2], $X_{p,sol.solids}$ is the soluble solid mass fraction [kg kg^{-1}] in the particle-phase, $X_{liq,diss.sol.solids}$ is the concentration of soluble solids in the interstitial liquid phase [kg kg^{-1}]. As sucrose diffuses from the surface of the gel the concentration of sucrose in the surface layer is lowered which consequently lowers its melting temperature below 37 °C. If the melting temperature is below the mouth temperature, melting is relatively fast and limited by the thermal diffusion into the gel. Wright and Hills (2003) showed that if the velocity of melting and particle area is known, the melting of a gel is given by

$$dV_{p,i} = -A_{p,i} v_m dt \qquad \textbf{Eq. 5-34}$$

where V_p is the volume of the gel, A_p is the surface area and v_m is the melting velocity. In the model presented here, the particles are tracked individually with Eq. 5-34 being applied to each particle between chew strokes. The dimensions of the cuboids are known and so the surface area for melting can be determined. The melting velocity for each of the gels is determined from in-vitro measurements and used in the simulations. Assumptions specific to the model for gelatine gels are stated below, the key nomenclature are given in Table 6-8.

- Only two daughter particles are produced when a particle is fragmented
- The particles have a constant melting velocity
- Saliva flow rate is constant
- Mechanical size reduction is instantaneous at each chew stroke
- No melting of the gel prior to the first chew stroke

Table 6-8: Nomenclature and units for the size reduction and melting of gelatine.

Symbol	definition		units
v_m	Melting velocity	$2.25*10^{-3}$ - $6.25*10^{-4}$	cm s^{-1}
qs	Saliva flow rate	5.9	ml min^{-1}
chewf	Chewing frequency	0.75	s^{-1}
chews	Number of chews	9 - 15	-
Xsuc	Sucrose concentration (v/v)	0.3,0.5	
rhog	gel density	1.2	g cm^{-3}
v	Fragmentation chance of whole cube	0.35-0.75	-
w	selection function power	1.5-1.75	-

The model starts with a 1 x 1 x 1 cm cube as served to the subject in the chewing trials. A schematic flow diagram of the model for the bolus formation of the gels is shown in Figure 6-27. The model was coded in MathWorks® MATLAB 2013a, files are contained in Appendix E.

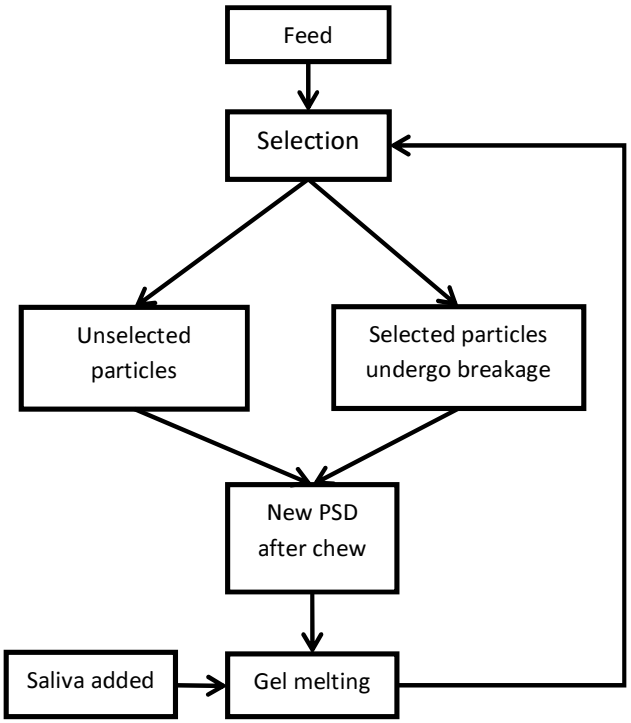

Figure 6-27: Schematic model flow diagram for the oral processing of gelatine gel, this is a specific case of the generalised diagram in Figure 5-5.

The PSD measured by image analysis is compared with the PSD in the model so that the validity of the selection and breakage functions could be determined. The methods employed for this are covered here. The particles in the bolus are put into size classes by assuming the projected area is a square. Size classes following a $2^{0.5}$ progression are used as it was in the other case studies, >8.0, 5.6, 4.0, 2.8, 2.0, 1.4, 1.0. For the simulated boluses, the maximum projected area for each particle was determined, thus each particle had a 'projected' 2D area and the particles in the simulated bolus could be compared directly with the data.

6.2.3 Experimental Results and Discussion

The results and discussion pertaining to the experiments carried out on the gels and with the subject are presented first. The outcome of the model and how it compares to the boluses from the subject is presented at the end of this section.

Gel Properties

The texture analyser was used to measure gels from the same recipe prepared on different days. The peak force from the first compression of the two-bite compression test is compared. The results for ten samples of the same recipe from different batches are summarized in Table 6-9.

Table 6-9: Reproducibility of the recipe 50%sucrose 15% gelatine, the hardness is defined as the peak force F1 value on the first compression cycle from a 'two-bite' compression test (displacement rate = 5 mm/s, compression ratio = 75%) this was performed on a rectangular piece of gel (1cm x 2 cm x 1 cm).

Batches	F1 peak force mean (N) value (n=10)	Standard deviation
Batch 1	175.14	13.82
Batch 2	165.12	4.64
Batch 3	170.38	10.04
Batch 4	166.00	7.34

The peak force measurements were consistent between samples although there was some variation between measurements. A one way ANOVA test showed that the mean peak force for the different batches was similar ($P > 0.05$). It was concluded that the preparation of the gels was consistent and the gels were reproducible and suitably similar from batch to batch.

One of the aims was to prepare gels that had different mechanical properties which would result in different rates of break down in the mouth. The peak force measured during the two bite compression test was compared for the four different gels to determine how the sucrose and gelatine concentration influenced the hardness of the gels, results shown in Table 6-10.

Table 6-10: Comparison of the hardness of the different recipes, the hardness is defined as the peak force F1 value on the first compression cycle from a 'two-bite' compression test (displacement rate = 5 mm/s, compression ratio = 75%) this was performed on a rectangular piece of gel (1cm x 2 cm x 1 cm), 10 replicate measurements were performed.

Recipe	F1 peak force mean value (N) (± standard deviation)
50% sucrose 15% gelatine	170.4 ± 10.1
30% sucrose 15% gelatine	145.8 ± 10.3
50% sucrose 10% gelatine	110.8 ± 5.7
30% sucrose 10% gelatine	73.8 ± 4.4

The four combinations of gelatine and sugar concentrations gave significantly different results for the peak force measurement from the two-bite test. The gelatine and sugar both contribute to the rigidity and firmness of the gel with gelatine having a larger influence. All the gels behaved elastically under the measurement conditions; they were not fractured and returned to their original shape after compression. Table 6-11 shows the Young's modulus for the different gels.

Table 6-11: Young's modulus of the gels derived from the stress-strain curve of the first compression in the 'two-bite' test, (mean and standard deviation of 10 replicate measurements.

Recipe	Young's Modulus (MPa) (± standard deviation)
50% sucrose 15% gelatine	0.63 ± 0.01
30% sucrose 15% gelatine	0.52 ± 0.04
50% sucrose 10% gelatine	0.42± 0.07
30% sucrose 10% gelatine	0.27± 0.02

Number of Chews to Swallow Point

The composition of the gels influenced the number of chews required to reach the natural swallow point. Table 6-12 shows the number of chews required for each gel and Table 6-13 shows the results of the two-way ANOVA comparing the chew number with recipe and hardness of the gels.

Table 6-12: Number of chews taken to swallow 1 cm^3 of the gel (mean ± stdv of six replicates, ^{a,b}means with different letters are significantly different)

Recipe	Number of chews
50% sucrose 15% gelatine	15.0 ± 0.37^{a}
30% sucrose 15% gelatine	14.0 ± 0.58^{a}
50% sucrose 10% gelatine	10.67 ± 0.56^{b}
30% sucrose 10% gelatine	9.50 ± 0.22^{b}

Table 6-13: P values from the two-way ANOVA showing the effect of the recipe and hardness on the number of chews before swallowing.

p	50%sucrose 15%gelatine	30%sucrose 15%gelatine	50%sucrose 10%gelatine	30%sucrose 10%gelatine
50%sucrose 15%gelatine	X	0.1358	< 0.0001	< 0.0001
30%sucrose 15%gelatine	0.1358	X	< 0.0001	< 0.0001
50%sucrose 10%gelatine	< 0.0001	< 0.0001	X	0.0848
30%sucrose 10%gelatine	< 0.0001	< 0.0001	0.0848	X

The number of chews before swallowing is significantly different between the gels with different gelatine concentrations but the difference was not significant for gels with the same gelatine concentration and different sucrose concentrations. The firmer gels required about 50% more chews before they were swallowed. If the fragmentation is the same for all the gels and the selection chance is independent of gel properties then the PSD at swallow point should be similar for the gels with the similar chew number.

Chewing Frequency

The chewing frequency was calculated from the test to find the natural swallow point for each of the gel recipes. The chewing frequency of the subject for the four different recipes is shown in Table 6-14.

Table 6-14: Chewing frequency of the subject for different gels when chewing to swallow point (mean ± stdv of six replicates).

Recipe	Frequency (1/s)
50%sucrose 15%gelatine	0.74 ± 0.036
30%sucrose 15%gelatine	0.74 ± 0.028
50%sucrose 10%gelatine	0.76 ± 0.037
30%sucrose 10%gelatine	0.77 ± 0.050

The properties of the gel had no significant influence on the chewing frequency ($F(3,20) = 1.44$, $P>0.05$). The chewing frequency for the subject is as an important parameter for the model as it defines the time between chews in which melting occurs.

Solids lost from the Bolus

The loss of solids from the bolus during mastication of the gels were very low for all the gels and the fraction of recovered solids was the same for all gel types ($F(3,20) = 0.507$, $P > 0.05$). Table 6-15 shows the solids recovered from the bolus at the swallow point for the different gels.

Table 6-15: Solids recovered in the bolus at the swallow point for the different gel recipes (mean ± stdv of six replicates)

Recipe	Recovered solids %
50%sucrose 15%gelatine	98.4 ± 1.3
30%sucrose 15%gelatine	98.6 ± 1.4
50%sucrose 10%gelatine	97.3 ± 1.0
30%sucrose 10%gelatine	97.7 ± 1.8

Saliva Content of the Bolus

The average saliva flow rate throughout mastication for each of the gels is shown in Figure 6-28.

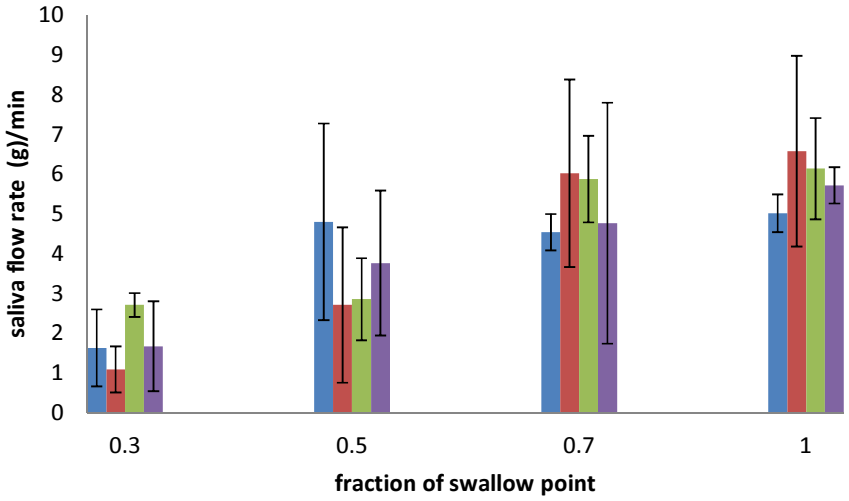

Figure 6-28: Saliva flow rate for the different recipes at different stages of mastication (mean ±stdv), (blue) 30% sucrose 15% gelatine, (red) 30% sucrose 10% gelatine, (green) 50% sucrose 15% gelatine and (purple) 50% sucrose 10% gelatine.

There was no significant difference in saliva flow rate at the swallow point between the gel recipes ($P > 0.05$). In the literature the saliva flow rate is typically reported for the bolus at swallow point and not at different points throughout mastication (Watanabe and Dawes., 1998, Engelen et al., 2003 and Gaviao et al., 2004). Here, the saliva flow rate increased as mastication progressed although there was significant variability between measurements. While variation between replicates is expected as saliva excretion is a physiological process, other factors also contribute to variability, for example the act of gathering up particles in the

mouth before spitting them out will incorporate more saliva than if the bolus is simply spat out with no sweep of the tongue to gather loose particles. The increase in saliva flow rate over the time of mastication could be related to the citric acid that enters the liquid phase and is known to stimulate more saliva production. The average flow rate at the swallow point for all gels was 5.92 ± 1.34 ml min^{-1}.

Particle Size Distribution

The particle size distribution of the bolus was analysed at different stages of mastication and at the swallow point. Two questions to be answered were, (i) do the number of chews for the firmer gels relate to the breakage rate, (ii) do the gel properties affect the particle size threshold for swallowing. Figure 6-29 shows the cumulative area fraction of the bolus at swallow point for the replicate blouses of the four different gels.

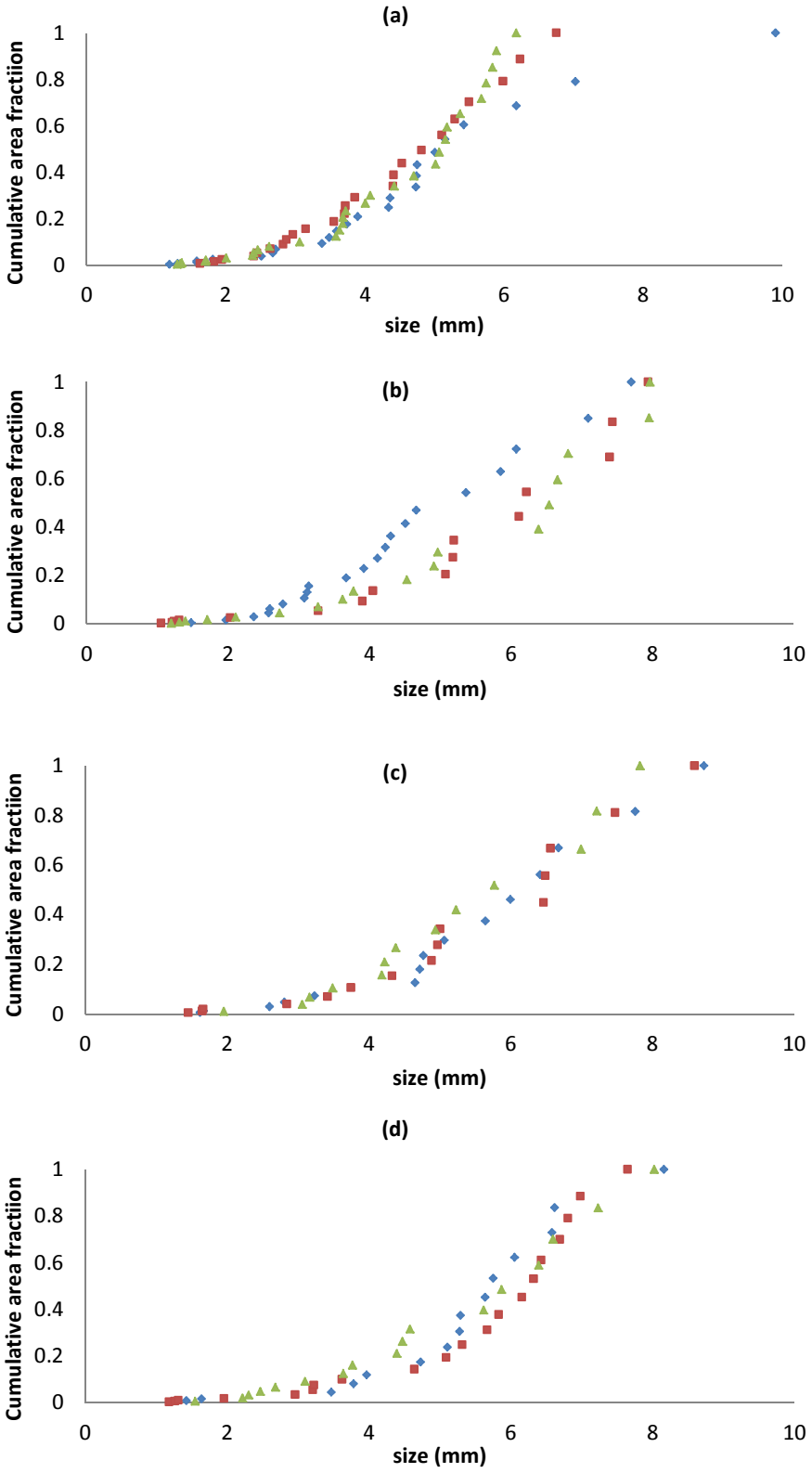

Figure 6-29: Cumulative area fraction of the bolus at swallow point for the three replicates of each type of gel, (a) 30% sucrose 15% gelatine, (b) 50% sucrose 15% gelatine, (c) 50% sucrose 10% gelatine and (d) 30% sucrose 10% gelatine.

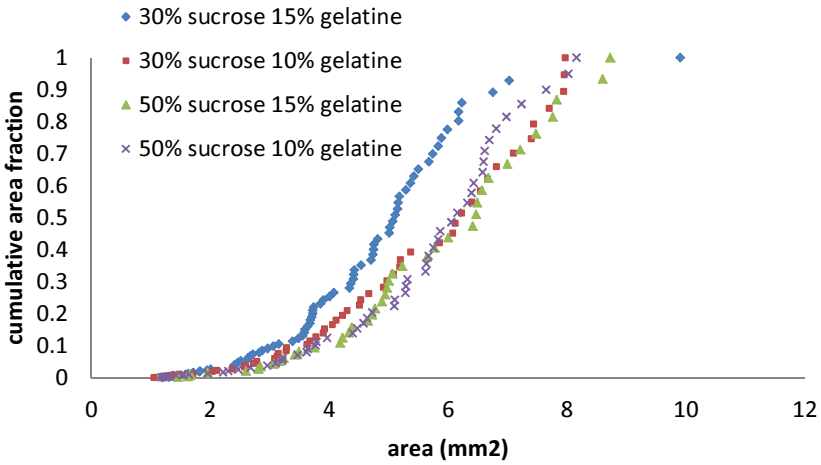

Figure 6-30: Cumulative area fraction of the gelatine boluses at swallow point where the three replicate boluses are combined into a single cumulative are a fraction.

To compare the distributions at the swallow point the d_{10}, d_{50} and d_{90} of the boluses from the different recipes were analysed, see Figure 6-31. Figure 6-32 shows the number of particles in the bolus at different stages of mastication. The 30% sucrose 15% gelatine gel produced boluses with a lower mean value for each of the size parameters. However, no significant difference was found between the recipes for the d_{10}, d_{50} and d_{90} respectively ($F(3,8) = 1.16$, $P > 0.05$), ($F(3,8) = 2.49$, $P > 0.05$), ($F(3,8) = 0.15$, $P > 0.05$). The number of particles in the bolus at the swallow point was different for 30% sucrose and 15% gelatine gel ($F(3,8) = 12.16$, $P < 0.05$).

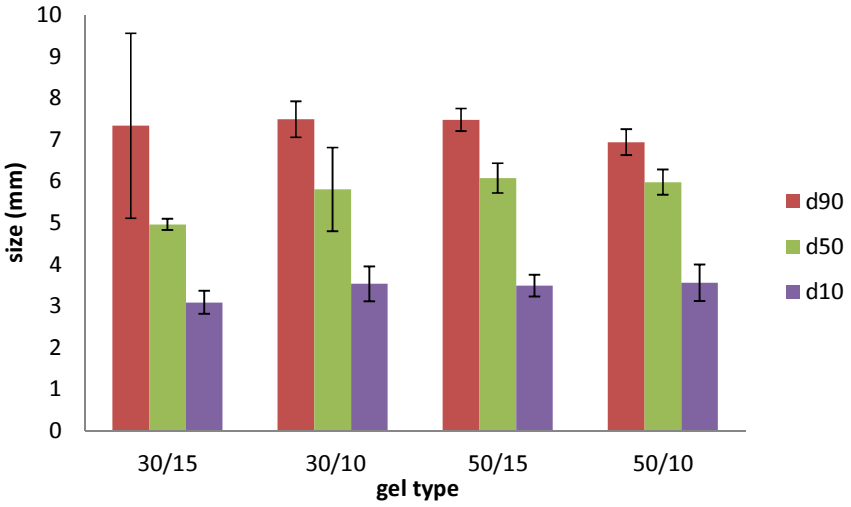

Figure 6-31: Key size parameters of the bolus at the swallow point for the different gels, (mean and standard deviation).

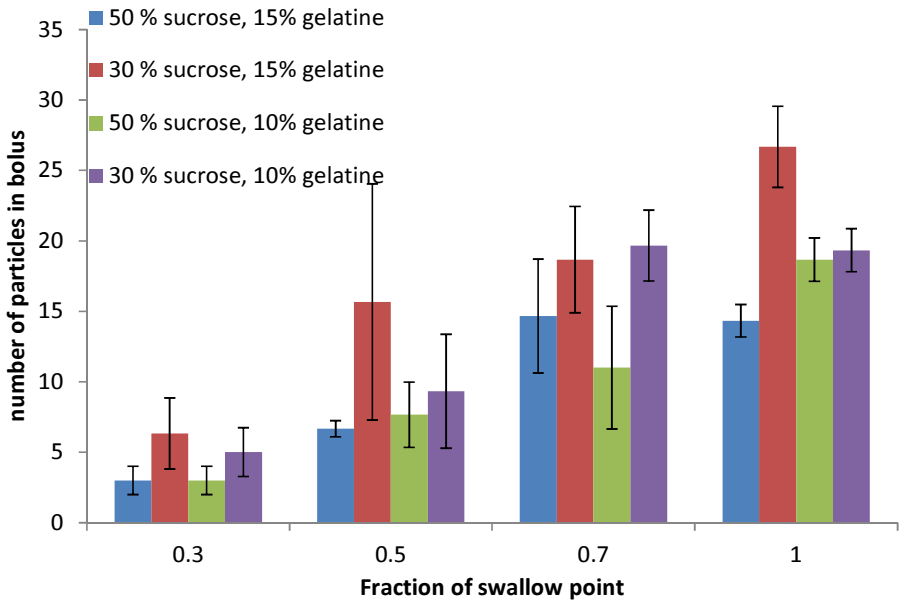

Figure 6-32: Number of particles in the bolus at different stages of mastication for the different gels, (mean and standard deviation).

The low number of particles in the bolus demonstrates the slow rate of mechanical size reduction, which contrasts starkly to a bolus of rice or peanuts which have thousands of particles at the swallow point. The variation between replicates can be large; this is typical for bolus data because of the physiological variables involved in oral processing. The 50/15 recipe produced a bolus with the fewest particles despite it requiring the most chews; demonstrating that the particles are often occluded without being cleaved into daughter particles.

In §4.3.2 and §4.4 the relationship between particle size and the inverse fragmentation ($(E/R)^{0.5}$) was discussed. It is proposed that the threshold particle size in the bolus is related to $(E/R)^{0.5}$. The toughness of the gels was not measured in this study; however, based on the values for other foods a sensible range for the gels can be assumed. Williams et al. (2005) measured the toughness of several foods including gummy bears which had toughness of 887 (J/m^2). Emmental cheese, raisin and dried apricot have values of 120, 306 and 565 (J/m^2) respectively (Agrawal et al., 1997, and Williams et al., 2005). It is reasonable to assume the gels in this study will have a toughness somewhere between 100 and 1000 (J/m^2). For the gels with 10 and 15% gelatine the $(E/R)^{0.5}$ is calculated with a toughness of 500 (J/m^2) and values of 100 and 1000 (J/m^2) to calculate likely range. Figure 6-33 shows the d_{90} of the gels at swallow point and their inverse fragmentation index fit the trend on the proposed state diagram for particle size threshold.

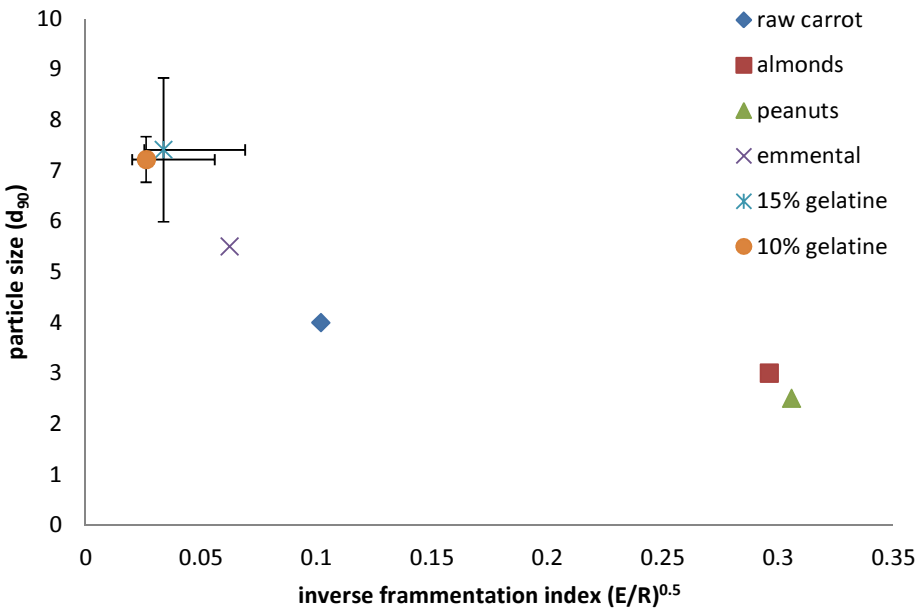

Figure 6-33: Relationship between the d_{90} in the bolus at the swallow point and the particle inverse fragmentation index for several foods, vertical error bars are the standard deviation of the d_{90}, horizontal error bars are the $(E/R)^{0.5}$ with toughness of 100 and 1000. (data for the other foods from Lucas et al. (2002), Peyron et al. (2004) and Jalabert-Malbos et al. (2007)).

Gelatine Melting Rate

The results of the in-vitro melting experiments, shown as the fraction melted with time, are shown in Figure 6-34 for the 30% sucrose gels and Figure 6-35 for the 50% sucrose gels.

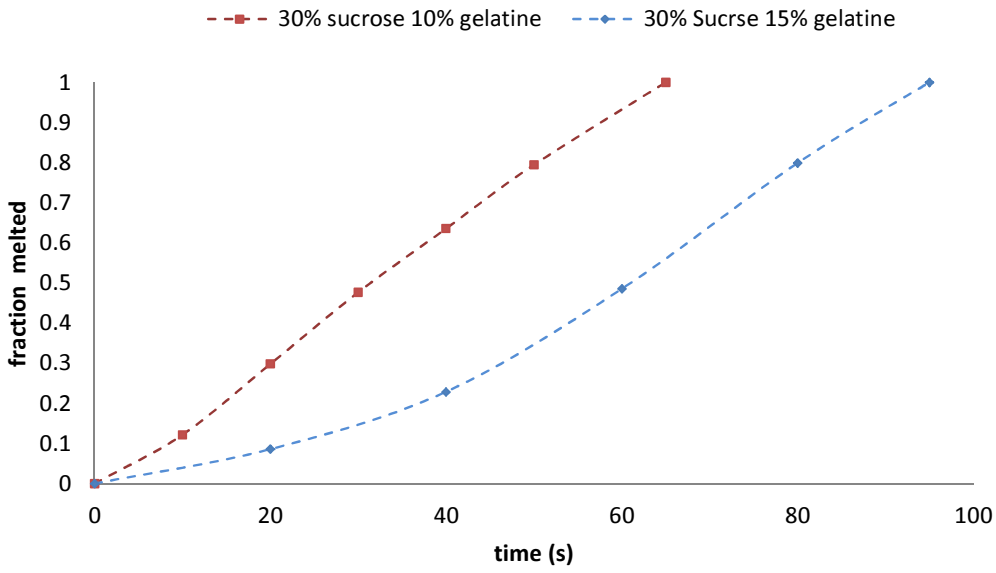

Figure 6-34: Fraction of the gelatine cube melted over time for the gels made with 30% sucrose, the cube was initially at 20° before being suspended in a beaker of water immersed in a water bath at 37°C.

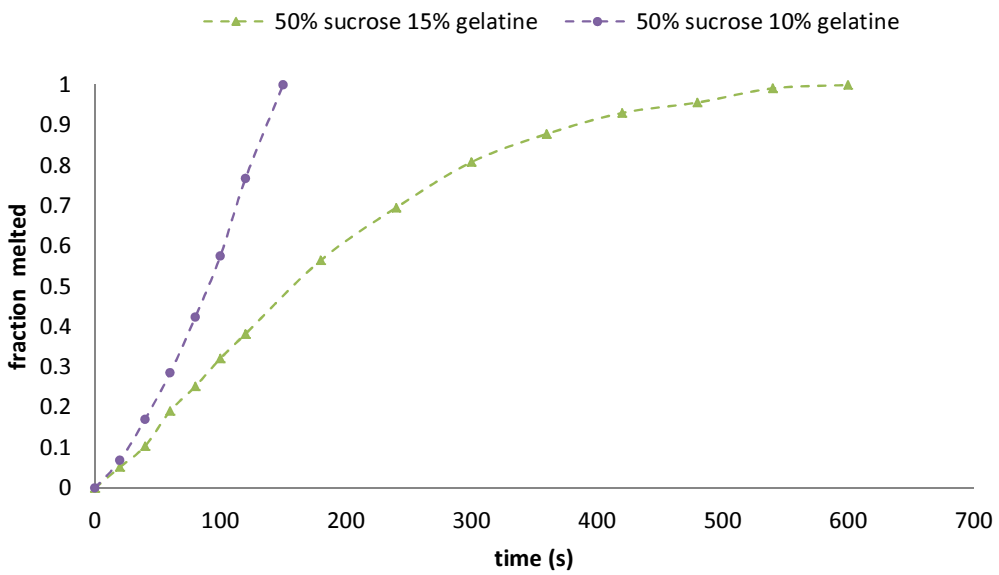

Figure 6-35: Fraction of the gelatine cube melted over time for the gels made with 50% sucrose, the cube was initially at 20°C before being suspended in a beaker of water immersed in a water bath at 37°C.

The gels took different lengths of time to completely melt, the 30/10 gel melted rapidly in 65 seconds, whilst the 50/15 gel took nearly ten times as long. Table 6-16, shows the initial melting velocity for the gels and the time taken to melt. This initial melting velocity is what will be used in the model to predict the amount of gel that melts in the bolus. It is expected to replicate the in-mouth melting rate during mastication of the gels.

The initial surface are of the cube is known and the size of the cube can be inferred from the measured sucrose concentration. Thus, the initial melting velocity was calculated by iteratively solving Eq. 5-34.

Table 6-16: Initial melting rate of the gels and time taken for the each gel to completely melt (mean ± stdv).

Gel type	Initial melting rate ($cm\ s^{-1}$)	Time to melt (s)
50% sucrose 15% gelatine	$5.50*10^{-4}$	600 ± 15
50% sucrose 10% gelatine	$5.85*10^{-4}$	150 ± 7.5
30% sucrose 15% gelatine	$6.25*10^{-4}$	95 ± 5.4
30% sucrose 10% gelatine	$2.25*10^{-3}$	65 ± 5.8

Despite the time taken to completely melt being different, the initial melting rate was similar for three of the gels, whilst the 30% sucrose 15% gelatine had a melting rate nearly an order of magnitude faster. The slope of the curves in the above figures (with the exception of the

50/15 gel) show that the effective melting velocity increases with time. The surface area for melting decreases and yet the rate at which the volume of is being remains constant or increases.

For gels that melt below 37°C, the melting rate is limited by thermal diffusion, as a temperature gradient develops in the gel and its mass average temperature increases, the melting front will move faster through the gel as the additional heat required to melt the surface layers decreases over time. If there was no temperature gradient in the gel, the melting velocity would remain constant. However, modelling a temperature gradient in the gels is not practical because the particles change size frequently as a result of occlusion. The complexity of the model required would not justify the potential increase in accuracy of the melting predictions. Because the oral processing time is short, assuming a constant melting velocity is reasonable.

Melting in the Bolus

The amount of each gel which melted during mastication correlates to the melting velocities from the *in-vitro* measurements. The 30% sucrose and 10% gelatine gel melted significantly more than the other gels and the 50% sucrose 15% gelatine gel melted the least. The amount of gel that melts per chew is expected to increase as mastication progresses because the surface area of the bolus increases as new particles are created through occlusion. Figure 6-36 shows the percentage of molten gel in the bolus at the swallow point is approximately 2.5 greater than at the half the half-way point for all the gels. This trend is in-line with the expectations. However, the amount of melting seen in the bolus is less than expected based on the initial melting rate observed *in-vitro*. Figure 6-36 shows how much of each gel melted in the mouth during mastication.

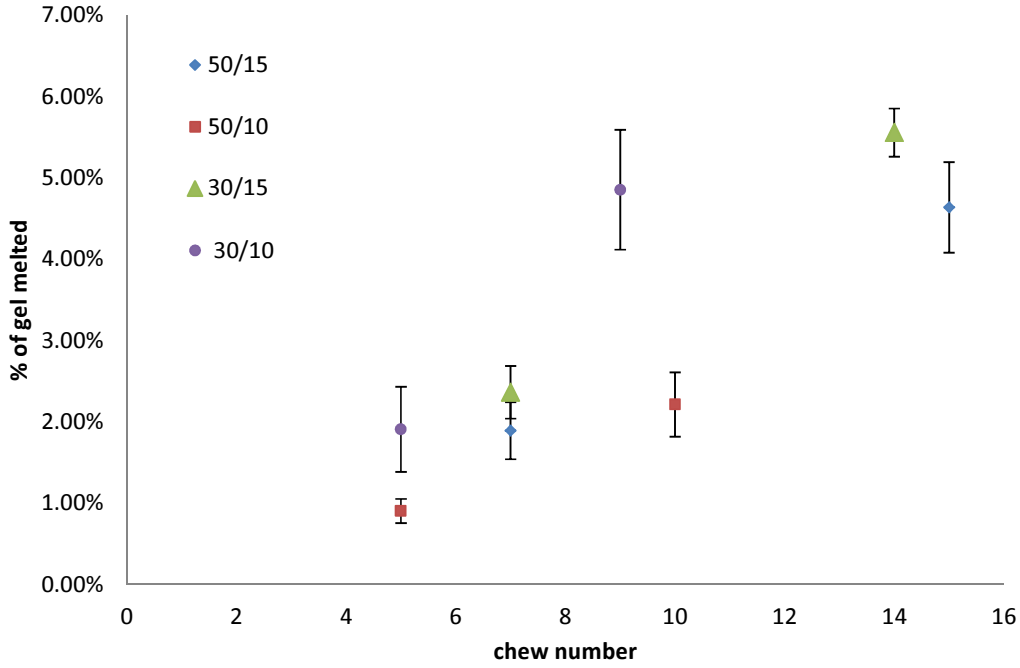

Figure 6-36: Amount of the gel cube that was melted during mastication for the different gel recipes (mean ± stdv).

6.2.4 Model Results

The results for the particle size predictions are discussed first followed by the melting of the particles in the bolus. The cumulative area fraction in each size class for the data and simulated boluses were compared. The model fit was optimised by minimising the sum of the squared residuals between the model and the data by changing the selection function parameters. The three replicate bolus measurements of the particle size at the swallow point were grouped together and the cumulative area fraction vs particle area is plotted.

Particle Size Distribution

Figure 6-37 to Figure 6-40 compare PSD of the boluses at the swallow at the swallow point to the simulation results for the four types of gel.

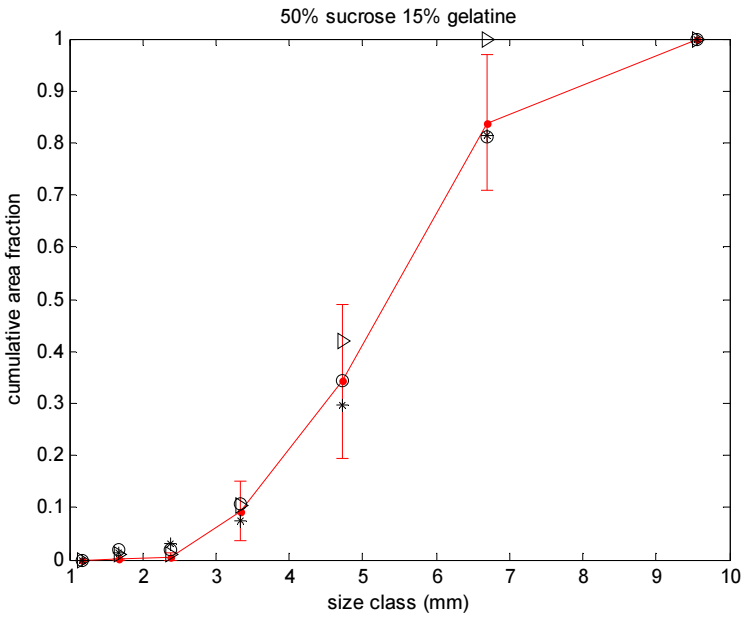

Figure 6-37: Cumulative area fraction in each size class for the three replicate boluses at the swallow point for the 50% sucrose 15% gelatine gel, the red dot and error bars show the model predictions (mean ± stdv of 25 replications)

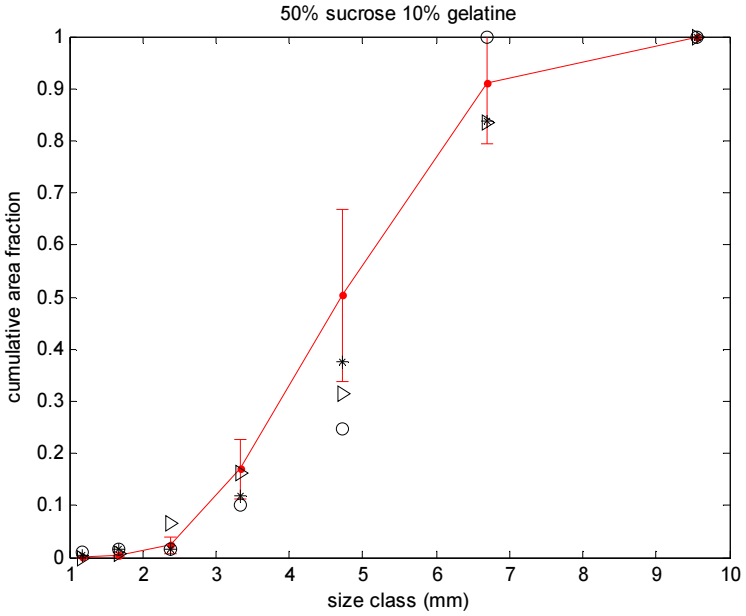

Figure 6-38: Cumulative area fraction in each size class for the three replicate boluses at the swallow point for the 50% sucrose 10% gelatine gel, the red dot and error bars show the model predictions (mean ± stdv of 25 replications).

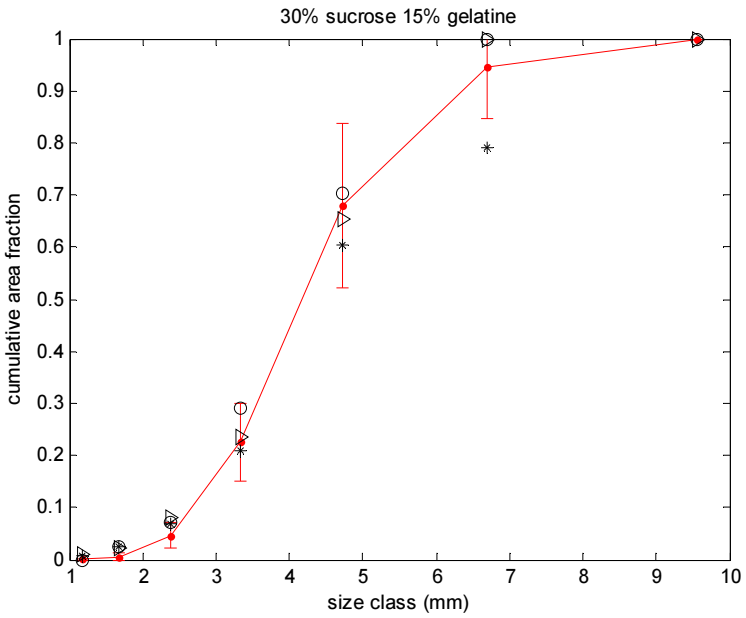

Figure 6-39: Cumulative area fraction in each size class for the three replicate boluses at the swallow point for the 30% sucrose 15% gelatine gel, the red dot and error bars show the model predictions (mean ± stdv of 25 replications).

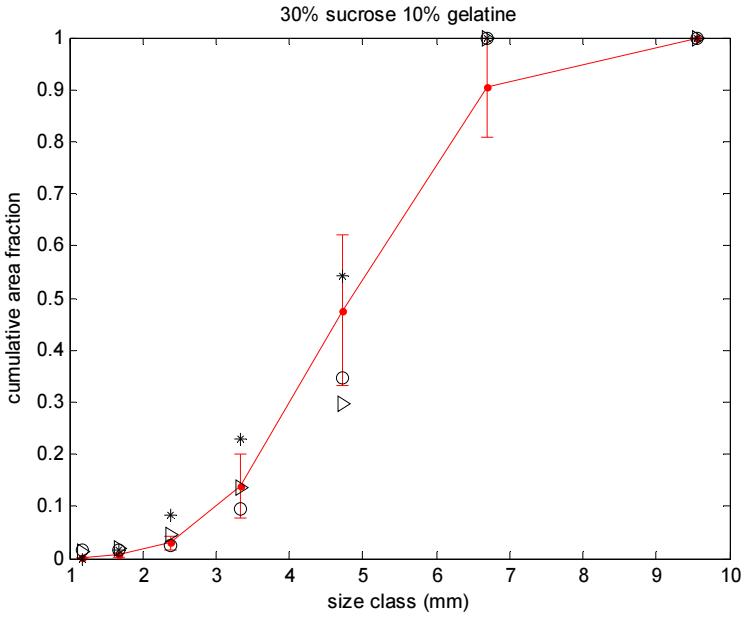

Figure 6-40: Cumulative area fraction in each size class for the three replicate boluses at the swallow point for the 30% sucrose 10% gelatine gel, the red dot and error bars show the model predictions (mean ± stdv of 25 replications).

The values of the selection function parameters are given in Table 6-17 as well as the r^2 value for the cumulative area fraction of the model fitted to the bolus data at swallow point. The high variability and standard deviations are because the gel boluses do not have many particles in them so one or two can skew the distribution, necessitating the relatively high number of

model replicates, n = 25. The important point is that the model provides a good representation of the oral processing of the gels. The sub-division method for breakage and particle selection based on size allows the PSD of the gel bolus to be simulated.

Table 6-17: Parameters of the selection function used to obtain the best fit for the area fraction in each size class, *v* and *w* are the fitted parameters in the power law selection function. The r^2 value for each gel is also shown.

	50% Suc 15% gel	30% Suc 15% gel	50% Suc 10% gel	30% Suc 10% gel
v	0.35	0.68	0.70	0.75
w	1.75	1.50	1.50	1.50
r^2	0.98	0.91	0.98	0.93

The selection chance was similar for three of the four gels with the 50% sucrose 15% gelatine gel having a lower chance of being fragmented than the other gels. The elastic nature of the gels meant they were sometimes squeezed between the teeth without fracturing. The slightly higher selection function exponent, *w*, for the 50/15 gel reflects the proportionally lower chance smaller particles have of being fragmented. The exponent is within the range found in previous comminution studies; where the values ranged from 1.0 to 2.0 van der Bilt et al. (1987) and 1.6 to 2.6 van der Glas et al. (1987) for subjects chewing on Optosil particles. The two gels with 10% gelatine had a comparable PSD and were chewed on average 9 and 10 times before the being swallowed, therefore the parameters governing their size reduction will be the same or very similar.

In the next section the melting mechanism is incorporated in the model and compared to the *in-vivo* experiments.

Gel Melting

The model results using a constant melting velocity obtained from *in-vitro* tests predict more melting than what was observed in the *in-vivo* boluses from the subject as shown in Figure 6-41 to Figure 6-44 for the four gels.

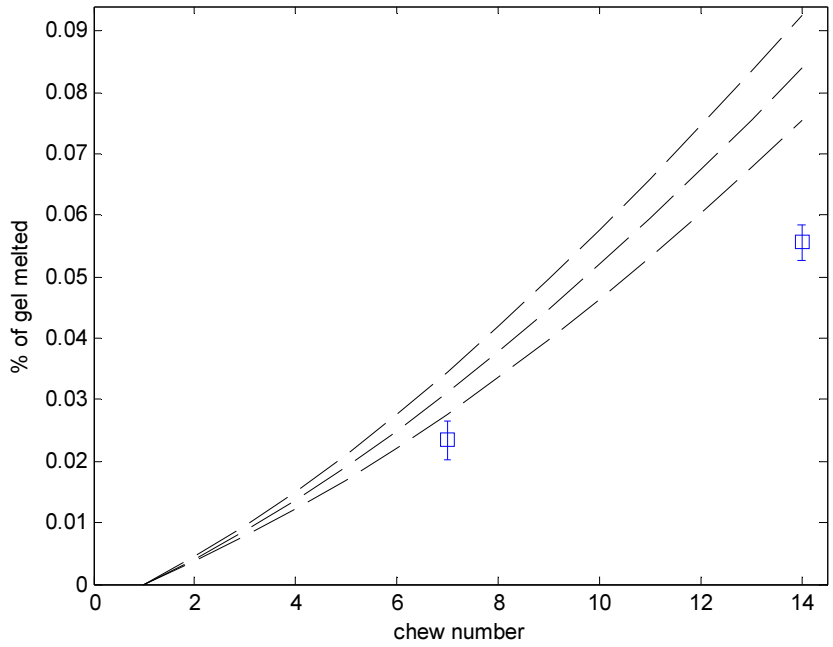

Figure 6-41: Amount of gel that melts during mastication of the 30% sucrose 15% gelatine recipe; -- is the means and standard deviation from 25 model simulations, □ mean and standard deviation of the *in-vivo* measurements with the subject.

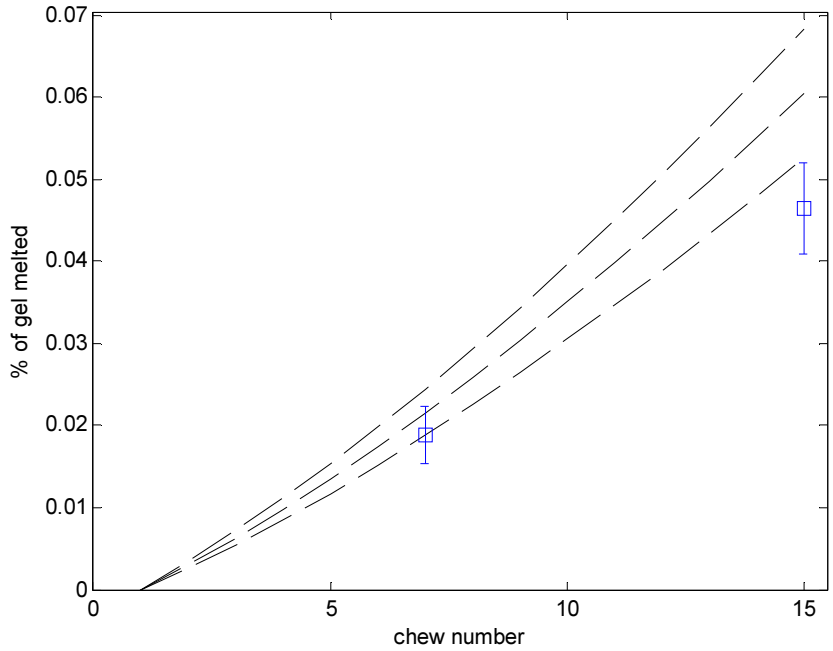

Figure 6-42: Amount of gel that melts during mastication of the 50% sucrose 15% gelatine recipe; -- is the means and standard deviation from 25 model simulations, □ mean and standard deviation of the *in-vivo* measurements with the subject.

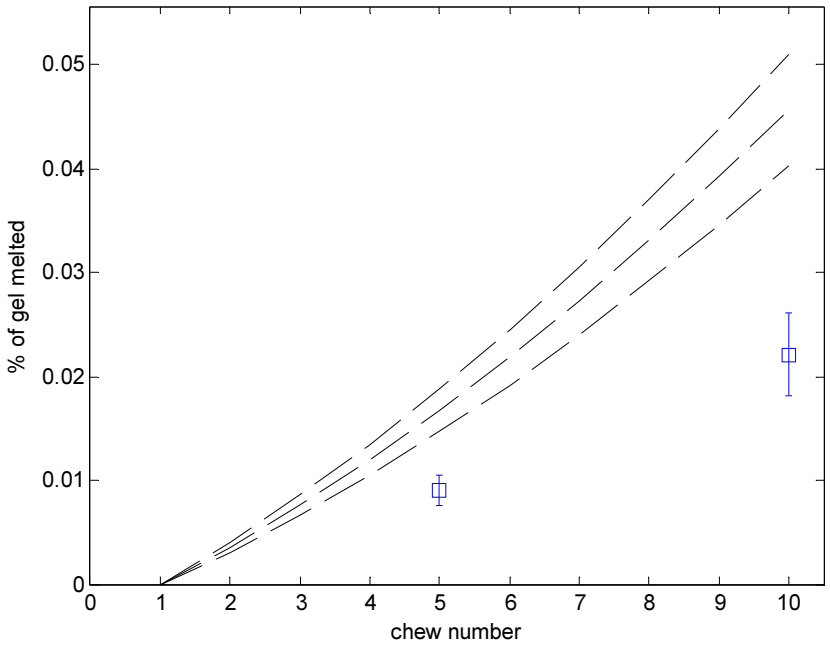

Figure 6-43: Amount of gel that melts during mastication of the 50% sucrose 10% gelatine recipe; -- is the means and standard deviation from 25 model simulations, □ mean and standard deviation of the *in-vivo* measurements with the subject.

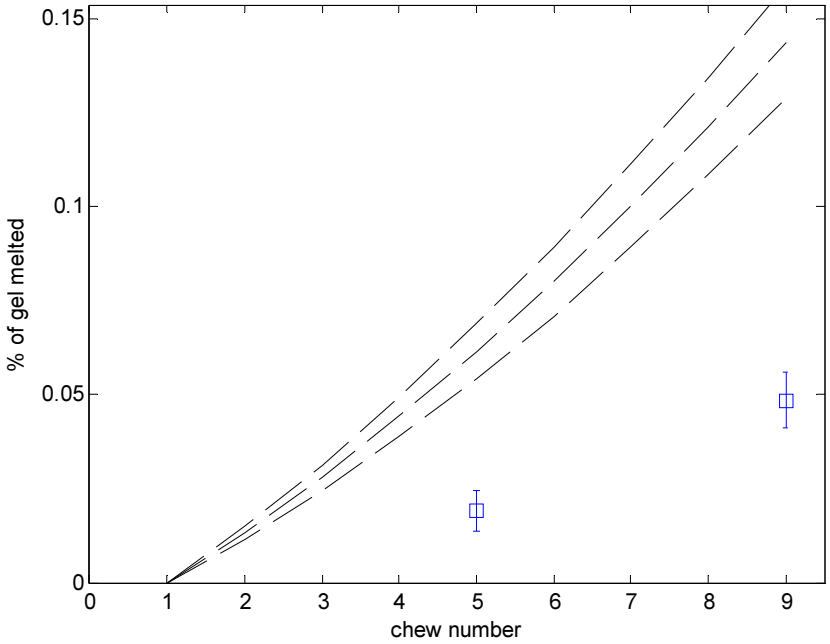

Figure 6-44: Amount of gel that melts during mastication of the 30% sucrose 10% gelatine recipe; -- is the means and standard deviation from 25 model simulations, □ mean and standard deviation of the *in-vivo* measurements with the subject.

The discrepancy between the model predictions and the in-vivo results show that the actual in-mouth melting velocity is less than what was measured from the in-vitro experiments. A couple of explanations account for the difference. The in-vitro melting experiments mimic an idealised situation in the mouth because the gel cubes are fully submerged in water which is well mixed ensuring the surface of the gel is ≈37°C. During mastication the gel particles are not always in perfect contact with sufficient liquid or oral surfaces, and the liquid phase of the bolus has less thermal mass than the water in the experiment. Furthermore, when a particle is fragmented new surface area is exposed. This new surface area will be close to the initial gel temperature. It will take some time for the new surface to be coated with saliva and heated to the melting temperature. As a result, melting from the newly exposed gel surfaces is likely to initially occur at a slower rate. The melting velocity from the in-vitro experiments is calculated from time zero to the first measurement. If the melting velocity changes over this initial period then it will be overestimated.

The model predictions for the gel melting can be fitted to the *in-vivo* data to determine the melting velocity of the gels during mastication. This is based on the assumption that the melting velocity in the mouth is constant. Figure 6-45 shows the best fit model for each of the gel recipes and the best fit velocities are compared to the *in-vitro* test velocities in Table 6-18

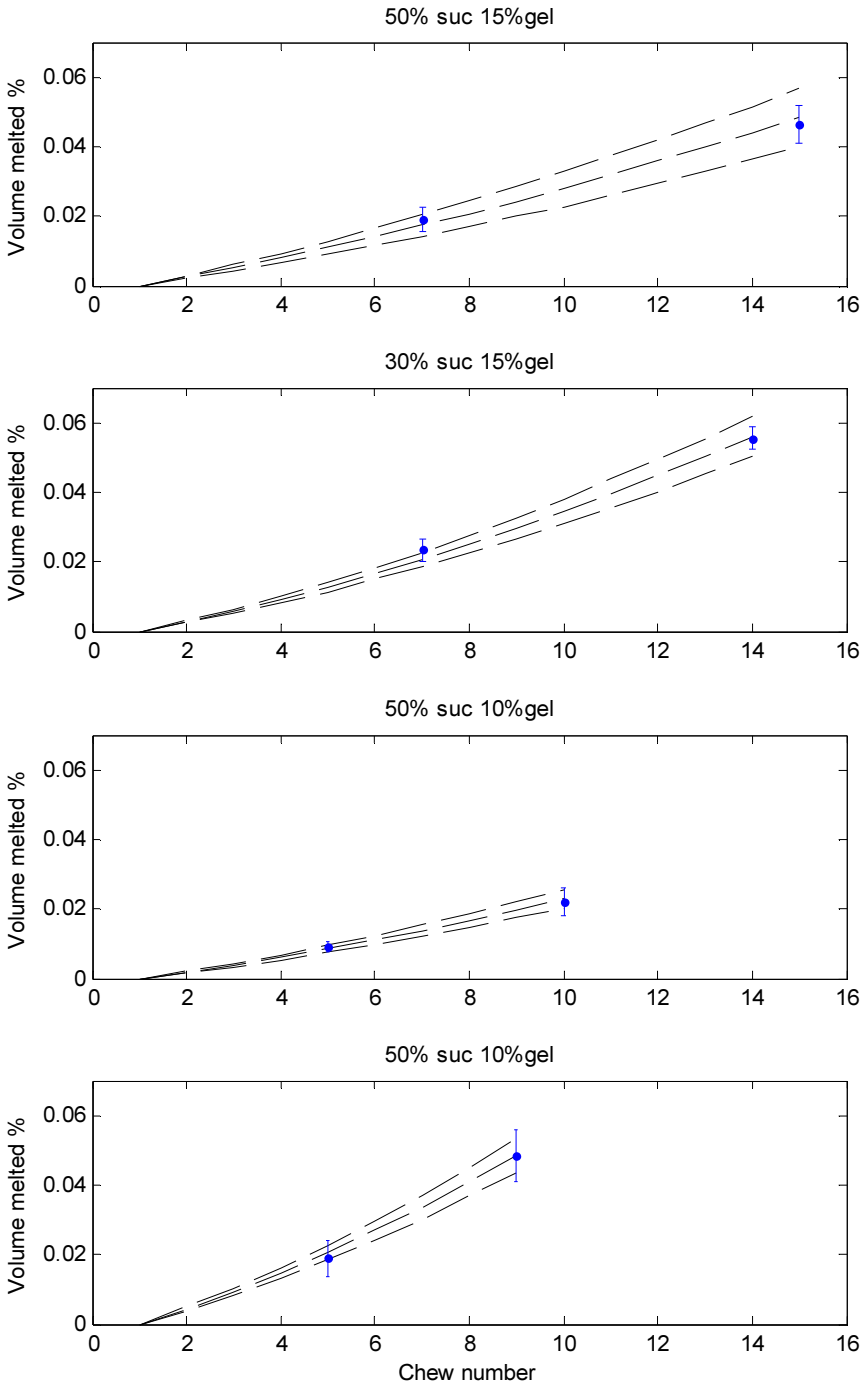

Figure 6-45: Fraction of gel that melts during mastication of the four gel recipes, the best fit model compared to the data; -- lines are the means and standard deviation from 25 model simulations, • is the mean and standard deviation of the *in-vivo* measurements with the subject.

Table 6-18: Comparison between the initial in-vitro melting rate and the melting rate that provided the best fit between the model and in-vivo experimental results.

Gel type	In-vitro melting rate ($cm\ s^{-1}$)	Best fit melting rate ($cm\ s^{-1}$)	% difference
50% sucrose 15% gelatine	$5.50*10^{-4}$	$4.50*10^{-4}$	18
50% sucrose 10% gelatine	$5.85*10^{-4}$	$2.80*10^{-4}$	52
30% sucrose 15% gelatine	$6.25*10^{-4}$	$4.35*10^{-4}$	30
30% sucrose 10% gelatine	$2.25*10^{-3}$	$6.75*10^{-4}$	70

These results show that melting rates observed in the mouth are considerably lower than in the in-vitro experiment. The difference between v_m measured in-vitro and in-vivo ranges from 18-70%. The 30% sucrose 10% gelatine recipe still had the highest v_m, however it is a lot closer to the other gels during mastication than when measured in-vitro. The rate limiting step for melting in the mouth is heat transfer to the surface of the gel which comes from the saliva produced and from the walls of the oral cavity. Therefore, for gels that melt below the mouth temperature an in-vivo experiment is likely to better characterise the melting behaviour.

Heat transfer in the mouth and how it relates to bolus properties is not widely studied in the literature. The overall heat transfer coefficient in the mouth is something that should be the focus of future research. It would enable a better understanding of the heat transfer between the mouth and bolus and could prove valuable when trying to understand the breakdown pathway of heat sensitive foods.

6.2.5 Summary and Conclusions

When the gels were occluded they predominantly subdivided into two daughter particles. Sometimes a gel particle would resist fracture and not be fragmented. This resulted in the boluses having a small number of particles in contrast to the rice and peanuts examined in the other case studies. Because there were fewer particles in the bolus, comparing the PSD in the early stages of mastication was difficult.

Four gels were produced by varying the concentration of gelatine (10 and 15%) and sucrose (30 and 50%). The hardness and Young's modulus was measured with a TPA compression test. These correlated to the number of chews needed to reach the swallow point with the two hardest gels requiring ≈50% more chews. However, the PSD of the boluses were similar at the swallow point, indicating the particle properties were not sufficiently different, resulting in the

gels having the same size threshold for swallowing. The inverse fragmentation index, calculated from the Young's modulus and toughness, is correlated to the particle size threshold (§4.3.2 and §4.4). This was calculated for the gels and plotted against their d_{90} at the swallow point. The gels fit the trend on the state diagram; they have the lowest inverse fragmentation index and the largest particles in the bolus at the swallow point.

The initial in-vitro melting rate was similar for three of the gels (5.5-6.25 x 10^{-4} cms^{-1}) with the 30% sucrose, 10% gelatine gel being faster by almost an order of magnitude (2.25 x 10^{-3} cms^{-1}). However, these in-vitro melting rates were not replicated in the mouth where to fit the model they needed to be 18-70% lower. The reason appears to be that in the mouth heat transfer is limited by both the available surface area and good contact between it and saliva and the oral surfaces. Certainly in the early stages this is compromised because there is little saliva present. Then as particle breakdown occurs, there is a lag time as the sensible heating occurs to bring the new surface up to the gel melting temperature. Heat transfer in the mouth could be better measured by melting cubes of gel in the mouth without chewing. The gel could either be held stationary between the tongue and palate or moved around the mouth. Weighing the gel after a fixed period of time in the mouth would give a better indication of the effective melting velocity in the mouth. Knowledge of the gels thermal properties would also enable the overall heat transfer coefficient to be measured.

6.3 Case Study - Peanuts Embedded in Different Food Matrices

In this section the mastication model is applied to peanuts embedded in two matrices, chocolate and gelatine, based on the data of Hutchings et al. (2011) who found that the matrices caused different breakdown rates of the peanut particles. The aim of this modelling exercise is to quantify how the type of matrix influences the selection process of the embedded peanuts.

So that the focus remains on the peanuts, this case study is a simplification of the mastication model, where all rate processes other than comminution and mixing are turned off. This is not strictly true, because the chocolate matrix both melts (the fats) and dissolves (the sugars) and some of the gelatine matrix dissolves. For the two included rate processes, mixing is captured mathematically by the selection function and comminution by the breakage function. Hutchings et al. (*ibid*.) were interested in the initial size distribution of peanuts, however the matrix is also broken down during chewing, but its size distribution could not be recovered due to the experimental techniques employed. Therefore assumptions about the breakdown dynamics of the chocolate and gelatine matrices were necessary.

The following section discusses the methodology and assumptions employed and the targeted observations for the modelling.

6.3.1 Methodology

Experimental

The study by Hutchings *et al*. (2011) was a single subject study with the subject being chosen after passing a screening process where their chewing behaviour was compared to a population (*n*=45) of healthy subjects with good dentition. The subject who had the lowest standard deviation for each measured chewing parameter compared to the population was chosen. The experiment involved two test foods, a gelatine gel (250 bloom) and a chocolate matrix, containing six embedded peanut quarters. The peanuts used were roasted and unsalted. The serving size was 9 cm^3 with each matrix containing 11.3% (v/v) peanut quarters.

The procedure of Hutchings (2011) is briefly described below as it is pertinent to the analysis carried out in this thesis. Boluses were collected after 5, 10, 15, 20 and 25 chews and at the natural swallow point. The subject did not know when they were going to expectorate; they were instructed by the researcher to do so. The chewing duration and order of test foods was randomised with each session containing 12 samples (six gelatine and six chocolate samples chewed to 5, 10, 15, 20, 25 chews or the swallowing point). After expectoration the subject rinsed their mouth with 25 ml of distilled water and expectorated into a separate container. The bolus and rinsings were weighed and then frozen at -18°C for further analysis. The expectorated boluses and debris were combined and washed with warm water over a 355 µm sieve to remove the matrix leaving only the peanut particles. A flatbed scanner was used to capture an image for processing. The particle size distribution (2D projected particle area) of the peanut particles was measured by image analysis using image J® software. The total peanut dry weight recovered at each chewing interval was significantly less than the initial dry weight, with the highest retention being after five chews in the gelatine matrix. After 25 chews ≈ 30% peanut solids were recovered from both matrices, as shown in Figure 6-46.

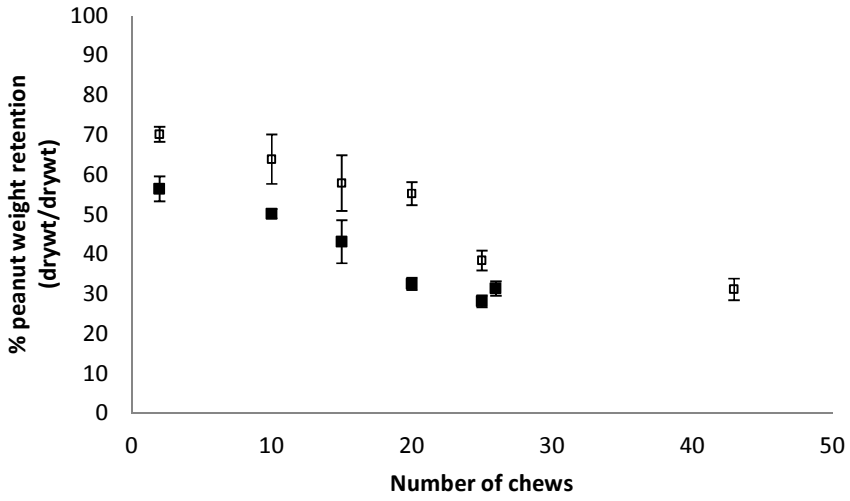

Figure 6-46: Recovered dry weight of peanuts in the bolus that are retained on a 355 μm sieve after different number of chews. Peanuts in chocolate matrix ■; peanuts in gelatine matrix □, (mean ±SE). Data from Hutchings (2011).

Hutchings (2011) results correspond with studies by Peyron et al. (2004), Jalabert-Malbos et al. (2007) and Flynn et al. (2011). Hutchings states that the likely sources of peanut loss are movement of particles into the oropharynx and during the wet sieving across the 355 μm sieve. Separating these two effects is by deduction. When boluses were simply dried and weighed without washing, the losses in dry weight were small, 10% for the chocolate and no significant loss for the gelatine boluses. This indicates that 0-10% of material is transported to the oropharynx which without more detailed data, we can assume is equally for both matrix and peanuts. After the matrix is washed from the peanuts on the 355 μm sieve, Figure 6-46 shows significant further loss of peanuts, up to ~70% at swallow point. These unrecovered particles must have passed the 355 μm sieve. Flynn's (2012) work supports this conclusion. She studied the particle size distribution for several foods including peanuts and conducted wet sieve analysis of the bolus and debris from a mouth rinsing after expectoration. For a 4 gram serving of peanuts, 38% was recovered above the 125 μm sieve, 46% of the total solids ingested were recovered in the pan below the 125 μm sieve, and approximately 16% of the solids were not recovered at all from the bolus or debris. Flynn (ibid) suggested that these particles may be still stuck in the oral cavity after rinsing the mouth or have been moved to the oral pharynx and swallowed during mastication. The subjects were instructed to chew in a natural manner so some intermediate swallowing may have occurred. These findings indicate that when a peanut particle is occluded a significant portion is crushed into very fine particles

during which lipids might also be expressed which are then washed away during the wet sieving process.

An experiment was carried out to quantify the fraction of a quarter peanut particle that will pass a 355 µm sieve after occlusion. This experiment is not conducted with the same subject used by Hutchings (2011), however, the differences in food particle fragmentation is significantly more dependent on the properties of the food than differences in oral physiology and chewing behaviour of individuals. Thus, the experiment provides an indication of the fragmentation behaviour and information that can be used in the model; roasted quarter peanuts (GO NUTZ food ltd) were used in this experiment. A similar protocol to that used by Mowlana and Heath (1993) was followed, where food particles are placed in a finger cot, which a subject chews once only. The particles and the fragments are then removed and examined. It is a convenient method which isolates the particles from the mouth meaning no particles or soluble solids are lost and the distribution of daughter particles is similar to fragmentation tests on samples chewed naturally. In this study, a quarter peanut was placed inside a latex finger cut off from a glove. The particle was placed in the occlusal zone and a single chew was performed, then the fragments were emptied into a pre weighed confoil aluminium container. This was repeated on eight quarter particles. There was negligible mass lost transferring particles from the cot to the container. The particles were then placed on a 355 µm sieve and washed with water at a flow rate of 2 L min^{-1} for 30 seconds. The retained particles were then scraped off the sieve and placed on a pre-weighed confoil dish and placed in an oven at 105°C for 24 hours. The dry solids content of the peanuts was determined by drying un-chewed quarter peanuts on a pre-weighed confoil container at 105°C for 24 hours. Table 6-20 shows that for 16 quarter peanut particles occluded individually, 17% passed the 355 µm. This fraction comprises fine particles and lipids expressed from surface of the particles as a result of fragmentation.

Table 6-19: Mean (± SEM) moisture content of the quarter peanuts

	Moisture content (g/100g dry food)
Peanuts	3.26 ±0.1

Table 6-20: Summary of 16 quarter peanut particles occluded and wet sieved on 355 µm mesh.

Mass of 1/4peanuts after chewing (g)	Dry solids retained on 355 µm sieve (g)	Fraction of quarter peanut occluded below 355 µm
3.52	2.82	17%

Conservation of volume and particle shape factor

As the particle size distribution evolves, volume needs to be conserved. A characteristic shape needs to be assumed so that particle volume can be calculated from the measured projected area of the particles. Hutchings (2011) assumed the particles were spherical and particle diameter was calculated assuming the projected area was circular. Particles were put into size classes based on the particle diameter. This assumption was justified by comparing the cumulative PSD of peanuts from wet sieving with the cumulative PSD given by image analysis using the above assumption on particle shape. The distributions were comparable which validated the approach; however, an actual volume balance was not shown. The cumulative distribution was shown as a fraction of the total volume. The assumption of spherical particles does not hold for the peanuts recovered from the chewing study with the matrices, where the retained peanut volume is over estimated by a factor of three. Thus, a new relationship between the projected 2D area and volume needs to be defined.

A whole peanut is an ellipsoid and a quarter peanut particle is analogous to a quarter of an ellipsoid whose volume is calculated by

$$V = \left(\frac{4}{3}\pi.a.b.c\right)/4 \qquad \textbf{Eq. 6-6}$$

where *a* is the major axis, *b* is the minor axis and c is the vertical axis. The axes have lengths 2*a*, 2*b* and 2*c*. Thus, the projected particle area is assumed to be half an ellipse, given by

$$A = 2(\pi.a.b) \qquad \textbf{Eq. 6-7}$$

If the major axis, *b*, is half *a* then the half area of the ellipse is equivalent to a circle with diameter *a.* To calculate the peanut particle volume, it was assumed that the minor and

vertical axes *b* and *c* are related to *a* by a shape factor *sf* which lumps the relationship that *b* and *c* have to *a* in one number. Thus the volume of a particle is given by Eq. 6-8,

$$V = \frac{1}{sf}\left(\left(\frac{4}{3}\pi a^3\right)/4\right) \qquad \textbf{Eq. 6-8}$$

It was found that the shape factor that accurately predicted the volume of a quarter peanut overestimated the total particle volume if used on all particles. Thus, different shape factors were given to each of the size classes. The shape factors were fitted by minimising the residual sum of squares between the predicted and recovered volume for all the expectorated boluses. Figure 6-47 shows the shape factors used for each of the particle size classes. Figure 6-48 compares the predicted bolus volume calculated from the 2D particle area with the actual volume of retained particles.

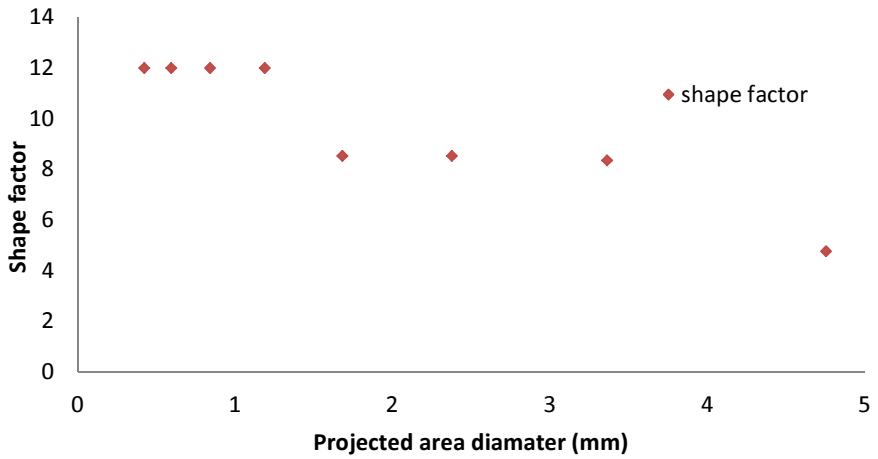

Figure 6-47: Values of the shape factors used to get the best fit for the peanut particle volume.

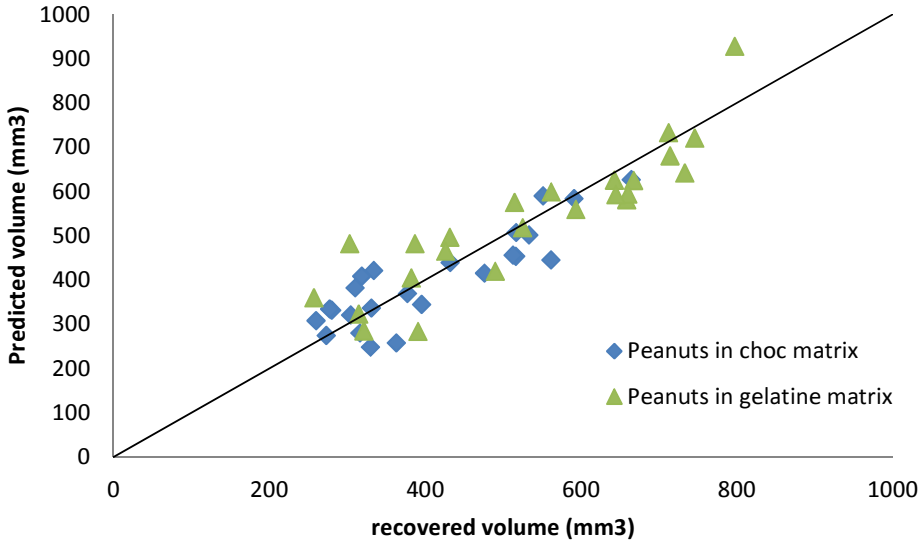

Figure 6-48: Predicted volume of retained particles vs actual volume of retained particles, where particles are assumed to be quarter ellipsoids.

6.3.2 Model Development

The mastication model has all rate processes switched off except comminution and mixing. This is done to investigate the evolution of particle size distribution of the embedded peanuts. For the two included rate processes, mixing is captured by the selection function and comminution by the breakage function. The comminution model has been described in §5.3.4. The particle size distribution (PSD) is sorted into size classes that follow a $2^{0.5}$ progression; ≥ 4.0, 2.8, 2.0, 1.4, 1.0, 0.71, 0.50, 0.355 and <355 (mm) To calculate the selection chance of particles in each size class the geometric mean diameter between size classes is used. The power law selection function is chosen here as it is has been used successfully in the previous comminution studies by van der Bilt et al. (1987), and Prinz and Lucas (1997). It is preferred over the competition model of selection (see §2.7.1) as that relies on knowing the number and size distribution of all the particles in the bolus which is not the case here because only data for the peanuts is available. Furthermore, the power law selection function is a simple approach with only two parameters to be fitted.

The fragmentation of peanuts was not measured by Hutchings et al. (2011). However, Kim et al. (2011) measured the distribution of particles resulting from a single chew of ½ and ¼ peanuts by a single human subject, a 2D chewing robot and uniaxial compression. The degree of fragmentation, *r*, calculated from their data of 20 replicates, is 1.8. Their analysis involved

washing the particles on a 312 µm sieve so the fragmentation variable only describes the distribution of the recovered particles above this size. A particle with a diameter of 4.0 mm in **Eq. 2-23** with *r* value of 1.8 only gives 1.9% below 355 µm. However, as shown in Table 6-20, 17% of a single occluded particle passed a 355 sieve. This suggests peanuts produce a bimodal distribution with the majority of peanut forming a distribution of larger particles and a second smaller distribution comprising fine particles and expressed lipids. Krifa (2009) showed that mixed cumulative distribution functions could be fitted to bimodal distributions resulting from size reduction of particulate and fibrous materials. Here, the size distribution of an occluded peanut is described by a mixed breakage function,

$$B(X, X_0) = Y * (1 - (1 + r_1.X/X_0).(1 - X/X_0)^{r_1}) + (1 - Y) * (1 - (1 + r_2.X/X_0).(1 - X/X_0)^{r_2}) \quad \textbf{Eq. 6-9}$$

where a portion, *Y*, of particle X_0 is distributed by the undersize distribution with fragmentation variable r_1 and (1-Y) of X_0 are distributed with r_2. The sensitivity of the model predictions to the breakage function is investigated and it is shown that variation in the breakage function has less influence on the size distribution of the peanuts than the selection function, indicating that the mixing changes markedly across the mastication cycle but that the peanut particle properties remain relatively constant.

Several assumptions are made to simplify the model.

- The breakage function of the peanut particles is constant across all particle sizes, so only the selection function is changed.
- Particles within each size class have the same chance of selection.
- The exponent of the selection function is constant; van der Glas et al. (1987) found that it did not change during mastication even when the bolus consisted of different mixtures of particles.
- The unrecovered peanut particles in the analysis by Hutchings (2011) are assumed to have been expectorated and subsequently all washed through the 355 µm sieve. Hutchings (2011) found ≈10% loss of solids from the chocolate bolus and no significant losses from the gelatine boluses (§6.3.1) so it is reasonable for the purpose of the model to assume all the peanut particles are retained in the bolus

A schematic flow diagram of the discrete comminution model is shown in Figure 6-49 below. The model was coded in MathWorks® MATLAB 2013a and the files are in Appendix E.

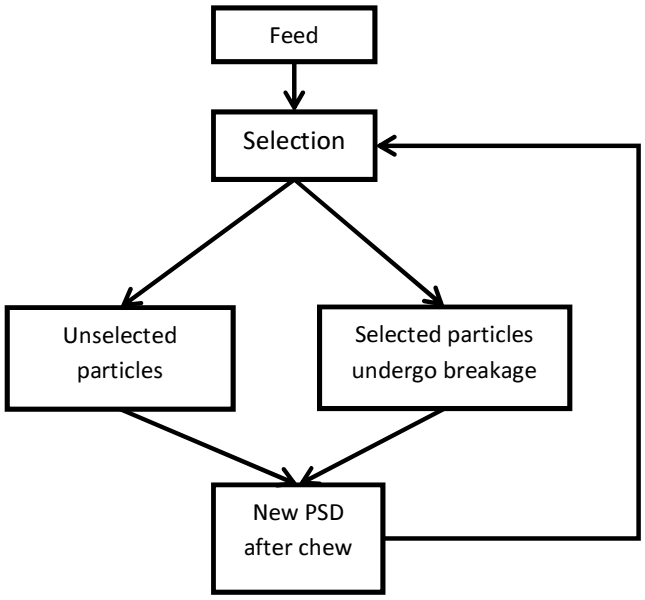

Figure 6-49: Schematic model flow diagram of the comminution model for the peanut component of the matrix, this is a specific case of the generalised diagram in Figure 5-5.

Peanut PSD data is available for five chew intervals up to 25 chews and at the swallow point. The particle size distribution of the model was compared to the mean PSD of the four replicate boluses at each of the five chew intervals. The model prediction was optimised by tuning the selection function parameters, where a different selection function was used for each of the chewing intervals. In reality the selection chance of the particles would not follow a rigid condition of changing every five chews. However, given the data available and the differences in the distributions at these chewing intervals it is a good starting point for this analysis. Fifty simulations were carried out with the mean PSD of the simulations compared to the mean PSD of the four data replicates. The best fit model was obtained by minimising the sum of the squared residuals between the model prediction and the data at each of the 5 chew intervals.

6.3.3 Results

Experimental Data

The particle size distributions using the data from the single subject study by Hutchings (2011) are shown in Figure 6-50. Eq. 6-8 and the shape factors from Figure 6-47 were applied to the projected area data to develop the volume fraction plots. The particles were put into size

classes based on the *a* axes from Eq. 6-6. The expectorated boluses and debris were washed on a 355 µm sieve prior to image analysis and the unrecovered dry weight is assumed to be made up of particles below this size. The average number of chews to swallow point is 26±1 and 43±1 for the chocolate and gelatine matrix respectively.

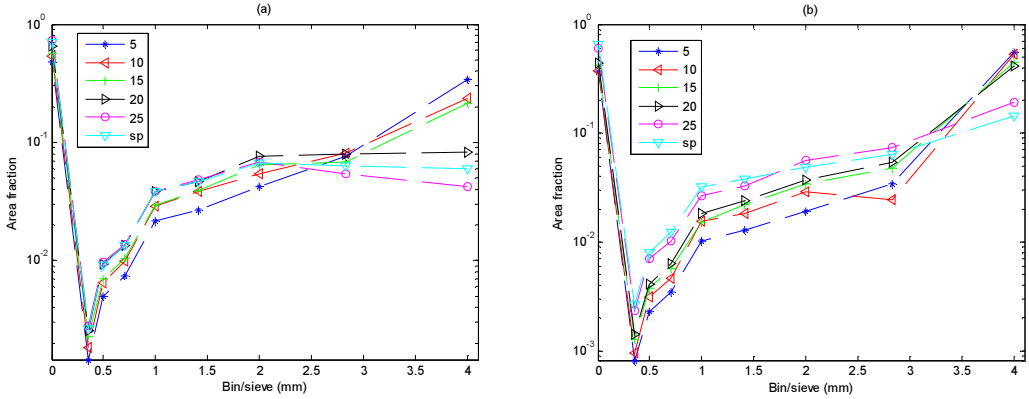

Figure 6-50: Volume fraction of particles in each size class, the recovered peanut particles was divided by the initial peanut volume ingested, (a) the chocolate matrix and (b) the gelatine matrix. Data from Hutchings et al. (2011).

The plots show similar trends for both matrices, with increasing chew number the proportion of large particles decreases and the proportion of small particles increases and the largest fraction is the unrecovered solid below 355 µm. The rate of peanut breakdown is faster in the chocolate matrix. For both matrices between the 5 chew intervals, the rate of peanut breakdown is not consistent. If the breakage function of the peanut particles is constant, the frequency which the particles are occluded must be changing throughout mastication. Excluding the first five chews, the biggest change in the PSD of peanuts in the chocolate matrix occurs between 15 and 20 chews, for the gelatine matrix the largest change is between 20 and 25 chews. The selection of peanut quarters in the first 5 chews is probably due to some the quarter peanut particles being fractionally occluded with the matrix. Once the peanuts and matrix are separated, the larger matrix particles will be preferentially selected over the peanut particles. The gelatine matrix is size reduced slower than the chocolate which leads to it having an average swallow point of 43 chews compared with 25 chews for the chocolate matrix.

Model Results – Peanuts Only

The comminution part of the model is applied to the peanuts in the chocolate and gelatine matrices. Firstly, the influence of the selection function to the breakdown on the peanuts is examined by assuming constant selection and breakage functions for the peanuts. Secondly, the best fit model prediction is obtained by varying the selection function whilst keeping the breakage function constant. The sensitivity of the model to the breakage function is also considered.

If the presence of the matrix does not influence the selection chance of the peanuts during mastication, keeping the selection function constant should provide a good fit for the data. Figure 6-51 shows the best fit of the model to the data with constant selection function; Figure 6-52 shows the same plots with a log scale on the y axis for the purpose of making it easier to distinguish the distribution of the small sizes.

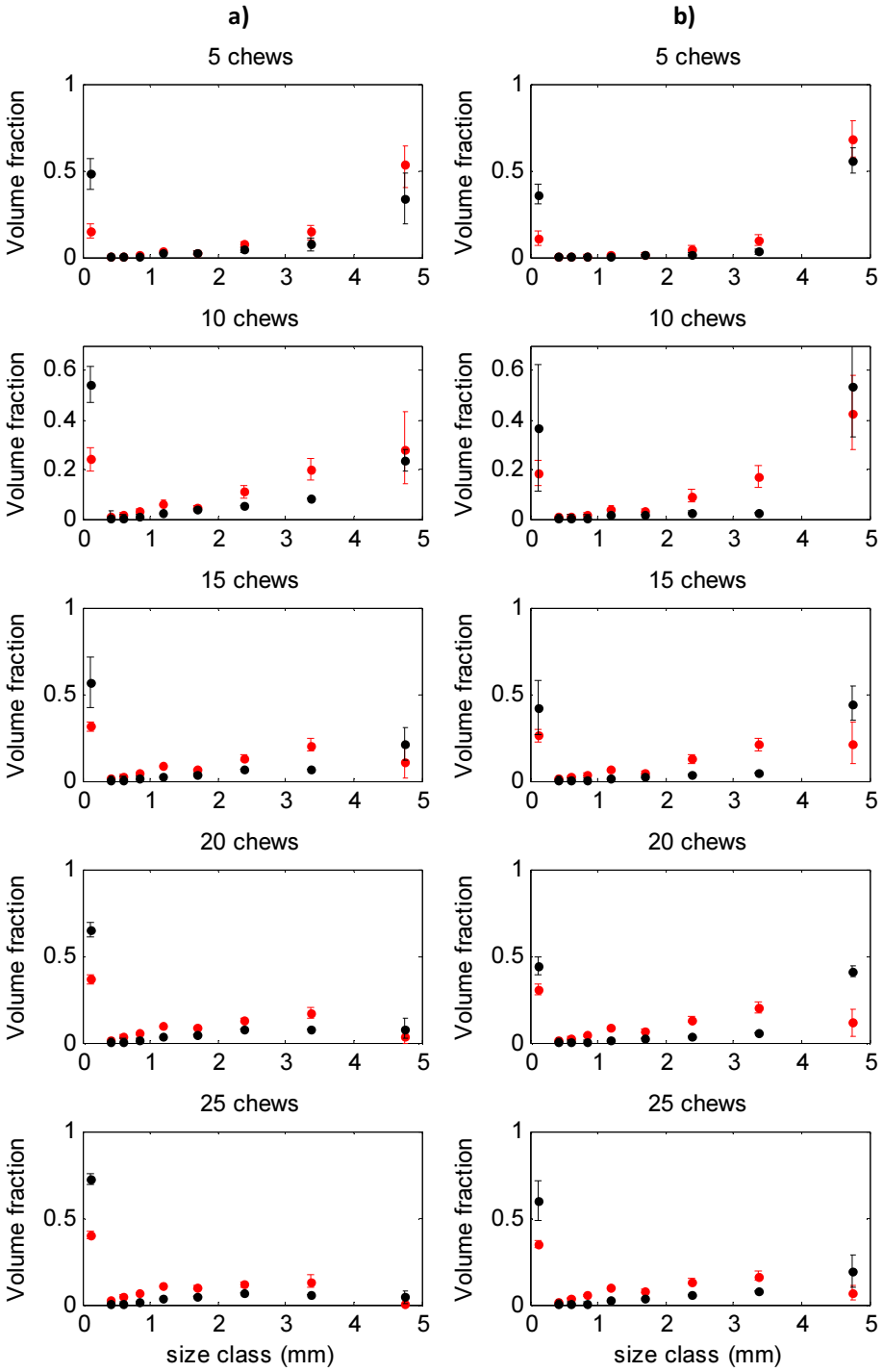

Figure 6-51: Best fit model prediction using a constant selection function that does not vary with chew number. PSD volume fraction of peanuts in (a) chocolate and (b) gelatine matrices after 5, 10, 15, 20 and 25 chews: model prediction red dot● is mean of 50 simulations with standard deviation vs experimental data black dot ●average with standard deviation error bars

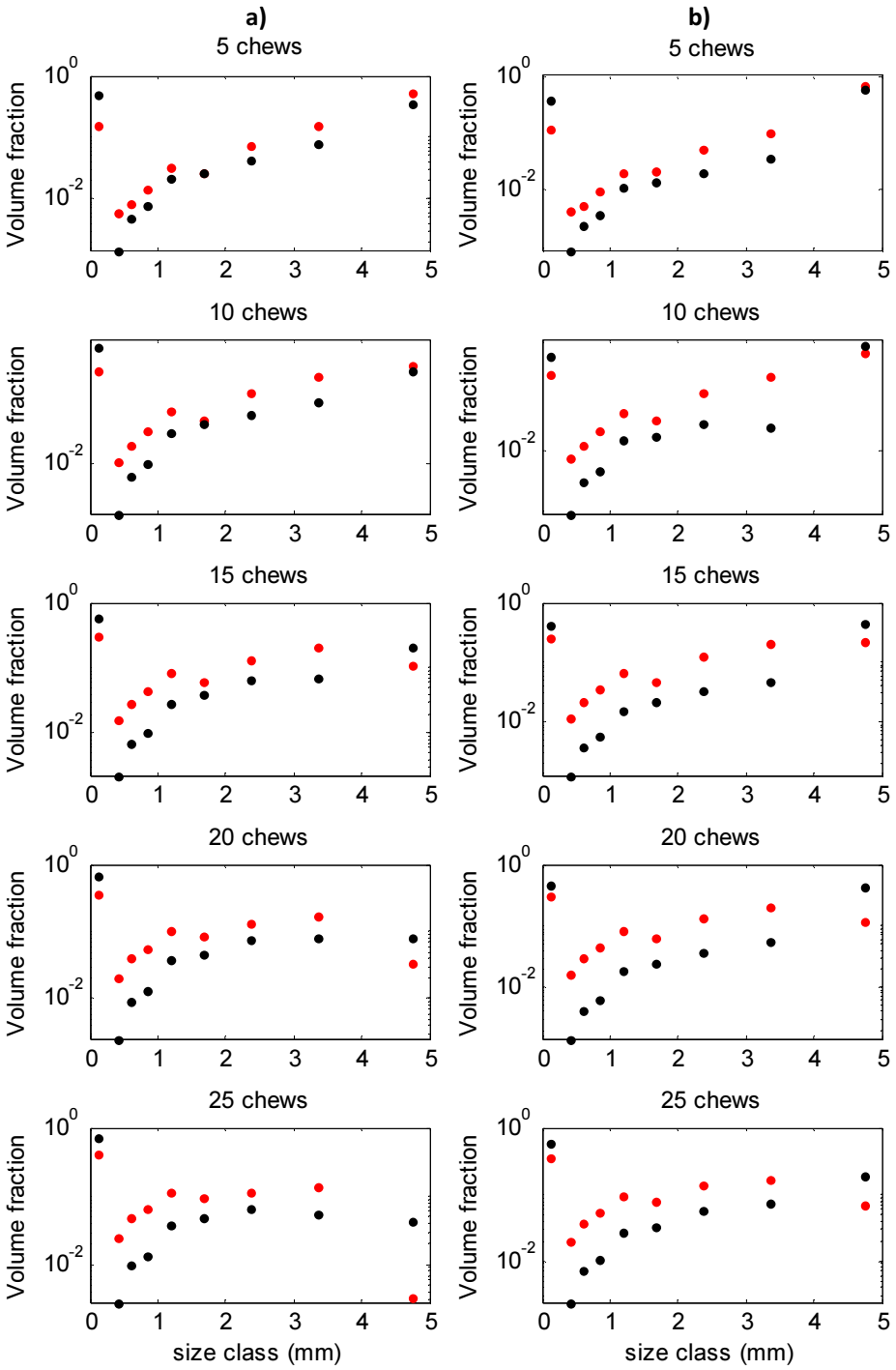

Figure 6-52: Best fit model prediction using a constant selection function that does not vary with chew number. PSD volume fraction of peanuts in (a) chocolate and (b) gelatine matrices after 5, 10, 15, 20 and 25 chews: model prediction ● is mean of 50 simulations vs experimental data mean ●.

Comparing the model results to the data, and comparing the two matrices shows a number of things; (i) that a constant selection function does not fit either data set particularly well but fits the peanuts in the chocolate matrix better than in the gelatine matrix; (ii), in the chocolate matrix the largest size class of particles are over predicted after five chews and slightly under predicted after 15 chews, which suggests that the chocolate does not influence the breakdown pathway of the peanut particles; (iii), in contrast, the model under predicts the peanut particle size distribution in the gelatine matrix which has a substantial influence as the PSD of the peanuts does not change much from 5 to 15 chews, which indicates that the mastication effort of the gelatine is preferential to the embedded peanuts. Figure 6-53 shows the volume fraction of peanuts occluded per chew in the chocolate and gelatine matrices. The fraction occluded is a fraction of the original peanut volume.

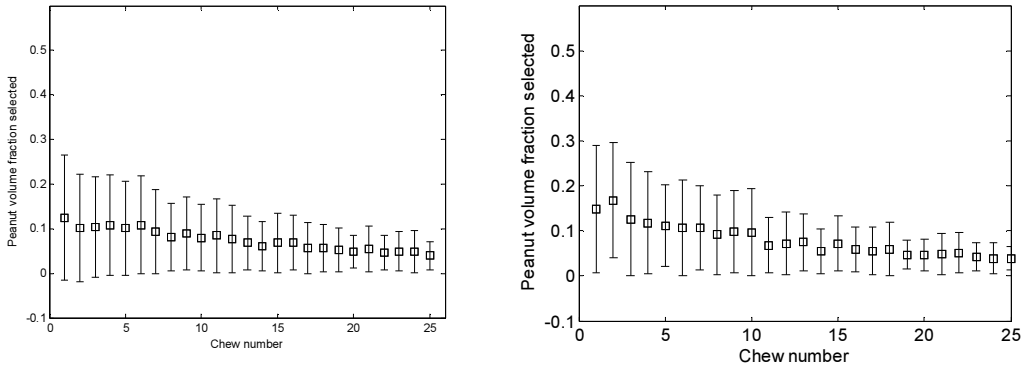

Figure 6-53: Mean and standard deviation of the volume fraction of peanut particles in the chocolate and gelatine matrix selected with a selection function parameters unchanged. The number of simulations was 50.

The constant selection function shows a gradual decline in the volume fraction peanuts selected. This is a natural phenomenon of oral processing when size reduction is occurring, as mastication progresses the number of larger particles decreases. The selection chance of the small particles is comparatively lower and the fraction below the minimum size for selection increases, thus the volume occluded reduces with an increasing number of chews. The high standard deviation is due to large particles contributing most of the food volume in the early stages of chewing. The total volume selected can vary considerably depending on the number of large particles selected. Assuming a constant selection function for the peanuts did not provide a good fit with the data so further simulations were carried out to get the best fit by changing the selection function. The selection probability of the peanuts for each of the five chew intervals was altered by changing the pre-exponential variable, *v*, in Eq. 2-7.

Figure 6-54 and Figure 6-55 give the best fit PSD for peanuts in the chocolate and gelatine matrices, the selection function variables are given in Table 6-21.

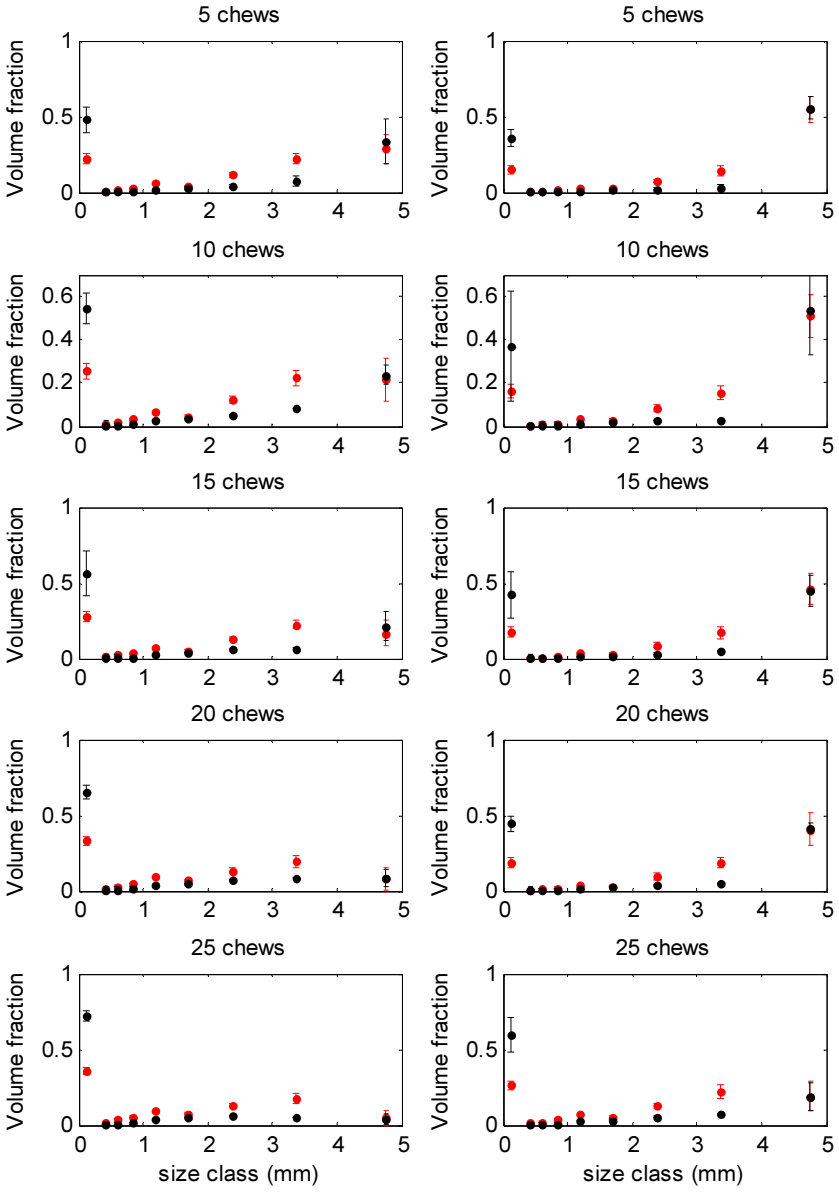

Figure 6-54: PSD volume fraction of peanuts in chocolate (left) and gelatine (right) matrices after 5, 10, 15, 20 and 25 chews using the selection parameters with parameters in Table 6-21: ● is the mean of 50 simulations with standard deviation vs experimental data ● average with standard deviation error bars.

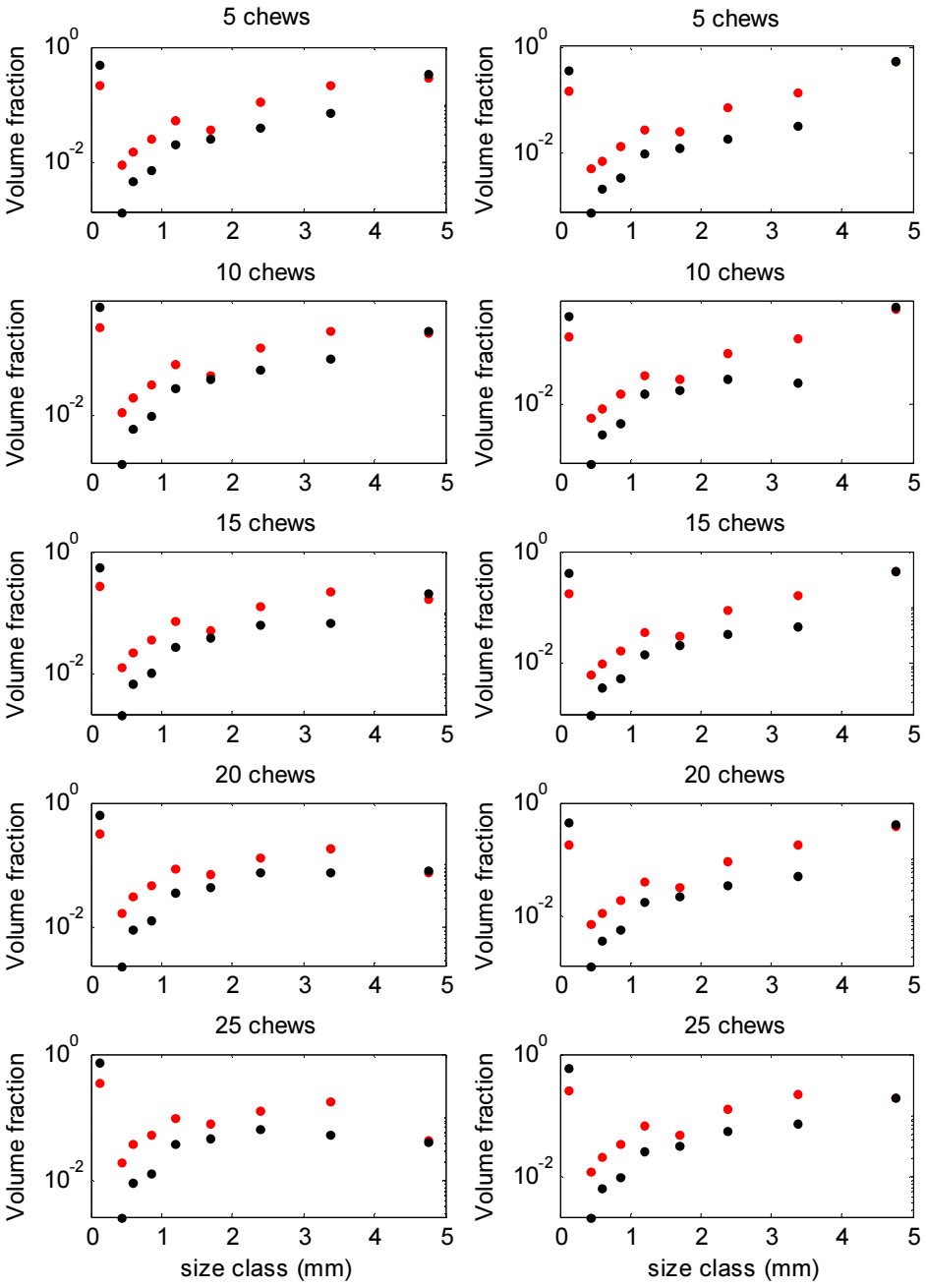

Figure 6-55: PSD volume fraction of peanuts in chocolate (left) and gelatine (right) matrices after 5, 10, 15, 20 and 25 chews using selection function with the parameters in Table 6-21 : ● is the mean of 50 simulations with standard deviation vs experimental data ● average with standard deviation error bars.

Table 6-21: Best fit selection function variables for the peanut particles in the chocolate and gelatine matrix.

	Chew #	1 to 5	6 to 10	11 to 15	16 to 20	21 to 25
Choc matrix	*v*	0.35	0.07	0.05	0.18	0.10
	w			1.5		
	R^2	0.61	0.54	0.55	0.61	0.61
Gel matrix	*v*	0.20	0.02	0.02	0.03	0.17
	w			1.5		
	R^2	0.81	0.80	0.70	0.67	0.53

The model is not able to exactly match the data; however, the fit is a lot better than for a constant selection function. The largest particle size is predicted accurately, but all other size classes throughout the mastication cycle are over predicted except for the smallest class which is the fraction that was unrecovered during Hutching's (2011) analysis. This was assumed to be smaller than the 355 µm sieve. It is likely that some of the unrecovered fraction consisted of larger particles and simply not recovered with the bolus or mouth rinsings. If that is the case then the model prediction would be closer to the actual size distribution in the bolus. Using a variable pre-exponential term on the selection function does provide significantly more accuracy than the previous constant term. For both the chocolate and the gelatine matrices, the selection chance decreases to a minimum in the middle of the chew cycle then increases at higher chew numbers. In both cases this indicates a lull in selection meaning the peanuts are less favourably selected in the middle of the chew cycle. This is demonstrated by Figure 6-56 which shows the volume fraction of peanuts selected per chew.

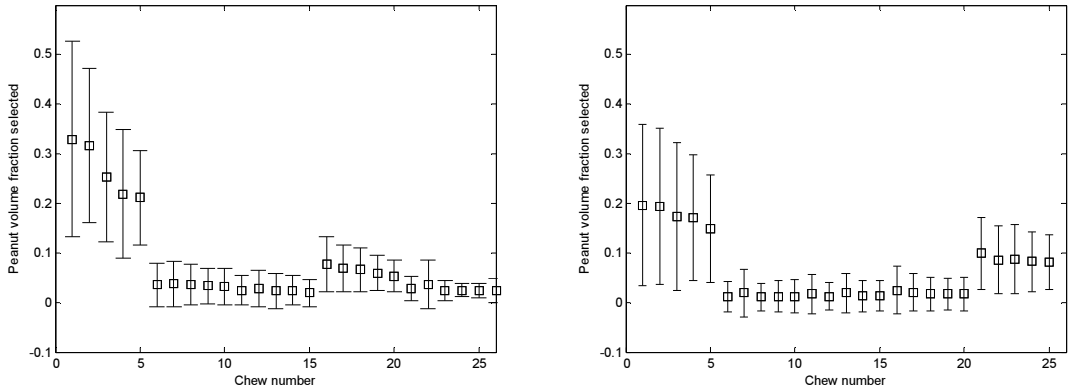

Figure 6-56: Mean and standard deviation of the fraction of original peanut volume selected per chew in the chocolate matrix (a) and gelatine matrix (b). The number of simulations was 50.

The variation in the peanuts selected per chew results from using a random number generator to help determine which particles are selected (see section 5.3.4). In the following section the sensitivity of the model prediction to changes to the breakage function is investigated.

Sensitivity of the PSD to the Breakage Function

The simulations shown so far have used a constant breakage function, given by Eq. 2-23, which was fitted to single chew experimental data. However, breakage may change during mastication as the properties of the material being chewed changes. Roasted peanuts tend to retain their physical properties over the time frame of mastication, but the matrices in which they are embedded will change due to temperature change, melting, dissolution and possibly its shear history. None of these effects are known, however. Therefore, it is worthwhile to examine the sensitivity of the PSD to the breakage function. Simulations were done by either changing the fragmentation variable, *r*, or the bimodal fraction *Y*. The selection variables in Table 6-21 for the peanuts in the chocolate matrix were used and the comparison between the model and experimental results are shown in Figure 6-57 and Figure 6-58.

Table 6-22: Values used to test sensitivity of model predictions to breakage

r	1.0	1.5	2.0	1.5	1.5	1.5
Y	0.84	0.84	0.84	0.74	0.84	0.94

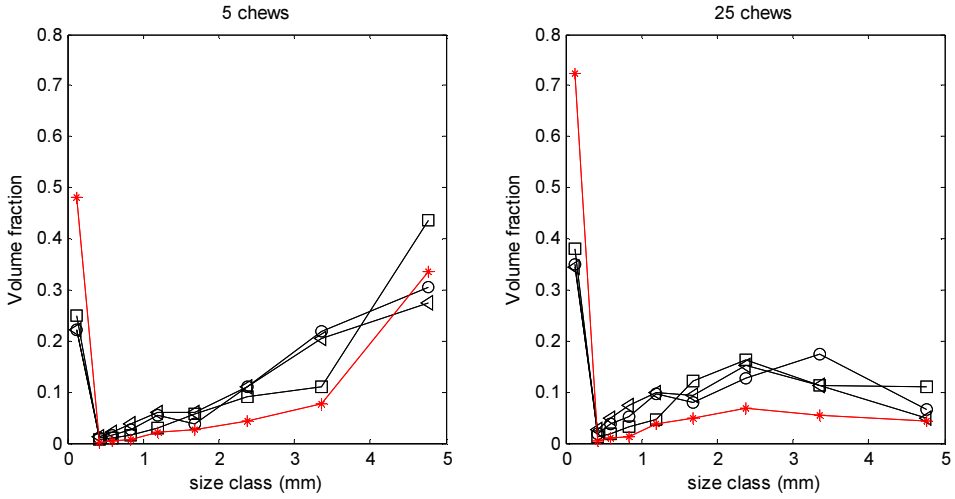

Figure 6-57: Sensitivity of PSD of the peanuts in the chocolate matrix to the fragmentation variable, *r*, after 5 and 25 chews. □ 1.0, ○ 1.5, < 2.0, * peanut data.

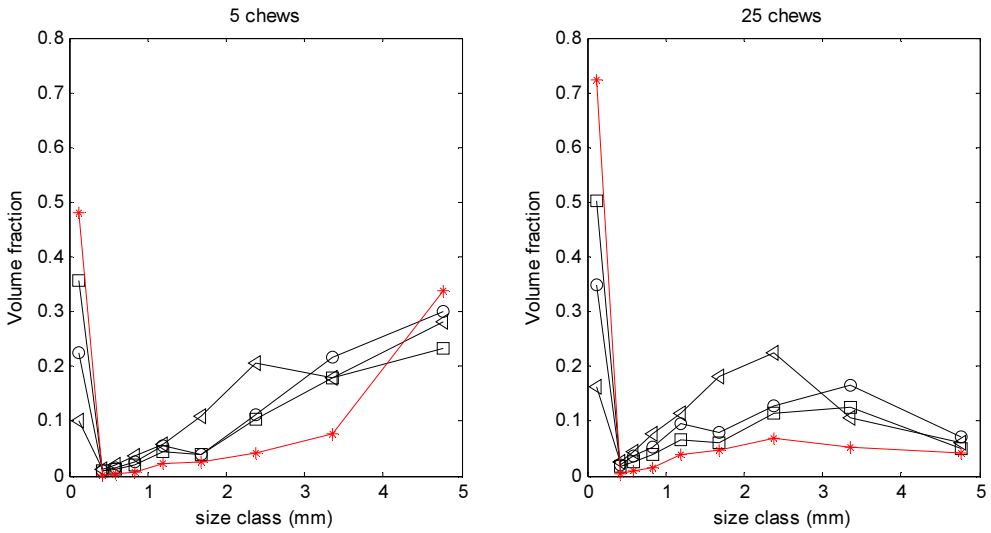

Figure 6-58: Sensitivity of PSD of the peanuts in the chocolate matrix to the bimodal variable (the pasted fraction) after 5 and 25 chews. □ 0.74, ○ 0.84, < 0.94 , * peanut data.

The predicated distributions have the same shape as the data; however, the largest discrepancy is under prediction of the fraction in the smallest size class. This is due to the assumption that all unrecovered particles were comminuted below 355 µm; however it is likely that much of this volume was simply lost and not recovered in the bolus and rinsings. The model is more accurate post the first five chews; where there is a large volume loss. After five chews the recovered peanut volume decreases linearly. When the PSD at five chews is used as the model input Figure 6-59 and Figure 6-60 show a close match between the simulated and experimental PSD at various chew intervals.

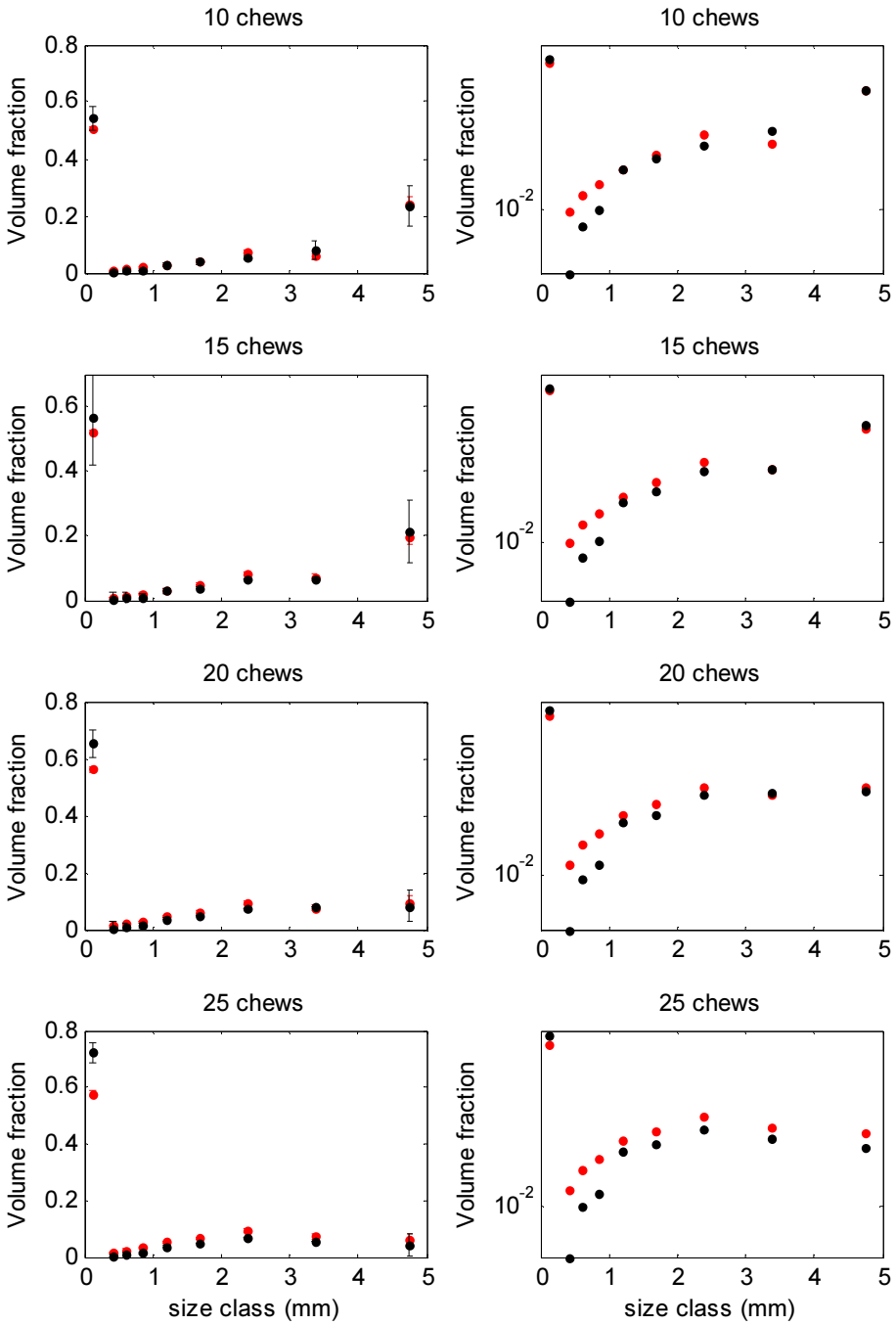

Figure 6-59: Model output for the PSD of the peanuts from the chocolate matrix using the data after five chews as the initial feed distribution. ● is the mean of 50 simulations with standard deviation vs experimental data ● mean with standard deviation error bars.

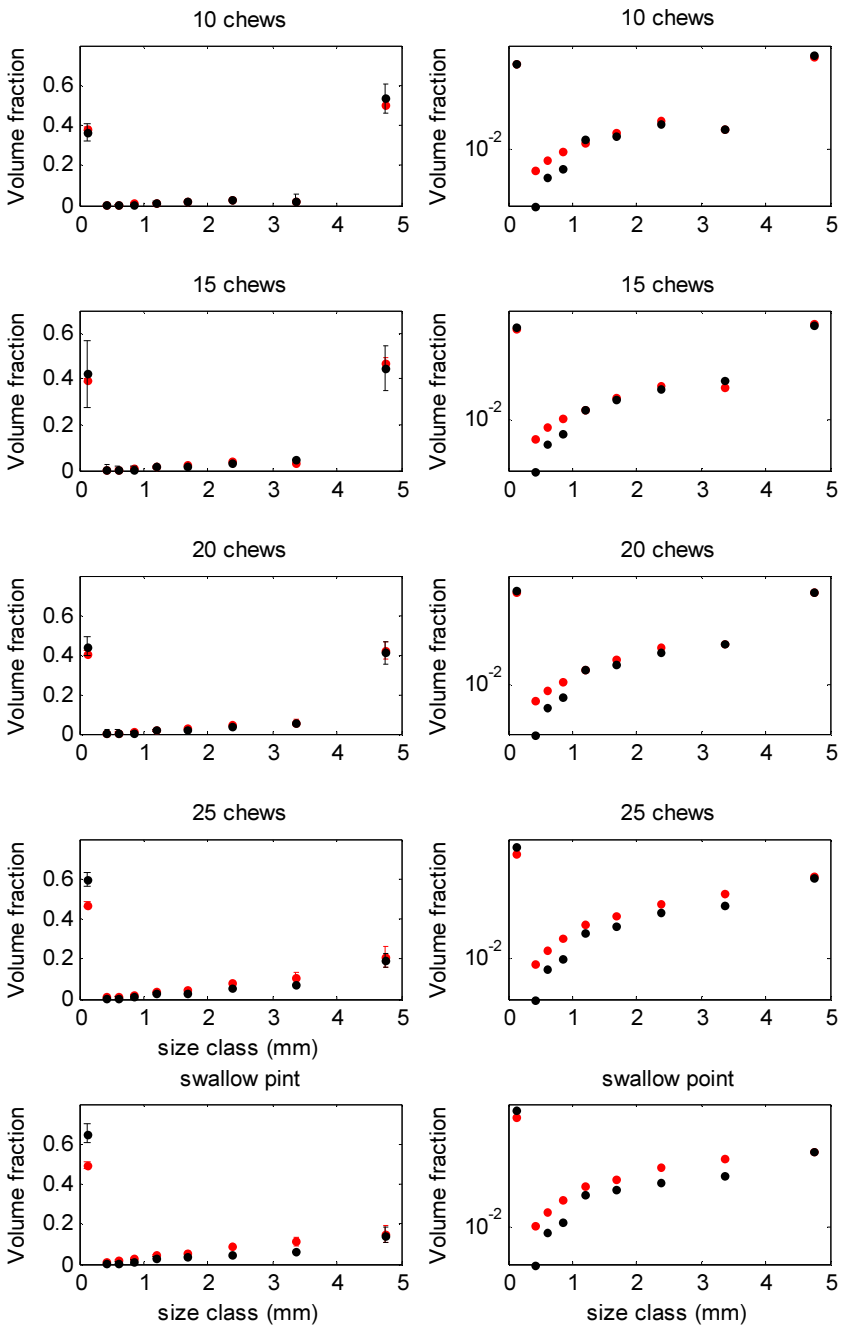

Figure 6-60: Model prediction of the PSD of the peanuts from the gelatine matrix using the data after five chews as the initial feed distribution, swalow point is fixed at 43 chews. ● mean of 50 simulations with standard deviation vs experimental data ● mean with standard deviation error bars.

In the next section, simulations are shown with the matrix included. These are largely hypothetical as the size distribution of the matrix was not obtained experimentally. However, it allows for discussion around why the distribution of the peanuts differs between the matrices and to get a better indication of the bolus composition throughout mastication.

Model with Food Matrix and Additional Rate Processes

The food matrix makes up most of the bolus by volume and is the reason the selection probability of the peanuts changes during mastication. Including the chocolate and gelatine in the model means the relevant rate processes need to be considered. For the chocolate this is melting and for gelatine this is dissolution of sugar but not melting of the gel which did not occur in this system. No particle size data for the matrix is available so some assumptions were made about the breakdown dynamics of the respective matrices.

Comminution of the Chocolate and Gelatine

No measured breakage functions for chocolate exist in the literature. However, it is known that chocolate is brittle when at room temperature and produces discrete particles when occluded. Eq. 2-23 is used with a low fragmentation variable of 0.5 as it predominantly produces larger particles when occluded and should be a reasonable approximation of the breakage of chocolate. As the chocolate increases in temperature during chewing its breakage function would change, however, for simplicity it will be assumed to remain constant throughout and be independent of size.

The gelatine did not readily break down into many discrete particles, and in the first few chews it may not have been completely cleaved when it was occluded. To approximate the size reduction of the gelatine a simple subdivision breakage function is used. An occluded particle will produce two daughter particles in the same manner as case study 2. The relative sizes are determined in a semi-random manner. A random number of 0.1, 0.2, 0.3, 0.4 or 0.5 will be generated for a selected particle to determine the sizes of the daughter particles. The matrix has a volume of 9 cm with dimensions of 2 x 3 x 1.5 cm, the daughter particles for the chocolate and gelatine are assumed to be cubes.

Melting

To include melting in the model some discussion about the heat transfer in the mouth and within the bolus is required. Melting of chocolate is complicated by the temperature range of melting, temperature gradients in the particles and constant size reduction during occlusion. To incorporate melting into the model it needs to be simplified.

The chocolate contains ≈ 30% cocoa butter which is solid at room temperature and typically melts over a temperature range of 30-33°C. As a result, a large portion of the chocolate is liquid when the bolus is ready to swallow. If the heat transfer through the chocolate is significantly slower than the rate of heat transferred to its surface, then melting will occur at the particle surface and a melting front will progress through the particle. Thus, a melting velocity can be used to describe how much chocolate is melted in between chew strokes. In reality there will be a temperature gradient in the larger chocolate particles and their mass average temperature will increase during mastication. However, because the size of the particles changes rapidly through comminution and many particles exist for only a single chew stroke, a melting velocity is assumed for simplicity in this instance.

The chocolate will gain heat from the liquid phase and from being in direct contact with the oral surfaces which can be assumed to be at 37°C. It depends on where the particles are in the bolus and where the bolus is in the mouth. Heat transfer will be simplified here; it is assumed that the chocolate gains all its heat from the liquid phase which is constant at 37°C. Thus, the heat transfer coefficient in the mouth needs to be estimated. The conditions in the mouth are likely to be that of low forced convection in a liquid. The Biot number gives the ratio of the heat transfer resistances inside and at the surface of the particle

$$Bi = \frac{hL_c}{k} \qquad \textbf{Eq. 6-10}$$

where *h* is the convective heat transfer coefficient, *L*c is the characteristic length which for a sphere is its radius, *k* is the thermal conductivity of the solid. If the Biot number is less than 0.1, conduction within the particle is much faster than convection from the surface and it can be assumed that there is no temperature gradient in the particle. A Biot number greater than 0.1 means heat transfer is more complex as temperature will be non-uniform in the particle. Table 6-23 shows the Biot number for spherical chocolate particles of differing sizes.

Table 6-23: Biot number for spherical chocolate particles where h = 250 W/(m^2.K)

particle diameter (mm)	Biot number
8.0	3.3
4.0	1.7
2.0	0.83
1.0	0.42
0.50	0.21
0.35	0.15
0.25	0.10
0.125	0.052

The Biot number values show that most particles will develop a temperature gradient whilst particles below 0.25 mm would gain heat uniformly. Because of the complex nature of melting and the comminution of the particles, a melting velocity is a sensible approach. A melting velocity can be calculated based on the largest size particle that would be completely melted during a chew stroke. To determine this size, a heat transfer model is developed based on the following assumptions.

- Heat transfer to the particle is by convection from the liquid phase, which is initially at a constant temperature of 37 °C.
- External resistance to heat transfer is limiting so that the particle temperature is uniform
- Thermal properties of chocolate are constant including thermal conductivity and specific heat capacity.
- Specific heat capacity is the same for solid and liquid chocolate.
- Heat of dissolution is negligible.
- Phase change occurs at 30°C, the particle remains at phase change temperature until all the cocoa butter is melted.
- Particle area is constant for heat transfer.
- A chewing frequency of 0.75 s^{-1}

The heat balance equations for particle temperature and melting are presented in §5.3.3. A reduction of the general equation is used here, where the temperature of the chocolate particle is given by

$$\frac{d\theta_p}{dt} = \frac{U_p A_{p,}(\theta_{liq} - \theta_p)}{M_{p,i} C_{p,p}} \qquad \textbf{Eq. 6-11}$$

when the particle reaches the phase change temperature the heat from the liquid phase melts the solid fat while the particle temperature remains constant,

$$\frac{dM_{sf}}{dt} = -\frac{U_p A_p(\theta_{liq} - \theta_p)}{h_{fat-oil}} \qquad \textbf{Eq. 6-12}$$

Figure 6-61 shows the temperature time profile and the solid fat for a spherical particle with a diameter of 100 µm.

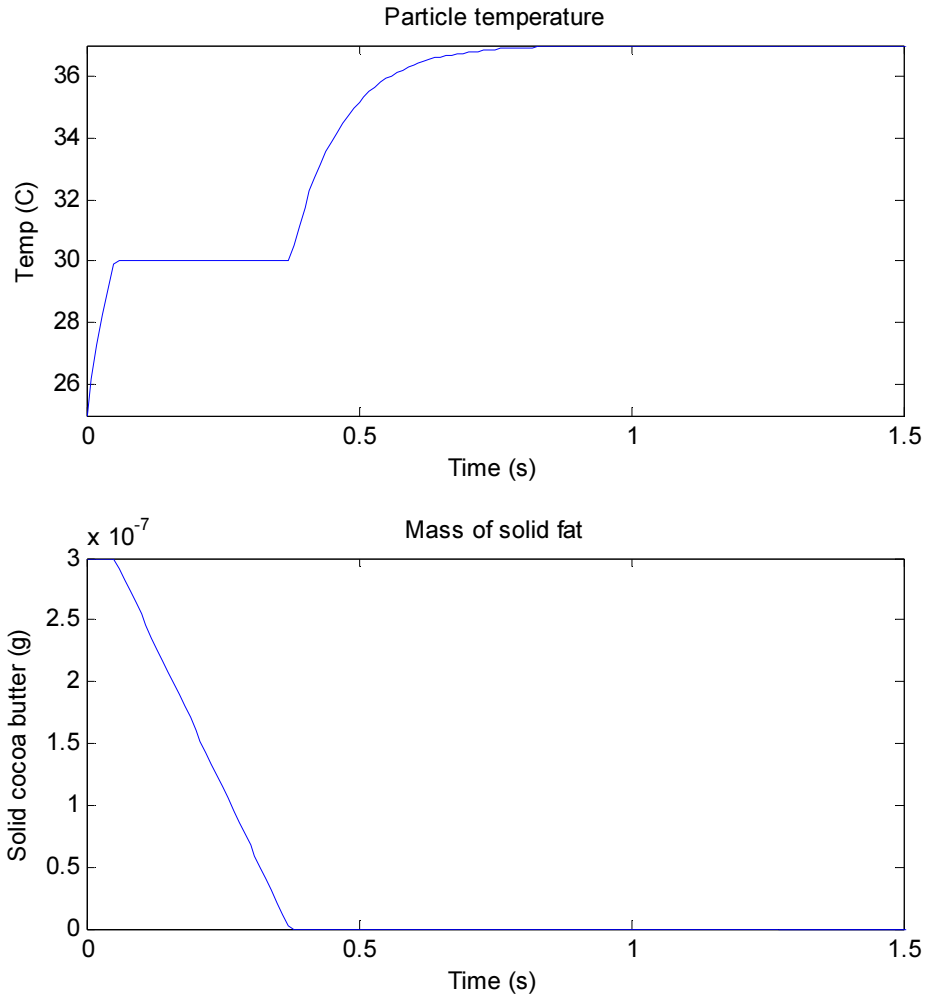

Figure 6-61: Change in the chocolate particle temperature and mass of solid fat in the particle with time.

In this example a spherical particle with a diameter of 100 µm is heated from an initial temperature of 25°C to the liquid phase temperature of 37°C in the time taken for a single chew stroke. The melting velocity for is thus 66.7 µm s^{-1}. The change in volume of each chocolate particle is given by,

$$dV_{p,i} = -A_{p,i} v_m dt \qquad \textbf{Eq. 6-13}$$

where $V_{p,i}$ is the volume of a given chocolate particle, $A_{p,i}$ is its surface area and v_m is the melting velocity.

Dissolution

The mechanism of dissolution and melting in gels has been discussed previously in section 5.4.4. If the melting temperature is above that of the mouth sucrose diffuses out from the surface gel, lowering the melting temperature of a thin layer on the surface of the gel which can then be melted. The gelatine matrix did not appreciably dissolve during mastication Hutchings (2012 (personal communication)), for a gel with a melting point above 37°C the rate of dissolution is given by,

$$\dot{M}_{k,dissolution}\big|_p = k_d \rho_{k,p,sol.solids} A_{p,i}\big|_p \left(X_{p,sol.solids}\big|_p - X_{liq,diss.sol.solids}\big|_p \right) \qquad \textbf{Eq. 6-14}$$

where k_d [m s^{-1}] is the mass transfer coefficient, $A_{p,i}|_p$ is the area of a particle [m^2], $X_{p,sol.solids}$ is the soluble solid mass fraction [kg kg^{-1}] in the particle-phase, $X_{liq,diss.sol.solids}$ is the concentration of soluble solids in the interstitial liquid phase [kg kg^{-1}].

Model Implementation

The model procedure is the same as shown in Figure 6-62, the matrix of either chocolate or gelatine is included and after the comminution process the rate process of melting or dissolution is implemented prior to the next chew stroke. The same selection function, Eq-2.8, is used for the peanuts and the matrices, thus matrix and peanut particles of equal size have the same chance of being occluded. The Matlab files are in Appendix E.

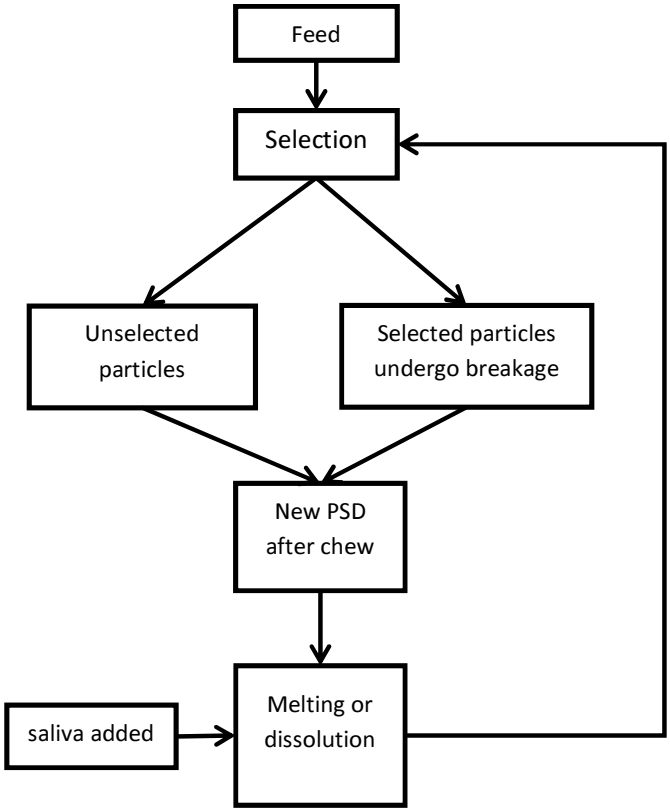

Figure 6-62: Schematic model flow diagram of the comminution model for the peanuts and matrix where the melting is included for the chocolate and dissolution in included for the gelatine, this is a specific case of the generalised diagram in Figure 5-5.

The model predictions for the PSD of the chocolate matrix and embedded peanut are compared to the experimental data for the peanuts in Figure 6-63 (normal y axis) and Figure 6-64 (log y axis). The volumes in each size class are normalised to the initial peanut volume. To preserve the volume of the matrix, the chocolate that has been melted is allocated the smallest size class. The peanut data is included so this can be compared with the model prediction. The cumulative volume of melted chocolate as predicted in the model is shown in Figure 6-65.

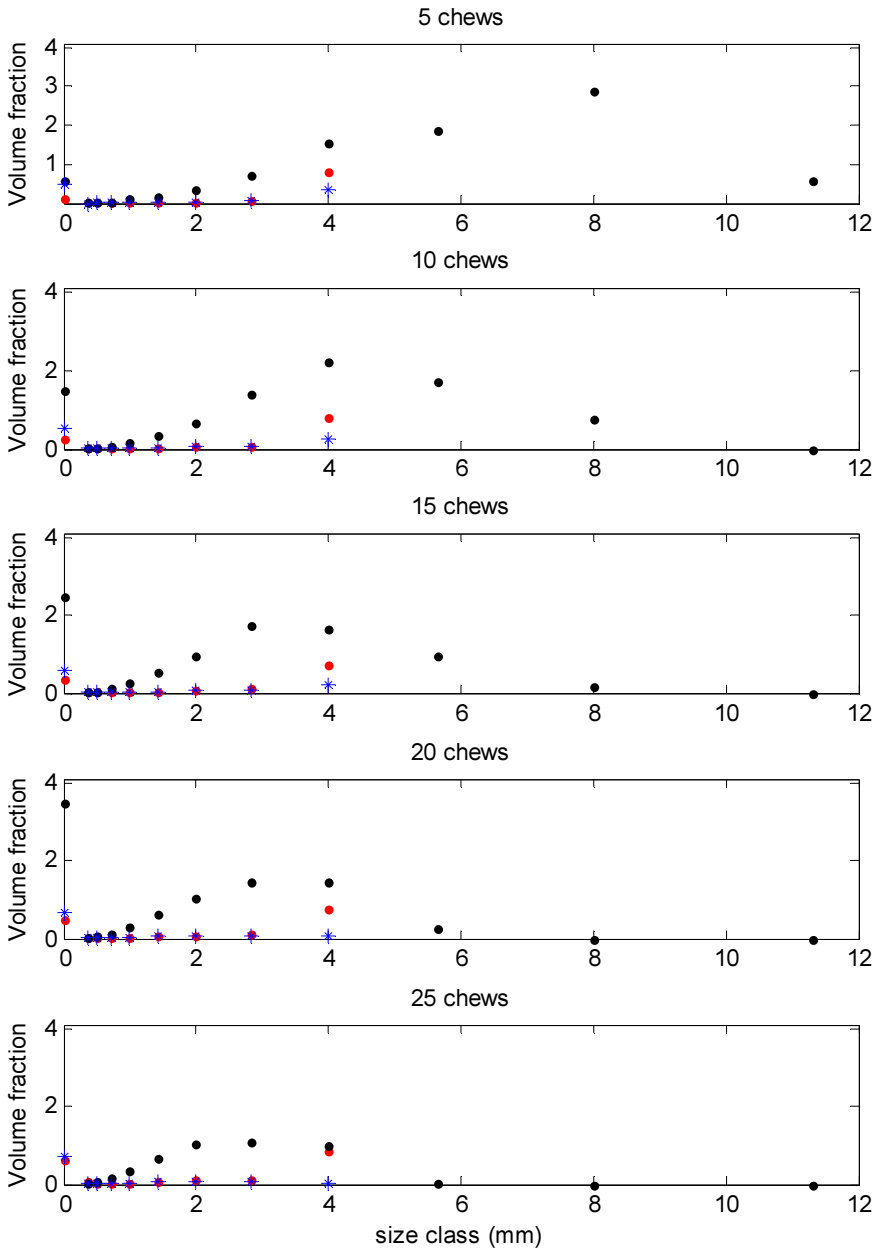

Figure 6-63: Model PSD of the chocolate matrix and embedded peanuts throughout mastication and the peanut bolus data, the volume in each size class is normalised to the initial peanut volume • chocolate matrix, • embedded peanuts, * peanut data

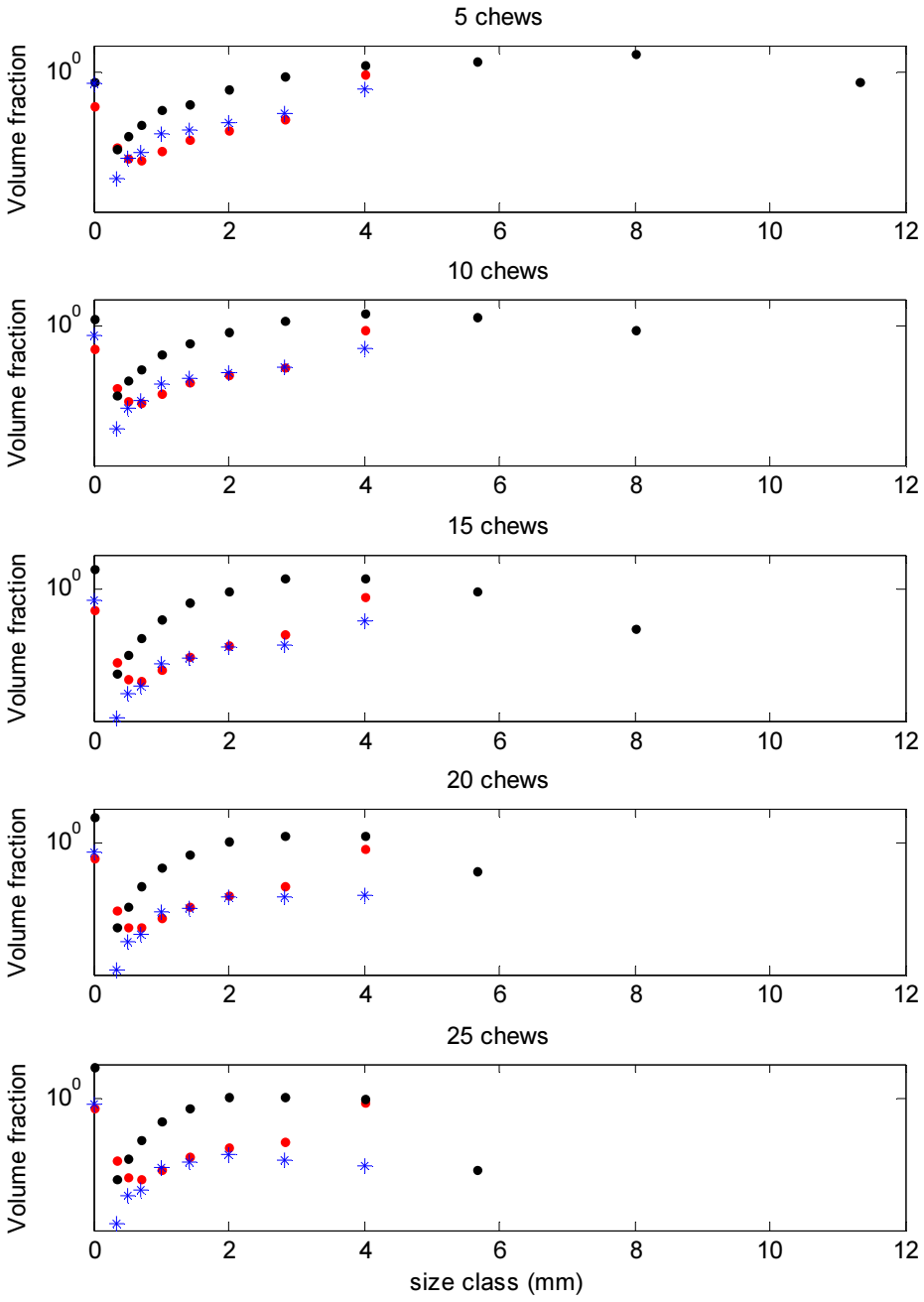

Figure 6-64: Model PSD of the chocolate matrix and embedded peanuts throughout mastication and the peanut bolus data, the volume fraction is on a log scale and the volume in each size class is normalised to the initial peanut volume; • chocolate matrix, • embedded peanuts, * peanut data.

The predicted particle size distribution of the chocolate is reasonable. Given the large initial size of the matrix there are particles in the bolus larger than the peanut quarters throughout mastication. At the swallow point ≈60% of the chocolate has melted, however, the volume of solid chocolate is still greater than the peanut volume. The data shows that the distribution of the peanuts does not change a lot from 20 chews onwards to the swallow point. This period could be more important for reducing the chocolate particles to an acceptable size for swallowing.

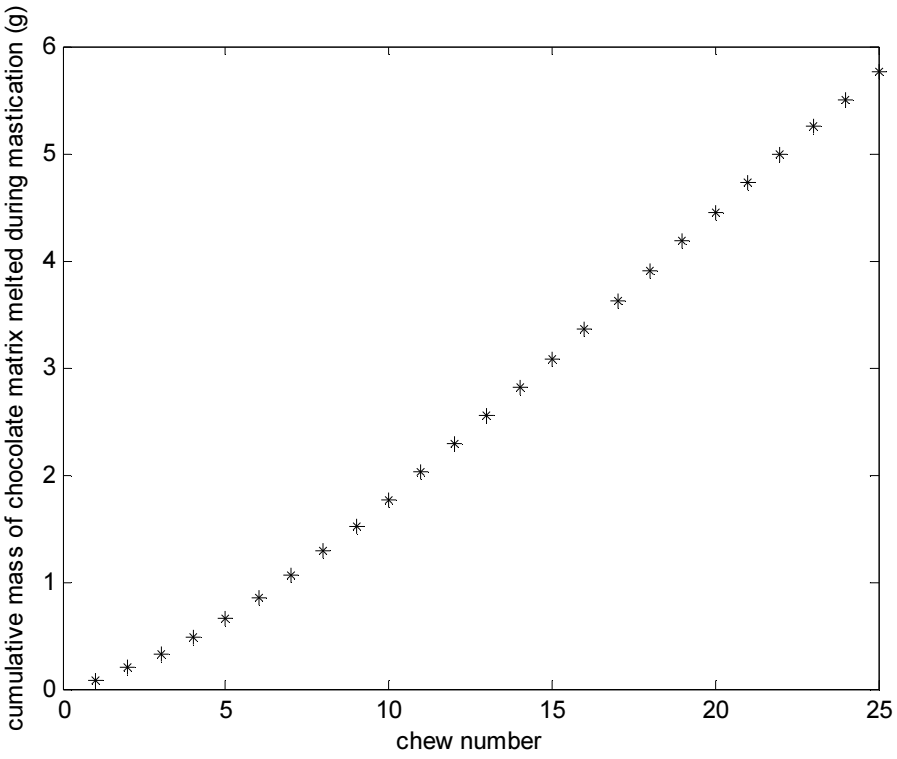

Figure 6-65: Cumulative mass of the chocolate matrix that is melted during mastication and enters the liquid-phase of the bolus predicted by the melting model (mean value of 10 model replications).

No data for chocolate size or melting was recorded by Hutchings (2011) because this was not their focus. However, from observations this conversion of solid to liquid chocolate appears to be a good approximation. The majority of chocolate melts before swallowing, however, there are still some solid particles in the bolus at swallow point. The model predictions for the gelatine matrix and embedded peanuts are shown in Figure 6-66 (normal y axis) and Figure 6-67 (log y axis). The volume in each size class is given as a fraction of the initial peanut volume. To preserve the volume of the matrix, the gelatine that has been melted is allocated the smallest size class. The peanut data is included so this can be compared with the model prediction.

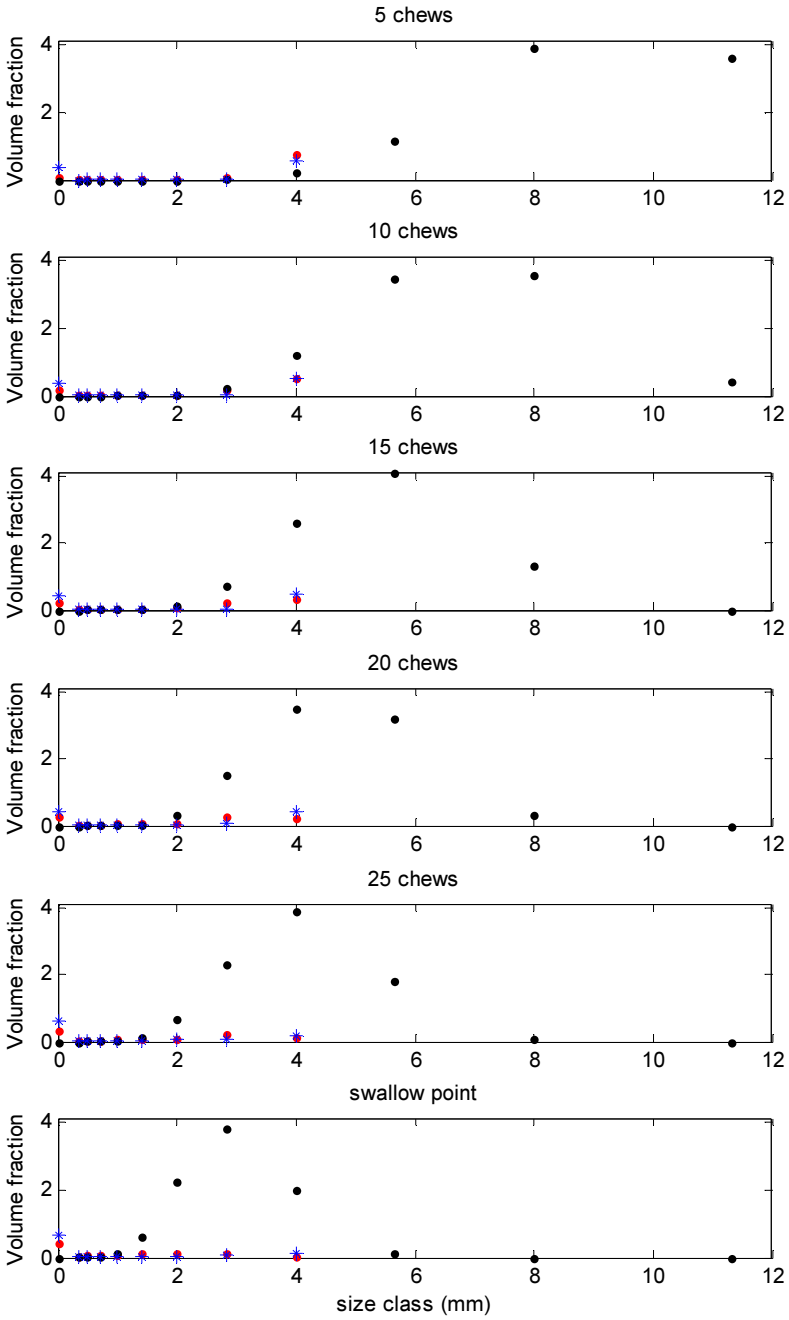

Figure 6-66: Model PSD of the gelatine matrix and embedded peanuts throughout mastication and the peanut bolus data, the volume in each size class is normalised to the initial peanut volume; • gelatine matrix, • embedded peanuts, * peanut data.

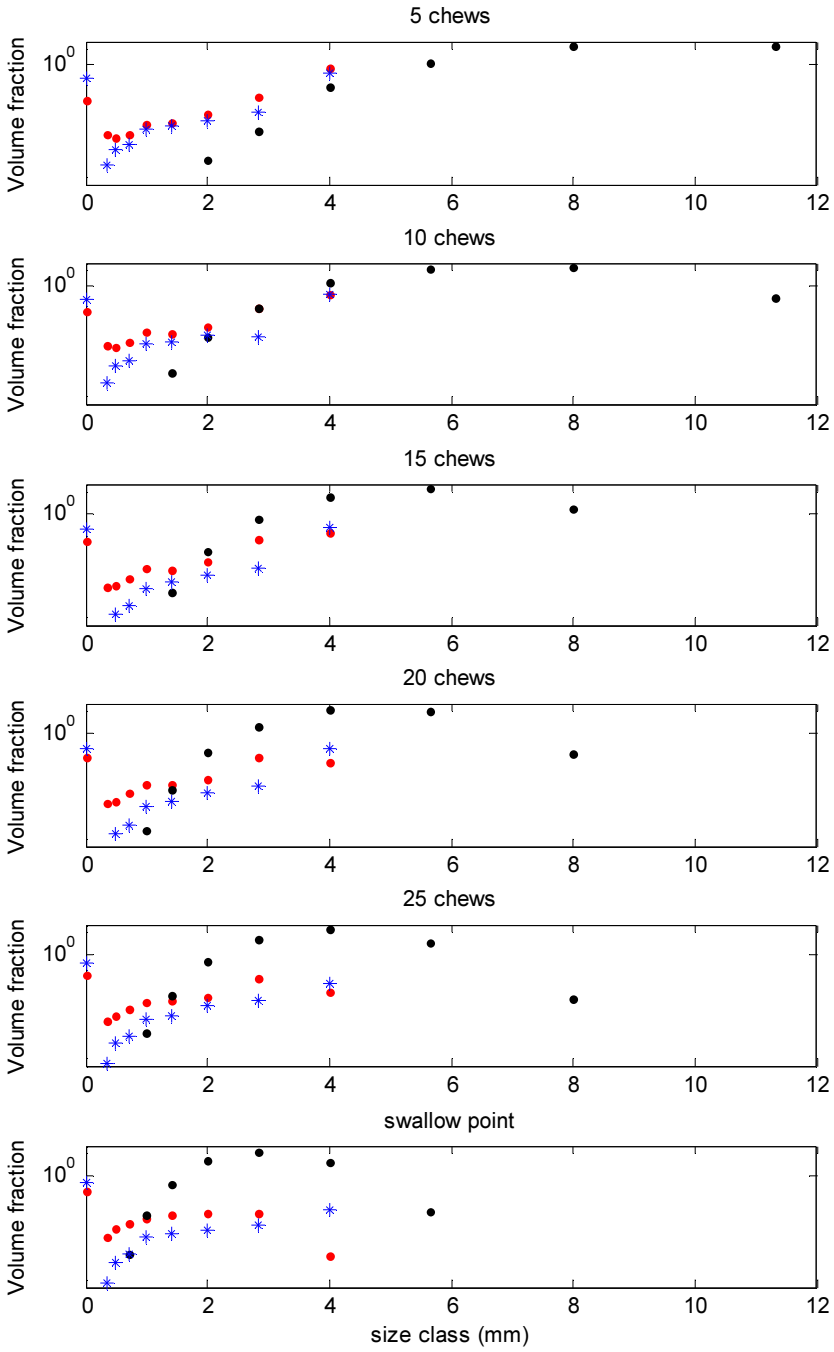

Figure 6-67: Model PSD of the gelatine matrix and embedded peanuts throughout mastication and the peanut bolus data, the volume fraction is on a log scale and the volume in each size class is normalised to the initial peanut volume; • gelatine matrix, • embedded peanuts, * peanut data.

The particle size reduction of the gelatine matrix is much slower than the chocolate. For the gelatine the sub-division breakage assumption meant only two daughter particles were produced when a particle is occluded. As a result there are no gelatine particles smaller than 1 mm throughout mastication. The volume fraction gelatine particles ≥ 5.6mm is more than double that of chocolate for each of the five chew intervals. This can explain why the peanuts in the gelatine matrix are selected less frequently because there are many large pieces of gelatine which will inhibit the selection of the peanut particles. The quarter peanuts in the gelatine between one and five chews have a comparatively high selection chance because when they are embedded in the matrix they can be occluded simultaneously with the matrix. After a few chews the peanuts will separate from the matrix resulting in occlusion being dominated by the larger gelatine particles. In contrast to the chocolate the rate process of dissolution did not contribute to the size reduction of the matrix; Figure 6-68 shows the mass of gelatine in the liquid phase of the bolus.

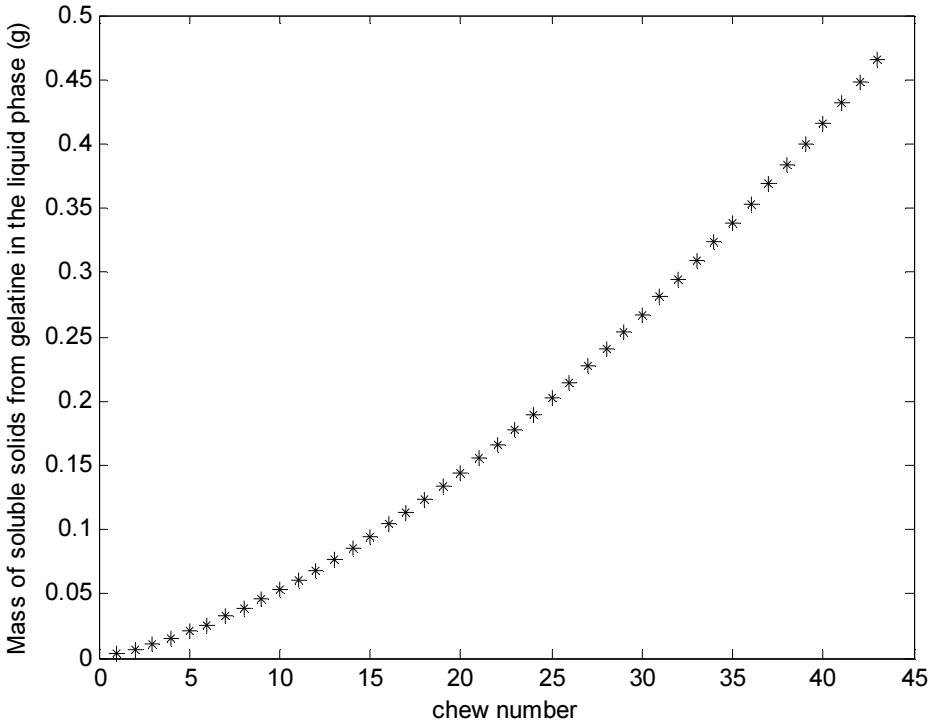

Figure 6-68: Cumulative mass of soluble solids in the liquid-phase of the bolus as a result of dissolution from the gelatine matrix.

Intermediate swallowing has not been included in the simulation so all the gelatine that has melted is in the liquid phase of the bolus. It is likely that the subject would have performed at

least one intermediate swallow to remove excess liquid from the bolus which would lower the amount of soluble solids in the liquid phase.

6.3.4 Summary and Conclusions

Hutchings (2011) found that the PSD of peanuts when embedded in either a chocolate or gelatine matrix were similar at the swallow point. However, the number of chews required to reach the swallow point was nearly double for the gelatine matrix indicating that the matrix played a significant role in modifying the breakdown rate of the peanuts. The discrete comminution model has been used to quantify this effect.

The PSD of the peanuts was simulated using a power law selection function and a breakage function fitted to single chew data. It was assumed that the matrix did not influence the fragmentation behaviour of the peanuts so a constant breakage function was used. It was found that when quarter peanuts were occluded over 15% of the mass passed a 355 µm sieve. This could explain why a significant amount of the peanuts were not recovered in Hutching's (2011) analysis where the peanut and matrix bolus was washed over the 355 µm aperture sieve. The model output was fitted to the peanut bolus data after various chews by changing the parameters of the selection function. The model fit showed that the chocolate and the gelatine matrices influence the selection chances of the peanuts throughout mastication.

In both matrices the most significant breakdown of peanuts occurred in the first five chews. This can be explained by the large quarter peanut particles being embedded in the matrix and occluded with the matrix. As mastication progresses the peanuts separate from the matrix and the larger matrix particles can be preferentially selected. It was found that the peanuts were occluded more frequently throughout the complete mastication sequence in the chocolate matrix. The chocolate is size reduced more rapidly and melting also contributes significantly to reducing the solid phase of the bolus. The gelatine was not readily fragmented and was reduced in size at a much slower rate than the chocolate. This resulted in the gelatine suppressing the selection of the peanuts more than the chocolate matrix.

CHAPTER 7 CONCLUSIONS AND RECOMMENDATIONS FOR FUTURE RESEARCH

7.1 Conclusions

A mathematical model framework has been developed which enables production of solid food breakdown and changes in bolus properties during mastication to be simulated. This has been demonstrated by using the model as part of an analysis on three separate food systems. Model outputs were fitted to bolus data from human subjects using experimentally determined model parameters and model tuning. The model has two potential uses; firstly, it can help formalise an understanding of how bolus properties change during mastication, secondly, it could help in food design by showing how the breakdown pathway can be manipulated by changing initial properties of the food.

Conceptual models of oral processing (Hiiemae, 2004 and Lucas et al. 2002) and bolus formation (Hutchings and Lillford 1988) have been postulated previously. However, none have captured the complete process of breakdown, mixing and in-mouth measuring of the food properties. The engineering approach used in this work considered the mouth as a unit operation into which the food, saliva and heat are added and out of which is the swallowed food. This conceptualisation addressed how food is transformed into a bolus via the rate processes of mastication; these are size reduction, work softening, absorption, dissolution, melting and mixing. During mixing, which is the circulation, selection and placement of food between occlusion cycles, the mouth performs mechanical sensory tests (MST). These MST assess the food and bolus properties. Those that are essential were confirmed using a reverse HAZOP analysis which is a risk mitigation tool. The determinant properties for safe swallowing are temperature, volume, adhesion, bolus deformation, particle deformation and particle size. Together, these describe a phase-space of threshold properties which each food must achieve in order to be swallowed. The descriptions of the mastication rate processes, the MST, the food properties that these assess and that are critical to safe swallowing, when regarded together, define a conceptual model of the food during mastication from after the first bite until the swallow point. This work then takes the next step and translates the conceptual model into a mathematical model.

Previously, mathematical models have been published describing aspects of food breakdown including; size reduction (Lucas and Luke 1983b, van der Bilt et al., 1987, van der Glas et al.,

1992), dissolution (de Loubens et al., 2011), and melting (Wright and Hills., 2003); however, none are as extensive as that described here. It tracks the structural breakdown of the food through size reduction and work softening and also the rate processes of dissolution, absorption and melting that result from the addition of saliva and heat to the bolus.

Case studies on the oral processing of brown rice, gelatine gel and peanuts embedded in food matrices were used to demonstrate the capability of the model to simulate food breakdown.

For the brown rice study, experiments with a single subject were conducted to obtain parameters for selection and breakage functions. The two-way completion model of selection (van der Glas et al., 1992) was used in the model; this is the first time it has been used in a simulation study of the bolus. The PSD of the model closely matched that of the boluses expectorated throughout mastication by the subject. The rice bolus at the swallow point consisted of ≈10 % un-chewed grains and the majority were retained on a 2.8 mm aperture sieve. It was found that the rice particle size does not appear to prevent the swallow threshold from being reached; rather, it is the lack of moisture. Therefore it is the adhesion threshold that determines when the bolus is safe-to-swallow. This is satisfied by saturating the interstitial space liquid-phase by the addition of saliva and the undersize particles entering the liquid-phase.

In the gelatine case study, four gels were made by varying the amount of sucrose (30 and 50%) and gelatine (10 and 15%). The gels had different properties which influenced their breakdown and melting behaviour. The two harder gels required ≈50% more chews, although there was no significant difference in the PSD between gels at the swallow point. It was found that the particle size of the gels at the swallow point agreed with the proposed state diagram which links the threshold size for swallowing with the particles inverse fragmentation index. The model was used to simulate melting and the size reduction of the gel. The size distribution predicted by the model was fitted to the bolus data by tuning the parameters of the selection function. It was found that the melting velocity measured *in-vitro* in a beaker of water at 37°C over-predicted the melting rate which was 18-70% lower for the human trials. This is expected because food in the mouth is not enveloped by a continuous fluid phase. Thus, the heat transfer rates are lower and subsequently so is the melting.

In the third case study peanuts were embedded in matrices of gelatine and chocolate. The experimental work was reported by Hutchings (2011) and. Hutchings et al. (2011) who showed

that, that at the swallow point, the PSD of the peanuts was similar despite those embedded in the gelatine matrix being chewed for nearly twice as long as for the chocolate. The comminution model was used to try and quantify the matrix effect on the peanut selection chance by fitting the power law selection function. The most significant breakdown of peanuts occurred in the first five chews for both matrices. The selection chance of peanuts in the chocolate was greater throughout mastication. This is because the chocolate, which is softer than the gelatine, is size reduced more rapidly, meaning the peanuts had more chance of being selected. For peanuts in gelatine, the gelatine was size reduced at a much slower rate. Effectively, its firmer structure and larger size means that it supresses the selection chance of the peanuts resulting in the peanuts in the gelatine matrix taking more chew cycles to break down.

7.2 Recommendations

Future work should be undertaken to further improve the model developed in this work. This includes; further case studies to isolate rate processes, developing constitutive relationships between food properties influenced by the rate processes and the food properties measured during MST, quantifying the heat transfer coefficients in the mouth, developing a mixing model for non-brittle foods, and expanding the model to include partial swallowing. These are discussed in more detail below.

Further case studies are needed that isolate rate processes in order to quantify them. Examples are; a dry porous food to investigate the absorption and wicking of the liquid phase into the particles, a fibrous cooked meat to investigate the work softening of the food. Further experimental work for Case study three will allow the model to be extended to include the competition model of selection, the influence of food hardness on selection, and the melting and dissolution of the matrices.

Developing a further understanding of the constitutive relationships between food properties influenced by the rate processes and the food properties measured during MST will improve the model. The bolus properties predicted in the model need to be relatable to the required properties for swallowing. Understanding these relationships would be improved through quantitative measurements and enable thresholds to be defined. Currently there is no existing device capable of this. Different rheological and textural analysis techniques have been applied to different food boluses with some success (Peyron et al. 2011, Nagatomi et al. 2008); however, the limitations of existing measurements is probably because they do not replicate

what happens to the bolus during swallowing and so are not measuring the relevant properties. Developing a device capable of this measurement is worth investigating and would be an exciting development.

Mixing is the management of the food within the mouth cavity; a generalised mixing model needs to be devolved to describe the occlusion of food that does not form discrete particles. Such a mixing model is likely to include stretching, folding and rotation and should for brittle foods give the same mathematical result as the selection functions arising from existing studies (e.g., the selection functions of Lucas and Luke, 1983a; van der Bilt et al., 1987; van der Glas et al., 1992). A mixing model could be based around masticatory efficiency which minimises the number of chew cycles as it makes energetic sense to chew the food in a sequential way without significant overlap.

The heat transfer and melting component of the model can be improved with some experimental work. The aim would be to measure the heat transfer coefficients in the mouth. Two values are important; the overall heat transfer coefficient (*htc*) between the walls of the oral cavity and the liquid phase and the *htc* between the liquid phase and the food particles. This could be achieved by measuring the rate of melting for gel particles in the mouth, where the gel is manoeuvred around the mouth but not chewed. If the thermal properties and melting point of the gel are known, a good approximation of the *htc* can be made. Experiments could then be extended to include chocolate following the same procedure.

The model will be improved if it can be multi-compartmentalised to account for mass flow between the main bolus and buccal pouches and also include partial swallows. Flynn (2012) found that solids are lost from the bolus throughout mastication and a significant portion is retained in the oral cavity after swallowing or expectoration. These solids have a different PSD to the main bolus that was expectorated. Other studies have found that, at the swallow point, the bolus can consist of as little as 50 percent of the ingested solids (Peyron et al. 2004, Jalbert-Malbos et al. 2007) where most of these losses were attributed to intermediate swallows. Including partial swallowing and the movement of the food between the main bolus and the buccal pouch would improve its predictive capability. This could enable a better understanding about how the bolus reaches the swallow point.

REFERENCES

Afoakwa, E. O. (2011). *Chocolate science and technology*. John Wiley & Sons

Agrawal, K. R., Lucas, P. W., Prinz, J. F, and Bruce, I. C. (1997) Mechanical properties of foods responsible for resisting food breakdown in human mastication. *Arcsh oral Biol,42,* 1-9.

Aguilera, J. M., & Lillford, P. J. (Eds.). (2007). *Food materials science: principles and practice*. Springer Science & Business Media.

Aguilera, J. M., & Stanley, D. W. (1999). *Microstructural principles of food processing and engineering*. Springer Science & Business Media.

Aps, J. K. M., & Martens, L. C. (2005) Review – The physiology of saliva and transfer of drugs into saliva. *Forensic Science International,* vol 150, pp 119-131

Ashby, M. F., & Medalist, R. M. (1983). The mechanical properties of cellular solids. *Metallurgical Transactions A*, *14*(9), 1755-1769.

Austin, L. G. (1971) A review; introduction to the mathematical description of grinding as a rate process. *Powder Technol, 5*. 1-17.

Berenbaum, R. (1961) Analysis of the shatter breakage of coal using a matrix model. *J. Inst. Fuel, 34*. 367-374.

Bornhorst, G. M., Hivert, H., & Singh, R. P. (2014). Rice bolus texture changes due to α-amylase. *LWT-Food Science and Technology*, *55*(1), 27-33.

Bourne, M. (2004) Relation between texture and mastication. *J. Textural Studies, 35,* 125-143.

Bourne, M. C. (1978). Texture profile analysis [Food acceptability]. *Food technology*.

Broadbent, S. R. and Callcott, T. G. (1956) I. A new analysis of coal breakage processes. II. A matrix representation of breakage. *J. Inst. Fuel, 29*, 524-539.

Burey, P., Bhandari, B. R., Rutgers, R. P. G., Halley, P. J., & Torley, P. J. (2009). Confectionery gels: a review on formulation, rheological and structural aspects. *International Journal of Food Properties*, *12*(1), 176-210.

Chen, J. (2007). Surface texture of foods: Perception and characterization. *Critical reviews in food science and nutrition*, *47*(6), 583-598.

Chen, J. (2009). Food oral processing – A review. *Food Hydrocolloids, 23,* 1-25.

Chen, J., Khandelwal, N., Liu, Z., & Funami, T. (2013). Influences of food hardness on the particle size distribution of food boluses. *Archives of oral biology*, *58*(3), 293-298.

Christen, A. G., & Christen, J. A. (1997). Horace Fletcher (1849-1919):" The Great Masticator.". *Journal of the History of Dentistry*, *45*(3), 95-100.

de Loubens, C., Saint-Eve, E., Deleris, I., Panouille, M., Doyenette, M., Trela, I. C., & Souchon, I. (2011) Mechanistic model of in vitro salt release from model dairy gels based on standardized breakdown test simulating mastication. *Journal of Food Engineering,* vol 59, pp 2534-2542.

DeMars, L. L., & Ziegler, G. R. (2001). Texture and structure of gelatin/pectin-based gummy confections. *Food Hydrocolloids*, *15*(4), 643-653.

Engelen, L., de Wijk, R. A., Prinz, J. F., van der Bilt, A., & Bosman, F. (2003) The relations between saliva flow after different stimulations and the perception of flavor and texture attributes in custard desserts. *Physiology and Behaviour*, vol 78, pp 165-169.

Engelen, L., Fontijn-Tekamp, A., & van der Bilt, A. (2005). The influence of product and oral characteristics on swallowing. *Archives of Oral Biology*, *50*(8), 739-746.

Epstein, B. (1947) The mathematical description of certain breakage mechanisms leading to the logorithmico-normal distribution. *J. Franklin Inst, 244.* 471-477.

Ertekin, C., Kiylioglu, N., Tartlaci, S., Keskin, A., & Aydogdu, I. (2000) Effect of mucosla anaesthesia on oropharyngeal swallowing. *Neurogastroenterology & Motility*, vol 12, no. 6, pp 567-572.

Flynn, C.S., Foster, K. D., Bronlund, J.E., Lentle, R. G., Jones, J.R, & Morgernstern, M. (2011) Identification of multiple food compartments present during the mastication of solid food. *Archives in Oral Biology*, vol 56, pp 345-352.

Flynn, C. S. (2012). *The particle size distribution of solid foods after human mastication*. Massey University, Auckland, New Zealand (Doctoral dissertation).

Foegeding, E. A., Daubert, C. R., Drake,M. A., ssick, G., Trulsson, M., Vinyard, C. J., & van de Velde, F. (2011) A comprehensive approach to understanding textural properties of semi- and soft-solid foods. *Journal of Texture Studies*. Vol 42, pp 103-129.

Fontijn-Tekamp, F.A., van der Bilt, A., Abbink, J. H, & Bosman, F. (2004) Swallowing threshold and masticatory performance in dentate adults. *Physiology & Behaviour*, 83, 431-436.

Foster, K. D., Woda, A., & Peyron, M. A. (2006). Effect of texture of plastic and elastic model foods on the parameters of mastication. *Journal of Neurophysiology*, *95*(6), 3469-3479.

Foster, K. D., Grigor, J., Cheong, J. N., Yoo, M. J., Bronlund, J. E., & Morgenstern, M. P. (2011). The role of oral processing in dynamic sensory perception. *Journal of Food Science*, *76*(2), R49-R61.

Froehlich, D. A., Pangborn, R, Whitikaer, J. R. (1986) The effect of oral stimulation on human parotid salivary flow rate and alpha amylase secretion. *Physiology and Behaviour, 41,* 209-217.

Gaviao, M. B. D., Engelen, L., van der Bilt, A. (2004) Chewing behaviour and salivary secretion. *J oral Sci, 112,* 19-24.

Gunasekaran, S., & Ak, M. M. (2002). *Cheese rheology and texture*. CRC press

Hapgood, K. P. (2000). *Nucleation and binder dispersion in wet granulation*. University of Queensland, Australia. (Doctoral dissertation).

Hapgood, K. P., Lister, J. D., Biggs, S. R., & Howes, T., (2002) Drop penetration into porous powder beds, *Journal of Colloid and Interface Science*, vol 253, pp 353-366.

Harrison, M., & Hills, B. P. (1996) A mathematical model to describe flavour release from gelatine gels. *International Journal of food Science and Technology,* vol 31, pp 167-176.

Hiiemae. K. M. (1983) Process and mechanism: Mechanoreceptors in the mouth as the primary modulators of rhythmic behaviour in feeding? In: Verrillo, R. T. ad. 1993. *Sensory research: multimodal perspectives*, Routledge, pp 263-284.

Hiiemae, K. M. & Palmer, J. B. (1999) Food transport and bolus formation during complete feeding sequences on foods of different initial consistency. *Dysphagia,* vol 14, pp 31-42.

Hiiemae, K. (2004) Mechanisms of food reduction, transport and deglutition: How the texture of food affects feeding behaviour. *Journal of Texture Studies,* 35, pp 171-200.

Hoebler, C., Karinthi, A., Devaux, M. F., Guillon, F., Gallant, D. J. G., Bouchet, B., ... & Barry, J. L. (1998). Physical and chemical transformations of cereal food during oral digestion in human subjects. *British Journal of Nutrition*, *80*(05), 429-436.

Hoebler, C., Decaux, M. F., Karinthi, A., Belleville, C., Barry, J. L. (2000) Particle size of solid food after human mastication and *in vitro* simulation or oral breakdown. *Int J of Food Sci and Nutr, 51,* 353-366.

Holm, K., Wendin, K., & Hermansson, A. M. (2009). Sweetness and texture perception in mixed pectin gels with 30% sugar and a designed rheology. *LWT-Food Science and Technology*, *42*(3), 788-795.

Humphrey, S. P, & Williamson, R. T. (2001) A review of saliva: Normal composition, flow, and function. *Journal of Prosthetic Dentistry,* vol 85, pp 162-169.

Hutchings, J. B., & Lillford, P. J. (1988). The perception of food texture. The philosophy of the breakdown path. *Journal of Texture Studies,* vol 19, pp 103–115.

Hutchings, S.C, Bronlund, J.E., Lentle, R. G., Foster, K. D., Jones, J. R, and Morgenstern, M. O. (2009) Variation in bite size with different types of food bars and implications for serving in mastication studies. *Food quality and preference*, 20, 456-460.

Hutchings, S. C. (2011). *Oral processing of heterogeneous foods.* Massey University, New Zealand (Doctoral dissertation).

Hutchings, S. (February 2012). Massey University, New Zealand. Personal communication.

Hutchings, S.C., Foster, K. D., Bronlund, J. E., Lentle, R. G., Jones, J. R., & Morgenstern, M. P. (2012) Particle breakdown dynamics of heterogeneous foods during mastication: peanuts inside different food matrices. *Journal of food Engineering*, vol 109, no. 4, pp 736-744.

IUPAC., 2012. *Compendium of Chemical Terminology, 2nd ed. (the "Gold Book").* [online] Available at:< http://goldbook.iupac.org/W06691.html>[Acessed 2 February 2012].

Iveson, S. M., & Page, N. W. (2005) Dynamic strength of liquid-bound granular materials: The effect of particle size and shape. *Powder Technology,* vol 152, pp 79-89.

Jacobs, r., Wu, C. H., Goosens, K., van Loven, K., van Hees, J, & van Steenberghe, D. (2002) Oral mucosal verses cutaneous sensory testing: a review of the literature. *Journal of Oral Rehabilitation*, vol 29, pp 923-950.

Jalabert-Malbos, M. Mischellany-Dutour, A., Woda, A., & Peyron, M. (2007) Particle distribution in the food bolus after mastication of natural foods. *Food quality and preference,* vol 18, pp 801-812.

Jeronimidis, G., 1991. Mechanical and fracture properties of cellular and fibrous materials. In: Vincent, J. F. V., & Lillford, P. J. eds. 1991. *Feeding and the texture of food*, Cambridge University Press, pp 1-18.

Kapur, K. K., Garrett, N. R., & Fischer, E. (1990) effects of anaesthesia of human oral structures on masticatory performance and food particle size reduction. *Archives of Oral Biology, 35*(5), 397-403.

Kelly, E. G., & Spottiswood, D. J. (1990). The breakage function; what is it really?. *Minerals Engineering*, *3*(5), 405-414.

Kim, E. H., Morgenstern, M. P., Bronlund, J.E., Foster, K.D., & Le Got, A. (2011). Food breakdown during human mastication – Quantitative characterization. In: *11th International Congress on Engineering and Food*, Athens, Greece, May 22-26, 2011.

Kokini,J. l., Kadane, J. B, & Cussler, E. l. (1977) Liquid texture perceived in the mouth. *Journal of Texture Studies*, vol 8, pp 195-218.

Krifa, M. (2009). A mixed Weibull model for size reduction of particulate and fibrous materials. *Powder Technology*, *194*(3), 233-238.

Kutter, A., hanesch, C., Rauh, C, & Delgado, A. (2011) Impact of proprioception and tactile sensations in the mouth on the perceived thickness of semi-solid foods. *Food Quality and Preference,* vol 22, pp 193-197.

Lassauzay, C., Peyron, M. A., Albuisson, E., Dransfield, E., & Woda, A. (2000). Variability of the masticatory process during chewing of elastic model foods. *European journal of oral sciences*, *108*(6), 484-492.

Lenfant, F., Loret, C., Pineau, N., Hartmann, C., & Martin, N. (2009). Perception of oral food breakdown. The concept of sensory trajectory. *Appetite*, *52*(3), 659-667.

Liedberg, B. and Owall, B. (1991) Masticatory ability in experimentally induced xerostomia. *Dysphagia, 6,* 211-213.

Lillford, P. J. (2011) The importance of food microstructure in fracture physics and texture perception. *Journal of Texture Studies,* vol 42, no. 2, pp 130-136.

Loret, C., Walter, M., Pineau, N., Peyron, M. A., Hartmann, C., & Martin, N. (2011) Physical and related sensory properties of a swallowable bolus. *Physiology and Behaviour*, vol 104, no. 5, pp 855-864.

Lucas, P. W. & Luke, D. A. (1983a) Methods for analysing the breakdown of food in human mastication. *Archives of Oral Biology,* vol 28*,* no 9, pp 813-819.

Lucas, P. W., & Luke, D. A. (1983b) Computer simulation of the breakdown of carrot particles during human mastication. *Archives of Oral Biology,* vol 28, no 9, pp 821-826

Lucas, P. W. and Luke, D. A. (1986) Is food particle size a criterion for swallowing? *F. Oral Rehabil, 13,* 127-136.

Lucas, P. W., Prinz, J. F., Agrawal, K.R., & Bruce, I. C. (2002) Food physics and oral physiology, *Food Quality and Preference,* vol 13, pp 202-213.

Medicis, S. W., & Hiiemae, K. M. (1998, January). Natural bite sizes for common foods. In *Journal of Dental Research* (Vol. 77, pp. 295-295). 1619 DUKE ST, ALEXANDRIA, VA 22314 USA: AMER ASSOC DENTAL RESEARCH.

Mioche, L., Bourdiol, P., Monier, S., & Martin, J-P., (2002a) The relationship between chewing activity and food bolus properties obtained from different meat textures. *Food Quality and Preference*, vol 13,pp 583-588.

Mioche, L., Hiiemae, K. M., & Palmer, J. B. (2002b) A posterior videoflurographic study of the intra-oral management of food in man. *Archives of Oral Biology*, vol 47, pp267-280.

Mishellany, A., Woda, A., Labas, R., & Peyron, M. A. (2006). The challenge of mastication: preparing a bolus suitable for deglutition. *Dysphagia*, *21*(2), 87-94.

Moongngarm, A., Bronlund, J. E., Grigg, N., & Sriwai, N. (2012). Chewing behavior and bolus properties as affected by different rice types. *Int. J. Med. Biol. Sci*, *6*, 51-56.

Mowlana, F., & Heath, R. (1993). Assessment of masticatory efficiency: new methods appropriate for clinical research in dental practice. *The European journal of prosthodontics and restorative dentistry*, *1*(3), 121-125.

Nagatomi, H., Yoshimine, M., Miura, H., Tanaka, Y, and Arai, I. (2008) Multivariate analysis of the mechanical properties of boluses during mastication with the normal dentitions. *J Med Dent Sci, 55,* 197-206.

Ng, M., Lawlor, J. B., Chandra, S., Chaya, C., Hewson, L., & Hort, J. (2012). Using quantitative descriptive analysis and temporal dominance of sensations analysis as complementary methods for profiling commercial blackcurrant squashes. *Food quality and Preference*, *25*(2), 121-134

Okada, A., Honma, M., Nomura, S., & Yamada, Y. (2007). Oral behavior from food intake until terminal swallow. *Physiology & Behavior*, *90*(1), 172-179.

Olthoff, L. W., Van Der Bilt, A., Bosman, F., & Kleizen, H. H. (1984). Distribution of particle sizes in food comminuted by human mastication. *Archives of Oral Biology,* vol 29, pp 899–903.

Pangborn, R. M, and Lundgren, B. (1977) Salivary secretion in response to mastication of crisp bread. *Journal of Texture Studies, 8,* 463-472.

Pederson, A. M., Bardow, A., Beir Jensen, S, and Nauntofte, B. (2002) Saliva and gastrointestinal functions of taste, mastication, swallowing and digestion. *Oral Diseases, 8,* 117-129.

Pereira, L. J. De Wijk, R. A. Gaviao, M. B. D. and van der Bilt, A. (2006) Effects of added fluids on the perception of solid food. *Physiology and behaviour*, *88,* 538-544.

Peyron, M. A., Mishellany, A, & Woda, A. (2004) Particle size distribution of food boluses after mastication of six natural foods. *Journal of Dental Research, vol 83*, pp 578-582.

Peyron, M-A, Gierczynski, I., Woda, A., Loret, C., Hartman, C, and Martin, N. (2007) Use of the Texture profile analysis (TPA) test for a rheological characterisation of food bolus collected in the course of mastication. *5th International Symposium on Food Rheology and Structure.* pp108-111.

Peyron, M-A. (2011) Food bolus properties: investigation, role and significance. In: *Biomouth 2011*. Palmerston North, New Zealand 28-29 November 2011.

Peyron , M-A., Gierczynski, I., Hartman, C., Loret, C., Darevet, D., Martin, N, & Woda, A. (2011). Role of bolus properties as sensory inputs in the trigger of swallowing. PLoS ONE 6(6): e21167. doi:10.1371/journal.pone.0021167

Pineau, N., Cordelle, S., & Schlich, P. (2003). Temporal Dominance of Sensations: A new technique to record several sensory attributes simultaneously over time. In *5th Pangborn symposium* (p. 121).

Pineau, N., Schlich, P., Cordelle, S., Mathonnière, C., Issanchou, S., Imbert, A., ... & Köster, E. (2009). Temporal Dominance of Sensations: Construction of the TDS curves and comparison with time–intensity. *Food Quality and Preference*, *20*(6), 450-455.

Prinz, J. F. and Lucas, P. W. (1994) Swallow thresholds in human mastication. *Archs oral Biol, 40,* 401-403.

Prinz, J. F., & Lucas, P. W. (1997) An optimization model for mastication and swallowing in mammals. *Proceedings: Biological Sciences,* vol 264*,* no. 1389, December, pp 1715-1721.

Prinz, J. F., Janssen, A. M., & De Wijk, R. A. (2007). In vitro simulation of the oral processing of semi-solid foods. *Food Hydrocolloids*, *21*(3), 397-401.

Salles, C., Tarrega, A., Mielle, P., Maratray, J., Gorria, P., Liaboeuf, J., & Liodenot, J. J. (2007). Development of a chewing simulator for food breakdown and the analysis of in vitro flavor compound release in a mouth environment. *Journal of Food Engineering*, *82*(2), 189-198.

Schimmel, M., Christou, P., Herrmann, F., & Müller, F. (2007). A two-colour chewing gum test for masticatory efficiency: development of different assessment methods. *Journal of oral rehabilitation*, *34*(9), 671-678.

Seo, H. S., Hwang, I. K., Han, T.R, & Kim, I. S. (2007) Sensory and instrumental analysis for slipperiness and compliance of food during swallowing. *Journal of food Science,* vol 72, pp 707-713.

Sprunt, J. C., & Smith, A. C. (2002). Measurement of surface area, gel weight and saliva weight in a gelatin-based gel over the course of mastication. *International journal of food sciences and nutrition*, *53*(3), 261-271.

Strassburg, J., Burbidge, A., Delgado, A., & Hartmann, C. (2007). Geometrical resolution limits and detection mechanisms in the oral cavity. *Journal of biomechanics*, *40*(16), 3533-3540

Strassburg, J., Burbidge, A., & Hartmann, C. (2009). Identification of tactile mechanisms for the evaluation of object sizes during texture perception. *Food quality and preference*, *20*(4), 329-334.

Swarts, D. R., Greaser, M. L. and Cantino, M. E (2009). Muscle Structure and Function. Du, M., & McCormick, R. J. (Eds.), *Applied muscle biology and meat science*. (pp 1-46). CRC Press.

Szczesniak, A. S. (1963). Classification of textural characteristics. *Journal of food science*, *28*(4), 385-389.

Szczesniak, A. S., Brandt, M. A., & Friedman, H. H. (1963). Development of standard rating scales for mechanical parameters of texture and correlation between the objective and the sensory methods of texture evaluation. *J. Food Sci*, *28*(4), 397-403.

Szczesniak, A. S. (2002) texture is a sensory property. *Food quality and preference, 13,* 215-225.

Tanabe, N, A., and Hofberger, R. (2006) Hui, Yiu H. (Ed), *Handbook of food science, technology, and engineering*. Vol. 149 (pp1-11). CRC press.

Trulsson, M, & Essick, G. K. (1997) Low-threshold mechanoreceptive afferents in the human lingual nerve. *Journal of Neurophysiology,* vol 77, pp 737-748.

Trulsson, M., & Johansson, R. S. (2002). Orofacial mechanoreceptors in humans: encoding characteristics and responses during natural orofacial behaviours. *Behavioural Brain research,* vol 135, pp 27-33.

Trulsson, M. (2007) Force encoding by human periodontal mechanoreceptors during mastication. *Archives in Oral Biology*, vol 52, pp 357-360.

Trulsson, M, & Essick, G. K. (2010) Sensations evoked by microstimulation of single mechanoreceptive afferents innervating the human face and mouth. *Journal of Neurophysiology,* vol 103, pp 1741-1747.

van Aken, G. A. (2010) Modelling texture perception of soft epithelial surfaces. *Soft Matter*, vol 10, pp 826-834.

van der Bilt, A. Olthoff, L. W. van der Glas, H. W. van der Weelen, K. & Bosman, F. (1987) A mathematical description of the comminution of food during mastication in man. *Archives of Oral Biology,* vol 32, pp 579-586.

van der Bilt, A. van der Glas, H. W. & Bosman, F. (1992) A computer simulation of the influence of selection and breakage of food on the chewing efficiency of human mastication. *Journal of Dental Research,* vol 71, pp 458-465.

van der Bilt, A., Engelen, L., Pereira, L. J., van der Glas, H. w., & Abbink, J. H. (2006) Oral physiology and mastication. *Physiology and Behaviour,* vol 89, pp 22-27.

van der Bilt, A., Mojet, J., Tekamp, F. A., & Abbink, J. H. (2010). Comparing masticatory performance and mixing ability. *Journal of oral rehabilitation*, *37*(2), 79-84.

van der Glas, H. W., van der Bilt, A., Olthoff L. W, & Bosman F. (1987) Measurement of selection chances and breakage functions during chewing in man. *Journal of Dental Research,* vol 66, no.10, pp 1547-1550

van der Glas, H. W., van der Bilt, A., & Bosman, F. (1992). A selection model to estimate the interaction between food particles and the post-canine teeth in human mastication. *Journal of theoretical biology*, *155*(1), 103-120.

Vincent, J. F., & Lillford, P. J. (1991). *Feeding and the Texture of Food* (Vol. 44). Cambridge University Press.

Voon, F. C. T., Lucas, P. W., Chew, K. L., & Luke, D. A. (1986) A simulation approach to understanding the masticatory process. *Journal of Theoretical Biology,* Vol 119*,* pp 251-262.

Walstra, P., Walstra, P., Wouters, J. T., & Geurts, T. J. (2005). *Dairy science and technology*. CRC press.

Watanabe, S., & Dawes, C. (1988) The effects of different foods and the concentrations of citric acid on the flow rate of whole saliva in man. *Archs oral Biol,* vol 33, pp 1-5.

Williams, S. H., Wright, B. W., Truong, V. D., Daubert, C. R., & Vinyard, C. J. (2005). Mechanical properties of foods used in experimental studies of primate masticatory function. *American journal of primatology*, *67*(3), 329.

Woda, A., Foster, K., Mishellany, A.,& Peyron, M-A. (2006[a]) Adaptation of healthy mastication to factors pertaining to the individual or to the food. *Physiology and Behaviour*, vol 98, pp 28-35.

Woda, A., Mishellany, A., & Peyron, M-A. (2006[b]) The regulation of masticatory function and food bolus formation. *Journal of Oral Rehabilitation*, vol 33, pp 840-849.

Wright, K. & Hills, B. (2003) Modelling flavour release from a chewed bolus in the mouth: Part II. The release kinetics. *International Journal of Food Science & Technology,* vol 38, pp 361–368.

Wright, K., Sprunt, J., Smith, A. & Hills, B. (2003) Modelling flavour release from a chewed bolus in the mouth: Part I. Mastication. *International Journal of Food Science & Technology,* vol 38, pp 351–360

APPENDIX A

This Appendix shows the complete derivation for the one-way and two-way completion model of van der Glas et al. (1992).

One-way completion model derivation

The selection chance of the largest particle in a mixture is the same as for the selection of a number of particles of a single size. Thus, the unoccupied fraction of breakage sites left by the largest particle size X_1 is:

$$U\left(X_1, n_{X_1}\right) = [1 - O_1(X_1, 1)]^{n_{X_1}}, \qquad \textbf{Eq. A-1}$$

where $O_1(X_1, 1)$is the particle affinity for X_1 (see equation 5). Once the largest particles have occupied breakage sites, the selection chance for a single particle X_2 proportionally decreases with the unoccupied fraction of breakage sites left by the larger particles. The selection chance for particle size X_2 is:

$$S_1'(X_2, 1) = S_1(X_2, 1).\, U\left(X_1, n_{X_1}\right) \qquad \textbf{Eq. A- 2}$$

The number of breakage sites available for X_2 is

$$n_b'(X_2) = n_b(X_2).\, U(X_1, n_{X_1}) \qquad \textbf{Eq. A-3}$$

The fraction of breakage sites left by the largest particles (X_1) and occupied by the first particle of the next largest size (X_2) is given by:

$$O_1'(X_2, 1) = S_1'(X_2, 1)/n_b'(X_2) \qquad \textbf{Eq. A-4}$$

The particle affinity of size X_2 is not affected by the large particles X_1. The breakage sites left by size X_1 and occupied by size X_2 is therefore:

$$O\left(X_2, n_{X_2}\right) = 1 - [1 - O_1(X_2, 1)]^{n_{X_2}} \qquad \textbf{Eq. A-5}$$

From equations 18 and 19, the number of selected particles of size X_2 is:

$$n_s(X_2, n_{X_2}) = [n_b(X_2).\, U(X_1, n_{X_1})].\, [1 - (1 - O_1(X_2, 1))^{n_{X_2}} \qquad \textbf{Eq. A- 6}$$

This can be applied for any particle size X_i with (i-1) classes of larger particles, the number of selected particles is:

Two-way completion model derivation

The selection chance of the i^{th} particle will decrease with the unoccupied fraction left by the previously selected particles, so:

$$S_i(X_{q_i}, i) = S_1(X_{q_i}, 1).\, U[Q(i-1), i-1] \qquad \textbf{Eq. A- 7}$$

X_{qi} is the size of the i^{th} selected particle of size class q_i, Q(i-1)denoted the size of the $I - 1$ previous particles. $S_1(X_{q_i}, 1)$ is the selection chance if the ith particle was the first particle to occupy the breakage sites, $U[Q(i-1), i-1]$ is the unoccupied fraction of the breakage sites left by the $I - 1$ previous particles. The occupied fraction of breakage sites by the ith particle is:

$$O_i(X_{q_i}, i) = [S_i(X_q, 1).\, U(Q(i-1), i-1)]/n_b(X_{q_i}) \qquad \textbf{Eq. A- 8}$$

Substituting for $S_i(X_q, 1)$ this reduces to:

$$O_i(X_{q_i}, i) = O_1(X_{q_i}, 1).\, U[Q(i-1), i-1] \qquad \textbf{Eq. A- 9}$$

The unoccupied fraction of breakage sites left by the previous $I - 1$ particles, $U[Q(i-1), i-1]$, decreases with $O_i(X_{q_i}, i)$. Thus, the unoccupied fraction of the breakage sites left by i particles is:

$$U(Q(i), i) = \left(1 - O_1(X_{q_i}, 1)\right).\, U[Q(i-1), i-1] \qquad \textbf{Eq. A-10}$$

For the total number of particle, n_T, this is equivalent to:

$$U[Q(n_T), n_T] = \prod_{j=1}^{n_T}[1 - O_1(X_{qj}, 1)] \qquad \textbf{Eq. A-11}$$

this is the total unoccupied fraction of breakage sites left by all particles where $O_1(X_{q1}, 1)$is the affinity factor of the first particle and $O_1(X_{q2}, 1)$is the affinity factor of the second particle etc, this is independent of the size of the size of the subsequent particles.

$$U[Q(n_T), n_T] = \prod_{j=1}^{k}\left[\left(1 - O_1(X_j, 1)\right)^{n_{x_j}}\right] \qquad \textbf{Eq. A-12}$$

By definition, the total occupied fraction is simply one minus the unoccupied fraction:

$$O[Q(n_T), n_T] = 1 - \prod_{j=1}^{k}\left[\left(1 - O_1(X_j, 1)\right)^{n_{x_j}}\right] \qquad \textbf{Eq. A-13}$$

The purpose of this derivation is to define an equation for the number selected particles $n_s(X_i, n_{X_1})$ of some arbitrary size X_i ($1 \le I \le k$) as a function of the number of these particles, n_{X_i}, while these particles are in part of a particle mixture of different particle sizes. Particles of size X_i occupy some breakage sites $n_s(X_i, n_{X_i})/n_b(X_i)$ which is only a fraction of the total breakage sites occupied by all particles, $O[Q(n_T), n_T]$ (equation28). If the number of particles of other sizes decreases, the total occupied fraction of breakage sites, $O[Q(n_T), n_T]$, could be maintained by increasing the number of particles X_i. A mixture of n_T particles of k size classes could be replaced by a certain number of a single class X_i (this number is denoted as n_{T,X_i}) and give the same value for the total occupied fraction of breakage sites $O[Q(n_T), n_T]$.

$$[1 - O_1(X_i, 1)]^{n_{T.X_i}} = \prod_{j=1}^{k}\left[1 - O_1(X_j, 1)\right]^{n_{T.X_j}} \qquad \textbf{Eq. A-14}$$

Simplifying and rearranging gives:

$$n_{T,X_i} = \sum_{j=1}^{k} [n_{X_j}.\ln(1 - O_1(X_j, 1))] / \ln[1 - O_1(X_i, 1)] \qquad \textbf{Eq. A-15}$$

Each of the particles of size X_i has on average the same chance of occupying a breakage site, the actual number of particles of size X_i in a mixture, n_{X_i}, will occupy a fraction of the total occupied breakage sites $O[Q(n_T), n_T]$, given by:

$$f_{X_i} = \frac{n_{X_i}}{n_{T.X_i}} \qquad \textbf{Eq. A-16}$$

The occupied fraction of the breakage sites by the number of X_i particles n_{X_i} is therefore:

$$n_s(X_i, n_{X_i})/n_b(X_i) = f_{X_i}.O(Q(n_T), n_T] \qquad \textbf{Eq. A-17}$$

Equations Eq. A-13, Eq. A-15 and Eq. A-16 are substituted to give the number of selected particles of size X_i in the mixture:

$$\begin{aligned} & n_s(X_i, n_{Xi}) \\ & = n_b(X_i).\left[n_{Xi}.\ln\big(1 - O_1(X_i, 1)\big) \Big/ \sum_{j=1}^{k} \Big(n_{Xj}.\ln\Big(1 - O_1\big(X_j, 1\big)\Big)\Big)\right] \\ & \qquad .\left[1 - \prod_{j=1}^{k} (1 - O_1(X_j, 1))^{n_{Xj}}\right] \end{aligned} \qquad \textbf{Eq. A-18}$$

APPENDIX B

Composition and nutritional information for the foods used in Chapter Three.

Beef Rump (Silver Fern Farms)

Nutritional information (per 100 g)	
Energy	483kj
Protein	21.9g
Fat - Total	3.0g
- Saturated	1.1g
Carbohydrates	Less than 1g
- Sugars	-
Sodium	42mg

Carrots

Nutritional information (per 100 g)	
Energy	160kJ
Protein	1.0g
Fat, total	Less than 1g
- saturated	0
Carbohydrates	10g
- sugars	5g
Dietary Fibre	3g
Sodium	69mg

Banana

Nutritional information (per 100 g)	
Energy	375kJ
Protein	1.0g
Fat, total	Less than 1g
- saturated	0
Carbohydrates	23g
- sugars	12g
Dietary Fibre	3g
Sodium	2mg

Eta™ Roasted Peanuts

Ingredients: Peanuts, Canola Oil [Antioxidant (319)], Sunflower Oil [Antioxidant (306)], Salt. (Contains Wheat & Soy).

Nutritional information (per 100 g)	
Energy	2440kJ
Protein	23.3g
Fat, total	52.2g
- saturated	6.8g
Carbohydrates	14.6g
- sugars	1.6g
Sodium	620mg

Griffins Super Wine ™ biscuits

Ingredients: Wheat Flour, Sugar, Vegetable Fat [Antioxidant (306)], Invert Syrup, Whey Powder, Salt, Raising Agents (500, 450), Flavours, Colour (Annatto Extracts).

Nutritional information (per 100 g)	
Energy	1970kJ
Protein	5.6g
Fat, Total	16.3g
- Saturated	10.0g
Carbohydrate, Total	74.5g
-Sugars	25.7g
Sodium	350mg

Tip Top White sandwich bread

Ingredients: Wheat Flour, Water, Bakers Yeast, Iodised Salt, Canola Oil, Soy Flour, Acidity Regulator (263), Emulsifiers (481, 472e, 471). (Contains Wheat & Soy).

Nutritional information (per 100 g)	
Energy	1050kJ
Protein	8.0g
Fat, total	2.0g
- saturated	0.2g
Carbohydrates	48.1g
- sugars	3.4g
Dietary Fibre	2.4g
Sodium	450mg

Mainland Edam Cheese:

Ingredients: Milk, culture, enzyme (non animal rennet).

Nutritional information (per 100 g)	
Energy	1440kJ
Protein	26.8g
Fat, Total	26.5g
- Saturated	18.7g
Carbohydrate, Total	Less than 1g
- Sugars	Less than 1g
Sodium	370mg

Cadbury Dairy Milk Milk Chocolate:

Ingredients: Full cream milk, sugar, cocoa butter, cocoa mass, milk solids, emulsifiers (soy lecithin, 476), flavours, milk solids minimum 24%. Milk chocolate contains cocoa solids 26%, milk solids minimum 24%

Nutritional information (per 100 g)	
Energy	2240kj
Protein	8.1g
Fat - Total	29.6g
- Saturated	18.7g
Carbohydrates	59.1g
- Sugars	57.3g
Sodium	87mg

APPENDIX C

MASSEY UNIVERSITY
COLLEGE OF SCIENCES
TE WĀHANGA PŪTAIAO

Measuring the effect of particle size and number on the oral selection and breakdown of rice particles

INFORMATION SHEET

Hello,

My name is Eli Gray-Stuart; I am a PhD student in the School of Engineering and Advanced Technology. I would like to invite you to participate in a chewing study.

The aim of the project is to determine how the number and size of rice particles influence the breakdown during chewing. This study will look at the number and size of particles that are broken in a single chewing stroke. The distribution of fragmented particles will also be analysed and the compared for brown and white rice.

Participant Involvement
The trials will involve you chewing on cooked rice (brown or white); the samples will consist of a specific number and size of particles prepared by the researcher. The samples will be served to you and you will be required to make a single natural chew before expectorating the particles. The expectorated particles will be collected and analysed by the researcher.

Before participating in the rice chewing experiments, you will be required to participate in a half hour session involving fruit and nut bars to ensure suitability for the study. This involves chewing several bars, where the bite weight and number of chews used before swallowing is measured. You will need to be able to consume all foods involved in the study, so please check carefully the food and ingredient list on the last page, especially noting that nuts are being used. Selection will be based on your age, dental, and health status and on the screening test using food bars. Please note that if you volunteer and are screened out it is not an indication that there is any issue with your dental health.

If you are selected after the initial 30 minute screening session you will be compensated for your time at $15 per hour. Payment will be in the form of supermarket vouchers (hours will be calculated by the researcher). You will be required for no more than 2 sessions of 1 hour each per week, over a period of approximately 8 weeks. Session times are very flexible and can be arranged to meet your schedule.

To protect your privacy, all of your data will be placed under a code so that you will not be identified in any publications, and a summary of the findings will be posted to you after data analysis and writing up.

You are under no obligation to accept this invitation. If you decide to participate, you have the right to:

- decline to answer any particular question;
- withdraw from the study at anytime
- ask any questions about the study at any time during participation;
- provide information on the understanding that your name will not be used unless you give permission to the researcher;
- be given access to a summary of the project findings when it is concluded.

If you are interested in taking part, or have any further questions about the project, please do not hesitate to contact any of the researchers listed below. Your interest will be greatly appreciated. A screening questionnaire will be given to see if you're eligible to take part.

Project Contacts

Eli Gray-Stuart 06 350 9099 ext 7439
E.M..Gray-Stuart@massey.ac.nz

Prof John Bronlund 06 350 5542
J.E.Bronlund@massey.ac.nz

Prof Jim Jones 04 801 5799 ext 6719
J.R.Jones@massey.ac.nz

MUHEC APPLICATIONS

Committee Approval Statement

"This project has been reviewed and approved by the Massey University Human Ethics Committee: Southern A, Application 11/33. If you have any concerns about the conduct of this research, please contact A/Prof Hugh Morton, Chair, Massey University Human Ethics Committee: Southern A telephone 06 350 5799 x 4265, email humanethicsoutha@massey.ac.nz."

Compensation for Injury

If physical injury results from your participation in this study, you should visit a treatment provider to make a claim to ACC as soon as possible. ACC cover and entitlements are not automatic and your claim will be assessed by ACC in accordance with the Injury Prevention, Rehabilitation and Compensation Act 2001. If your claim is accepted, ACC must inform you of your entitlements, and must help you access those entitlements. Entitlements may include, but not be limited to, treatment costs, travel costs for rehabilitation, loss of earnings, and/or lump sum for permanent impairment. Compensation for mental trauma may also be included, but only if this is incurred as a result of physical injury.

If your ACC claim is not accepted you should immediately contact the researcher. The researcher will initiate processes to ensure you receive compensation equivalent to that to which you would have been entitled had ACC accepted your claim.

List of the ingredients that will be used in the test foods

Rice (Brown and White)

May contain traces of nuts.

Fruit and nut bar (Tasti brand)

Nuts (almonds and peanuts),Glucose, Milk solids, Dates, Sultanas, Milk Chocolate, Vegetable fat, Vegetable oil, Cocoa powder, Antioxidant (306), Emulsifiers (Soy Lecithin 492, 476), Citric acid, Puffed wheat, Sunflower oil, Sunflower seeds, Honey, Caramelised sugar and Salt

Measuring the effect of particle size and number on the oral selection and breakdown of rice particles

Primary questionnaire

Thank you for expressing interest in this study. Prior to your participation, please answer the following questions.

1. Is your age between 18 and 30?
   Y N

2. Do you have 8 post canine teeth?
   Y N

3. Do you experience any pain/discomfort while chewing?
   Y N

4. Have you suffered any serious jaw injuries in the past?
   Y N

5. Do you currently wear tooth braces?
   Y N

6. Do you have a problem with dry mouth or salivary flow?
   Y N

7. Do you wear dentures?
   Y N

8. Do you currently take any medication that might affect saliva flow, such as oxybutynin or amitriptyline?
   Y N

9. Do you have a disorder of the mouth?
   Y N

10. Do you currently have any significant problems with tooth decay or gum disease?
    Y N

11. Have you noticed any tooth grinding or excessive tooth clenching while chewing?
    Y N

12. Are you aware of any other health problems that may inhibit your ability to take part in this study or put your health at risk in any way?
    Y N

13. Do you suffer from any blood borne infectious disease?
    Y N

14. Are you allergic to any of the ingredients that will be used in this study? (Listed in information sheet)
    Y N

If you are able to answer YES to Q1 and NO to all other questions above, you are invited to come and look at the laboratory where the experiments will take place and discuss the project and the role of a participant in more detail.

MASSEY UNIVERSITY
COLLEGE OF SCIENCES
TE WĀHANGA PŪTAIAO

Measuring the effect of particle size and number on the oral selection and breakdown of rice particles

PARTICIPANT CONSENT FORM - INDIVIDUAL

I have read the Information Sheet and have had the details of the study explained to me. My questions have been answered to my satisfaction, and I understand that I may ask further questions at any time.

I agree to participate in this study under the conditions set out in the Information Sheet.

Signature: ..... **Date:** .....

Full Name - printed .....

MASSEY UNIVERSITY
COLLEGE OF SCIENCES
TE WĀHANGA PŪTAIAO

Rice Chewing Study

You are invited to take part in a study investigating the breakdown of rice during chewing. The effect of size and number of rice particles on the rate of breakdown during mastication will be investigated for brown and white rice.

If you are aged between 18 and 30 years, have a healthy and complete set of teeth, are happy to have your chewed food analysed, and would like to find out more about the study, please contact:

Eli Gray-Stuart
PhD student
School of Engineering and Advanced Technology
Massey University, Palmerston North
Tel: 06 356 9099 ext. 7439
E mail: e.m.gray-stuart@massey.ac.nz

Subjects will be compensated for participating

"This project has been reviewed and approved by the Massey University Human Ethics Committee: Southern A, Application 11/33. If you have any concerns about the conduct of this research, please contact A/Prof Hugh Morton, Chair, Massey University Human Ethics Committee: Southern A telephone 06 350 5799 x 4265, email humanethicsoutha@massey.ac.nz*."*

APPENDIX D

Measuring the particle size distribution and sugar leaching of a masticated gelatine sweet

INFORMATION SHEET

Hello,

My name is Eli Gray-Stuart; I am a PhD student in the School of Engineering and Advanced Technology. I am conducting a research project in conjunction with Camille Ollier, a second year food technology student from Dijon University in France. We would like to invite you to participate in a chewing study.

The aim of the project is to determine how the initial physical properties of a gel affect the rate of breakdown during chewing. Breakdown of solid foods during chewing involves mechanical size reduction via the teeth and simultaneous interactions between the food and saliva, including absorption and dissolution. This study will compare the particle size distribution in the bolus and the leaching rate of sugar during chewing for three different gelatine sweets.

Participant Involvement
The trials will involve you chewing on samples of gelatine gel with different physical properties and sugar concentrations and spitting them out at the point of swallowing or at a point specified by the researcher.

You will be required to participate in a half hour session involving fruit and nut bars to ensure suitability for the study. This involves chewing several bars, where the bite weight and number of chews used before swallowing is measured. You will need to be able to consume all foods involved in the study, so please check carefully the food and ingredient list on the last page, especially noting that nuts and gelatine are being used. The gelatine being used is derived from animal products so vegetarians or vegans are not able to participate. Selection will be based on your age, dental, and health status and on the screening test using food bars. Please note that if you volunteer and are screened out it is not an indication that there is any issue with your dental health.

If you are selected after the initial 30 minute screening session you will be compensated for your time at $15 per hour. Payment will be in the form of supermarket vouchers (hours will be calculated by the researcher). You will be required for no more than 2 sessions of 1 hour each per week, over a period of approximately 8 weeks. Session times are very flexible and can be arranged to meet your schedule.

To protect your privacy, all of your data will be placed under a code so that you will not be identified in any publications, and a summary of the findings will be posted to you after data analysis and writing up.

You are under no obligation to accept this invitation. If you decide to participate, you have the right to:

- decline to answer any particular question;
- withdraw from the study at anytime
- ask any questions about the study at any time during participation;
- provide information on the understanding that your name will not be used unless you give permission to the researcher;
- be given access to a summary of the project findings when it is concluded.

If you are interested in taking part, or have any further questions about the project, please do not hesitate to contact any of the researchers listed below. Your interest will be greatly appreciated. A screening questionnaire will be given to see if you're eligible to take part.

Project Contacts

Eli Gray-Stuart 06 350 9099 ext 7439
E.M..Gray-Stuart@massey.ac.nz

Camille Ollier
C.Ollier@agrosupdijon.fr

A/Prof John Bronlund 06 350 5542
J.E.Bronlund@massey.ac.nz

Prof Jim Jones 04 801 5799 ext 6719
J.R.Jones@massey.ac.nz

MUHEC APPLICATIONS

Committee Approval Statement

"This project has been reviewed and approved by the Massey University Human Ethics Committee: Southern A, Application 10/29. If you have any concerns about the conduct of this research, please contact Professor Julie Boddy, Chair, Massey University Human Ethics Committee: Southern A telephone 06 350 5799 x 2541, email humanethicsoutha@massey.ac.nz."

Compensation for Injury

If physical injury results from your participation in this study, you should visit a treatment provider to make a claim to ACC as soon as possible. ACC cover and entitlements are not automatic and your claim will be assessed by ACC in accordance with the Injury Prevention, Rehabilitation and Compensation Act 2001. If your claim is accepted, ACC must inform you of your entitlements, and must help you access those entitlements. Entitlements may include, but not be limited to, treatment costs, travel costs for rehabilitation, loss of earnings, and/or lump sum for permanent impairment. Compensation for mental trauma may also be included, but only if this is incurred as a result of physical injury.

If your ACC claim is not accepted you should immediately contact the researcher. The researcher will initiate processes to ensure you receive compensation equivalent to that to which you would have been entitled had ACC accepted your claim.

List of the ingredients that will be used in the test foods

Gelatine gels
Gelatine (derived from beef and pork), Sucrose, Glucose syrup, Citric acid powder, Colour

Fruit and nut bar (Tasti brand)
Nuts (almonds and peanuts),Glucose, Milk solids, Dates, Sultanas, Milk Chocolate, Vegetable fat, Vegetable oil, Cocoa powder, Antioxidant (306), Emulsifiers (Soy Lecithin 492, 476), Citric acid, Puffed wheat, Sunflower oil, Sunflower seeds, Honey, Caramelised sugar and Salt

Measuring the particle size distribution and sugar leaching of a masticated gelatine sweet

Primary questionnaire

Thank you for expressing interest in this study. Prior to your participation, please answer the following questions.

1. Is your age less than 18 or greater than 30?
   Y N

2. Do you have any missing teeth?
   Y N

3. Do you experience any pain/discomfort while chewing?
   Y N

4. Have you suffered any serious jaw injuries in the past?
   Y N

5. Do you currently wear tooth braces?
   Y N

6. Do you have a problem with dry mouth or salivary flow?
7. Y N

8. Do you currently take any medication that might affect saliva flow, such as oxybutynin or amitriptyline?
   Y N

9. Do you have a disorder of the mouth?
   Y N

10. Do you currently have any significant problems with tooth decay or gum disease?
    Y N

11. Have you noticed any tooth grinding or excessive tooth clenching while chewing?
    Y N

12. Are you aware of any other health problems that may inhibit your ability to take part in this study or put your health at risk in any way?
    Y N

13. Do you suffer from any blood borne infectious disease?
    Y N

14. Are you allergic to any of the ingredients that will be used in this study? (Listed in information sheet)
    Y N

If you are able to answer NO to all of the questions above, you are invited to come and look at the laboratory where the experiments will take place and discuss the project and the role of a participant in more detail.

MASSEY UNIVERSITY
COLLEGE OF SCIENCES
TE WĀHANGA PŪTAIAO

Measuring the particle size distribution and sugar leaching of a masticated gelatine sweet

PARTICIPANT CONSENT FORM - INDIVIDUAL

I have read the Information Sheet and have had the details of the study explained to me. My questions have been answered to my satisfaction, and I understand that I may ask further questions at any time.

I agree to participate in this study under the conditions set out in the Information Sheet.

Signature: ..... **Date:** .....

Full Name - printed .....

APPENDIX E

The Matlab files for the general model and case studies are contained on the CD attached.

General model folder

MATLAB files

- Bolus_model.m
- Selection_of_particlesCOMP.m
- Selection_of_particlesPLAW.m
- Discrete_Breakage_of_particles.m
- mycon.m
- myfun.m
- run_fmincon.m
- Bolus_figures.m

Case study 1

MATLAB files

- Rice_breakdown_model.m
- Selection_competiton_rice.m
- Rice_BreakageFCN.m
- mycon.m
- myfun.m
- run_fmincon.m
- rice_Graphs
- rice_bolus_paramaters.m

Excel files

- Brownricedata.xlsx

Case study 2

MATLAB files

- Gels_subdivison_model
- Selection_gels
- Gel_breakage
- Gel_figures
- Subject_data

Excel files

- Gels_bolsdata.xlsx

Case study 3

MATLAB files

- Shapefactorchocpeanutanalysis.m
- peanutchocolatedata.m
- ShapefactorJelpeanutanalysis.m
- peanutgelatinedata.m
- ShapeFactorPooledareaschoc.m
- ShapeFactorPooledareasjel.m
- Peanuts_in_matrix_Discrete_Model.m
- Breakage_peanuts.m
- Selection_of_peanuts.m
- Simulation_vs_chocpeanut_data.m
- Peanuts_Matrix_choc.m
- Peanuts_Matrix_gelatine.m
- SelectionOfNutsAndMatrix.m
- Simulation_Bolus_Averages.m
- Peanut_and_Matrix_GRAPHS
- graphswithmatrixandDATA.m
-

Excel files

- Pooledareapeanutdata.xlsx
- subject peanut bolus data (c-5c-s1-a.xlsx)

Discrete model

MATLAB files

- Discrete_comminution_vs_matrix_algebra.m
- Discrete_breakage_model.m
- Compare_discretePSD_vs_matrixmodel.m
- run_fmincon.m
- mycon.m
- myfun.m

APPENDIX F

Previous mastication studies have simulated the PSD on a volume basis with volume fractions being apportioned into size classes, as outlined in section 2-7. Discretising the distribution has some key benefits, notably the rate processes important during mastication involve the exposed surface area of the food. Furthermore if bulk properties of particles are changing between chews, the particle properties can be passed on to daughter particles resulting from occlusion. Another advantage is that image analysis is an increasingly popular method of particle size analysis, in which the size (2D projected area) and number of individual particles are measured. The MATLAB code for this is discrete PSD model is given in Appendix E.

The distribution of daughter particles needs to best fit the breakage function while conserving the volume of the occluded particle. Upon breakage, fractions of the parent particle are apportioned to a $2^{3/2}$ volume series (equates to a √2 particle diameter series) from which the exact size and number of particles within each size bin are calculated. To conserve volume, the size is somewhere within the bin size range. However, if the volume apportioned to a bin is less than the volume of a minimum sized particle within that bin, then adjustments have to be made otherwise the distribution generated will not represent the distribution given by the breakage function. This is best illustrated by considering the following example. Consider a spherical particle, V_i, with a diameter of 10 mm is occluded, Eq 2-23 is used with a fragmentation variable, r, of 1.0 to describe the resulting PSD. Assuming that all the daughter particles are spherical, this gives a PSD shown in Table F-1. The volume retained on the 8 mm sieve is insufficient to form a whole particle. Therefore, the volume distribution cannot be simply translated to a distribution of discrete particles.

Table F-1: Theoretical volume retained in each size class resulting from a 10 mm spherical particle being occluded with a fragmentation variable of 1.0.

Sieve aperture (mm)	Minimum particle volume (mm^3)	Volume fraction in each size class	Theoretical volume on sieve (mm^3)
8.00	268.1	0.36	187.6
5.66	94.9	0.32	167.7
4.00	33.5	0.16	83.8
2.83	11.9	0.08	41.9
2.00	4.2	0.04	21.0
1.41	1.5	0.02	10.5
1.00	0.52	0.01	5.2
0.71	0.19	0.005	2.6
0.50	0.07	0.003	1.3
0.35	0.02	0.001	0.66
pan	0.00	0.001	0.66

In this instance where one or more of the size classes has a volume apportioned which is less than that of the minimum required for a particle. To resolve this problem two alternate distributions are derived. These two distributions, $ALT1_{psd}$ and $ALT2_{psd}$, are generated so that they are similar to the PSD given by the breakage function, $theoryvol_{psd}$, whilst conserving the volume. The fmincon function in MATLAB® is used to find the ratio of these two distributions which most closely matches the volume distribution given by the breakage function, $theoryvol_{psd}$. The ratio is found by minimising the sum of the squared residuals between $theoryvol_{psd}$ and the product of the two alternate distributions and their associated ratios, Eq. F-1.

$$f = sum\left(theoryvol_{psd} - \left(xin_1 * Alt1_{psd} + xin_2 * Alt2_{psd}\right)\right)^2 \qquad \textbf{Eq. F-1}$$

The first alternate distribution, $ALT1_{psd}$, is generated by assuming that none of the original particle is retained on the largest sieve. This extra volume is then apportioned to the remaining size classes relative to the volume fraction in each size class. For $ALT2_{psd}$ a particle in the largest size class is generated. The particle is of the minimum size required to be retained in the 8mm sieve. The remaining volume, $V_i - V_p$ is distributed amongst the other size classes relative to the original volume fraction distribution. Figure F-1 shows that the combination of the discrete distributions generated at the optimum ratio produce a PSD close to that given by the breakage function.

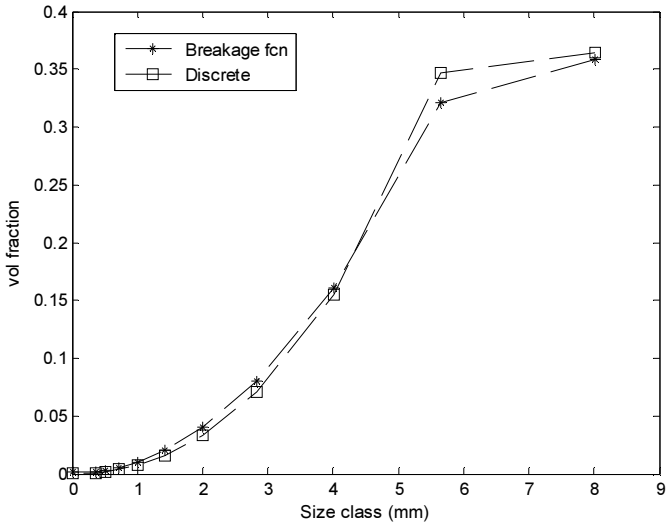

Figure F-1: PSD generated by the breakage function on a volume basis and the PSD given by the ratio of the two alternate distributions.

The breakage function is usually fitted to single chew data pooled from several particles, thus, it is the average distribution of several individually occluded particles. This distribution of daughter particles is not necessarily describing accurately the distribution obtained from a single particle, as particles of the same size produce different distributions depending on how they are positioned on the teeth. The method used here overcomes this problem and will produce daughter particles with a distribution similar to that measured experimentally.

APPENDIX G

Figure G-1 below shows the standard curve which enabled the sucrose concentration in the saliva from the expectorated bolus to be determined. Dilutions were prepared from the water and melted gel solution and the absorbance was measured at a wavelength of 510 nm.

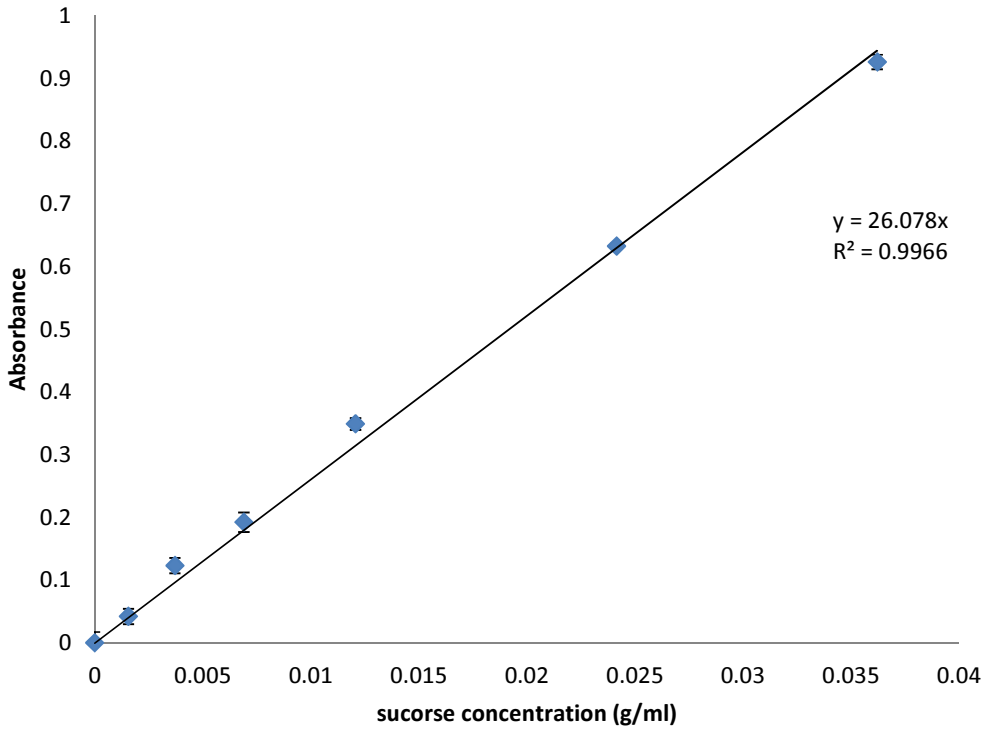

Figure G-1: Standard curve for the sucrose concentration in water obtained from melting two 1cm^3 of the 50%sucorse/15% gelatine cubes in 50ml of water.